UNIVERSITÀ
DEGLI STUDI
DI PADOVA

Administrative unit: **University of Padova**

Department: **Land Environment Agriculture and Forestry (TESAF)**

PhD Program: **Land Environment Resources and Health (LERH)**
Batch: **XXXI**

CABLE TENSILE FORCE MONITORING IN STEEP SLOPE FOREST OPERATIONS

DISSERTATION
submitted in partial fulfillment of the requirements
for the Degree of Doctor of Philosophy in
Forest Engineering

PhD Program Coordinator: Prof. Davide Matteo Pettenella
Supervisor: Prof. Stefano Grigolato
Co-supervisor: Prof. Raffaele Cavalli

PhD candidate: Omar Mologni

Summary

The interest on active sustainable management of mountain forests is increasing around the world. Great effort, in particular, is focusing on the identification of efficient, safe, and sustainable steep slope harvesting solutions adapted to the different environmental conditions. The main attention is moving toward winch-assist harvesting systems on trafficable terrain and European designed standing skyline mobile tower yarders on non-trafficable terrain. These cable-supported harvesting solutions have similar safety issues related to the use of tensioned wire ropes and the use of natural anchors. This research focused on the analysis of cable tensile force while operating with these harvesting solutions in ordinary harvesting sites and operational conditions.

First a state-of-the-art about the steep slope cable-supported harvesting solutions and their main safety issues was completed. A particular focus was dedicated to the significant works on cable tensile force monitoring. Following, field studies were successfully carried out to monitor the cable tensile forces on ordinary logging operations. The surveys interested eleven mobile tower yarders, observed on twelve different cable lines in the Italian Alps, and three large integrated-winch forwarders, observed on eight trails in the interior of British Columbia (Canada). A similar approach, based on the integration of tensile force monitoring, video recording of the operations, ground profile analysis, and load measurement/estimation, was applied to both the cable-supported systems. The case studies, the methodological approach used for the data collection and analysis, and the results of the monitoring are presented and reported in detail.

Riassunto

L'interesse per la gestione attiva e sostenibile delle foreste montane è in costante aumento in tutto il mondo. Un'attenzione particolare è dedicata all'individuazione di sistemi di utilizzazione forestale per terreni pendenti che siano efficienti, sicuri e sostenibili, adattati alle diverse condizioni ambientali. L'attenzione si sta attualmente focalizzando su sistemi basati sull'impiego di macchine terrestri a trazione assistita mediante impiego di funi e verricelli, in caso di terreni non accidentati, e sull'impiego di gru a cavo a portante fissa in caso di terreni molto pendenti e/o inaccessibili. Entrambi questi sistemi presentano rischi di sicurezza comparabili legati all'impiego di funi metalliche in tensione e, in parte, all'uso di ancoraggi e supporti naturali. Questo studio si è concentrato sull'analisi del comportamento delle funi in tensione utilizzate durante cantieri forestali ordinari e in condizioni operative. Inizialmente è stato analizzato lo stato dell'arte relativamente ai sistemi di utilizzazione forestale per terreni pendenti e alle loro principali problematiche in termini di sicurezza. Particolare attenzione è stata dedicata ai lavori più significativi inerenti al monitoraggio delle tensioni delle funi. In seguito, vari rilievi di campo per il monitoraggio diretto delle tensioni delle funi sono stati condotti in cantieri ordinari di utilizzazione forestale. Il monitoraggio ha interessato undici gru a cavo a stazione motrice mobile con ritto, osservate su dodici diverse linee di esbosco nelle Alpi italiane, e tre forwarder con verricello integrato, osservati su otto piste di esbosco in British Columbia (Canada). Un approccio simile, basato sull'integrazione del monitoraggio delle tensioni delle funi, la video registrazione delle attività lavorative, l'analisi del profilo del suolo e la misurazione del carico, è stato applicato a entrambi i sistemi analizzati. I casi studio, l'approccio metodologico utilizzato per la raccolta e l'analisi dei dati e i risultati del monitoraggio sono presentati e riportati in dettaglio.

Part of the information reported in this dissertation have been published or submitted to scientific Journals:

[1]. Mologni O., Lyons C.K., Zambon G., Proto A.R., Zimbalatti G., Cavalli R., Grigolato S. (submitted). ***Skyline tensile force monitoring of mobile tower yarders operating in the Italian Alps****. European Journal of Forest Research.*

[2]. Mologni O., Dyson P., Amishev D., Proto A.R., Zimbalatti G., Cavalli R., Grigolato S. (2018). ***Tensile force monitoring on large winch-assist forwarders operating in British Columbia****. Croatian Journal of Forest Engineering 39(2): 193-204.*

[3]. Mologni O., Grigolato S., Cavalli R. (2016). ***Harvesting systems for steep terrain in the Italian Alps: state of the art and future prospect****. Contemporary Engineering Sciences 9(25): 1229-1242. http://dx.doi.org/ 10.12988/ces.2016.68137.*

Acknowledgments

There are many people to whom I would like to recognize my appreciation for the support to my research activities during the three years of doctorate program.

Prof. Andrea Rosario Proto and Prof. Giuseppe Zimbalatti, from the *Department of Agriculture* of the *University of Reggio Calabria*, who provided the tensile force monitoring system used in the field studies and collaborated to the setting of the tools and to the elaborations of the research outcomes.

Dr. Paul Magaud, from the French *Institute of Technology for Forest-based and Furniture Sectors*; Prof. Eric Labelle, from the *Technical University of Munich*, and Prof. Martin Ziesak, from the *University of Applied sciences in Bern,* for the great effort done looking for collaboration with contractors operating with winch-assist harvesting systems in their countries.

Prof. Woodam Chung, from the *Oregon State University*, for the hospitality and the support during my visit to Oregon and for financing of my participation to the COFE Meeting DEMO International in Vancouver in October 2016.

Prof. C. Kevin Lyons, from the *University of British Columbia* (currently at the *Oregon State University*), for support my visit in British Columbia, for the pleasant discussions about the cable yarding systems, and for his great collaboration in the elaboration of the research outcomes.

Dr. Dzhamal Amishev from the *FPInnovations*, for his effort in the organization of my visit and my field studies in British Columbia, for his great hospitality, and for the fruitful collaborations started during my stays in Vancouver.

All the other people from *FPInnovations*, in particular Dr. Peter Dyson, Dr. James Hunt, Dr. Brian Boswell, Dr. Craig Evans, Dr. Domink Röeser, Dr. Ken Byrne, and Dr. Nico Petch for the great work environment and the pleasant time spent together.

Dr. Ilario Valentini and Dr. Francesca Ziller, from the *Valentini Srl*, for the continuous support and collaboration during these years of research activities.

All the numerous Italian contractor and forest operators which gave their fundamental contribution to the research activities, allowing the monitoring of their harvesting studies and giving full availability and collaboration to the project. A special thanks to Marco

Dorigato, Davide Dorigato, Paolo Sandri, Mirco Cigliani, Luigi Concina, Lucchini Giancarlo, Andrea Ciaponi, Emanuele Sansi, Giacometti Antonio Guido, Fiorenzo Pellegatta.

The Canadian forest companies Canfor e Interfor and their contractors Volktrans-Canada Ltd., Bill Todd Logging Ltd., and Lo-Bar Log Transport Co. Ltd. for their essential support in the field studies monitoring winch-assist harvesting operations.

Prof. Stefano Grigolato and Prof. Raffaele Cavalli, my supervisor and co-supervisor, respectively, for their trust in me and their substantial and continuous supports during these years.

Finally, Dr. Gianni Picchi, from CNR-IVALSA, and Dr. Martin Kühmaier, from BOKU University, for the excellent review of this dissertation and the useful suggestions that allowed me to improve my work.

TABLE OF CONTENTS

1. BACKGROUND AND LITERATURE REVIEW

1.1. FORESTS AND THEIR ROLE FOR THE SUSTAINABLE DEVELOPMENT

The last *Global Forest Resources Assessment* (FAO 2015a), published by the *Food and Agriculture Organization of the United Nations* (FAO) in 2015, provides an overview of the state of the world forests. The report, representing the most recent and consolidated assessment of forest data, shows a world forest area covering almost four billion hectares, representing more than 30% of the global land area. The majority of the forests are located in the tropical and sub-tropical areas, which together comprise 52% of the world forests. Countries classified as temperate and boreal include 26 and 22%, respectively.

The dynamic of the world forest area is the result of loss (forest deforestation) and gain (forest expansion) processes in different world regions. The trend is still negative and the net forest loss account 129 million hectares from 1990 to 2015. The rate of forest area net loss in the 2010-2015 period, however, was reduced by more than 50% compared to the 1990-2010 period. The loss of forests occurs mainly in developing countries located in tropics, particularly in sub-Saharan Africa, Latin America and Southeast Asia, due to a complex combination of economic, political and demographic factors, which lead to the conversion of forest lands to agriculture and other soil use. Forest area is declining also in the others climatic domain except for the temperate one.

Deforestation affects natural forests, which currently account for most of the forest area (93%), both as primary forests (26%) and naturally regenerated forest (74%). At the opposite, planted forests increased by over 105 million hectares since 1990. The average annual increment rate of planted forests in the 2010-2015 period, however, decreased compared to the previous two decades for a reduction of planting operations in several world regions.

However, large-scale afforestation programs and the related increase of planted forests, as well as the spontaneous reforestation of low-productive agricultural lands back to the forest, mainly in mountainous areas, are the main factors of increasing the forest area in some parts of Asia, North America and Europe.

The global forest resources provide multiple ecosystem services to the human being (Millennium Ecosystem Assessment 2005). These ecosystem services include provisioning services (e.g., wood and fuel production); regulating and supporting services (e.g., carbon sequestration, reliable water supplies, protection against natural hazards, mitigation of climate change, biodiversity); cultural services (e.g., the role of forests in local belief systems and customs, recreation and tourism). The fundamental role of forests for the human well-being and the life on the planet have been empathized by the *United Nations* in the *2030 Agenda for Sustainable Development* (United Nations 2015), where sustainable development is defined as a "development that meets the needs of the present without compromising the ability of future generations to meet their own needs", according to the *World Commission on Environment and Development report* (WCED 1987).
The *2030 Agenda* has four main objectives (eradicate poverty; heal the planet; secure prosperity for all; foster peace and justice) distributed in 17 *Sustainable Development Goals* (SDGs) and articulated in 169 targets. The *State of the World's Forest* (FAO 2018a), published by FAO in 2018, highlighted the role of forests in achieving ten of these 17 SDGs, five of them (SDG 1, SDG 2, SDG 7, SDG 8, SDG 12) related to the active forest management:

SDG 1 - End poverty in all its forms everywhere

Forest are recognized as vital sources of income, livelihoods and well-being for rural populations, particularly indigenous people, smallholders, and those living in close proximity to forests.

SDG 2 - End hunger, achieve food security and improved nutrition and promote sustainable agriculture

Forests contribute directly to food security by providing edible *non-wood-forest-products* and dietary diversity, supplying wood energy for cooking

food, and enhancing the resilience of the ecological and social systems surrounding agriculture.

SDG 5 - Achieve gender equality and empower all women and girls

Forests have significant potential to empower women by enhancing their rights, increasing their income and employment. According to the *Global Report on Women in Tourism 2010* (Twining-Ward 2010), women make up the majority of the tourism workforce. Nature-based tourism is growing three times faster than the tourism industry as a whole and now accounts for approximately 20% of the global market.

SDG 6 - Ensure availability and sustainable management of water and sanitation for all

Forests are an integral component of the hydrological cycle and are essential for supporting life on Earth. They regulate the precipitation and evaporation rates and control the fresh water supply and groundwater recharge. They filter water and reduce soil erosion and sedimentation of water bodies. According to the *Millennium Ecosystem Assessment* (Vinet and Zhedanov 2011), over 75% of the world's accessible freshwater comes from forested watersheds; over half of the Earth's population is dependent on these areas for water used for domestic, agricultural, industrial and environmental purposes.

SDG 7 - Ensure access to affordable, reliable, sustainable and modern energy for all

Forests have an important role in ensuring sustainable energy supply both providing woodfuel for cooking, heating and industrial needs (including power generation and cogeneration of heat and power) and protecting watersheds to enable hydropower generation.

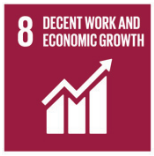

SDG 8 - Promote sustained, inclusive and sustainable economic growth, full and productive employment and decent work for all

Forests and their value chains are of critical importance for sustainable economic growth, full and productive employment and decent work for all, especially in remote rural areas.

SDG 11 - Make cities and human settlements inclusive, safe, resilient and sustainable

Urban and peri-urban forests can make a valuable contribution to the protection of cities' local cultural and natural heritage by providing settings for recreational and physical activities, fostering local tourism, and increasing aesthetic appreciation of the surrounding environment.

SDG 12 - Ensure sustainable production and consumption patterns

Resource efficiency, renewability and responsible sourcing of forest products are at the base of the sustainable production and consumption concepts. The resource efficiency and durability of wood products and responsible gathering of *non-wood-forest-products* can reduce the environmental burden of production to meet a growing world population.

SDG 13 - Take urgent action to combat climate change and its impacts

Forests store globally an estimated 296 billion tons of carbon and absorb roughly two billion tons of carbon dioxide equivalent each year. As highlighted by the IPCC's Fifth Assessment Report (IPCC 2014), forests have crucial role against global warming due to their ability to mitigate and adapt to climate change by reducing the carbon emissions caused by deforestation and forest degradation, and by increased carbon sink through afforestation and sustainable forest management.

SDG 15 - Protect, restore and promote sustainable use of terrestrial ecosystems, sustainably manage forests, combat desertification, and halt and reverse land degradation and halt biodiversity loss

Forests constitute an integral part of the global mosaic of landscapes and ecosystems. They interact with other living organisms, with soil, water and the atmosphere, and provide a wide range of goods and services that are important for society. Forests are among the most important repositories of biodiversity. Tropical forests host at least two-thirds of terrestrial species, while other types of forest are species-rich ecosystems in their own contexts (Vinet and Zhedanov, 2011).

The role of forests as a primary ecosystem for the human being and planet health have been reinforced and centralized also through the *Paris Agreement* (UNFCCC 2015), adopted in 2015 under the *United Nations Framework Convention on Climate Change*. The agreement recognizes the urgency of climate change and calls for limiting the increase in global temperatures. The *IPCC's Fifth Assessment Report* (IPCC 2014), showed the potentiality of forestry in this goal and most of the signatories included the forests in their *Intended Nationally Determined Contributions* for mitigation of climate change, but also for their contribution to adaptation. While reducing deforestation and forest degradation dominate the forestry mitigation potential in Latin America, Middle East and Africa, the active sustainable forest management, followed by afforestation, offers the best cost-effective mitigation option for contrasting the climate change in most of the developed countries.

Again, the *United Nations Strategic Plan for Forests 2017-2030* (United Nations 2017a) reports the forest-related contributions to the implementation of both the *2030 Agenda for Sustainable Development* and the *Paris Agreement*, as well as to the *Convention on Biological Diversity*, the *United Nations Convention to Combat Desertification*. This *Strategic Plan* highlighted the capacity of sustainable forest management to maintain healthy, productive, resilient and renewable ecosystems, providing essential goods and services to people worldwide. This was strengthened in 1992 during the *United Nations Conference on Environment and Development* in Rio de Janeiro from which derives also the *Agenda 21* (an action plan adopted by the *United Nations* previous the *2030 Agenda*) (UNCED 1992).

Also, according to the *Forestry for a low-carbon future* report (FAO 2016), not only forests but also the forest products play a strategic function in mitigation and adaptation to climate change through the potential for wider use of wood products and wood energy to displace more fossil fuel intense products, creating a virtuous cycle towards low-carbon economies. Several life-cycle assessments of wood-based products in the construction sector indicates that wood-based materials have a lower greenhouse gasses footprint than comparable non-wood materials over the complete life cycle of the product, including the production stage, use and disposal (González-García et al. 2011). Moreover, wood-products have great potential for carbon storage (SFC 2010). The woodfuel, currently accounting for about 6% of the world's total primary energy supply and 40% of the world's renewable energy supply (FAO 2017), have a significant lower greenhouse gasses emission per unit of produced energy compared to other energy sources (Wihersaari 2005; Zhang et al. 2010; Baral and Malins 2014). Also, sustainable wood energy production has a high mitigation potential, mainly in using wood residues effectively, improving the conversion efficiency of woodfuel and improving the combustion and heating efficiency of end-use devices and facilities. With a growing stock of 531 billion m^3 (FAO 2015a), the world's forests contain a vast quantity of energy, as about 142 billion tons of oil equivalent, which corresponds to roughly ten times the annual global primary energy consumption (FAO 2018a).

Global population and the wood mobilization strategy

The world population, currently accounting 7.6 billion people, is expected to reach 8.6 billion in 2030, 9.8 billion in 2050, and 11.2 billion in 2100 (United Nations 2017b). The income per capita of the world population is expected to triple by 2050 with a substantial increase demand for energy, food and natural resources (OECD 2016). As already shown in the last 50 years, both the economic growth and the population growth lead to a non-linear increased consumption of ecosystem services, even if the efficiency of the technologies used in the production of any particular level of service strongly influence its potential impacts (Vinet and Zhedanov 2011).

Growing population and the food-related demand, mainly occurring in the developing countries, is directly associated to the deforestation level (FAO 2015b). By 2050 the agriculture production is expected to increase by 70-85%, with a consistent land expansion mainly at the expenses of the natural forests (Bruinsma 2009). At the same time, wood

demand and removals are continuously increasing. Figure 1.1 shows the wood removal trend from 1960, when the world population accounted for 3 billion people, to 2016, in which wood removals reached 3.7 billion m^3 (FAO 2018b).

In this context, international policies - mainly in the developed regions - have been largely oriented to promote the active sustainable forest management, as well as the use of wood-based products and wood-energy, for both the mitigation effects of the human carbon-footprint and for emerging a sustainable bio-based economy as a long-term strategy for satisfying the increasing wood demand (Orazio et al. 2017). This is the case of the global forest goals of the *Strategic Plan for Forests 2017-2030* of the *United Nation* (United Nations 2017a) and of the forest policies in the European countries, currently oriented to the mobilization of the large unutilized domestic wood resources through the improvement of the harvesting intensity (Forest Europe 2011).

1.2. Mountain forests and the Sustainable Forest Management

Mountain forests have a crucial role in achieving the SDGs of the *2030 Agenda*, ensuring water supply and sanitation (SDG 6) and being a huge repository of biodiversity (SDG 15) (FAO 2018c). More than half of humanity relies on the fresh water that accumulates in

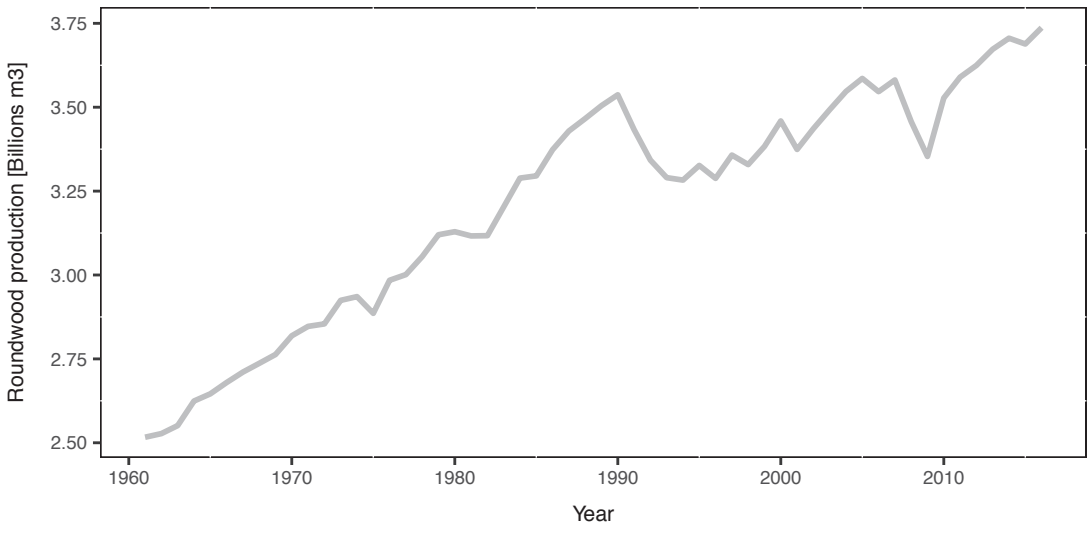

Figure 1.1: Global roundwood production from 1961 to 2016 (FAO 2018b)

mountains. Mountain areas constitute a relatively small proportion of river basins, but they provide the greater part of the river flows downstream (Liniger and Weingartner 2000). On the other hand, most of the world's highly significant species, ecosystems and genetic material are in the mountain forests, as well as many of the world's endemic species and plants with high value for pharmaceutical and agricultural industries (Grabherr 2000).

Mountain forests have a crucial position in terms of climate change, representing fundamental ecosystems for the health of the planet and a major carbon sinks (Price et al. 2011). They have a huge relevance in the tourist industry offering a vastity of recreational activities and providing important social psychological benefits to millions of people (Mccool and Lachapelle 2000). Also, mountain forests have a relevant cultural value in most of the long-time populated areas, representing a natural repository of events and history of its inhabitants. They host cultures as diverse as the mountains themselves (Zanzi Sulli 2000).

The role of the mountain forests to human life and activities is crucial for both highland and lowland communities. The interdependency between the mountain and lowland populations is particularly relevant when considering forests as sources of downstream water and soil erosion control, market goods and sociocultural diversity (Zingari 2000). Some of the mountain forests also have a fundamental role for direct protection of the human environment against natural hazards such as avalanches, landslides, rockfall, erosion and floods.

According to Schönenberger (2000), a direct protective function could occur when i) the forests are on slopes from which direct risks of natural hazards such as snow avalanches, landslides, erosion, debris flows, rockfall or torrents arise; ii) the hazards are threatening people or objects of significant value; iii) the forest is effective in preventing or reducing these hazards. The interaction between natural hazards and human activities is particularly relevant in densely populated areas, where it shaped the development of societies and infrastructure, i.e., settlements and agricultural land are found on the flat terrain while forested areas occur on steeper terrain (Bont 2012).

One of the most effective maps of the mountain forests was published by Kapos et al., (2000) in the *IUFRO Research series 5 - Forests in sustainable mountain development: a state of knowledge report for 2000* (Price and Butt 2000). The mapping process included the preliminary identification of the mountain area around the globe and the overlap of a digital maps of global forest. The criteria for defying the mountains were the altitude, the

slope, and the local elevation range, which combine to generate environmental gradients and unstable environments. Later, an update of the tree cover map of mountainous regions was published by Blyth et al. (2002). The update of the criteria identifies seven different classes of mountainous areas:

- class 1: elevation less or equal to 4500 m;
- class 2: elevation ranging between 3500 and 4499 m;
- class 3: elevation ranging between 2500 and 3499 m;
- class 4: elevation ranging between 1500 and 2499 m, and slope higher than two degrees;
- class 5: elevation ranging between 1000 and 1499 m, and slope higher than five degrees; or elevation ranging between 1000 and 1499 m and local (7 km radius) elevation range higher than 300 m;
- class 6: elevation ranging between 300 and 999 m and local (7 km radius) elevation range higher 300 m;
- class 7: inner isolated areas (less than 25 km^2 in size) that do not meet criteria but surrounded with mountains.

Results showed that almost a quarter of the global forests (23%), covering more than 900 million hectares, are located in mountainous area, representing a significant land proportion of these regions. Mountain forests grow from the equator to high latitudes, north and south, comprising both coniferous needleleaf and broadleaf species. Coniferous forests dominate in the European, North American and, partly, the Asian mountains, while deciduous forests are more common in Russia (Figure 1.2). The mountain forests are particularly relevant in North America, from the Pacific West Coast, to the Rocky Mountains and the Appalachians, in Central and South America, from the Andes Mountain Range to the Guiana Highlands, in the mountains of Central Africa, Southeast Asia, Borneo, New Guinea, and in the Australian Alps. Their relevance is particularly high also in Europe where they cover more than 40% of the total mountainous area and over half of the Alps, Balkans, Carpathians, and Pyrenees (Price et al. 2011). Without forests, large parts of these regions would be inhabitable, due to their ecological and socio-economic importance (Glück 2002).

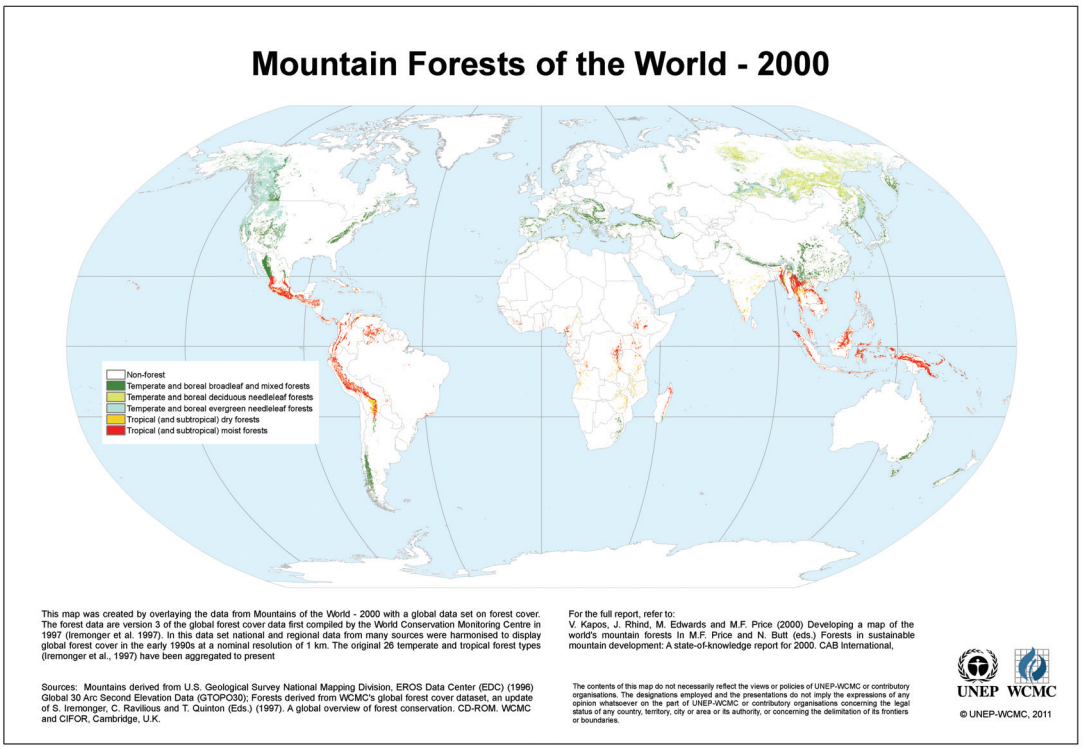

Figure 1.2: Mountain forests of the world (Kapos et al. 2000)

Compared to forests in general, mountain forests have some specific characteristics which are decisive for their management. Glück (2002) highlighted three main distinctive elements for the mountain forests: i) the harvesting costs comparatively higher than the average, mainly because of the difficult terrain in mountain forests, but also for the lack of the forest road network (Grigolato et al. 2013; Pellegrini et al. 2013); ii) the relevance of their protection function; iii) the fragility of their ecosystems, frequently exposed to heavy strains by several factors as storm.

The objectives of forest management and silviculture in mountain forest changed greatly since the '70 in many regions around the world. This was because of the recognizance of the numerous ecosystem services provided by these ecosystems, leading to a multifunctional approach to forestry (Buttoud 2000). The multifunctional approach and the related protectionism - combined with the mountain abandonment and depopulation - led to the under exploitation of several mountain forests in the developed countries.

While the fragile, and often vulnerable, environment of the mountain forests require a particular care in the management regime, the under exploitation of these forest led to an increased rot and decay - with consequent implications for water supplies - and increased

areas of windthrown timber with potentials for serious insect and disease problems. Also, the under exploitation caused a loss of income and benefits derived by the use of mountain timber and wood-based products. The active management of mountain forests have a fundamental role to limit the abandonment and the consequent decay of forest stands, maximizing forest resiliency, and guaranteeing timely regeneration (Valente et al. 2011; Spinelli et al. 2016). Also, in stands with a direct protective function, the disintegration phase of the natural forest development cycle must be prevented by silvicultural measures aimed at providing an uninterrupted protective effect (Schönenberger 2000).

In this context, the development and adoption of sustainable forest management systems that provide a balance between land use and conservation of all the ecosystems services offered by the mountain forests result strategic (Cavalli and Amishev 2017). Even in a multifunctional approach, however, the wood harvesting remains a central aspect of sustainable mountain forest management (Price and Butt 2000). Although information about timber production from mountain forests is not available at a global level, these forests are crucial sources of wood for satisfying the increased global demand (Valente et al. 2014), especially in an increasingly urbanized world, where the global timber trade is expanding rapidly (Price et al. 2011).

1.3. SUSTAINABLE FOREST OPERATIONS AND STEEP SLOPE HARVESTING SOLUTIONS

The forest management is directly and unavoidably linked to the forest operations. In this context, the debate on the value of implementing a sustainable approach to the forest operations has increased (Marchi et al. 2018a). Sessions and Garland (1999) defined the forest operations as all the technical and administrative processes required to develop technical structures and facilities, to harvest the wood, to prepare sites for regeneration, to maintain and improve quality of stands and habitats.

The sustainable concept applied to the forest operations evolved from the 1992, when the focus was on the *environmentally sound forest harvesting concept* proposed by Dykstra and Heinrich (1992), in which the mission was to promote economically viable forest operations with minimal environmental impacts at local and regional scale. Following, the approach

moved to the so called *reduced-impact logging concept*, summarized by FAO (2004), which focused on the minimization of the impact of wood harvesting on forest stand and soil at local scale. Later, Heinimann (2007) introduced the concept of *forest ecology operations* extending the approach from local and regional scale to a global scale. This concept suggested to develop environmentally sound forest operation technologies, to improve efficiently in the use of the wood resources, to reduce the waste and emissions due to the harvesting operations, and to minimize impacts to the structures and functions of the environment, including atmosphere, biosphere, hydrosphere, and lithosphere. The author proposed the development and promotion of forest operations which are:

- bio-physically effective, considering the physical laws, engineering knowledge, and environmental relationship to the forest ecosystems;
- economically efficient, considering costs and benefits of short and long-range consequences;
- individually compatible, preventing adverse effects on the health or the psychosocial well-being, promoting the development of personal skills and attitudes, and social reasonability;
- environmentally sound, considering impacts on the environment and efficient use of natural resources;
- institutionally feasible, considering the laws and regulations governing operations, landowner objectives, and social values.

More recently, Marchi et al. (2018a) proposed an update of the *sustainable forest operations* criteria for a local, general and global scale, integrating two more aspects: quality optimization and ergonomics. This new concept of sustainable forest operation was defined as "a complex system of relationships that encompasses a set of technologies, methods, systems and practices applied in forest operations planning, implementation, monitoring and improvement with the consideration of five performance areas including: environment; ergonomics; economics; quality optimization; people and the society". The key aspects of each performance area which contribute to the success of this last sustainable forest operations concept include:

- **environment:** minimization of the environmental impacts of forest operations at local, general and global scale, regarding energy consumption, soil, air, water, residual stands, and biodiversity;
- **economics:** maximization of the profitability (expressed in terms of productivity, costs, and added value) of the forest operations to improve the forest management and maintain a stable and solid forest sector;
- **ergonomics:** guarantee of the safeguard and protection for undue risks of the forest workers. Ergonomics is related to the comfort of the operations, but it also pursues the health and safety of forest workers;
- **quality optimization:** maximization of the utilization rates of harvested trees, reduction of waste materials, and enhancement of product quality and profitability during in-forest operations. In this context, the extraction of forest residues should be carefully assessed in relation to local environmental conditions, considering nutrient recycling and protection of soil and water resources. Preserve the quality of future products avoiding the residual stand damages;
- **people and society:** maximization of the multiple ecosystem services provided by the forests ecosystems in term of provisioning services, regulating and maintenance services, cultural services, employment services.

Further relevant components of the sustainable forest operations criteria suggested by Marchi et al. (2018a) include the involvement and participation of the different stakeholders in the forest operations decisions and the compliance of forest operations with the laws and regulations at different levels.

In a sustainable approach to the forest operations, a primary concern is the carefully selection of the proper harvesting system because of its potential strong effect on environmental, economic and social performances. Pentek et al. (2008) defined a wood harvesting system as the tools, equipment and machines used to exploit a forest area. The depth knowledge of the elements and factors that could affect the efficiency of the harvesting solutions is the base information for selecting the best system in a sustainable point of view. While many studies have been conducted to evaluate physically feasible machine

solutions and improve harvesting economics, since the later part of the 20th century, social and environmental conservation assumed growing importance in public discussions (Harrill 2014) and into the definition of criteria for selecting the proper harvesting system (Kühmaier and Stampfer 2010; Horodnic 2015).

Modern harvesting systems are strictly influenced by the increased global competition that is imposing a growing strain on all commercial activities, including wood harvesting. This requires an increasing in the productivity while decreasing production costs in order to maintain the profitability of the harvesting operation, according to the sustainable criteria (Marchi et al. 2018a). In the last decades, this resulted in a massive effort towards forest mechanization (Spinelli and Magagnotti 2011).

The process of wood harvesting is carried out in a succession of interrelated operations, including felling, delimbing, bucking and transportation (Gerasimov and Sokolov 2014). Transportation consists of two phases, off-road and on-road, which are heavily dependent on each other (Heinimann 2004). Off-road transportation (wood extraction) has the role to concentrate the harvested wood to a permanent transportation construction (Alexandru and Ticu 2012). This phase has a significant impact on the overall operational and environmental efficiency in managing the entire forest. Therefore, the development of the most appropriate transportation scheme is a crucial task when planning a forest harvesting operation (Bont 2012; Horodnic 2015). In this context, trafficability, defined as the quality of the terrain that expresses the capability to bear traffic, directly determined by stand accessibility and terrain characteristics (Cavalli 2015), is the main factor in the identification of the harvesting systems suitable at particular locations within a defined project area (Kühmaier and Stampfer 2010). Heinimann (2004) identified four main basic harvesting concepts, mainly in terms of off-road transportation (Figure 1.3): i) ground vehicles moving on natural terrain, ii) ground vehicles moving on skid roads iii) carriages moving on cable structures, and (iv) airships moving in the atmosphere. The four main concepts were categorized in three groups named ground-based, cable-based, and airship-based harvesting systems.

Ground-based harvesting systems refer to any harvesting system that uses an extraction machine or equipment driven into the forest (Horodnic 2015) on a path over natural terrain or, if the terrain conditions become too complex, over geotechnical structures (built skid roads) (Erickson and Virginia 1991; Heinimann 2004). Slope feasibility limit for ground-

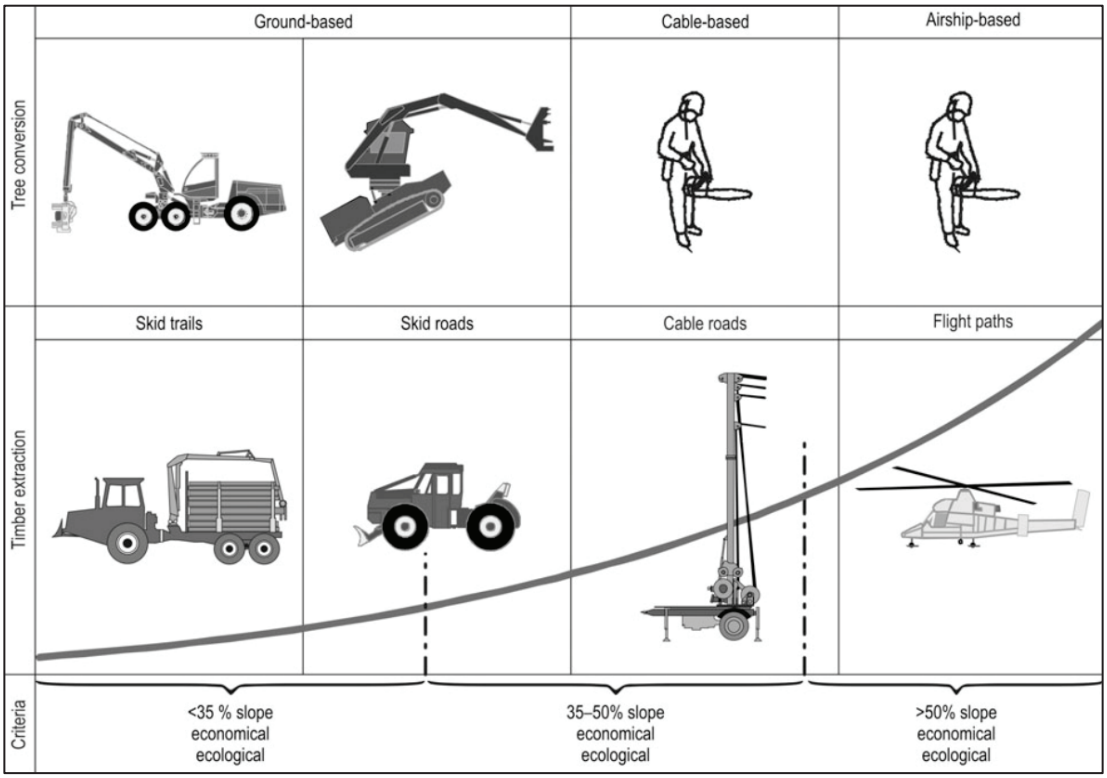

Figure 1.3: Basic harvesting system concepts (Heinimann 2004)

based systems is often not well defined (Visser 2014). For example, slope limits were fixed for downhill skidding at a slope gradient of 50% for wheeled skidders and 60% for crawler tractors, depending on surface roughness. Practical experience later demonstrated that those limits had to be reduced in order to keep the machine slippage and soil erosion within acceptable limits (Hittenbeck 2007). Slope limits of 30% and 40% for wheeled and tracked machines, respectively, were related primarily to machine traction and soil erosion, and these values have since been presented and propagated in many subsequent reports and guidelines (Visser and Stampfer 2015).

Steeper slopes require motor-manual felling for tree conversion and different yarding systems. At slope gradient exceeding 35%, cable yarders enable the transport of partially or fully suspended loads over large distances and are the determinant technology of harvesting system (Heinimann 2004; Bont 2012). The use of helicopters for timber extraction is burdened with high operational costs but could play an important role in timber transport in specific site conditions when road costs are high, the speed of operations is important

or soil and stand damage must be avoided due to special functions of forests (Stampfer et al. 2002; Lyons and McNeel 2004; Manzone and Balsari 2011; Grigolato et al. 2016).
The slope is a primary determinant of travel speed and machine stability and, as a consequence, of proper selection of harvesting system, but is not the only factor that should be considered when assessing safe operations or system productivity on steep terrain. Other two terrain characteristics are also important: ground strength and surface roughness (Owende et al. 2002). Ground strength is a measure of the bearing capacity of the soil and is able to affect the productivity of harvesting machines and to indicate the potential level of environmental damage caused by the machines. Surface roughness is a measure of the size and distribution of obstacles and is able to directly affect machine stability and travel speed (Davis and Reisinger 1990).

Relevance of steep slope forest operations

The decline in per capital forest area at global level, coupled with steady increases in wood removals, indicates that more wood will be needed from less land in coming years (FAO 2015b). As already shown several years ago, moreover, flat lands are progressively monopolized by farming and urban development, displacing the forest to increasingly difficult mountain terrain (Carson 1983; FAO 1985). Also, several forest areas, as occurred for example in British Columbia (Canada), representing one of the largest forest industries in the world, have been intensively logged in the last 150 years on their easy-access areas and the loggers have to move on steepest mountainous areas previously avoided (Bennett 2016). Forest operations in mountain forests are challenging because of the steep slope, the complexity in the morphology, and limited accessibility of the stands which strongly limit the technological solution available for the exploitation of a forest areas. Efficient, safe and sustainable steep slope harvesting solutions for mountain forest harvesting operations represent a main challenge in the forest industry around the world.
The relevance and the specificity of this theme is highlighted by one of the few specifically mountain-focused topics of a research unit (3.06.00) of the *International Union of Forest Research* (IUFRO). This includes a sub-unit on *Accessibility of mountain forests* (3.06.01), as this is the most critical factor affecting these operations, given the difficulties of harvesting and extracting wood in steep terrain (Price and Butt 2000).

1.3.1. CABLE-BASED HARVESTING SYSTEMS

Cable-based harvesting systems historically represent the most common systems for steep slope forest operations around the world. The possibility to operate efficiently in non-trafficable terrain allowed the widespread of this system where commercial forestry is partially or totally related to steep grounds, such as the Pacific West Coast, New Zealand, and Central Europe (Heinimann et al. 2001; Raymond 2012; Visser and Harrill 2017).

The diverse forestry conditions in these areas led to the development of different technological solutions, rigging configurations, machines sizes, and equipment described in several handbooks and best practice guidelines (Studier and Binkley 1974; Samset 1985; FITEC 2005; Work Safe BC 2006; OR-OSHA 2010; Safe Work Australia 2013; Ackerman et al. 2017). According to the several handbooks published in the forty years, the cable harvesting systems, defined by the type, number, and the functions of the cables, could be classified in four main categories: high-lead; live skyline, running skyline, and standing skyline.

The *high-lead system* is the simplest cable yarding system. It consists of an inhaul drum and cable (mainline), and an outhaul drum and cable (haul-back). This system is simple in operation and set-up, but the lack of lift poses problems for the level of ground disturbance, breaking of gear and stems, and low productivity. In a skyline system, instead, the skyline supplies lift for the rigging, the carriage, and the logs. Skyline systems are preferred over high-lead systems as they ensure adequate suspension of the loads above the ground to minimize site disturbance or eliminate it altogether, and they also allow for longer extraction distance in multi-span systems (Owende et al. 2002).

In a *live skyline configuration*, the skyline is fixed at only one end support, with a mechanism to control the tensile force of deflection of the skyline at the other end support. A *running configuration* involves a mechanism at each end of the support to control the tensile forces. To make such a system operable, the two control mechanisms are integrated at the head end while a pulley at the tail end diverts the tensile force. A difference between tensile forces is required to produce lift and to move a load. Running configurations can vary the deflection at any point of the span, adjusting itself to the weight of the load, the deflection increases with heavier loads to provide the lift to the suspended load without adding to the line tensile force (Talbot et al. 2015). Live and running skyline systems are the common

cable yarding systems in North America, New Zealand and north of Europe (Bont 2012; Talbot et al. 2015; Visser and Harrill 2017).

In Central Europe, and in particular in the Alps, where forestry is based on partial retention cuts and thinning operations, the *single and multi-span standing skyline configurations* represent the primary cable yarding system (Stampfer et al. 2006). In this configuration, as shown in Figure 1.4, a skyline is fixed to both ends and the load, hooked to a carriage, is moved on the skylines by the mainline, which in some cases has to be combined with haulback lines for valley mounted yarders and downhill wood extraction (Heinimann et al. 2001; Dupire et al. 2015).

Compared to the North American and New Zealand forestry, the Central European adoption of a small-scale harvesting regime, the relatively limited log size, and the need of frequent relocations of the machines, moved and positioned on the existing forest road network, lead to the development of limited-size machines, with a relatively low payload capability but settled explicitly for speed of operations and relocation. However, the interest in European designed cable yarders, that provide energy and fuel cost savings as well as automated controls for improved safety and worker satisfaction, is increasing even in the industries where traditionally expensive large and robust yarders used to operate (Harrill and Visser 2017; Visser and Harrill 2017).

The European designed cable yarders are provided by several manufactures, mainly distributed around the Alps (Figure 1.5). Two main categories of standing skyline technologies are available: the sledge yarders and the mobile tower yarders. The first category

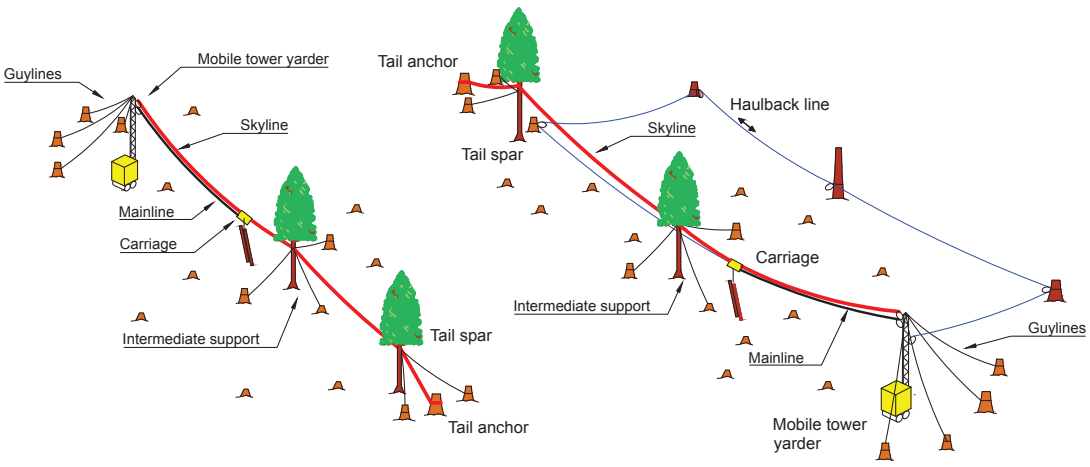

Figure 1.4: Uphill and downhill standing skyline cable yarding (Marchi et al. 2018b) modified

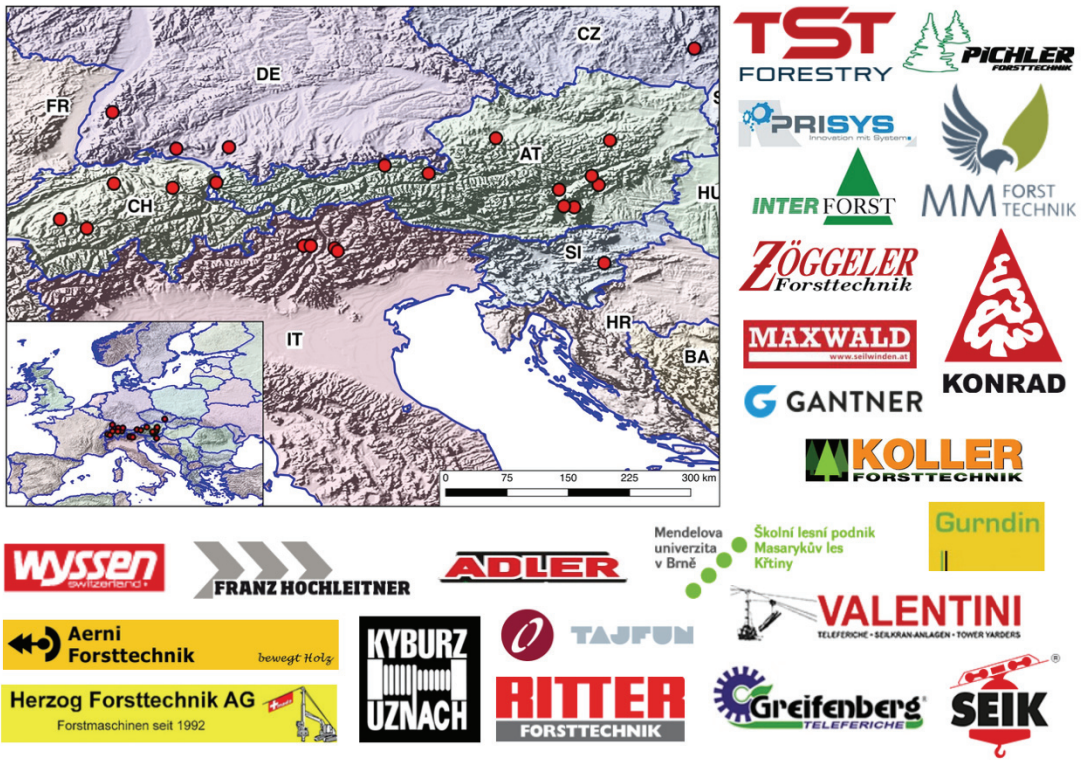

Figure 1.5: Standing skyline system manufactures. This includes manufactures of sledge yarders, mobile tower yarders and carriages. Red point shows the locations of the manufactures

represents the traditional system based on a winch with, normally, a single drum installed on a sled chassis. It is still quite common in some areas but limited to the most prohibitive conditions (Mologni and Cavalli 2015; Mologni et al. 2017). The tower yarders are mobile machines equipped with the drums for all the wire ropes required for the cable system functionality and with a hinged or telescoped mast mounted on a carrying base. The mobile tower yarders represent the state of the art of the technological development of the standing skyline configurations (Heinimann et al. 2001). They are particularly common in the Alpine area, in particular in Austria (Ghaffariyan et al. 2010), Switzerland (Magaud et al. 2018), and Italy (Spinelli et al. 2013).

The base vehicle equipment (e.g., tractor, trailer, truck and self-propelled track undercarriage) is normally used as parameter to classify the different technological solutions of mobile tower yarders available on the market. The *tractor-based cable yarders* (Figure 1.6) are typically small machines mounted on the three-point hydraulic system of a tractor or on its own axes. These machines are powered by the power-take-off (PTO) of the tractor or,

rarely, have their own engine. This type of machine is usually available in the two-lines configuration for uphill wood extraction, but some models are provided in the three-lines option. The skyline length is generally included between 300 and 500 m, with diameters ranging from 12 to 17 mm. The power required to the tractor ranges between 40 to 100 kW. The total maximum weight of these machine reaches five tons. The maximum pulling forces and speeds of the mainline drum (measured at half drum) are generally limited to 30 kN and 5.6 ms^{-1}, respectively.

The *trailer-based cable yarders* (Figure 1.7) are cable cranes built on a single or dual towed wheel trailer, generally pulled by tractors. Differently by the tractor-based tower yarders, these machines are independents and have their own engine (power ranging from 40 to 175 kW), able to control the functionality of the hydraulic systems. The skyline length ranges between 500 and 1100 m with diameter ranging between 14 and 22 mm. The maximum mainline pulling force and speed at half drum reach 50 kN and 9 ms^{-1}, respectively. The weight of these machines range between six to 20 tons.

The self-propelled cable yarders with a track undercarriage - subsequently named *track-based cable yarders* - (Figure 1.8) have their own engine with a power ranging from 130 to 190 kW. Despite the high machine weight (15-20 tons), they have generally high mobility capacity and can be installed and positioned in difficult landings, but usually they require a special permit for their transport to the harvesting site. The skylines range between 500 and 1000 m in length and 16-22 mm in diameter. The mainline drum reaches a maximum pulling force and speed (measured at half drum) of 50 kN and 9.5 ms^{-1}, respectively.

Truck-based cable yarders (Figure 1.9) are generally realized on a two or three axes truck. They are usually powered by the motor of carrying truck, with a power ranging between 280 and 350 kW. These machines are typically the heaviest (weight ranging from 26 to 40 tons, with a maximum of 48 tons) and powerful Central European tower yarders. The skyline reaches 1100 (1500) m in length and diameters up to 24 (26) mm. The maximum mainline drum pulling force and speed (at half drum) reach 55 kN and 9.5 ms^{-1}, respectively.

Another important type of European designed cable yarder is represented by the *Processor Tower Yarders*. These machines integrate a tower yarder with a processor on the same base vehicle which is normally represented by a three of four axes truck. The presence of these machines in the Italian mountains is limited because of the required high-quality standards in the forest road network.

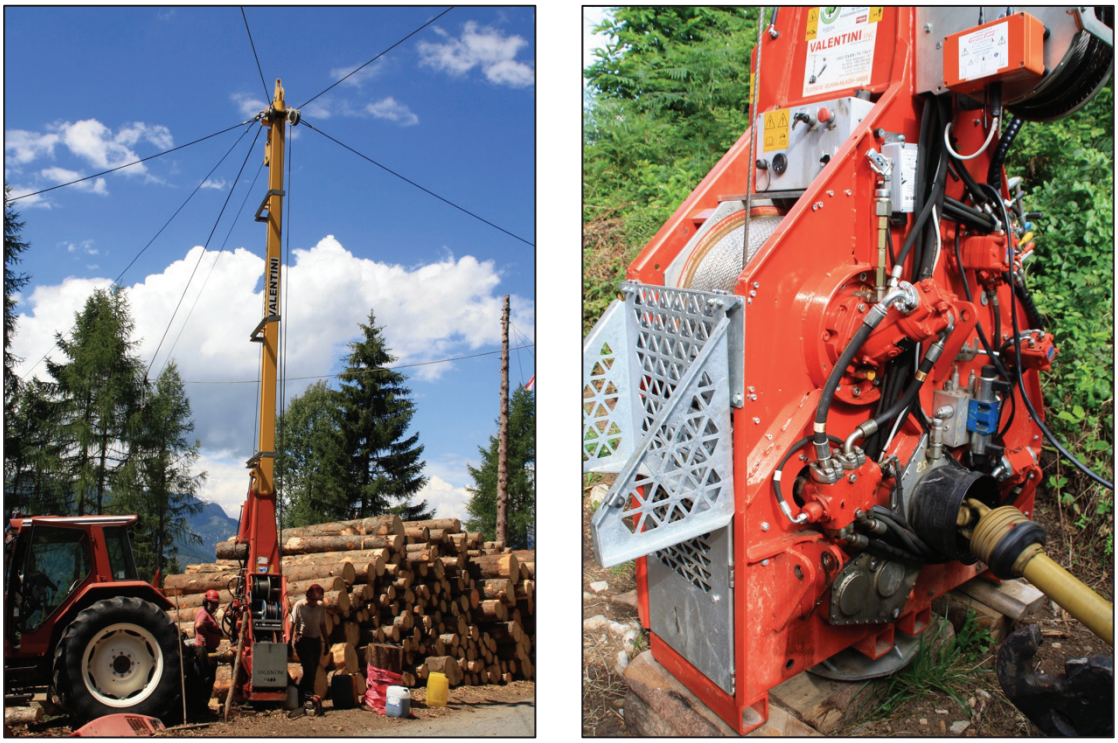

Figure 1.6: Tractor-based tower yarders

Figure 1.7: Trailer-based tower yarders

Figure 1.8: Track-based tower yarders

Figure 1.9: Truck-based and Processor tower yarders

A base component of the cable system which interact with the base machine and the cable system for completing the yarding operations is the carriage. Modern type of standing skyline carriages effectively used in the logging industry include automatic clamped carriages, motorized carriages and self-propelled carriages (Figure 1.10).

The *automatically clamped carriages* are characterized by the presence of automatic clamps for locking the carriage at the hooking or unloading positions. The clamping control can occur in different ways, including radio control and time triggered. The skidding line is represented by the mainline. Simple carriages work as gravity system, more complex carriages have a dedicated system for slack-pulling the mainline. The slack-pulling mechanism can work through the use of a cable (the haul-back line or an auxiliary line), a hydraulic motor, an electric motor, or a combustion engine.

The *motorized carriages* are characterized by the presence of a combustion engine, a self-built winch hydraulically activated by the engine, and an independent drop line. These carriages can be manufactured as clamped or unclamped carriages. The size and dimensions of these carriages are normally higher than simple automatic carriages. Limitedly, a combination of automatically clamped carriages and a motorized carriage or a combination of two different motorized carriages is adopted for fully suspension of whole trees.

Finally, the *self-propelled carriages* are carriages with a self-built winch and independent dropline. In this kind of carriages, the translation along the skyline is not given by the mainline but directly by two or more driving pulleys. These carriages allow to work in the one-line configuration and does not need necessarily the tower yarders to operate. However, the combined use of this carriages with tower yarders is common because of the easiest installation procedures. These carriages do not use clamps on the skyline, they just use the hydraulic brake of the driving pulleys.

Figure 1.10: Carriages used in standing skyline cable yarding. From the top left: ACC; ACC slack-pulling -hydraulic motor; ACC slack-pulling -electric motor; ACC slack-pulling – combustion engine; motorized carriage; self-propelled carriage; double-carriage for fully suspension of whole trees

The introduction of new procedures and technological developments in the last two decades have improved the general performances of cable yarding operations in terms of productivity, efficiency, ergonomics, and safety. Some examples are the introduction of radio controlled chockers (Stampfer et al. 2010); the use of active slack-pulling and/or self-propelled carriages (Heinimann et al. 2001); the development of automatic systems for controlling the hauling phases, which are common and well developed in the European cable yarders (Visser et al. 2014; Visser and Harrill 2017). The increasing diffusion of the whole-tree harvesting method also represented an improvement in the cable logging operations. Operating with this method, the trees are felled and the stem, intact with branches, is transported to the landing. The processing operations are then performed at the roadside (Heinimann et al. 2001; Ghaffarian et al. 2009; Gerasimov and Sokolov 2014). This solution allows higher profitability and safety of the processing operation and gives the possibility to recover large quantity of biomass for use as energy wood, representing an additional source of income (Spinelli et al. 2016).

The cable-based harvesting system, and particularly the skyline configurations (Gumus and Acar 2010), is generally considered an environmentally friendly system because of the limited soil interaction (Owende et al. 2001, 2002). This whole-tree method, however, raised recent concerns in terms of long-term sustainability because of the removal of most of the nutrient-rich components of a tree from the harvesting site (Huber and Stampfer 2015). Moreover, the high set-up (Stampfer et al. 2006) and running costs (Ghaffariyan et al. 2013; Spinelli et al. 2015), and the safety issues, related to both the linked motor-manual tree felling (Tsioras et al. 2014) and the cable yarding activity itself (Tsioras et al. 2011), are pressing the forest industries around the world to expand the operational range of ground-based systems on steep grounds, both as a support for the felling process but mainly in totally substitution of cable yarding operations (Visser and Stampfer 2015).

1.3.2. MECHANIZING STEEP SLOPE FORESTS OPERATIONS: THE WINCH-ASSIST SOLUTION

The mechanization process of forest harvesting operations contributes to reducing both the risks and the frequency of accidents and/or occupational diseases (Bell 2002; Klun and Medved 2007) and improving profitability (Enache et al. 2016), in compliance with the

criteria of a sustainable forest operation (Marchi et al. 2018a). For this reason, research in steep slope forest operations is currently oriented into the extension of the safety operation range of ground-based harvesting system through the development of special traction devices and under-carriages (Cavalli 2015). Similarly to the mechanization phase in forestry occurred in 70's with the vision for safety in the forest based on "no foot on the ground, no hand on the tree", the vision for steep slope forest operations is moving towards a "no worker on the slope and no hand on the chainsaw" according with the New Zealand Future Forests Research Program (Bayne and Parker 2012). While modern fully mechanized ground-based systems are a default option for safe and productive harvesting in gentle terrain, they have always been limited by terrain factors such as slope, soil strength, and/or roughness. Improvements to allow machines to operate on steeper areas are two-fold: the need for increased stability of the base machine on the slope itself and improved ergonomics for the operator (Visser and Stampfer 2015).

Various steep-slope harvesting machines have been shown to safely access and operate on terrain up to 70% slope without external support thanks to self-levelling cab and boom and specialized undercarriages and carriers (Stampfer 1999; Stampfer and Steinmüller 2001; Strandgard et al. 2014; Visser and Berkett 2015). Also, improved control systems, swivel seats, 360-degree windows and/or rear facing cameras provided for greater visibility and improved operator performance. Modern self-levelling machines also redistribute the center of gravity uphill to improve overall stability (Visser and Stampfer 2015).

Recent worldwide effort is focusing on improving traction and stability of ground-based forestry machines on steep slopes, supporting them with winches and cables anchored to various anchor types (Amishev 2016). Terms such as winch-assist, traction-assist, cable-assist and tethering all refer to technology that helps a forestry machine climb a steep slope (Cavalli and Amishev 2017). This technology is based on the use of a cable, pulled or braked by a winch, synchronized with the machine vehicle speed (Cavalli et al. 2009) and able to increase traction control during felling or extraction operations (Kühmaier and Stampfer 2010). The safety principle is that machines are not suspended from the cables and primary machines should be able to stop in full control at all times without reliance on the cable (Amishev 2016).

Options for extending mechanized forestry operations to steep slopes were examined during the 70's through a feasibility study of a self-contained cable tether system (McKenzie

and Richardson 1978). Winch-assist forwarders has been available in Europe since the 90's to match the wheeled harvesters capable of working on steep slopes, even if the first commercial solutions were introduced in 2004 by Herzog Forsttechnik AG (Holzfeind et al. 2018; Holzleitner et al. 2018). Later, winch-assist technology was extended to harvesters (Visser 2013; Visser and Stampfer 2015). In New Zealand the first winch-assist harvesting machine was pioneered in 2006. The first winch-assist unit designed and manufactured in North America was in 2012. The subsequent developments in purpose-built winch-assist machines over the last decade have proven this concept as a well-defined harvesting system (Cavalli and Amishev 2017). Depending on the location and power source of the winch, two main design options spread on the forest industries around the world (Visser and Stampfer 2015; Amishev 2016): integrated-winch machines and anchor machine winches.

Integrated-winch systems

In the integrated-winch system, the winch is built into or bolted onto the primary forestry machine. The anchor normally is a stump or a tree, sometimes another machine or a properly constructed deadman. The rope is not moving along the ground. This allows to reduce the abrasion but expose to localized rope damages. With this system, a single machine is able to exploit down site and upper site of a forest road. A strawline allows the pull-up the cable if required. Logistic, maintenance, and transportation costs are related to a single machine.

Most of the integrated-winch harvesting machines allow to remove the winch unit when not required. However, adding a winch system to the machine itself adds both weight and power requirements. In addition to the winch itself, modifications are required in terms of integrating the control system as well as some fairlead to ensure that the cable is not dragged over the ground or subjected to bending fatigue. In case of winch-assist forwarders, is normally not possible to easily remove the winch.

This option includes purpose-built harvesting machines, as the New Zealand *ClimbMAX*, and the European solutions for harvesters and forwarders, such as the *HAAS on John Deere* machines and the *Herzog on Ponsse* machines. Other forestry equipment manufactures designed and integrated their own winch, as *Komatsu* (previously partnered with Ritter) and *HSM* (Figure 1.11).

Figure 1.11: Integrated-winch machines. From the top left: ClimbMAX; Komatsu harvester; John Deere-Haas forwarder; John Deere - Haas harvester; Ponsse-Herzog forwarder; Ponsse-Herzog harvester; HSM forwarder; HSM harvester

Notes: The HSM forwarder photo has been provided by FPinnovations. The other photos, excluding the John Deere-Hass machines, have been downloaded from the official web pages and Youtube channels of the manufacturers

Anchor machine winch systems

The anchor machine design option is a two-part system with the winch mounted on and powered by a second machine, typically a bulldozer, an excavator, or a purpose-built mobile winch system. In addition to removing the weight and power requirements from the machine on the slope, this option provides flexibility because the assisted machines can be detached and operate independently, while the anchor machine can be used for assisting another machine. The full power of the anchor machine (usually a second-hand converted machine) can be used in the winch-assist function pulling the primary machine. Thus, there is greater capacity in term of drum size, cable length and pulling force. The cables move along the ground following the primary machine with a potential increased abrasion and risk of sparking a fire during the dry season. The operations are limited by access the anchor machine from a road or a back-spar trail and required two machines instead of one whit the related capital and maintenance costs. Both single and double rope systems are available. The first one guarantee less maintenance and easier monitoring. A double system allows a safety backup in case of cable failure and an increased safe working load and pulling force.

This design option includes machines from New Zealand, both as double-ropes (*Remote Operated Bulldozer; EMS Tractionline*) and single-rope machines (*Falcon FFE Winch-assist*), and North America, as the *T-Mar LC 150* and the *LC 190* and the *Summit* winch. Examples of European technology include the *Ecoforst T-winch*, an Austrian small purpose built mobile tracked winch system with significantly lower power and fuel requirements compared to converting a conventional bulldozer or excavator. Another European-designed solution is the *Herzog Synchrowinch MV500*, composed by two dynamic anchor winches and one traction winch built on a Ponsse machine. Other options included winches attached on adapted machines, as the *Haas three-point-winch* for installation on tractors (Figure 1.12).

Figure 1.12: Anchor based winch-assist systems. From the top left: EMS Tractionline; Remote Operated Bulldozer; FFE winch-assist; Summit; T-Mar LC150; Ecoforst T-Winch; Herzog MW500; Haas three-point-winch

Notes: The T-Winch and the Herzog MW500 photos have been provided by FPInnovations. The other photos have been downloaded from the official web pages and Youtube channels of the manufacturers.

Winch-assist machines have been shown to safely operate on terrain up to 85-100% slope (Cavalli 2015; Cavalli and Amishev 2017), even if there is a limit about the physical feasibility of operating machines on steep slopes that needs to be better defined and understood (Berkett 2012). These specialized forestry machines, however, can often exceed the upper slope limits established in safety codes in many countries throughout the world (Alam et al. 2013; Visser and Berkett 2015; Sessions et al. 2017). As example, the *Safety and Health in Forestry Work* (ILO 1998), published by the *International Labour Office* (ILO), defines that forestry equipment specifically designed for use on steep slopes should not be operated on a slope which exceeds 50%. The *Workers' Compensation Act* of British Columbia (Canada) (B.C. Reg. 296/97) has updated its *Occupational Health and Safety Regulations* for the use of ground-based logging equipment in 2008. The slope limits are the same as reported by ILO. However, the regulation included the possibility to operate beyond the maximum slope operating stability limits developing and following specific steep slope protocols for stability and safety concerns. In Oregon (US), the *Occupational Safety and Health Administration* (OSHA) revised the 437-007-0935 section related to *Operation of Ground Skidding Machines and Vehicles* during 2016 (OR-OSHA 2016). The slope limits are the same as reported by ILO, unless differently specified by the manufacturer of the equipment. If there are not official specification of the manufacture, the contractors must apply for and be granted a research variance prior to using the harvesting machine above its slope limit with a winch-assist system. The variance has to be designed to demonstrate or validate new and improved safety or health techniques or products. In New Zealand, the revised *Approved Code of Practice for Safety and Health in Forest Operations* (MBIE 2012) contains a section for winch-assist harvesting on steep slopes where references to specific slope limits have been removed. It requires "*All mobile plant using the assistance of a wire rope and/or winch shall be specifically designed, tested, demonstrated to be safe*" and that "*The tension on the wire rope shall be restricted to 33* percent *of its breaking load at all times*". Conversely, no European country has yet implemented specific winch-assist rules, although machine manufacturers have started to develop their own guidelines (Visser and Stampfer 2015).
At international level, the *International Standards Organization* (ISO) is currently developing a new version of the ISO 19472 (*Machinery for Forestry. Winches - Dimensions, performance and safety - Part 2: Tethering and Tractions Assistance Winches*), still not published, including and regulating the winch-assist functions (ISO 2018).

According to the multi-criteria decision model developed by Kühmaier and Stampfer (2010), the broader potentiality of the winch-assist systems might be attributed to higher system productivity and limited set-up times; higher contribution margin because of lower harvesting costs; greater working safety as a result of fully mechanized harvesting system; fewer impacts on the remaining stand because of a more careful extraction process; lower greenhouse gas emissions. On the other hand, the use of ground-based harvesting systems on steep terrain could increase the impact on the soil due to the high bearing pressure of heavy machines and reduce the number of employees needed for harvesting the same timber volume.

The winch-assist systems have huge potentials for improving the machine mobility, as well as for increasing the efficiency (Evanson and Amishev 2010; Dyson and Boswell 2016) and the profitability of steep slope forest operations (Holzfeind et al. 2018). This system allows to extend the safe operative range of ground-based machine onto steep grounds while reducing soil disturbance from slippage (Visser and Stampfer 2015). As shown in the previous paragraph, however, the slope is not the only limiting factor, and fully mechanized ground-based systems - being limited by the soil strength and/or roughness (Amishev et al. 2009) – are still limited to trafficable terrain.

The winch-assist systems are quickly spreading in the main forest industries around the world. As example, in New Zealand in 2006 there were not more than six machines and currently there are more than 50 of them (Visser 2016). Similarly, first machine in British Columbia was introduce no more than six years ago and today there are more than 40 machines (Amishev 2016). In both countries, the primary driving forces in the promotion of the system were the necessity to reduce the risk during tree hand-felling and the needed to find an efficient solution to exploit stands in steep grounds. No information about the distribution of the winch-assist machines in Central Europe were found.

The rapid growth of this harvesting system is a great success in innovating steep slope harvesting operations, but it also presents inherent risks as there are challenges in adapting off-shore technology to the varied geography. Industry, operators, and contractors still face knowledge gaps in engineering and are not yet fully familiar with safe operating procedures.

1.4. SAFETY CONCERNS IN STEEP SLOPE HARVESTING SYSTEMS

Forest harvesting operations are one of the most hazardous activities worldwide (Klun and Medved 2007). A crucial dimension of the social aspects of sustainable forest operations is the impact of forest work on the safety and health of the operators (Heinimann 2004, 2007; Marchi et al. 2018a). Operating in mountainous conditions, thus typically on steep grounds, require the use of specific harvesting solutions as the cable-based harvesting systems or the winch-assist systems. Both these cable-supported systems, as defined by Marchi et al. (2018b), even if conceptually different, have similar safety issues related to the presence of tensioned wire ropes and natural anchors, such as stumps or trees (Figure 1.13).

Tensioned cables and anchors represent the basic element for effectively operate in steep stands with the specialized equipment. Their failures represent serious safety concerns for the operators and the forest industry as a whole. Anchor and cable failures could lead to tower collapses or overturning in the cable yarding (Hartsough 1993; Fraser 1996; Fraser and Bennett 1996), while the cables, the anchors or the supports could fatally hurt the operators. In case of winch-assist systems, forestry machines should be able to stop in full control at all times without reliance on the cable, but field evidences show that consequences in case of anchor or rope failure could be serious (BC Forest Safety Council 2017).

Anchor stability

Natural anchors are the most common anchoring solutions for the cable yarders and integrated-winch machines. The use of existing green trees or stumps available in the working site rather than providing artificial and usually more work-demanding solutions like pickets and anchors buried in the earth, is normally the more economical solution (Studier and Binkley 1974). However, both Cavalli (2012) and Marchi et al. (2018b) highlighted a critical lack of research regarding the behavior of trees and stumps used as anchors in steep slope forest operations.

Reference data used for the estimation of tree resistance for anchoring purposes is mainly derived from the empirical work of Pestal (1961), who defined the tree strength directly proportional to the tree diameter squared. Further stability tests were applied to different tree species, mainly to evaluate the reliability of mechanistic models that predict the

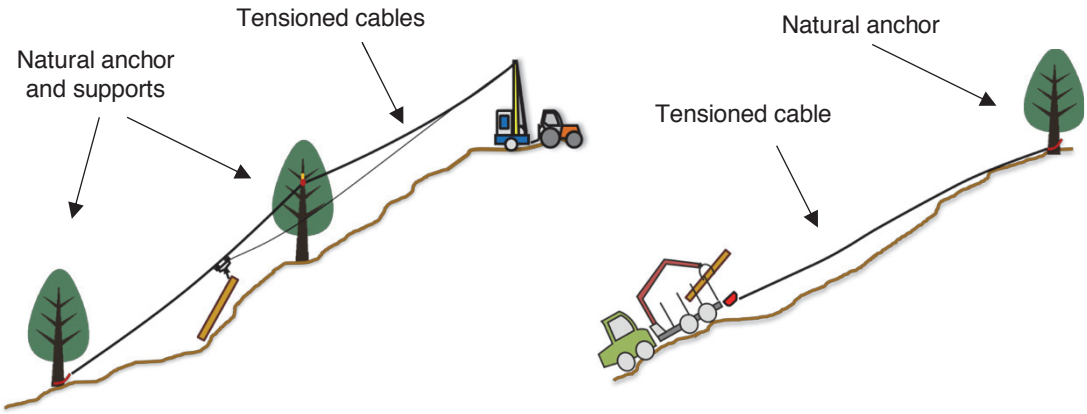

Figure 1.13: Main safety risk elements in cable-supported steep slope wood extraction

effects of wind forces. Part of these studies (Fraser 1962; Fraser and Gardiner 1967; Coutts 1983; Peltola et al. 2000; Nicoll et al. 2005) might be correlated to the analyses of anchoring systems in cable-supported forest operations. However, these works focused on the behavior of small diameter trees, not suitable as anchors in forest harvesting operations.

The size of a tree influences the magnitude of the forces and the modes of failure (James et al. 2013), and there is a lack of information regarding pulling tests of trees with relatively large diameters. Only Papesch et al. (1997); Moore (2000); Moore and Gardiner (2001) - testing radiata pine (*Pinus radiata*) and Douglas-fir (*Pseudotsuga menziesii*) in New Zealand; Lundström et al. (2007a, b) - testing Norway spruce (*Picea abies*), silver fir (*Abies alba*) and Scots pine (*Pinus sylvestris*) in Switzerland; Byrne and Mitchell (2007) - testing western hemlock (*Tsuga heterophylla*) and western cedar (*Thuja plicata*) in British Columbia, analyzed larger tree diameters.

The literature for stump bearing capacity is even more limited due to the absence of leverage effects, typically used in tree pulling tests, which increases the difficulties in this kind of analyses. Toupin et al. (1985) investigated the load transmission in multiple anchors, identifying that less than 50% of the load is transferred to the second stump. Biller and Baumgras (1987) tested small-diameter stumps, while Pyles and Stoupa (1987) and Pyles et al. (1991) tested several stumps of second-growth Douglas-fir and western hemlock for studying their load carrying capacity for cable logging applications. The data were used for developing a load-slip hyperbolic function to predict the load for a given stump

displacement based on the diameter. More consistent research works were carried out in New Zealand, where Smith and McMahon (1995) tested several large stumps of radiata pine, with diameters up to 72 cm. To date, however, there is still a considerable lack of knowledge regarding the resistance of medium-large trees and stumps used as anchors, as well as in regarding its interaction with cyclic loads (O'Sullivan and Ritchie 1993).

Cable tensile forces

Another primary concern for both the cable-supported harvesting systems is the excessive cable tensile force, which is the main reason for broken supports, anchor trees, and cables (Tsioras et al. 2011). The deep understanding and knowledge of the effective cable tensile force in forestry operations is fundamental for safety reasons. Ensuring rope tensile force remain within safe limits not only reduces rope breakage but reducing excessive stress on the rope breakage will maintain wire rope integrity and improve rope life (Scion 2009).

The engineering limits of a wire rope include the elastic limit and the endurance limit (Ackerman et al. 2017). The *elastic limit* represents the limit up to which there is a permanent deformation when the rope is unloaded. For commonly used wire rope, this limit is at 60-65% of the *minimum breaking load* (MBL) of the cable. The *endurance limit* is a limit, demonstrated through tests, lower than the elastic limit, with a greater important in the life of a wire rope and, consequently, also in the safety assessment. This limit is approximately the 50% of the MBL (Wenger 1984). If a wire rope is repeated pulls and jerks greater than the endurance limit, the life of the wire rope is comparatively short, and it will finally break, even though it has never been strained to its breaking strength nor its elastic limit.

A third operational cable working load limit, named *safe working load* (SWL), is applied in industrial cable applications. This limit is calculated as ratio between the MBL and a safety factor. The SWL represent the recommended maximum cable working load. The inclusion of a safety factor in static load calculations is a prudential approach for considering the dynamic forces, which are mostly unknow.

In cable logging, the SWL normally refers to a safety factor of three. The draft version of the EN 16517 (*Agricultural and forestry machinery - Mobile yarders for timber logging - Safety*), however, suggest a safety factor of 2.5 for cable yarders with an effective load limiter during the operations (CEN 2017). The proposal version of the ISO 19472-2 (ISO 2018) for winch-assist operations considers a safety factor of two (Holzleitner et al. 2018).

1.4.1. SKYLINE TENSILE FORCES IN CABLE YARDING OPERATIONS

The cable yarders in standing skyline configuration use several wire ropes. The skyline, the mainline, and the guylines are the basic fundamental cables for yarding the logs. For downhill wood extraction it is normally used also a haul-back line. A strawline could be used for pulling the other lines during the set-up. Moreover, some technical solutions include an auxiliary line for slack pulling the mainline. The skyline, however, is the primary line in the cable structure. It is the most stressed - with the highest tensile forces - and potentially more dangerous cable in case of failure. For this reason, most of the research works and attention focused on the analysis of its behavior during the logging operations.

In Central Europe, the payload and skyline pretension calculations, representing the main aspect in the cable layout design of standing skyline configurations (Fabiano et al. 2011), are generally based on the empirical approach prosed by Pestal (1961). Further models for optimizing the cable layout have been proposed after the Pestal formulation (Falk 1981; Jarmer and Sessions 1992; Charland et al. 1994; Chung and Sessions 2003; Bont and Heinimann 2012; Dupire et al. 2015), but little effort has been done on inclusion of dynamic amplifications (Womack 1989; Womack et al. 1994; Knobloch and Bont 2018). The calculations, thus, are still based on static assumptions. Missing information on the dynamic amplifications does not allow to predict the real skyline tensile forces properly (Spinelli et al. 2017).

Only a few researchers focused on field measurement of skyline tensile forces and just a small minority of them analyzed the dynamic amplifications. These studies include observations on scaled or experimental sites and, more limitedly, ordinary forest yards. Preliminary works based on electronic measurement of cable tensile forces, representing the only solution for medium-high frequency recording (Visser 1998), started in the late 70's and 80' and were initially limited to guylines (Binkley et al. 1978), mainlines, and chokers (Henshaw 1977; Falk 1980; Peters and Biller 1984). Later, Pertlik (1992) extended the monitoring to the skyline through the development of a dedicated bending system, tested on two mobile tower yarders and a self-propelled carriage-based cable yarder. These measurements showed preliminary results on skyline dynamic oscillations, measured as the difference between one record to the next one, recording with a frequency of 2 Hz. Another remote tensile force monitor system, developed by the *Logging Industries Research*

Organization -LIRO (Smith 1992), was tested by Hartsough (1993) on 14 cable yarders operating in New Zealand. The aim of these tests was to demonstrate the potential benefits, in terms of safety and productivity, of continuous tensile force monitoring.

A first consistent work on skyline tensile force dynamic analysis was conducted by Pyles et al. (1994). The authors applied several dynamic tests to a short experimental single span cable line for identifying natural frequency, damping, and dynamic amplifications of skyline, guylines, and tail spar. In the same year, these authors (Womack et al. 1994) published the simplified model cited in the previous paragraphs for determining the fluctuations in tensile force of a skyline that hangs up and subsequently breaks out and validated the model through five tests in a short single span configuration. A few years later, Visser (1998) developed and tested a continuous skyline tensile force monitoring system based on the measurement of the strain in the sheave mounting plates at the top of the yarder's tower. During the tool trial, the author collected data on skyline tensile forces on a small and a medium-size cable yarder operating in Austria. The first one was monitored during non-forestry applications, the second one was monitored while operating in three different harvesting sites. Both uphill and downhill-oriented cable lines, as well as cut-to-length and tree length harvesting methods, were considered. This work included brief information on dynamic amplifications in cable yarding, expressed in terms of tensile force oscillation magnitude during inhaul.

Further skyline tensile force monitoring are reported by Fabiano et al. (2002, 2011), who summarized a decade of investigations carried out in Italy and published between the 1989 and 1997. The authors proposed several multiple regression analyses for peak tensile force calculations. Most of their results derived by scaled lines (13 cable lines in single and multi-span configurations) and experimental sites (40 mobile tower yarders cable lines in single span uphill-oriented configuration). Also, results included sixteen cable lines operating with traditional cable yarders (sledge yarders) in ordinary harvesting sites, both in single and multi-span configurations. More recently, Harrill and Visser (2013) investigated the dynamic forces in a scaled cable logging system. The aim was to quantify and compare the peak skyline tensile forces between three different rigging configurations by simulating common situations that are known to cause shock loading, throughout drop tests, impact tests, and bridling tests.

Other skyline tensile force data are reported by Dupire et al. (2015) and Leshchinsky et al. (2016). Dupire et al. (2015) showed the static tests used for validating the assumptions of the proposed predicting model for the skyline tensile force and cable profiles at different loads. The tests interested seven single span and three multi-span experimental lines. Also, 30 static measurements of load path and skyline tensile force were collected on a mobile tower yarder in single span uphill-oriented configuration. Leshchinsky et al. (2016) reported field measurements of skyline tensile forces while presenting their design approach for mobile anchors in cable logging.

Recent field measurements on ordinary harvesting sites, specifically conducted with the aim of analyzing the skyline peak tensile forces and dynamic behaviors in cable logging operations, are shown by Harrill and Visser (2016) and Spinelli et al. (2017). Harrill and Visser (2016) compared different New Zealand rigging configurations, monitoring 259 work cycles of 12 large mobile tower yarders operating on 16 different profiles. Spinelli et al. (2017) monitored the skyline tensile forces in 83 work cycles of a large European mobile tower yarder operating, under controlled environment at the same pre-defined stops, with two different carriage types in a short uphill-oriented single span configuration. Harrill and Visser (2017) also analyzed the dynamic amplifications in cable logging, but they monitored the choker tensile forces - recording 60 work cycles in two different cable logging operations in New Zealand – and not the skyline ones.

The literature accounts several research works reporting skyline tensile force data in cable yarding. However, there is still clear evidence of broad gaps of knowledge and missing information on the skyline tensile force behaviors during ordinary forest harvesting operations, in terms of both peak tensile forces and dynamic amplifications.

1.4.2. Cable tensile forces in winch-assist operations

In the winch-assist harvesting systems one or two cable lines support the machine movements on steep ground. Even if a scientific and anecdotal evidence provided for increased knowledge and understanding (Sessions et al. 2017), there is still a limited quantitative framework with which to evaluate the relationship between cable tensile force, stability, ground pressures, and slip, especially in terms of site operative conditions and machine

specifications. Moreover, there are currently no high-resolution onboard information systems installed to provide detailed information about the actual tensile force on the cable/s (Amishev 2016) and the research works analyzing the cable tensile force behavior in this system are extremely limited.

Recently, Holzleitner et al. (2018) developed a scientific approach with a robust workflow for in-depth monitoring and analysis of cable tensile force for harvesters and forwarders equipped with integrated-winch . The authors tested the methodology and presented results from a short-term study of tensile forces of harvester and forwarder operations in Central Europe. In terms of anchor-based systems, only one technical note from the *Future Forest Research Limited* (Visser 2013) and one from the *FPInnovations* (Amishev et al. 2017) reported some brief examples of tensile forces measurements, analyzing winch-assist operations on large feller-directors in New Zealand and British Columbia, respectively. There is no evidence of any other publication on actual tensile force on winch-assist systems, excluding test reports on different machines drew up by the German *Kuratorium für Waldarbeit und Forsttechnik e.V.* (KWF), as for example the tests conducted by Weise and Burk (2011, 2016) and Debnar (2014).

While it is relatively easy to calculate the static forces applied to the cables, in both the cable-based and the winch-assist harvesting system, the assessment of dynamic forces and shock loadings is still challenging due to the many factors at play and the difficulty to reflect them in theoretical models (Visser 2013; Spinelli et al. 2017).

1.5. Aim and Objectives

This study focuses on the analysis of the cable tensile forces on both the cable-based and the winch-assist systems, recognized as one of the primary elements for the risk assessment in steep slope forest operations, and thus a base criterion for compliance with the sustainable forest operations criteria. The research, in particular, aims to reduce the gap of knowledge on the cable tensile forces in steep slope forest operations, analyzing the operational conditions and tensile forces behavior during ordinary harvesting sites. The objectives of the work include:

- to analyze the cable (skyline) tensile forces of **mobile tower yarders in standing skyline configuration** operating in ordinary harvesting sites, and in particular:
    - to quantify the frequency with which the cable safe working load is exceeded;
    - to determine the peak tensile forces for each cycle elements, identifying the most critical aspects;
    - to investigate the tensile force dynamic amplifications.

- to analyze the cable tensile forces of **integrated-winch forwarders** operating in ordinary harvesting sites, and in particular:
    - to quantify the frequency with which the cable safe working load is exceeded;
    - to determine the peak tensile forces for each cycle elements, identifying the most critical aspects;
    - to investigate the shock loads in tensile force behavior.

2. METHODOLOGY

The analysis of the cable tensile forces in steep slope forest operations was based on a similar approach for both the analyzed cable-supported harvesting systems (cable-based and winch-assist system). The tensile force monitoring was integrated with the video recording for the time and motion study of the logging operations; the monitoring of the carriage/machine positions and movements; the measurement of the yarded loads; the analysis of the ground profile of the trail where the machines were operating.
The processing of the data collected in the ordinary harvesting sites provided the frequency in exceeding the safe working limits. Also, dynamic amplifications, shock loads, and main variables influencing the cable tensile force behavior were analyzed.

2.1. GENERAL APPROACH AND TOOLS

The tools and procedures used for the cable tensile force monitoring, the video recording, and the machine movements monitoring are described in the Chapters 2.1.1 and 2.1.2. They were the same for both the harvesting systems. Different approaches, instead, were used for load measurement and marking of the structural element measurements (as shown in Chapter 2.2.1 and 2.2.2), because of different conditions and available tools and resources.

2.1.1. CABLE TENSILE FORCE MONITORING SYSTEM

Cable tensile force measurement methods in harvesting operations account several options, well summarized and explained by Visser (1998). Lots of these methods, however, are not technically usable for the continuous high-frequency monitoring of the cable tensile force, as request by the aim of this research work (e.g., the cable vibration and cable deflection methods; the use of strain gauges onto the wire ropes; the use of mechanical dynamometers; etc.). Other solutions are potentially more applicable but have difficulties in easily access the data. The drum oil pressure approach, for example, is largely used on several technological solutions and by lots of machine manufacturers for both cable logging and winch-assist systems. This method is based on the principle of measuring the force exerted on the cable knowing the moment generated by the drum and the moment arm. The moment generated by the drum can be measured using a hydraulic pressure gauge considering the drums specifications. The amount of cable on the drum must be considered because of its direct influence on the moment arm. For this reason, this system is normally used for indirectly measuring the skyline pretension on mobile tower yarders, positioning the skyline in the tensioning compartment of the drum. Also, it is used in the winch-assist systems based on capstan unit, where the pulling drum is separated by the storage drum. This approach, however, does not allow an easily monitoring and recording of the cable tensile forces.

The only methods practically usable for accurate continuous high-frequency cable tensile force monitoring and recording are based on the use of electronic load cells which convert the forces into electrical signals. Two main systems of electronic load cells are available for the tensile force monitoring: the in-line systems and the clamped-on systems. The *in-line systems* are probably the most accurate system available for measuring the cable tensile forces since no bending forces need to be taken into consideration. The sensors have to be located in a broken rope. Operatively, this mean that the sensor has to be located between the end of the rope and the anchor connection. The older types of these sensor used springs or hydraulic ram mechanisms. The modern types are accurate electronic load cells which use internal strain gauge technology, lots of them available with wireless connection and dedicated App for mobile electronic devices. The inconvenience in using this kind of sensors is that they could represent a weak link in the machine connection to the anchor,

which also include a taking responsibility for the researcher who is monitoring the system. Moreover, they cannot be applied on the cable when the machines are operating, and they have to be installed during the set-up of the harvesting system.

The *clamped-on sensors* are normally based on externally mounted load cell positioned in the central of three hardened steel skids. This kind of sensors allow the quick installation on pretensioned cables without linking the cable systems and without any interruption of the work flow. Potentially they can be located in any point of the cable line. For this reason, a clamped-on sensor was selected for monitoring the cable tensile forces in this research.

The selected sensor was a clamped-on *CableBull® SR22/800 XR* tensiometer (Figure 2.1), manufactured by the German *Honigmann Industrielle Elektronik GmbH.* The same sensor was already successfully used in tensile force monitoring of winch-assist forestry machines operating on steep ground by Holzleitner et al. (2018).

A compensator enables measurement on wire ropes with diameter ranging from 14 to 22 mm. The resolution is 0.0127 kN and the rated load capacity is 200 kN, with tolerance on measuring higher loads -up to 300 kN - without damages. Data were recorded using the dedicated *HCC-Easy* software (version 6.02.23) installed on a field laptop and connected to the sensor through an analogical-digital converter unit. The recording frequency could be set in 100, 200, 1000, and 2000 Hz. The connections, reinforced and isolated for protection against the elements and hard contact with the ground, allow the position of the laptop at 5 m far from the measuring sensor. An external laptop power bank was used to guarantee the full-day registration.

Figure 2.1: CableBull SR22/800XR tensiometer and recording set-up

2.1.2. MACHINE CONTROL UNIT

A preliminary development of a *machine control unit* started in 2015, in collaboration with Dr. Marek Pierzkala from the *Norwegian Institute on Bioeconomy Research* (NIBIO), through the integration of an *inertial measurement unit* (IMU), a GNSS sensor, and two action cameras. This monitoring system was tested on a long-distance cable system based on the use of a sledge yarder and a motorized carriage (Figure 2.2). Next, these sensors and instrument were integrated on a wood panel - laminated with an aluminum foil - equipped with five magnets and vibration dampers for a quick installation on the machines. Finally, a new version of machine control unit, based on an action camera joined with a GNSS sensor integrated and synchronized with an inertial measurement unit on a single board microcontroller *Arduino*® (following named "GNSS-IMU sensor"), was developed. The *GNSS-IMU sensor* is able to collect data in terms of speed, position, tilt and roll inclinations at a registration frequency of 5 Hz. It was specifically developed and assembled for supporting the time study and the machine movements monitoring in forest operations. The performances of this sensor were tested on both a scaled environment and in ordinary harvesting sites in collaboration with Dr. Alessandro Lezier, as part of his Master thesis discussed in late 2016 (Lezier 2016).

Figure 2.2: Preliminary version of machine control unit

The main components of the GNSS-IMU sensor are:

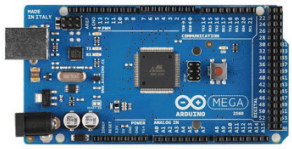

Electronic board Arduino MEGA 2560

This electronic board is based on a microcontroller AT-mega2560 with 54 pins for digital input and output and 16 pins for analogical input. It has both a USB connection and a power source connection on the left side.

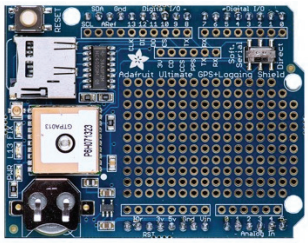

GNSS sensor Adafruit Ultimate GPS Logger Shield

This electronic board integrates the GPS MTK3329 module with a microSD reader, achieving also the function of data-logger. The position is provided in the standard NMEA 0138 with a frequency of 10 Hz. Also, it provides the clock time, the date, and the number of connected satellites. This sensor has and integrated antenna and a *SubMiniature A-version* connector (SMA) for external antennas

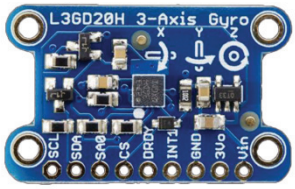

Gyroscope Adafruit L3GD20H

This sensor provides the rate of variation of the inclination over time, i.e. the angular velocity measured in degrees per second. The inclination is calculated as integral of the angular velocity. This sensor can be set to three measure scales with sensibility of 250; 500; 2000 degrees per second.

Accelerometer Adafruit LIS3DH

This sensor measures the acceleration over the three axes (x, y, z), that is a variation of speed over time. Through the application of trigonometric functions is possible to calculate the inclination. The sensor has a resolution of 2; 4; 8; 16 g and a recording frequency of one or 5 Hz.

The integration of the gyroscope and the accelerometer are the base component of an inertial measurement unit, which represent the best solution to optimize the accuracy of the angular position measurements. The gyroscope provides the most accurate inclination value. However, the calculation of the inclination based on the gyroscope needs the solution of a continue integral of the angular velocity. This is not possible, and an approximation based on the sum of a finite sample measured at a constant time is required. This led to drift errors when the sample recording frequency is lower than the frequency with which the data provided by the sensor change. The error continuously increases during the time and the gyroscope inclination data is usable only for short periods.

The use of accelerometers for tilt applications, instead, is subject and disturbed by the external forces which move the measured object even if without any rotation. Thus, the inclination values derived for this sensor are accurate in the long time, but they have to be cleaned by the noise throughout the application of filters. The combination of the gyroscope and accelerometer data was achieved through the application of a filter favoring the data provided by the gyroscope, set to a sample recording frequency of 100 Hz, in the short time, and the inclinations data provided by the accelerometer in the long time. The used filter formula was:

$$Incl = 0.9(Incl + gyr\_data * dt) + 0.1(acc\_data) \quad [1]$$

Where *Incl* represent the tilt or roll angle, expressed as degrees; *gyr_data* the data input from the gyroscope sensor; *acc_data* the input information from the accelerometer.

The full set of electronic boards and sensors, a control panel, and a power supply able to guarantee more than 30 hours of recording, were installed in a plastic box with dimension of 20x15x8 cm. The box was modified and equipped with a front water-proof door for access to the control panel and check of the different notification led. The box was painted with high visibility orange color and covered with reflective bands for targeting with laser rangefinders, if required. On the upper section of the box was installed a SMA connector for mounting external GNSS antennas, improving the position data quality. On the right side of the box was created an opening to easily access to the microSD memory card.

The control panel hosts four switches, five notification led, and a plug-in system for recharge the battery. The four switches functions include power, recording, axis inversion

(for vertical or horizontal applications), and instant position recording. The notifications led provide information in terms of energy supply, GNSS data quality (considering the number of connected satellites), active recording, and evidence of problems. Two aluminum bars equipped with four magnetics and a Velcro were used to fix the tools on the monitored machines. A dedicated software developed in C++ language was loaded in the electronic board for recording the whole set of data.

The action camera coupled with the GNSS-IMU sensor was with a *Drift Ghost 1080* equipped with a 20.000 mAh power bank and a 64 GB microSD memory card for full-day registration purpose (Figure 2.3). This camera had the aim to record the whole logging operation for the further time and motion study, as well as for identifying eventual shock events. Video recording for backup and time study have already been used in several previous works on productivity analyses (Inoue and Kobayashi 1996; Amishev and Evanson 2010; Strandgard et al. 2014; Holzfeind et al. 2018). The camera was set to record videos at 720 ppm at 30 frames per second. This combination was considered a good compromise between data quality and memory usage. The setting, as well as the shot control and the start/stop function of the camera were activated throughout the dedicated App installed on a field tablet.

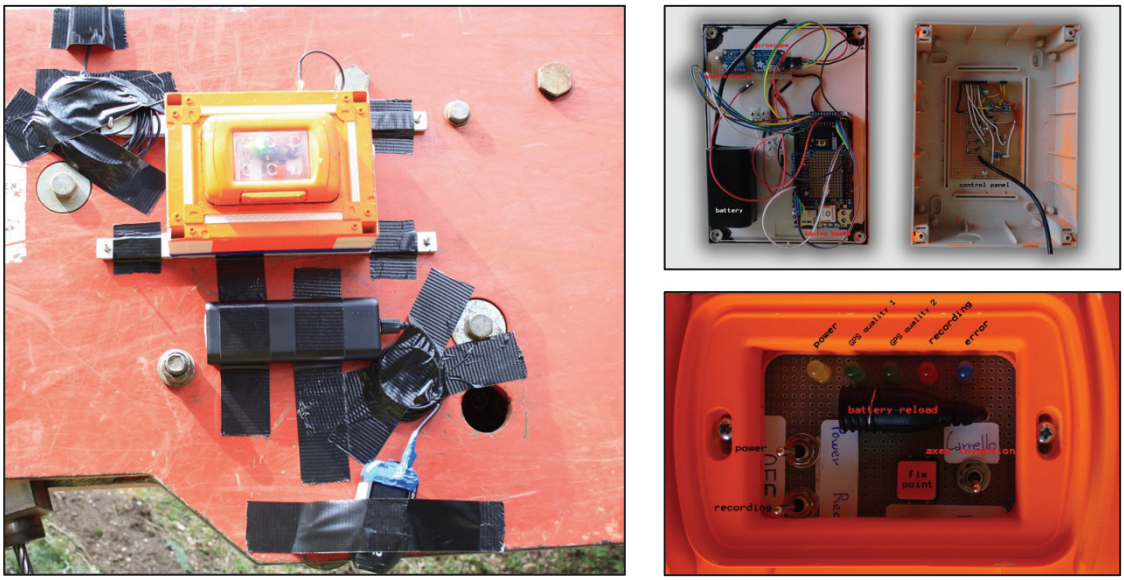

Figure 2.3: Machine control unit. On the left side the unit installed on a carriage; on the right side details of the GNSS-IMU sensor control paned and internal connections

2.2. STUDY SITES AND MACHINES DESCRIPTION

The cable tensile force analysis of steep slope forest operations was applied in two different forestry contexts. The cable-based harvesting system was analyzed in the Central-Eastern Italian Alps, where the mobile tower yarders of interest in the present study are largely widespread. The winch-assist system was analyzed in British Columbia (Canada), representing one of the biggest forest industries worldwide (annually cutting more than 65 million m^3 of wood), and where there are more than 40 machines actively operating on large scale. Winch-assist machines are well distributed also in Central Europe (Austria, Switzerland, Germany, and more limitedly in France), but their presence in Italy is currently limited to just one low-utilized machine, for what is in the knowledge of the author research team. The detailed analysis of logging operation requires the active collaborations of the logging companies operating the machines. While no collaborations were found in the European context, the *FPInnovations*, a non-for-profit research institution from British Columbia (Canada), provided its active collaboration to monitor the winch-assist harvesting system.

2.2.1. CABLE-BASED HARVESTING SYSTEMS CASE STUDIES

The monitoring of the cable-based harvesting system was conducted during the spring and summer 2017 in the Central-Eastern Italian Alps, covering three Italian regions: Lombardy, Trentino-Alto Adige, and Friuli-Venezia Giulia (Figure 2.4). Data were collected on eleven different cable yarders, owned by ten logging companies and operating on twelve different profiles. The study included both single span and multi-span cable lines, oriented for uphill and downhill yarding. Single and multi-span configurations were categorized considering spans longer than 30 m and excluding spans next to the tail spar. Depending on the base vehicle equipment, the study considered tractor, trailer, and truck-mounted European designed mobile tower yarders. Also, a self-propelled tower yarder with a track undercarriage (subsequently named “track-based tower yarder”) was monitored. Most of the carriages (nine out of eleven) used in combination with these yarders were automatic clamped carriages. Also, a motorized carriage with an independent drop line and a self-propelled

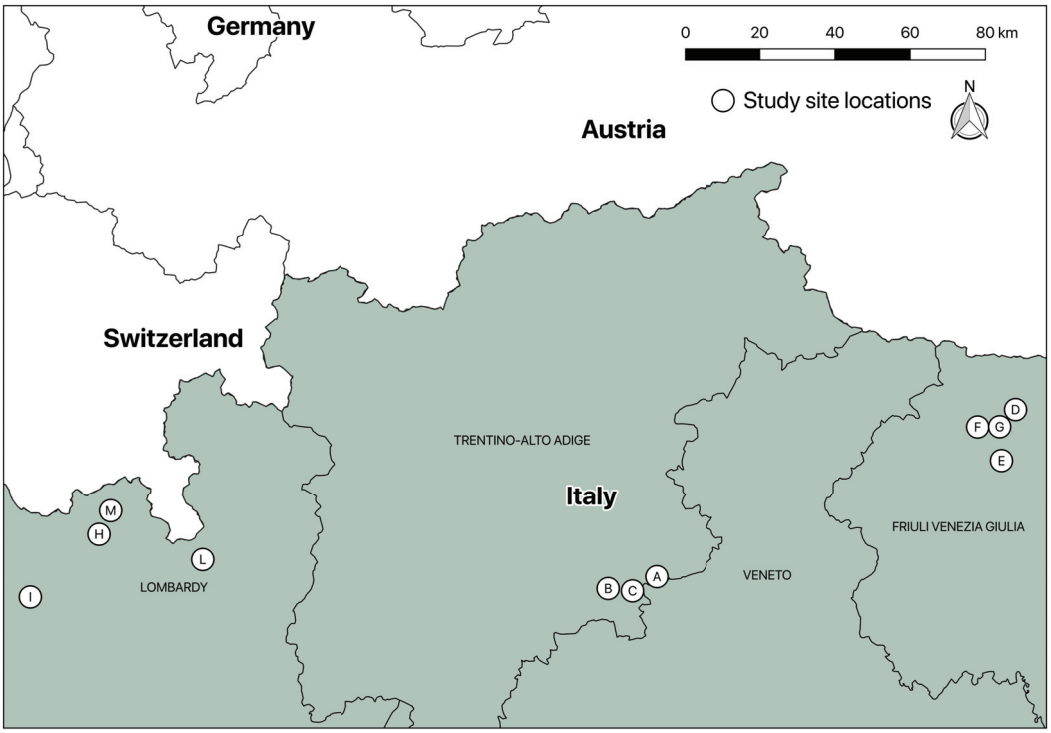

Figure 2.4: Locations of the cable-based harvesting system study sites

carriage were considered. Details on tower yarders, carriages, and skylines are shown in Table 2.2 and Table 2.3, related to the two-lines (skyline and mainline) and the three-lines (skyline, mainline, haul-back line) cable yarding systems, respectively.

All the logging contractors included in this study were experienced cable loggers (more than 15 years of experience in cable logging). The team of operators employed in the operations had different experience levels and ages. However, low-experienced operators were always assisted by expert operators. The operations considered Norway spruce (*Picea abies*) dominated plantations and semi-natural mixed stands of spruce, beech (*Fagus sylvatica*), silver fir (*Abies alba*), larch (*Larix decidua*), and Scots pine (*Pinus sylvestris*). The harvesting treatments included both clear-cuts and partial retention cuts (selective cuts, patch-cuts, shelter wood). All the harvesting sites adopted the whole-tree method for most of the monitored cycles, integrating partial processing when there were troubles in rotating the stems parallel to the skylines (in downhill cable yarding) or in case of too large loads. Details on stand characteristics and forest operations on each harvesting site are reported in Table 2.1. A detailed description of the study sites is reported in the Annex 3.

Table 2.1: Timber cruise data of the cable-based study sites

Parameter	Unit	Site A	Site B	Site C	Site D	Site E	Site F	Site G	Site H	Site I	Site L	Site M
Harvested area	ha	5.0	1.5	2.0	21.7	17.6	0.6	2.2	20.2	10	3.3	2.8
Treatment[1]	-	P	P	C	SH	SH	P	SE	P	P	P	P
Harvested volume	m^3	465	152	1072	2624	1111	54	197	2100	1028	457	279
Harvested density	$m^3\ ha^{-1}$	93	101	536	121	63	84	90	104	103	138	100
Mean tree volume	m^3	2.41	2.11	0.80	2.22	0.93	0.84	1.17	1.72	2.11	1.66	1.11
Species composition by volume												
Norway spruce	%	43	95	87	82	25	94	46	64	68	66	44
silver fir	%	57	-	-	15	-	-	-	-	25	-	-
beech	%	-	-	-	3	75	6	52	-	7	-	-
larch	%	-	-	13	-	-	-	-	36	-	34	28
Scotch pine	%	-	5	-	-	-	-	2	-	-	-	28

Notes: [1] Treatment: P=Patch-cut; C= Clearcut; SH=Shelter wood; SE= Selective

Table 2.2: Two-lines cable yarding systems

Cable yarding system		1A	2A	3A	4A	5A	6A
Tower yarders	**Unit**	**Valentini V400/2T**	**Valentini V400/2T**	**Greif. TG700**	**Valentini V600/M/2/ 1000**	**Greif. TG860**	**Konrad KMS12U**
Vehicle base	-	tractor	tractor	trailer (1 axe)	trailer (2 axes)	trailer (2 axes)	trailer (2 axes)
Engine power	kW	81[1]	81[1]	69	104	118	212
Tower height	m	10.0	10.0	9.0	12.5	9.0	11.0
Mass	kg	3200	3600	6500	10800	12000	13700
Carriages	**Unit**	**Koller HSK2002**	**Hochleit. BW3000**	**Greif. CRG15**	**Konrad Woodliner 3000**	**Greif. HT30**	**Konrad Liftliner 4000**
Type	-	ACC gravity	ACC gravity	ACC gravity	Self-propelled	ACC hydraulic	Motorized
Mass	Kg	220	200	145	1170	290	950
Max payload	kN	20	30	15	27.5	32	40
Skylines	**Unit**	**6x31WS FC**	**6x26WS IWRC (C+S)**	**6x19S FC**	**8x26WS IWRC (C+S)**	**6x26WS IWRC (C+S)**	**8x26WS IWRC (C+S)**
Nom. diam.	mm	20	16	20	22	22	22
Grade	$N\ mm^{-2}$	1770	1960	1770	1960	1960	1960
Mass	$kg\ m^{-1}$	1.42	1.14	1.44	2.34	2.3	2.3
MBL	kN	234	201	234	451	485	469

Notes: [1] Engine power required at the Power-Take-Off of the tractor. Manufactures: Greif.= Greifenberg; Hochleit.=Hochleitner. Carriage type: ACC-gravity= Automatic clamped carriage working through gravity system; ACC-hydraulic= Automatic clamped carriage with active slack -pulling through hydraulic motor. Skyline technical features are described in Annex 2.

Table 2.3: Three-lines cable yarding systems

Cable yarding system		1B	2B	3B	4B	5B
Tower yarders	**Unit**	**Valentini V600/M/3 850 spec.**	**Greifenberg TG T3**	**Valentini V600/M/3 1000**	**Valentini V600/M/3 1000/B10/R**	**Valentini V600/M/3 1000/LKW**
Vehicle base	-	trailer (2 axes)	trailer (2 axes)	trailer (2 axes)	track undercarriage	truck (2 axes)
Engine power	kW	104	149	134	177	104
Tower height	m	12.5	9.8	12.5	12.5	13.0
Mass	kg	12000	12180	12000	20000	26000
Carriages	**Unit**	**Hochleitner BW4000**	**Koller HUSK2002**	**Hochleitner BW4000**	**Hochleitner BW4000**	**Hochleitner BW4000**
Type	-	ACC - cable	ACC - cable	ACC - cable	ACC - cable	ACC - cable
Mass	kg	650	400	650	650	650
Max payload	kN	40	20	40	40	40
Skylines	**Unit**	**6x19S IWRC (C+S)**	**6x19F IWRC (C)**	**6x19S IWRC**	**6x19S IWRC (C)**	**6x19S IWRC (C)**
Nom. diam.	mm	22	22	22	22	22
Grade	N mm^{-2}	1960	1960	2160	1960	2160
Mass	kg m^{-1}	2.40	2.34	2.32	2.28	2.32
MBL	kN	425	431	435	448	435

Notes: Nom.diam.= nominal diameter. Carriage type: ACC - cable= Automatic clamped carriage with active slack-pulling through the haul-back line

The twelve cable lines were codified dividing single and multi-span configurations and progressively numbering them functionality to the cable system type and power. A summary of the machines involved in each cable line, as well as the contractor abbreviation and the other features of the harvesting sites are reported in Table 2.4.

Table 2.4: Summary information of machines and contractors per cable line

Cable line	Site[1]	Contractor[1]	Cable system[2]	Tower yarder type	Carriage type	Processor
S01	F	F3	2A	Tractor-based	ACC - gravity	No
S02	G	F4	3A	Trailer-based (1 axe)	ACC - gravity	No
S03	E	F2	2B	Trailer-based (2 axes)	ACC - cable	Yes
S04	C	T2	3B	Trailer-based (2 axes)	ACC - cable	Yes
S05	C	T2	5B	Truck-based	ACC - cable	Yes
S06	B	T2	5B	Truck-based	ACC - cable	No
M01	L	L3	1A	Tractor-based	ACC - gravity	No
M02	M	L4	4A	Trailer-based (2 axes)	Self-propelled	No
M03	I	L2	5A	Trailer-based (2 axes)	ACC - hydraulic	Yes
M04	H	L1	6A	Trailer-based (2 axes)	Motorized	No
M05	D	F1	1B	Trailer-based (2 axes)	ACC - cable	No
M06	A	T1	4B	Track-based	ACC - cable	Yes

Notes: Carriage type: ACC - gravity= gravity system; - hydraulic= active slack -pulling through hydraulic motor; - cable= active slack-pulling through haul-back line. [1] As described in the Annex 2; [2] As reported in Table 2.2 and Table 2.3

2.2.2. WINCH-ASSIST HARVESTING SYSTEMS CASE STUDIES

The monitoring of the winch-assist harvesting system was conducted in the fall of 2017, in conditions of snow and freezing temperatures, in three different harvesting blocks located in the interior of British Columbia (Canada), between Clearwater, Kamloops, and Prince George (Figure 2.5). The analysis focused on three John Deere 1910E eight wheels winch-assist forwarders (Table 2.5) - representing one of the largest winch-assist forwarders available on the market - owned by three different contractors.

The 21.8-ton forwarders have a maximum payload of 19 tons and are powered by a 186-kW engine. The cabs were self-levelling and rotated automatically following the tilt crane movements. A traction aid cable winch *Highgrade GEN2*, manufactured by the German *HAAS Maschinenbau GmbH*, was mounted on the rear frame of each forwarder. The capstan style winch has a drive drum which provides tensile force to the cable, separately from the storage drum.

The winch provides a consistent pulling power synchronized with the forwarder wheel rotation. The operator can adjust the tensile force to ten different settings ranging from zero

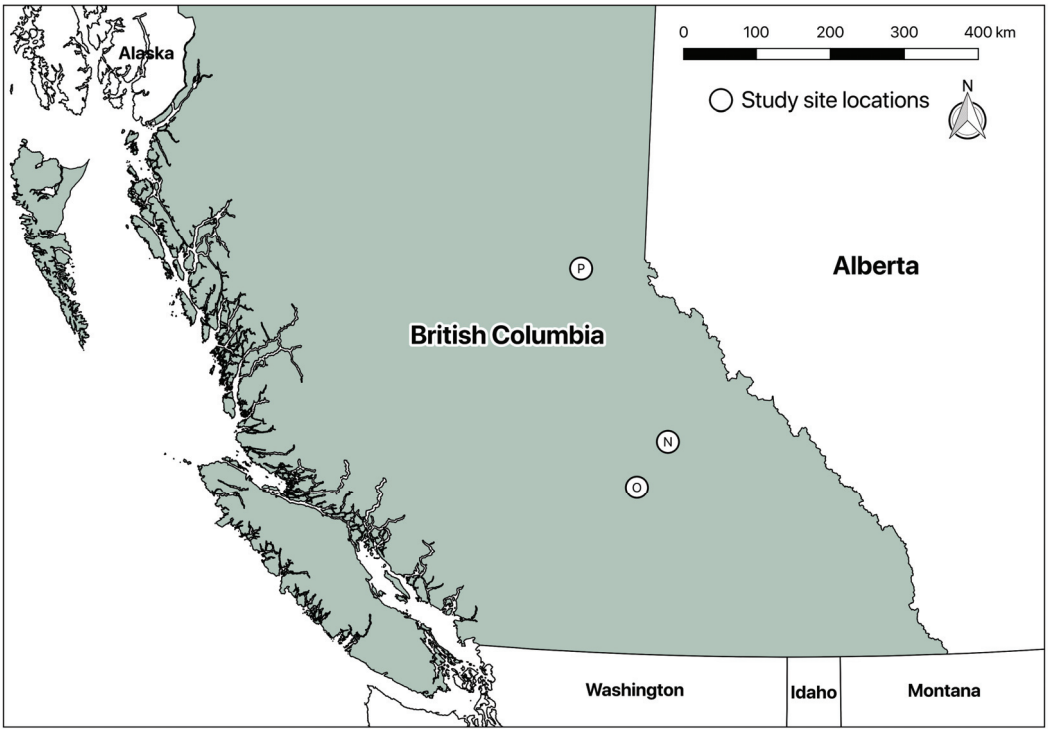

Figure 2.5: Locations of the winch-assist harvesting system study sites

Table 2.5: Technical features of the integrated-winch forwarders

Parameter	Unit	Measure
Forwarder John Deere 1910E		
Engine	-	John Deere 6090
Engine power	kW (rpm)	186 (1900)
Engine cylinders	n.	6
Engine displacement	cm^3	9000
Engine torque	Nm (rpm)	1090 (1400)
Fuel tank capacity	l	184
Transmission	-	hydrostatic-mechanical 2-speed gear box
Pump size	cm^3	180
Working pressure	bar	240
Max speed	km h^{-1}	7-21
Tractive force	kN	220
Wheels	n.	8
Wheel type	-	700/26.5-20
Cabin	-	rotating and leveling
Rotating angle	°	290
Tilt front/backward	°	10/6
Loading rating	ton	19
Length/width	mm/mm	10370/3120
Transport height	mm	3900
Mass	kg	21800
Ground clearance	mm	710

Parameter	Unit	Measure
Boom CF8		
Maximum reach	m	8.5
Gross lift torque	kNm	151
Gross slewing torque	kNm	41
Slewing angle	°	380
Tilt angle	°	-3/+26
Traction aid winch HAAS Highgrade GEN2		
Tensile force	kN	0-90
Mass	kg	1950
Max storing capacity	m	400
Cable diameter	mm	14
Cable MBL	kN	211
Cable speed	km h^{-1}	0-5

to 90 kN. Forwarder maximum speed is 6 km h^{-1} when winch-assist is active. The store drum holds 400 m of cable with a diameter of 14 mm and a MBL of 211 kN. The *Haas* winch has a radio control used while testing the anchors before the operation. Also, the it incorporates a radio controlled auxiliary strawline winch - with 300 m of 6-mm synthetic rope - for supporting the setup of the cable. The total weight of the winch, including the cable, is 1.9 tons.

All three harvested study sites were comprised of old-grow forests dominated by hybrid spruce (*Picea glauca var. albertiana*), subalpine fir (*Abies lasiocarpa*) and lodgepole pine (*Pinus contorta*), with varying stand characteristics. The study took place in ordinary harvesting operations where stands were clearcut using a combination of fully mechanized winch-assist and conventional ground-based operations. The winch-assist operations were limited to the steepest sections of the blocks, interesting between 57 to 70% of the areas (Table 2.6). All operators involved in the analysis were younger than 40 years old and had

Table 2.6: Timber cruise data of the winch-assist study sites

Parameter	Unit	Site N	Site O	Site P
Total harvested area	ha	50.2	17.1	116.2
Winch-assist harvested area	ha	29.0	9.7	81.0
Winch-assist harvested area	%	57.8	56.7	69.7
Harvesting treatment[1]	-	C	C	C
Harvested wood volume	m^3	18233	6988	42321
Harvested wood density	$m^3\ ha^{-1}$	364	409	374
Average tree volume	m^3	0.63	0.45	1.10
Average DBH[2]	cm	32.9	27.2	41.3
Stand density	stems ha^{-1}	577	909	340
Species composition by volume		–	–	–
Douglas-fir	%	–	7	–
hybrid spruce	%	63	10	68
lodgepole pine	%	–	50	–
subalpine fir	%	37	33	31
western hemlock	%	–	–	1

Notes: [1]Harvesting treatment: C= Clearcut; [2] DBH = diameter at breast height

at least two years' experience in winch-assist operations. A detailed description of the harvesting case studies is reported in Annex 4.

The trails were the forwarder operated were numbered progressively, following the chronological order of the monitoring. A summary of the machines involved in each trail, as well as the contractors, and the other features of the harvesting sites are reported in Table 2.7.

Table 2.7: Summary information of machines and contractors per trail

Trail	Site	Contractor	Harvesting machine	Harvester head	Harvester winch	Forwarder	Forwarder winch
CR01	N	BC1	JD 1470G	War. H290	HAAS sw	JD 1910E	HAAS sw
CR02	O	BC2	JD 1470G	War. H290	HAAS sw	JD 1910E	HAAS sw
CR03	P	BC3	Tig. 1185	Tig. 570	EF T-winch	JD 1910E	HAAS sw
CR04	P	BC3	Tig. 1185	Tig. 570	EF T-winch	JD 1910E	HAAS sw
CR05	P	BC3	Tig. 1185	Tig. 570	EF T-winch	JD 1910E	HAAS sw
CR06	P	BC3	Tig. 1185	Tig. 570	EF T-winch	JD 1910E	HAAS sw
CR07	P	BC3	Tig. 1185	Tig. 570	EF T-winch	JD 1910E	HAAS sw
CR08	P	BC3	Tig. 1185	Tig. 570	EF T-winch	JD 1910E	HAAS sw

Notes: JD= John Deere; Tig.=Tigercat; War.=Waratah; EF=EcoForst; sw=Highgrade Synchro-winch GEN 2

2.3. DATA COLLECTION

The protocol for the field studies followed the suggestions of the limited previously published papers, optimizing the procedures, the resolution, and the data quality when possible. The data collection was based on the installation of the cable tensile force monitoring system and the machine control unit on the carriages and forwarders operating in the different case studies (Figure 2.6). Also, further information on ground profile, machine technical features, yarded volume, and structural element position and features were collected. A preliminary daily synchronization of the laptop clock time was carried out through a web connection. Subsequently, the clock time of the action camera composing the machine control unit was set to the same clock time of the laptop. The action camera was then also used to record a video backup of the laptop clock time for the further double checked of the synchronization process.

The GNSS-IMU sensor was turned on at least 30 minutes before starting the recording to allow enough time to connect with a proper number of satellites. The machine control unit was then installed on the machines in collaboration with the operators employed in the logging operations at the beginning of the working day. Once the researchers were ready and positioned, the tensile force monitoring system was clamped on the pretensioned cables, waiting for that the system was temporally stopped.

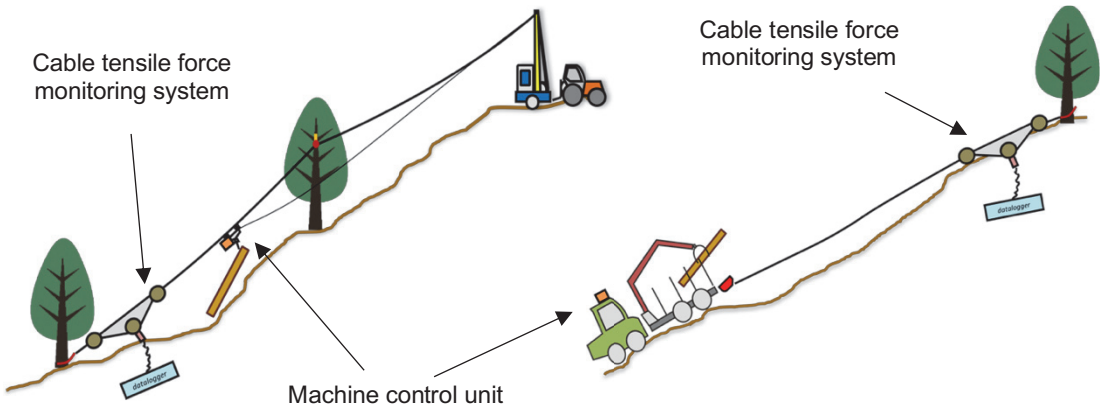

Figure 2.6: Schematic representation of the monitoring systems set-up

The system was able to record for the whole day and the researchers had just to periodically check the tensiometer, starting new recording sessions every two to four hours. When the logging operations – during the team breaks or at the end of the working day - the position of the main elements (e.g., tower yarder, tail spar, support, anchor, landing, road center line, access road, deviating stump, as applicable for the different systems, were marked. Also, specie, diameter, height, type of anchors and supports were noted.

2.3.1. Details on data collection of the cable-based harvesting system case studies

The data collection protocol for the cable tensile force monitoring of the cable-based harvesting systems was similar to the protocols successfully adopted by Harrill and Visser (2016) and Spinelli et al. (2017). The set-up of the machine control unit required the active collaboration of the logging companies which had to drop down the skyline at ground level to mount the GNSS-IMU sensor and the action camera on the carriages (Figure 2.7). These sensors continuously recorded the operations until the end of the working day when the skylines were dropped again to remove them. Each monitoring day accounted more than 30 GB of video.

The tensiometer, set for recording at 100 Hz, was positioned close to the tail anchor, at uphill or downhill position functionally to the yarding direction (Figure 2.7). The set-up of the cable tensile force monitoring system close to the anchor instead of in proximity of the tower yarder was selected because of safety and technical reasons. The anchors were normally out of the active logging areas and no machines were operating at close distance. Monitoring the tensile force at the anchor, thus, allowed a safer environment for the researcher who had to mount the system and periodically check its functionality.

The sensor was positioned as far as possible from the anchor (at a maximum distance of 5 m) and the researcher move out as soon as the sensor was set-up to reduce the risks in case of cable or anchor failure.

The load volume yarded during the cable tensile force monitoring was measured scaling every log of each cycle using a caliper and a meter tape. The diameter was taken at mid-length. Each log was also classified in term of specie and, similarly to what was done in

Figure 2.7: Sensors and tools mounted on a cable line. From the top left: cable tensile force monitoring system mounted on the skyline; CableBull tensiometer; Machine control unit mounted on a carriage; View of the Drift camera from the carriage

other studies (Spinelli et al. 2017), in terms of branch density (clean, low branching, average branching, heavy branching).

The position of each structural element, including tower yarders, anchors, tail spars, and intermediate supports, as well as the landing and access road were marked using a *Garmin GPSmap64*. Tree species, diameters, heights (tree heights, cable heights, force application heights), as well as type of anchors and supports were noted. Information about the tower yarders, the carriages, and the skylines were collected from data reported on the machines, the documents provided by the contractors, and the indications from the manufacturers. The timber cruise information derived directly from the harvesting plan provided by the logging contractors.

The data collection monitoring the cable-based harvesting systems required 14 days for getting the desired amount of data. A minimum of two researchers were involved in the surveys. One dedicated to the tensiometer set-up and control, a second dedicated to scale the logs. In case of short time cycles, a third researcher was involved in the wood volume measure.

2.3.2. DETAILS ON DATA COLLECTION OF THE WINCH-ASSIST HARVESTING SYSTEM CASE STUDIES

The data collection monitoring the winch-assist harvesting systems adapted the approach proposed by Holzleitner et al. (2018), integrating the profile field survey and the load volume estimation. The initial idea of mounting the machine control unit out of the forwarder cabs was abandoned because of the presence of a thick layer of ice and snow on the machines. Thus, the GNSS-IMU sensor was installed into the forwarder cabs, with an external GPS antenna mounted on the roof of the machines. For this reason, considering the use of self-levelling cabs, the tilt and roll data were not usable to measure the real machine inclination.

Two action cameras were mounted in the forwarder cabs (Figure 2.8). The drift camera, used also in the analysis of the cable yarders, was mounted at the operator point of view, recording the whole operations. A second action camera (*GoPro Hero4*), set to acquire videos at 720 ppm with 30 frames per second, was positioned for recording the winch settings chosen by the operators. For each working day, more than 90 GB of video were collected.

The tensiometer, set for recording at a frequency of 100 Hz, was located close to the anchor (Figure 2.8). When available, the sensor was located few meters far from the anchor, in proximity of the access road. This shrewdness allowed to avoid the sensor damage due to ground and stump contacts but required the installation of small chains between the sensor connection avoiding any damages.

The wood volume forwarded per each cycle was noted taking several high-quality photos during the unloading of the logs at the road side, while the cable was on the ground with no tensile force. Both back and lateral photos were taken orthogonally to the machine, reducing at the minimum the distortions. Sample of sorted piles were scaled for comparison of the data. However, no real extended field measurements of the log dimensions were possible in most of the cases.

Forwarding trail terrain profiles were surveyed by measuring slope and distance using a *Truepulse® 200* rangefinder at each significant change in ground slope. Anchor positions and significant points were marked using the *AvenzaMap®* App installed on a field tablet where were loaded the harvesting plan of the area. Anchor trees species, diameters, and heights were noted. Information about the machines and the support cables were collected directly from data reported on the machines and documents provided by the logging

Figure 2.8: Sensors and tools mounted on integrated-winch forwarders. From the top left: Tensile force monitoring system installed on the support cable; CableBull tensiometer; Drift Ghost 1080HD camera; View of the Drift camera; GoPro Hero4 camera; View of the GoPro camera

companies. Timber cruise information were derived directly from the harvesting plan provided by the forest companies.

The data collection monitoring the integrated-winch cable-forwarders required six working days. Two researchers were involved in the tools set-up, scaling the piled logs (as control system), and measuring the ground profiles. Once the monitoring systems were installed, the data collection was managed directly by one researcher because the cycle time was long enough to move up and down the hill taken the load pictures and the check the tensiometer.

2.4. DATA ANALYSIS

The management of a large amount of data collected required the definition of a systematic work flow able to the effectively analyze the data (Figure 2.9). The procedure was standardized for both the analyzed cable-supported harvesting systems, even if with same peculiarity and differences.

2.4.1. RAW DATA PRE-ELABORATION AND SYNCHRONIZATION

This preliminary step included the pre-elaboration of the output files provided by the different tools and sensor applied in order to add the proper headers and get compatible file formats for the further analyses. The pre-elaboration was carried out using the *Microsoft Excel*® software. This included the pre-elaboration of the output file reported by the GNSS

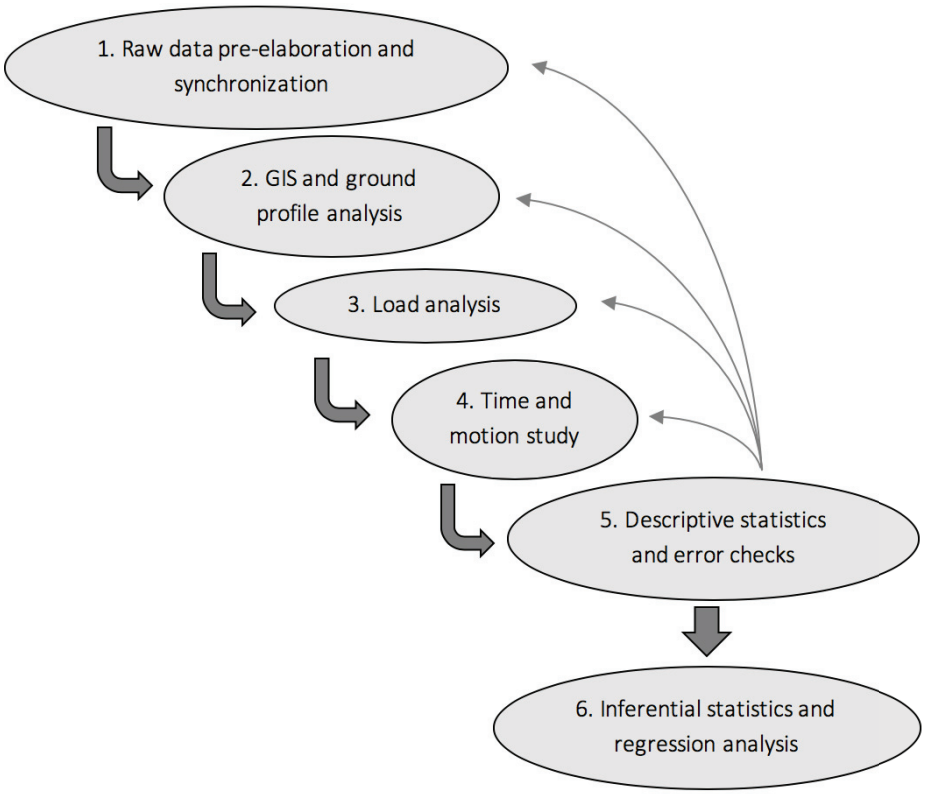

Figure 2.9: Flowchart of the data analysis process

sensor/device used for collecting the position of the structural element, the GNSS-IMU sensor, and the tensiometer.

The position data of the main structural elements were elaborated setting the proper headers and adding the descriptive notes collected in the field, as applicable (i.e., element type, specie, diameter at breast height, total height; rope height). The GNSS-IMU sensor data were elaborated selecting the columns needed in the following analyses, inserting the proper headers, and selecting the proper formats of the columns. These data included a clock time column formatted as "h:min:s.00". A new time column, reporting the time from starting the recording, expressed in seconds, was added for an easy synchronization in the following analyses. The format conversion from values expresses as "h:min:s.00" to values expressed in seconds was carried out using the following formula:

$$Time\ (s) = Time\ (h{:}\,min{:}\,s.00) * 24 * 3600 \qquad [2]$$

The output file of this preliminary elaboration reported - for each row - the clock time [h:min:s.00]; the time since the starting recording [s]; the carriage/machine speed [m s^{-1}], pitch [degree], and roll [degree]; the geographic coordinates [degree].

The output file of the cable tensile force monitoring system included two text (Figure 2.10). One file reported two columns: the time since the start of the recording and the related non-linearized measured tensile force. The second file was a text file reporting the multiple statistics of the survey and the last modification time. This information was used to calculate the start time using the following formula:

$$Start\ time\ (h{:}\,min{:}\,s.00)\ =\ stop\ time\ -\ (total\ duration * 3600^{-1} * 24^{-1}) \qquad [3]$$

The clock time of the other rows was simply calculate adding to the starting time one cent of second (00:00:00.01). Similarly to the GNSS-IMU sensor data pre-elaboration, a column reporting the time in seconds (with two decimal) since the starting time of the GNSS-IMU sensor started to record was added for an easily synchronization between the data.

The backup videos recorded every morning with the *Drift* action camera were used double checking the tool synchronization and correct eventual differences.

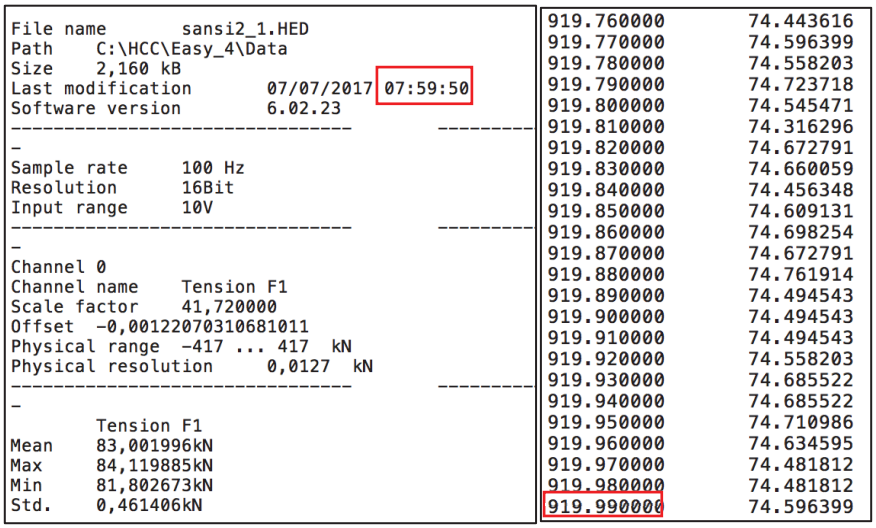

```
File name       sansi2_1.HED
Path    C:\HCC\Easy_4\Data
Size    2,160 kB
Last modification       07/07/2017 07:59:50
Software version        6.02.23
--------------------------------        ---------
-
Sample rate     100 Hz
Resolution      16Bit
Input range     10V
--------------------------------        ---------
-
Channel 0
Channel name    Tension F1
Scale factor    41,720000
Offset  -0,00122070310681011
Physical range  -417 ... 417  kN
Physical resolution     0,0127  kN
--------------------------------        ---------
-
        Tension F1
Mean    83,001996kN
Max     84,119885kN
Min     81,802673kN
Std.    0,461406kN
```

```
919.760000      74.443616
919.770000      74.596399
919.780000      74.558203
919.790000      74.723718
919.800000      74.545471
919.810000      74.316296
919.820000      74.672791
919.830000      74.660059
919.840000      74.456348
919.850000      74.609131
919.860000      74.698254
919.870000      74.672791
919.880000      74.761914
919.890000      74.494543
919.900000      74.494543
919.910000      74.494543
919.920000      74.558203
919.930000      74.685522
919.940000      74.685522
919.950000      74.710986
919.960000      74.634595
919.970000      74.481812
919.980000      74.481812
919.990000      74.596399
```

Figure 2.10: Tensiometer output files used for the synchronization

The resolution in the time study was in the order of a second, while the cable tensile force data were recorded in cents of second. However, this was not a real problem because the only consequence was eventual small differences (less than a second) in the starting and final time of each work element, which normally had no significant values in the tensile force analysis.

During the pre-elaboration process of the cable tensile force data includes also two other columns were added in the dataset: i) the work cycle column, reporting a progressive number - following a chronological order - from the first harvesting site to the last one; ii) the work element column in which was reported the specific element observed at each moment. The final output file, thus, included for each row the clock time [h:min:s.00]; the time since the starting recording [s]; the non-linearized cable tensile force [kN]; the work cycle progressive number; the work element.

Each recording sections normally ranged from one to four hours. The pre-elaboration of the tensile force data was also used to equally distribute the data in text files no longer than 700.000 rows (equal to two hours of monitoring) for guaranteeing the fluid analysis working with the data analysis software. Each harvesting site was thus subdivided in up to five text files.

2.4.2. GIS AND GROUND PROFILE ANALYSIS

The GNSS-IMU sensor data and the GPS position of the relevant point marked in the harvesting sites were loaded in a GIS software (*QGIS* version 2.14.3) to visualize the profile locations and the machine movements, as well as for checking eventual grossly position errors. Geographic coordinates were projected to *Universal Transverse Mercator* (UTM) metric coordinates, selecting the proper zone functionally to the harvesting site locations. Zone 11 was set for the Canadian case studies; zone 32 for the Italian ones. Line shape files reporting the cable line and trails were created connecting the market positions of the structural elements.

When good quality *Digital Elevation Models* (DEMs) were available, as occurred in the cable-base harvesting systems case studies, the ground profiles were extrapolated directly through GIS analysis. The DEM were downloaded from the public geodatabase provided by the regional and provincial administrations (Table 2.8). The DEMs provided by the Autonomous Province of Trento and the Autonomous Region of Friuli Venezia Giulia derived from LiDAR elaboration. The Lombardian DEMs derived from integration of LiDAR data and previously available geographical information. The distance of the points used for extrapolating the profile information was set longer than the DEMs grid diagonal length to avoid the inclusion of two sample points in the same grid. Thus, for the 1m-grid resolution DEMs a distance of 1.5 m was used, while for the 5m-grid resolution DEMs a distance of 7.5 m was used.

For the winch-assist harvesting system case studies only DEMs with a grid resolution of 30 m were available (https://www2.gov.bc.ca/gov/data/geographic-data-services). This resolution was not considered suitable for the ground profile information extraction. In this

Table 2.8: Data source of DEMs used in the ground profile extraction process

Site	Provider	Projection	Grid resolution	Link
A-B-C	Autonomous Province of Trento	WGS84 UTM32	1 m	http://www.lidar.provincia.tn.it:8081/WebGisIT/pages/webgis.faces
D-E-F-G-H	Autonomous Region of Friuli-Venezia Giulia	Gauss Boaga East zone	1 m	http://irdat.regione.fvg.it/CTRN/ricerca-cartografia/
I-L-M-N	Lombardy Region	WGS84 UTM32	5 m	http://www.geoportale.regione.lombardia.it/download-ricerca

case, the direct field measure of distance and slope taken at any significant slope change in the ground profile were plotted in a CAD software (*AutoCAD*® 2017) software with which were extracted the relative vertical distance (altitude) from the polyline information through the "list" command. Using the GPS information at the upper point was attribute the absolute altitude value at each point. The data were exported as text files and were also used to create the longitudinal profiles reported in Annex 5 and Annex 6.

The profile data of both the analyzed cable-supported harvesting systems were than plotted in the *R* software (version 3.2.4) where, at the same defined distances, it was calculated the ground slope, expressed in percentage values. The profiles were thus analyzed and summarized in term of slope and length (horizontal, vertical and inclined length). In case of the cable-based harvesting system, this step also included the cable line geometry calculations.

2.4.3. LOAD ANALYSIS

The load yarded at each cycle was quantified differently between the two harvesting systems because of the different input data source. However, the final common output of the load analysis included - per each work cycle - the total wood volume, the number of logs, and the average log size. In the cable-based harvesting system case studies, the wood volume of each log yarded during the monitored operations was calculated using the *Huber's formula* (West 2014), considering the logs as pure cylinders and inputting the length and the diameter, at mid-length, measured in the field. For the cable-based harvesting systems, also the total load applied to the cable structure was estimated.

Most of the cable-based case studies adopted whole tree harvesting method or a mixed method - exploiting mid-length stems not debranched - for mechanizing the processing phase at the landing and/or for interest in the biomass recovering. For the load calculation, thus, the values of green wood load per unit of volume (Giordano 1981), differentiated per species, were increased functionally to the branch density - visually estimated during the data collection - adopting both bibliography data (Spinelli et al. 2006) and operator suggestions. This approximation was introduced to account for the branch load which was relevant in several cases. The class of estimated branch load were set as:

- Clean: 0.0 kN per unit of wood volume (m^3)
- Low branching: 0.5 kN per unit of wood volume (m^3)
- Average branching: 1.0 kN per unit of wood volume (m^3)
- Heavy branching: 2.0 kN per unit of wood volume (m^3)

This procedure allowed to approximate the wood load, the branch load, and the total *payload*, expressed ad their sum. Adding also the carriage load, the *estimated total load* applied on the cable structure was calculated. The mainline and the haul-back line load effect on the cable structure were neglected in this study.

In the winch-assist case studies, based on the use of harvester and forwarders, the work flow was based on the cut-to-length method. The logistic organization of the harvesting sites did not allow a detail direct random or total field measurement of the log dimension, and the volume data derived from post-processing analysis of the forwarder photos collected at the landing before unloading the logs. Loaded forwarder photos were uploaded into a CAD software (*AutoCAD® 2017*), following a perspective correction through *Adobe Photoshop®* to reduce eventual minimal distortions. Field measurements of forwarder bunk dimensions were used for scaling the photos. The wood volume forwarded per work cycle was then calculated as sum of the volume of each log, calculated assuming the logs as pure cylinders and measuring their length and diameters on the back side of the forwarder directly in the CAD software. Considering that each load included at least two different log lengths, several pictures were analyzed for the same load estimation. No information on each log specie was available and thus no conversions volume-load were considered to reduce the uncertainty of the data.

2.4.4. TIME AND MOTION STUDY

The 30-min mp4 videos recorded through the action cameras were elaborated using the *QuickTime Player* software creating an independent video for each work cycle. These videos were then analyzed for completing a time and motion study, following the elemental

level method defined by the internationally recognized procedures (Björheden 1991). Element level measurement consists of splitting the work cycle into functional steps (elements) and recording time consumption separately for each of them. This method allows to separate effective work time from delay time, which may contribute to a better understanding of process dynamics.

Delays are interruptions of the work process and are commonly subdivided into three main categories depending on their origin (Acuna et al. 2012): i) *mechanical delays* are caused by the need to service or repair the machine used for performing the work task; ii) *personal delays* are interruptions caused by the operator and include rest breaks; iii) *operational delays* are related to organizational causes, work planning, and site reconnaissance. The main problem with delays is their large variability, due to the erratic occurrence. A reliable estimate of delay time (or overall time including delays) will require a very large number of replications and a comparably long observation time. Therefore, two main solutions have been devised to overcome this problem: i) including into the study only those delay events that fall within a maximum duration limit (e.g. 10 or 15 minutes); ii) excluding delays from data recording (considering just the delay-free work cycle) and accounting for delay time through specific coefficients applied to the productive time.

In this research, only delays lower than 15 minutes were included in the time study. Time measurements were thus expressed in term of *Productive Machine Hour* (PMH_{15}) representing the effective working hours, excluding time lost to machine relocation, rigging, and mechanical or other delays exceeding 15 minutes. Analyzing short time work cycle, as was the case of the monitored case studies, is useful to use the *Productive Machine Minutes* unit (PMmin), equivalent to PMH, but rescaled to minutes for improved readability (Talbot et al. 2015).

The time study from video analysis was carried out filling the work cycle and work element columns of the output file derived from the pre-elaboration process. For the cable-base harvesting systems case studies the work elements were defined as:

- outhaul: begins when the operator is ready to move the carriage from the landing out to the choker setter and ends when the carriage stops at the hooking area;
- hook: begins at the end of the outhaul and ends when the choker setter hooks the load and is in the safety area ready to pull the load;

- lateral skid: begins at the end of hook and ends when the load is pulled up to the carriage and the carriage begins to move on the trail;
- inhaul: begins at the end of the lateral skid and ends when the load reaches the unloading position at the landing;
- unload: begins at the end of the inhaul and ends when the chokers return to the carriage and the carriage is ready to move;
- delay: includes all delays less than 15 minutes.

The video analysis was also used to define the prevalent transportation system (semi-suspended, fully suspended) and the detect eventual variation of load volume between lateral skid and inhaul due to intermediate partial processing.

In the winch-assist harvesting systems, priorities were assigned at each work element. If two elements overlap, the activity with the higher priority (1: highest; 3: lowest) was recorded, following the method described by Fernandez-Lacruz et al. (2013) and Erber et al. (2016) adapted to the present time study. The work elements for the winch-assist case studies were defined as:

- travel empty: time spent moving (empty) to the loading; starts when the forwarder wheels begin to rotate and ends when the boom begins to swing (priority 2);
- loading: time spent loading logs in one trip; starts when the boom begins to swing and finishes when the boom stops swinging (priority 1);
- driving - loading: time spent moving between the different loading spots; starts when the forwarder wheels begin to rotate and ends when the boom begins to swing (priority 2);
- travel loaded: time the loaded machine spends moving to the landing; starts when wheels begin to rotate and ends when the boom begins its swing (priority 2);
- unloading: time spent unloading logs at the landing; starts when the boom begins to swing and finishes when the boom stops its swing (priority 1);

- driving - unloading: time spent moving between different sort piles at the unloading site; starts when the forwarder wheels begin to rotate and ends when the boom begins to swing (priority 2);
- winch control: time the operator spent changing the force settings on the winch control panel (priority 3);
- delay: includes all delays less than 15 minutes.

The in-cab videos were analyzed also identifying the forwarder actual snapshot travel direction-uphill, downhill or stationary. The videos of the operator settings – recorded through the second action camera installed in the cabs - were analyzed only for one of the operators working in two different trails.

2.4.5. DESCRIPTIVE STATISTICS AND ERRORS CHECK

The data derived from the previous analysis were merged and analyzed using the *R* software. A first analysis was applied independently at each harvesting site, developing dedicated scripts. During this analysis, the yarding distance and the load volume were calculated. Mean and peak tensile forces, different tensile force parameters, factors, and indexes, as well as the time duration were calculated at both work cycle and work element level. The analysis briefly differed between the two harvesting sites, and the detailed explanation is reported in the following chapters. Subsequently, graphs reporting the tensile forces and the machine positions over the time were plotted to check errors in the previously analyses. If this was the case, previously analyses were double checked. The scripts developed for each harvesting site were organized in four main sections:

- Section 1: GNSS-IMU data elaboration;
- Section 2: Time study data elaboration;
- Section 3: Profile analysis;
- Section 4: Cable tensile force data elaboration;
- Section 5: Graph production.

Section 1 - GNSS-IMU data elaboration

The GNSS-IMU data analysis included the calculation of the relative distance of each point respect to a reference point which was set as the tower yarder position in cable-based harvesting system and the road center line in winch-assist system. This calculation was based on the Pythagoras theorem applied to the UTM metric coordinate difference between each recorded point and the reference point. In the cable-base harvesting systems, the tower yarder positions were set as reference points, and the yarding distance was defined as the farthest horizontal distance reached by the carriage in the cycle (Figure 2.11). In the winch-assist harvesting systems, the road center line in proximity to the trail was set as the reference point. The forwarder distance traveled on the trail was measured as the farthest loading point reached during each cycle. The forwarder distance traveled on the road was measured as the farthest unloading point reached during the cycle (Figure 2.12). The GNSS-IMU data were collected with a frequency of about 5 Hz, but the clock time from derived from the satellites was expressed in integer seconds. Thus, at the same clock time, resulted several measures. Through an aggregate function, it was calculated the average distance and speed per second, as well as the average tilt and roll - when applicable – changing the frequency from 5 Hz to 1 Hz. These data were then connected to the cable tensile force information through the application of linear models to approximate the resolution from one to 100 Hz. Descriptive summary information (minimum, maximum, mean, standard deviation) was calculated for each variable at cycle level. The maximum distance from the reference point was assumed as the cycle yarding distance.

Section 2 - Time study and productivity elaborations

The filled cable tensile force data sheets reporting the work cycle and the work elements indications were analyzed to complete the time study at element level. The analysis was based on the row data sum, considering that each record accounted for 0.01 second. Delays longer than 15 minutes were excluded from the analysis. The total time recorded for each case study, as well as the summary information were calculated at element level using the cycle as the observational unit. Also, work cycle time, expressed in terms of both $PMmin_{15}$ and delay-free cycle time ($PMmin_0$), was calculated.

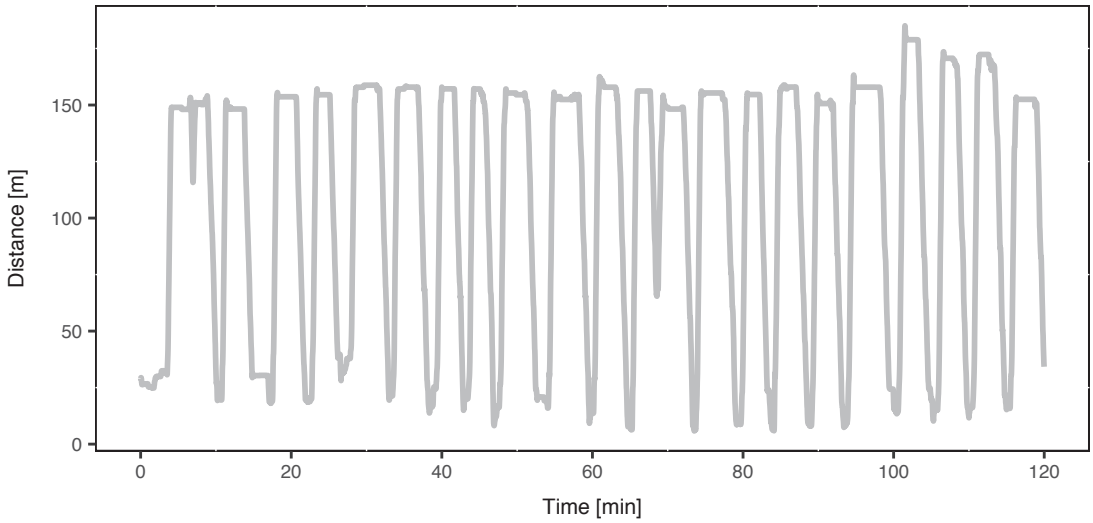

Figure 2.11: Example of relative yarding distance (Site A, cable line M06, session 1A, 120 min)

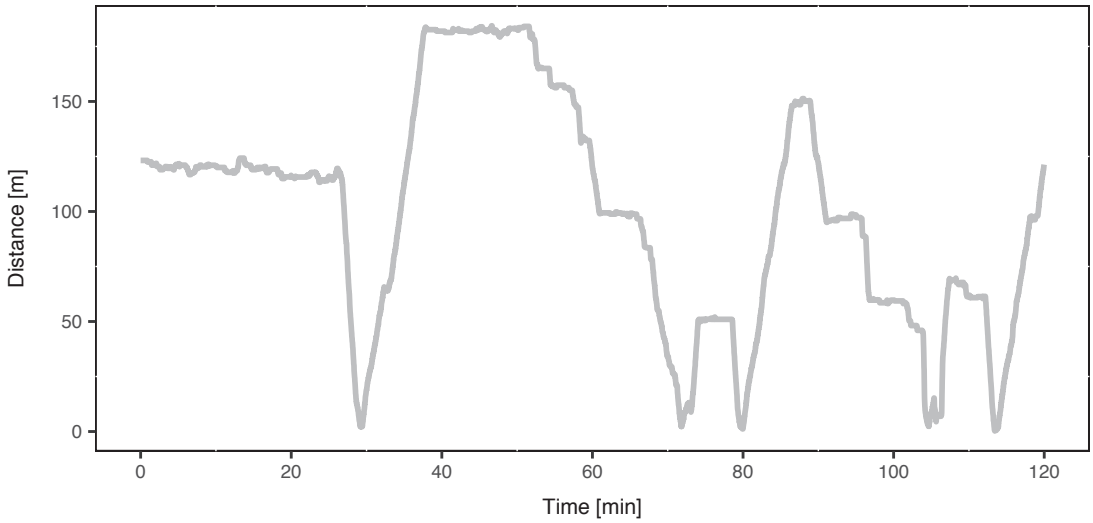

Figure 2.12: Example of relative forwarding distance (Site P, trail CR08, session 4A, 120 min)

The wood volume information was then connected to the time study to get the productivity recorded at each harvesting site, expressed in terms of m^3 PMH_{15}^{-1}. Summary information were then derived for the productivity data.

Section 3 - Cable tensile force data elaboration

The raw data of the cable tensile forces were initially corrected through the application of the following linearization formula:

$$TF = (0.004086\, rTF^2) + (0.829576\, rTF) + 0.829576) \quad [4]$$

Where "*TF*" is the linearized tensile force, expressed in kN; "*rTF*" is the raw tensile force provided as output file from the pre-elaboration step, expressed in kN. This formula is directly applied by the dedicated *HCC-Easy* software when visualizing the data but is not applied to the raw data during the exporting process. Thus, using a different software for the data analysis, the data have to be corrected.

Descriptive statistic of the cable tensile force data was applied considering the cycle as the observational unit. Further analysis related to dynamic amplification analyses, as well as parameters and indexes calculation, differed between the cable-based and the winch-assist harvesting systems and are treated separately in the next chapters. The tensile force analysis initially focused on the maximum working loads, defined as the percentage value of the ratio between the tensile force and the MBL (provided by the manufacturers) of the cable, both expressed in kN.

$$Cable\ working\ load = \frac{cable\ tensile\ force}{minimum\ breaking\ load}\ 100 \quad [5]$$

The working load was then compared to the SWL in order to quantify the frequency in exceeding the safety limits, as reported in the chapter 1.4.2. Cable mean and peak tensile forces and other summary information were then calculated at element level assuming the cycle as observational unit.

Also, according to Pyles et al. (1994), for the cable tensile forces recorded in the cable-based harvesting systems case studies, two dynamic amplification parameters were calculated: i) the *Break-out Tensile Force* (BOTF) associated with starting the load moving (Figure 2.13); ii) the *Maximum Cyclic Load Amplitude* (MCLA), defined as the greatest peak to peak difference in a cyclic load (Figure 2.14). The MCLA represents the maximum momentary excursion in the cable tensile force during outhaul and inhaul and is a combination of vibrations of the system and changes of the load applied to the system (e.g., carriage moving along the cable and load moving along the ground).

The BOTF was automatically identified as the maximum cable tensile force measured during lateral skid. The MCLA was identified through a peaks and valleys detection algorithm

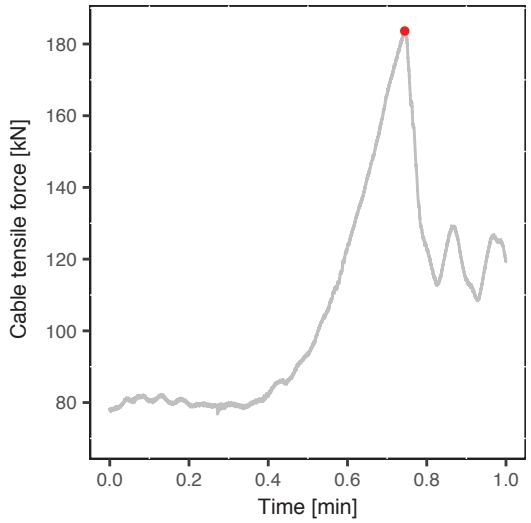

Figure 2.13: Example of lateral skid and evidence of the break out (red point)

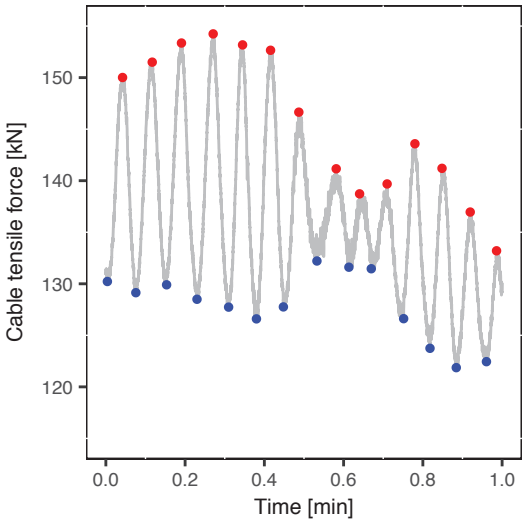

Figure 2.14: Example of peaks (red points) and valleys (blue points) identification for MCLA calculation

developed in the *R* environment, operating in a mobile time-window of two seconds. Factors - in relation to the pretension - and indexes - in relation to the payload - were also calculated. The *pretension* is defined as the unloaded cable (skyline) tensile forces set-up tensile force of the cable structure (Samset 1985). Operatively, this value was detected in multi-span configuration identifying the unloaded cable tensile force in proximity of the intermediate support during the outhaul. In single span configurations, pretension was detected periodically moving the carriage close to the tower yarders.

Section 4 – Graphs

The last section of the scripts plotted the cable tensile forces and the machine positions over the time, per each cycle, using a loop procedure. In the case of cable-harvesting systems, further plots related to the outhaul and inhaul MCLA analysis were plotted as well. These graphs were used to detect unusual behavior or eventual grossly errors in the previously analysis.

2.4.6. INFERENTIAL STATISTICS AND REGRESSION ANALYSIS

Once the data and the previously analyses were verified. The output files derived from the descriptive analysis of each harvesting site were merged in a single text file for each harvesting system. These datasets reported for each work cycle all the information and parameters calculated in the previous analyses.

The work cycle was assumed as the observational unit also in the inferential statistics. The significance of the differences between mean values was tested through *t-test* and *Analysis of Variance* (ANOVA). In case of violation of the normal distribution assumptions, logarithm and square root transformations were attempted for normalizing the data. If the normalization process was not successful, the *Kruskal-Wallis and Mann-Whitney-Wilcoxon* non-parametric tests were used instead of *t-test* and ANOVA for verifying statistical differences between mean values. The same non-parametric tests were also use in case of violation of the homogeneity of variance assumption, tested with the *Leven's test*.

The regression analysis differed between the two harvesting systems. In cable-based harvesting systems the spread and magnitude of the tensile force parameters varied within the cable lines, with at least some lines reporting values largely different from the overall average. This justified considering the response variables to be repeated measures within a class, and possibly showing heteroscedasticity. Given this observation, a random intercept for the different cable lines was included in the regression analysis, leading to the adoption of linear mixed-effect models. The significance of the single variables was evaluated through the application of the *Likelihood Ratio test*, testing the difference in two nested models using the *Chi square* distribution. The significance level of the statistical analysis was set to 0.05. Statistical assumptions were checked analyzing the residual plot distributions. In case of non-normal distribution of the residuals, logarithm and square root transformations were tested, as appropriate, on both response variables and explanatory continuous variables.

The goodness-of-fit of linear mixed-effect models was tested considering the *Akaike Information Criterion* (AIC) and the *Bayesian Information Criterion* (BIC), comparing different model options. Also, the coefficient of determination (R^2_{LR}) proposed by Magee (1990) was

considered in this work. This coefficient is based on the *Likelihood Ratio joint significance test* and is calculated as:

$$R^2_{LR} = 1 - exp\left(\frac{-2}{n}\left(l_M - l_0\right)\right) \quad [6]$$

Where l_M and l_0 are respectively the log likelihoods of the model of interest and the intercept only model, and n is the number of observations. According to Nagelkerke (1992), this coefficient is consistent with the classical coefficient of determination (R^2). It does not have any unit and rages between zero and one, with zero denoting that model does not explain any variation, and one denoting that it perfectly explains the observed variation.

In winch-assist harvesting system case studies, the regression analysis was based on simple and multiple linear regression analyses, tested at a significance level of 0.05. Similarly to the analysis based on the application of mixed-effect models, the statistical assumptions were checked analyzing the residual plot distributions. Again, in case of non-normal distribution of the residuals, logarithm and square root transformations were used, as appropriate, on both response variables and explanatory continuous variables.

Note: most of the results are presented though the use of boxplots where the grey boxes include the data between the 25th and 75th percentile; the whiskers extend to the most extreme data point which is no more than 1.5 times the length of the box away from the box; the black point represents out-layers (considering the "1.5 rule"); the vertical/horizontal (considering the graph direction) black line in the grey boxes represents the median; the rhombus represents the mean.

3. RESULTS

The cable tensile force monitoring interested almost 90 PMH_{15} of steep slope forest operations, distributed in 15 different harvesting sites and two different countries and continents. Tensile force data were recorded with a frequency of 100 Hz, collecting almost 32 million row data, related to 502 work cycles in cable yarding and 28 cycles in winch-assist forwarding. Video recording of the logging operations collected more than 1.2 TB of data. Log scaling and photo analysis measured 1360 m^3 of wood.

3.1. RESULTS RELATED TO THE CABLE-BASED HARVESTING SYSTEM CASE STUDIES

A total of 72.1 PMH_{15} of cable yarding operations were monitored, collecting more than 26 million rows tensile force data of 502 complete work cycles. The number of cycles observed for each cable line ranged from 25 to 71, recording between 3.4 to 9.3 PMH_{15} per line, during one or two working days.

The horizontal length of the cable lines, measured from the tower yarder to the tail anchor, ranged from 138 to 600 m with an average of 202 m for single span cable line and 460 m for multi-span configurations. The vertical length, ranging from 14 to 213 m, averaged 149 m for multi-span cable lines and 67 m for single span configuration. The average geometric chord length was 132 m, with a minimum of 7 m and a maximum of 391 m. The average chord slope was 18.3%, ranging from 0.6 to 53.6%. Details on the geometric features of the analyzed cable lines are reported in Table 3.1.

Table 3.1: Cable line configurations and geometries

Cable line	Line config.	HL	VL	Span 1		Span 2		Span 3		Span 4		Span 5	
				IL	Slp	IL	Slp	IL	Slp	IL	Slp	IL	Slp
-	-	m	m	m	%	m	%	m	%	m	%	m	%
S01	up	138	62	7	60	99	53	49	48	-	-	-	-
S02	up	166	14	151	10	17	44	-	-	-	-	-	-
S03	down	349	187	391	51	-	-	-	-	-	-	-	-
S04	down	213	56	217	20	-	-	-	-	-	-	-	-
S05	down	175	46	178	18	-	-	-	-	-	-	-	-
S06	up	172	39	160	25	22	78	-	-	-	-	-	-
M01	up	490	213	40	31	131	40	265	44	81	58	24	84
M02	down	222	63	144	24	84	21	-	-	-	-	-	
M03	up	600	195	362	20	97	43	138	47	50	128	-	-
M04	up	588	200	85	28	192	41	293	32	55	52	-	-
M05	up	426	105	45	1	122	11	180	38	100	43	-	-
M06	up	438	120	311	35	97	13	49	12	-	-	-	-

Notes: Line config.= Line configuration (up = uphill-oriented yarding; down = downhill-oriented yarding); HL= Horizontal length - measured from the tower yarder basement to the anchor; VL= Vertical length - measured from the tower yarder basement to the anchor; IL= inclined chord length; Slp= chord slope. In blue the span over the tail spar.

3.1.1. TIME STUDY AND PRODUCTIVITY

The average delay-free work cycle was 7.44 $PMmin_0$ long. Hook interested almost one-third of the time (29.6% of the delay-free time), followed by inhaul (24.9%) and outhaul (17.9%). Lateral skid and unloading involved 14.4 and 13.2% of the delay-free time, respectively. Most of the cycles (73%) included delays shorter than 15 minutes, with an average duration of 1.63 minutes (Figure 3.1).

A total of 837 m^3 of wood were scaled at the landings. The average wood volume yarded per cycle was 1.67 m^3. The log size ranged from 0.49 to 6.06 m^3, with an average of 0.94 m^3. All the harvesting sites adopted the whole-tree harvesting method for most of the monitored cycles, integrating partial processing in case of problems in yarding the logs or too large loads. Table 3.2 reports details on work time, yarding distances, and loads aggregate per cable line.

Integrating the volume information with the time study and considering all the work cycles recorded in the cable tensile force monitoring, the average productivity was 13.6 m^3 PMH_{15}^{-1}. Large differences were recorded between the different cable lines, with average values ranging from less than 4 m^3 PMH_{15}^{-1} up to more than 30 m^3 PMH_{15}^{-1} (Figure 3.2).

The average yarding distance (horizontal distance) was 223 m long, with a maximum of 569 m recorded in cable line M03. More than 75% of the cycles, however, recorded a yarding distance shorter than 300 m.

3.1.2. CABLE WORKING LOAD AND TENSILE FORCES VARIABILITY

The cable working load (expression of the tensile force as the relative percentage of MBL) recorded for the whole dataset highlighted a prevalence of tensile forces lowers than the SWL, but also a consistent portion even exceeding this limit and reaching a maximum of 54.7% (Figure 3.3). Considering the cycle as the observational unit, however, the maximum cycle cable working load exceeded the SWL in almost 55% of the observations. Also, in nearly 20%, the cycles the skyline working load exceeded a value of 40%, and in six cycles (1.2% of the total) on two different single span cable lines, exceeded the endurance limit (50% of the MBL). The frequency of exceeding the safety limits, however, changed between the different cable lines (Figure 3.4): six lines out of twelve (four of them in single span configuration) exceeded the SWL in more than 80% of the cycles. The other six lines exceed the SWL in less than one-third of the cycles, with one of them never reaching the SWL (cable line M02).

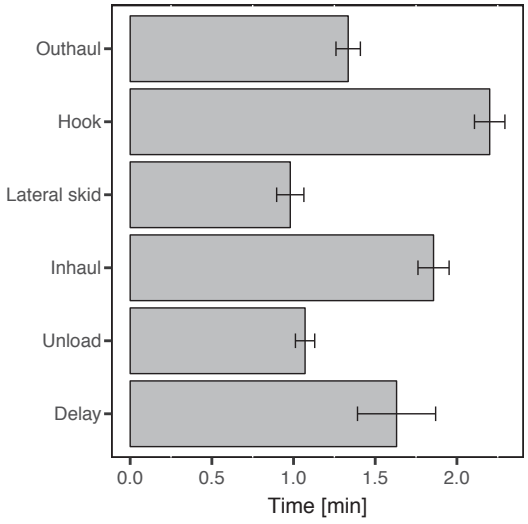

Figure 3.1: Work element time distribution in cable yarding

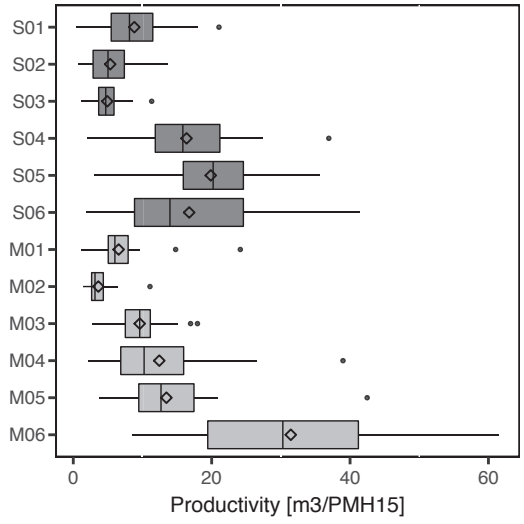

Figure 3.2: Cable yarding cycle productivity recorded per cable lines

Notes: The error bars report the 95% confidence interval

Table 3.2: Cycle time, yarding distance, and volume data per cable line

Cable line	Total time	Work cycles	Work cycle duration	Yarding distance	Total wood volume	Load volume	Estimated cycle load	Log size
-	PMH_{15}	no.	$PMmin_{15}$	m	m^3	m^3	kN	m^3
S01	4.3	37	7.0 (2.7)	76 (10)	34.8	0.9 (0.4)	8.2 (3.5)	0.69 (0.45)
S02	5.4	38	8.6 (2.8)	101 (36)	27.4	0.7 (0.5)	7.6 (4.8)	0.17 (0.12)
S03	4.9	25	11.7 (4.1)	256 (21)	22.6	0.9 (0.4)	9.7 (4.4)	0.36 (0.24)
S04	4.2	36	6.9 (2.2)	120 (23)	64.1	1.8 (0.8)	16.2 (7.0)	0.65 (0.41)
S05	3.4	33	6.1 (2.1)	129 (13)	62.9	1.9 (0.7)	16.4 (5.6)	0.56 (0.18)
S06	5.7	39	8.8 (4.5)	137 (17)	82.0	2.1 (1.1)	18.5 (9.1)	1.45 (0.95)
M01	8.9	44	12.2 (1.8)	442 (9)	57.6	1.3 (0.7)	11.9 (5.8)	0.48 (0.33)
M02	4.3	43	6.0 (1.3)	147 (15)	15.6	0.4 (0.2)	3.3 (1.8)	0.10 (0.13)
M03	9.3	47	11.9 (2.3)	527 (38)	88.8	1.9 (0.6)	17.5 (5.4)	0.91 (0.51)
M04	7.4	52	8.6 (3.2)	266 (144)	81.4	1.6 (0.8)	14.5 (6.6)	1.06 (0.72)
M05	7.2	37	11.6 (5.7)	141 (22)	80.4	2.2 (0.6)	19.4 (4.7)	1.37 (0.65)
M06	7.1	71	6.0 (1.3)	215 (40)	219.4	3.1 (1.3)	26.2 (10.5)	2.19 (1.28)

Notes: The values between the brackets report the standard deviations

A deeper analysis of the cable working load distribution is possible considering separately each cable line (Figure 3.5) and the distribution between the different work elements (Figure 3.6). The cable working load plots distribution per cable line showed a first high frequency at lower values, followed by a smoothed long tail decay distribution at higher working loads, sometimes including a second limited peak in the distribution. The difference between the cable lines justified the cable working load distribution of the whole dataset, as already partially conceivable from the maximum cable work load boxplot (Figure 3.4). Four cable lines, mainly in multi-span configuration (cable line S01, M02, M03, M04) mainly interested cable working load ranging from 10 to 20%. Cable lines S03, S04, S06, M05, and M06, instead, recorded highest frequency at cable working load ranging from 20 to 30%. The portion of the data exceeding the SWL is mainly due to the cable contribution of cable line S02 and S04, both in single span configuration, and by the largest working load values recorded during lateral skid and inhaul in the other cable lines, excluding cable line M02.

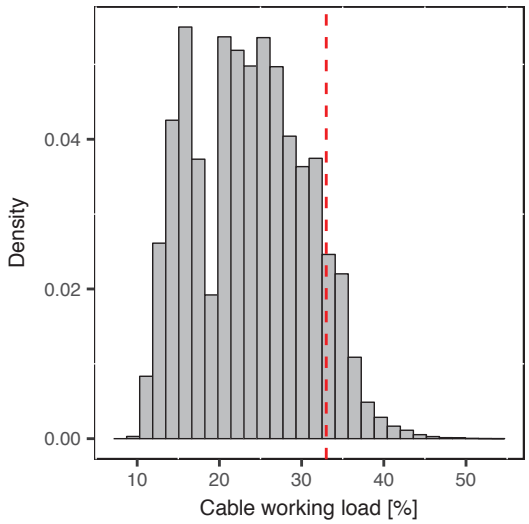

Figure 3.3: Cable working load recorded in the whole dataset

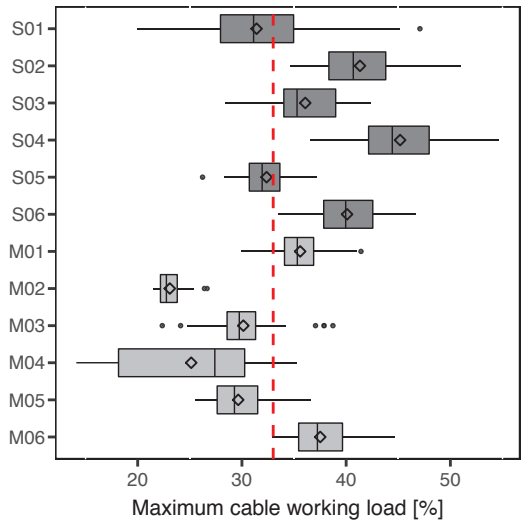

Figure 3.4: Maximum cycle cable working load per cable line

Notes: The dashed red lines indicate the cable Safe Working Load (one-third of the Minimum Breaking Load)

The cable tensile force behaviors of whole cycles are reported in Figure 3.7 and Figure 3.8, showing a single and a multi-span configuration, respectively. During outhaul, the tensile force progressively increased moving the carriage farther from the tower, reaching a maximum at the mid-span, and decreasing again reducing the distance to the tail anchor, the tail spar or an intermediate support. The tensile force in this work element assumed a cyclic load behavior, but with a limited amplitude. Once the carriage stopped, the tensile force assumed a typical initial cyclic load decay and then, while hooking up the load, tent to stabilize to a constant vibration. During lateral skid, the tensile force recorded an initial sharp increase due to the application of the pulling force and the resisting load initial friction and resistance on the ground, reaching a maximum at the break-out point and decreasing with the following movement of the logs close to the skyline. Further multiple peaks normally occurred because of logs striking obstacles such as stumps or rocks. During inhaul, similarly to outhaul, the tensile force increased up to the mid-span and decrease again moving closer to the tower yarder. In the case of multi-span configurations, the highest peak tensile force during inhaul was recorded at the mid-span of the main span. The cyclic load magnitude during inhaul was much more relevant compared to outhaul. Finally, the unloading of the load, occurring close to the tower yarder, showed a general limited tensile force, but the initial releasing of the load led to sporadic peaks in tensile force.

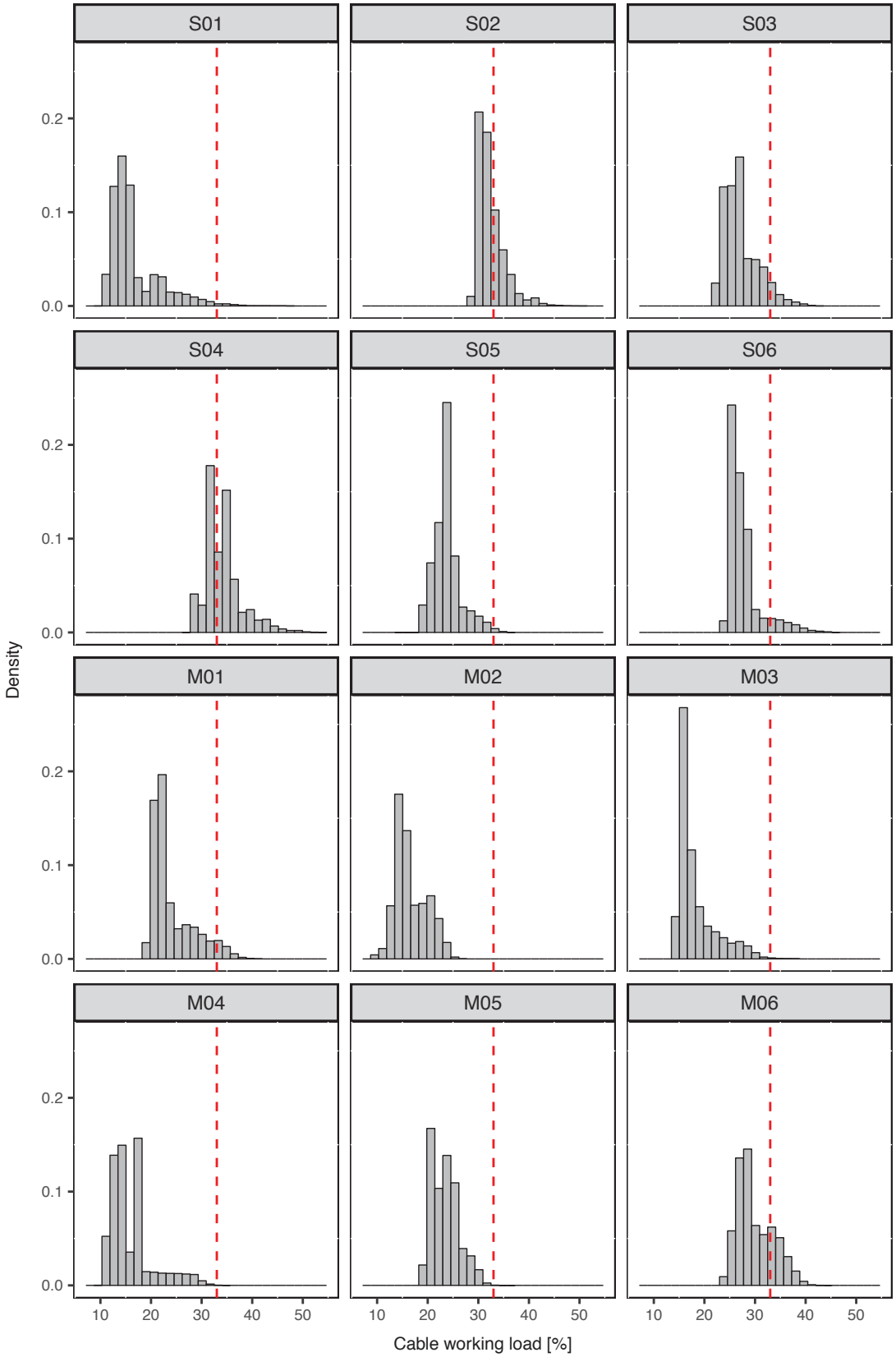

Figure 3.5: Cable working load distribution per cable line

Notes: The dashed red lines indicate the cable Safe Working Load (one-third of the Minimum Breaking Load)

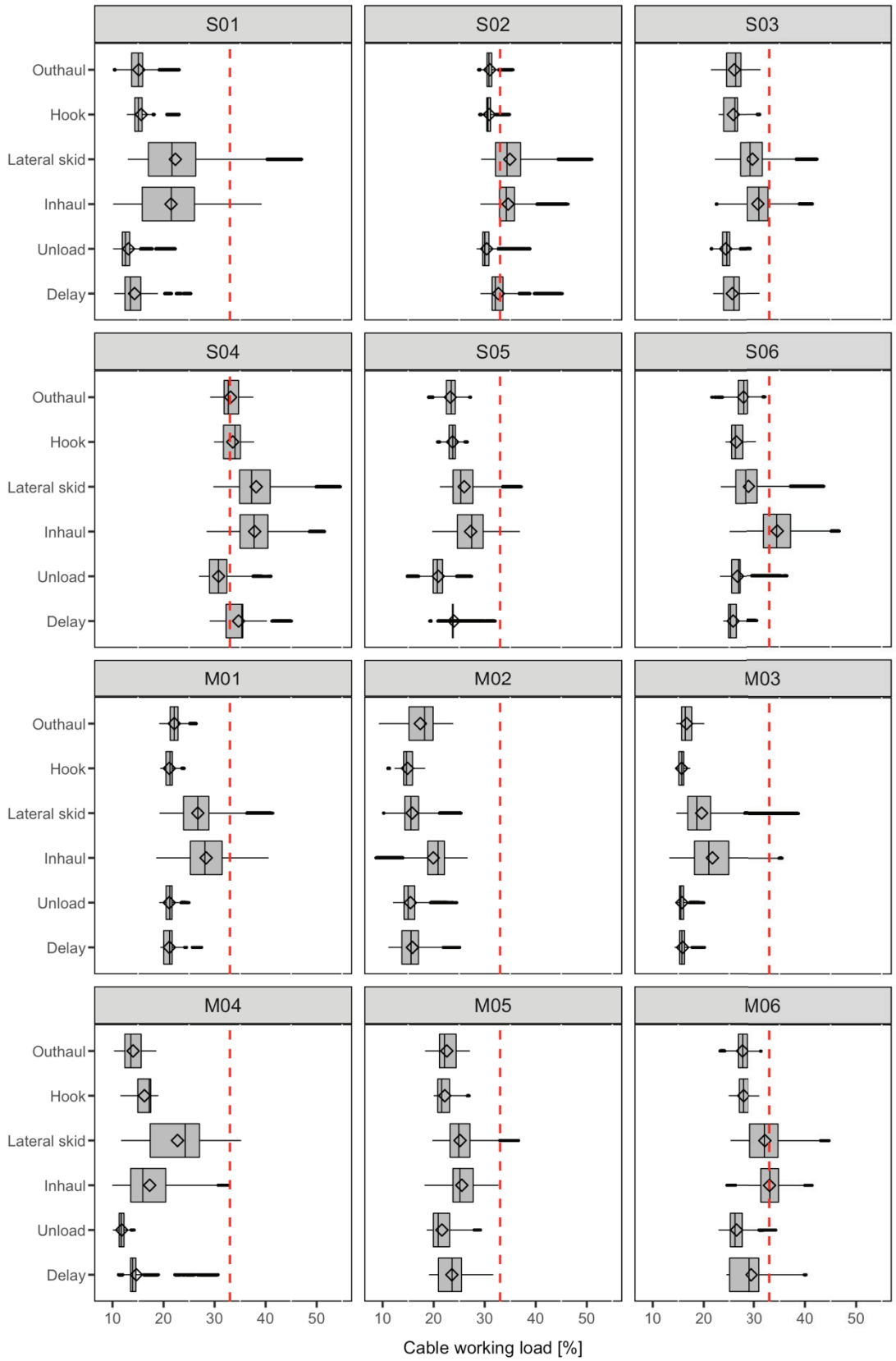

Figure 3.6: Cable working load distribution per cable line and work element

Notes: The dashed red lines indicate the cable Safe Working Load (one-third of the Minimum Breaking Load)

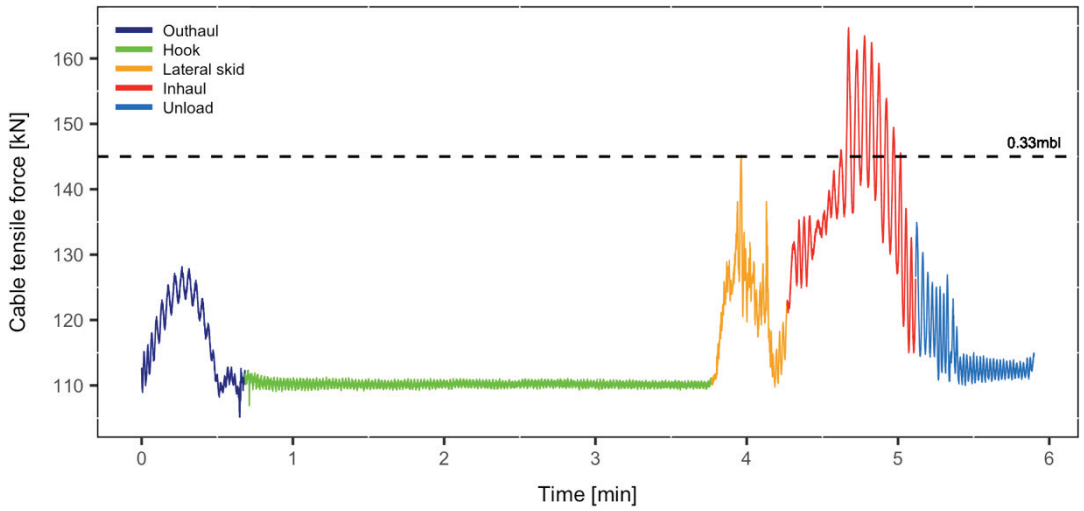

Figure 3.7: Example of cable tensile force plotted over the time for a work cycle in single span configuration (Site B, cable line S06, yarding distance= 147 m, estimated total load= 26.5 kN)

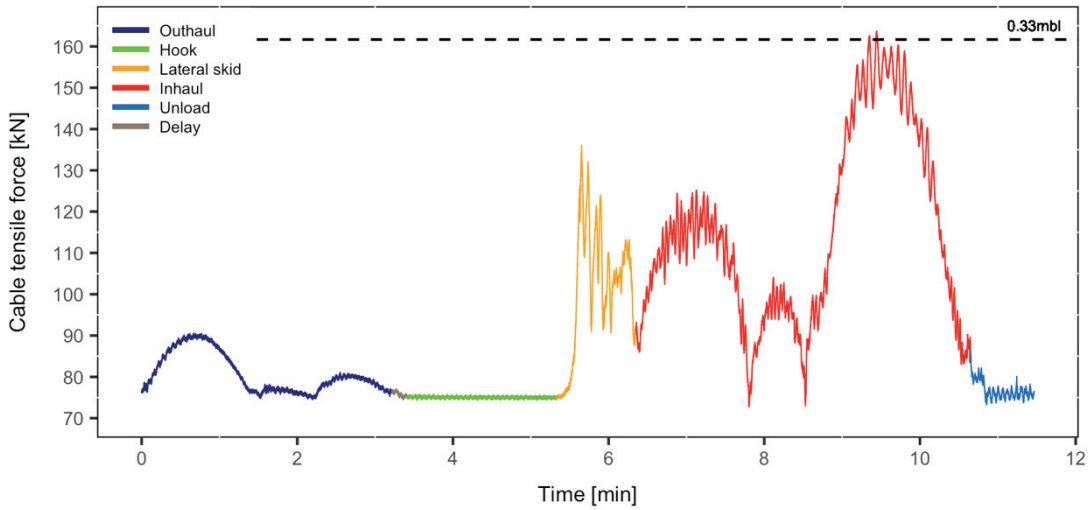

Figure 3.8: Example of cable tensile force plotted over the time for a work cycle in multi-span configuration (Site I, cable line M03, yarding distance= 551 m, estimated total load= 23.3 kN)

The pretension ranged from 20 to 120 kN proportionally to the cable yarding system size and power (Figure 3.9). In relative percentage terms (Figure 3.10), pretension ranged from a minimum of 29% up to a maximum of 86% of the SWL, with a significant difference (p-value <0.001), tested through the Kruskal-Wallis test, between single span (67%) and multi-span cable lines (52%).

3.1.3. PEAK CABLE TENSILE FORCES

Cable peak tensile forces exceeded 180 kN in nearly 13% of the work cycles, distributed in five cable lines, with a maximum of 237.8 kN recorded in the cable line S04 (Table 3.3). Peak tensile forces resulted statistically different between the different base vehicles - directly correlated to the machine power - with maximum values recorded for the larger truck and track-based machines, followed by trailer (single and double axes) and tractor-based tower yarders (Figure 3.11).

The highest cycle peak tensile forces were recorded during lateral skid (51.6% of the work cycles) and inhaul (48.4%). Considering the data aggregated per cable line, there was normally a predominance of one of these two work elements in recording the maximum cycle tensile force (Figure 3.12), mostly because the monitoring interested a limited portion of the yarding operations (one or two working days), and the work cycles were partially concentrated at a similar yarding distance. However, significant differences between the average peak tensile forces recorded in lateral skid and inhaul were recorded only in five cable lines out of twelve (Table 3.2)

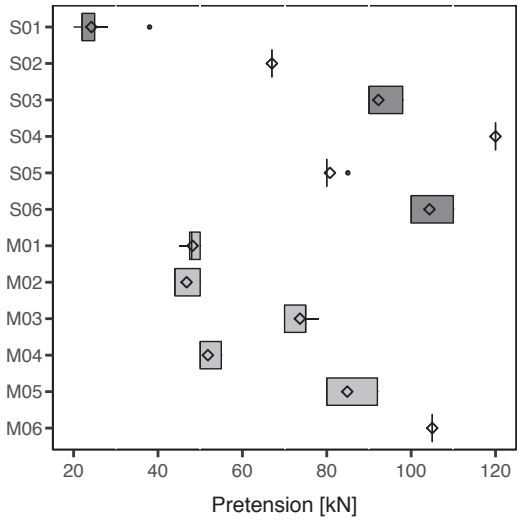

Figure 3.9: Pretension recorded per cable line

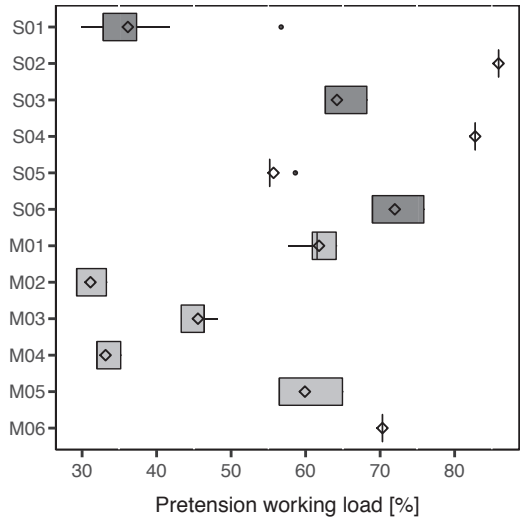

Figure 3.10: Pretension recorded per cable line, expressed as percentage ratio with SWL

Table 3.3: Average and maximum peak cable tensile forces per work element and cable line

Cable line	SWL	Peak tensile force					
		Outhaul	Hook	Lateral skid	Inhaul	Unload	Abs. max
-	kN	kN	kN	kN	kN	kN	kN
S01	67	33.9[a] (3.7)	33.2[a] (3.9)	61.3[b] (13.0)	57.5[b] (8.3)	31.4[c] (4.5)	94.6 - LS
S02	78	74.6[a] (2.4)	73.9[a] (2.7)	96.0[b] (9.3)	89.0[c] (6.9)	78.0[d] (4.3)	119.4 - LS
S03	144	118.3[a] (7.0)	114.1[b] (7.4)	153.2[c] (15.9)	150.7[c] (14.3)	112.8[b] (6.6)	182.6 - LS
S04	145	151.9[a] (6.9)	150.9[a] (8.1)	196.0[b] (19.6)	187.2[b] (15.2)	151.8[a] (11.5)	237.8 - LS
S05	145	108.7[a] (4.0)	108.3[a] (3.8)	139.8[b] (11.1)	135.7[b] (10.5)	108.7[a] (5.9)	161.7 - LS
S06	145	129.4[a] (4.5)	119.2[b] (6.5)	152.4[c] (16.8)	173.4[d] (15.1)	135.2[e] (9.8)	203.2 - IN
M01	78	55.1[a] (2.1)	50.1[b] (2.2)	75.3[c] (8.3)	81.8[d] (5.6)	54.6[a] (1.8)	96.9 - LS
M02	150	93.3[a] (3.3)	68.0[b] (6.0)	77.9[c] (7.7)	104.1[d] (5.6)	90.9[e] (7.7)	120.2 - IN
M03	162	90.4[a] (2.4)	77.1[b] (3.0)	122.5[c] (27.0)	142.3[d] (12.2)	86.0[e] (5.0)	187.8 - LS
M04	156	77.4[a] (9.1)	76.7[a] (10.6)	116.4[b] (30.3)	113.8[b] (27.6)	60.3[c] (3.2)	165.2 - LS
M05	142	100.3[a] (8.4)	97.2[a] (7.1)	124.5[b] (11.7)	120.3[b] (9.9)	105.9[c] (8.4)	155.7 - LS
M06	149	130.9[a] (4.0)	128.9[b] (5.1)	166.4[c] (11.6)	164.3[c] (10.2)	133.5[d] (7.7)	200.2 - LS

Notes: SWL: Safe Working Load. Abs. max (absolute max): highest tensile force recorded per cable line with indication of the element in which was recorded (LS= lateral skid, IN= inhaul). The values between the brackets report the standard deviations. The letters in the apices show the significance of the differences between the elements at line level tested through the Kruskal- Wallis and Mann-Whitney-Wilcoxon non-parametric tests because of ANOVA assumptions violations.

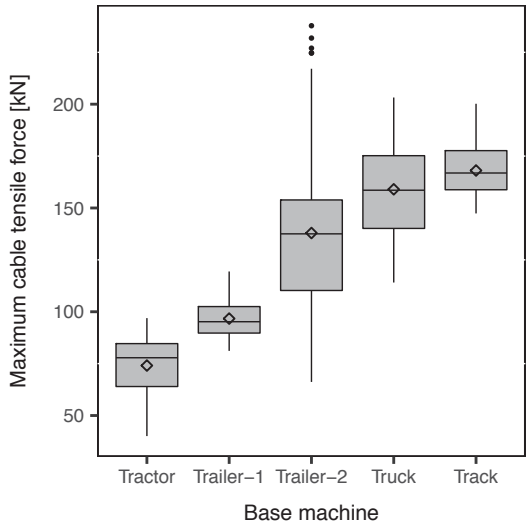

Figure 3.11: Maximum cycle cable tensile force recorded per base vehicle

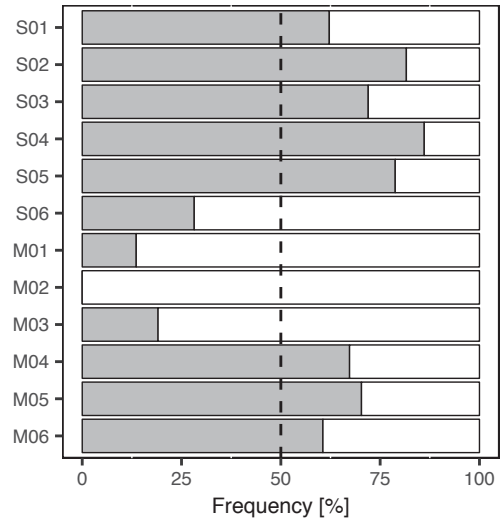

Figure 3.12: Work element frequency in recording the highest cycle tensile force between lateral skid (grey) and inhaul (white)

3.1.4. LATERAL SKID AND BREAK-OUT TENSILE FORCES

The average lateral skid peaks were statistically higher than inhaul peaks just in one cable line (cable line S02). However, in ten lines out of twelve the BOTF was the absolute maximum peak tensile force recorded per cable line (Table 3.3), Also, the BOTF during lateral

skid was the cause of exceeding the endurance limit in the six cycles in which this happened, suggesting this event as one of the most relevant aspects in the tensile force analysis of cable yarding operations.

Fifty-nine cycles in the cable-base case studies included a partial processing of the logs between lateral skid and inhaul, changing the typical work cycle organization. This was mainly because of the need of reducing residual stand damages while rotating the stems parallel to the skyline, operating with the whole-tree harvesting method in partial retention cuts. In these cycles, the estimated total load derived from the volume measurement at the landing was different from the load pulled during lateral skid. Thus, these cycles were excluded from the analysis of the BOTF.

Absolute maximum peak tensile force recorded per cable line at the break-out point ranged from 40 kN up to more than 237 kN (Figure 3.13). The tensile force increase at the break-out point (*BOTF increase*), expressed as the difference between BOTF and pretension, ranged from a minimum of 11.8 kN up to values exceeding 117 kN (Figure 3.14), with average values largely different between the cable lines. Similarly, the *BOTF increase factor*, expressed as ratio between BOTF increase and pretension, ranged from a minimum of 0.18 up to values of 2.30 (Figure 3.15), with 75% of the cycles, however, not exceeding a factor of one. The *BOTF increase index*, calculated as ratio between BOTF increase and estimated total load, ranged from 0.66 up to extreme values exceeding nine (Figure 3.16), with nearly 25% of the work cycles exceeding a value of four. Large differences were recorded considering the cable line configuration. On average, the BOTF increase index ranged between 1.5 to 2.8 in multi-span configurations, and between 2.1 to 4.6 in single span cable lines.

3.1.5. Inhaul and Maximum Cyclic Load Amplitude

The average peak tensile forces recorded during inhaul resulted statistically higher than lateral skid in one-third of the monitored cable lines and in three-quarter of the cable lines in which was recorded a significant difference between the two work elements (Table 3.3). Inhaul showed peak tensile forces ranging from 39 to 224 kN, following a general linear increment with the machine power and size.

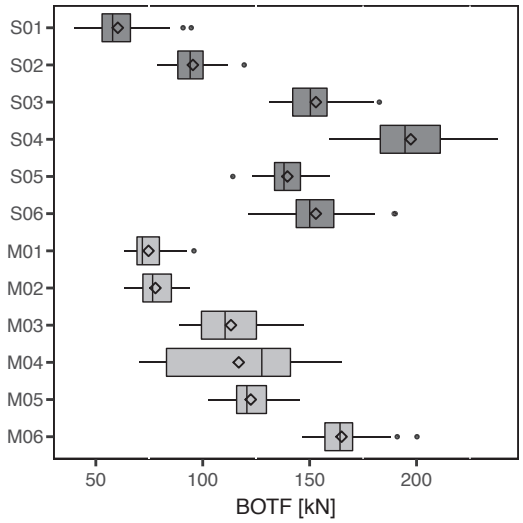

Figure 3.13: BOTF per cable line

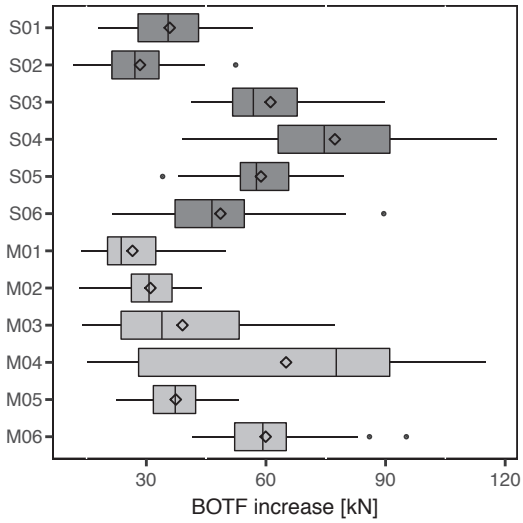

Figure 3.14: BOTF increase per cable line

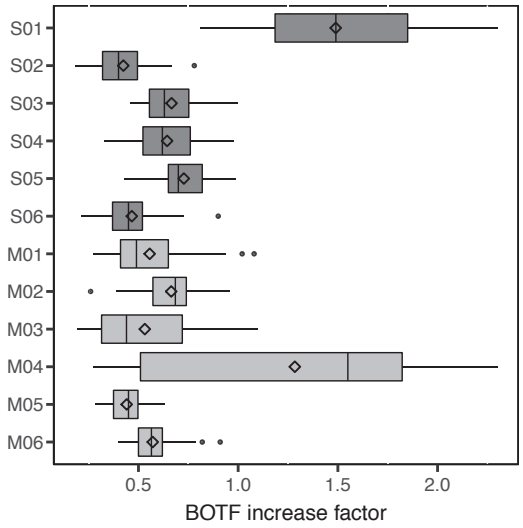

Figure 3.15: BOTF increase factor per cable line

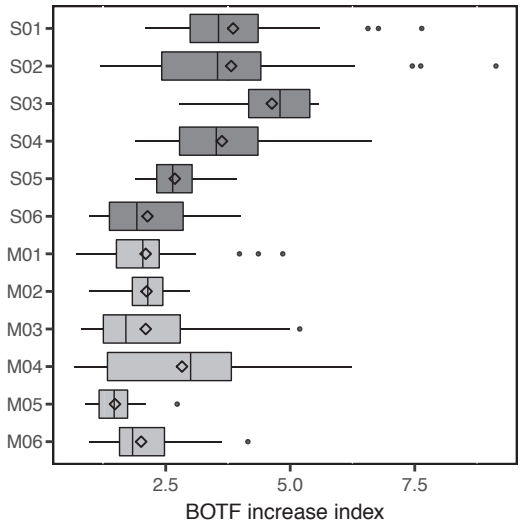

Figure 3.16: BOTF increase index per cable line

The inhaul was characterized by a cyclic load behavior for which was calculated, as reported by Pyles et al. (1994), its maximum cycle magnitude (MCLA) and the related factors and indexes. The inhaul MCLA ranged from 2.8 to 47.3 kN (Figure 3.18), with almost 85% of the work cycles recording values ranging from 5 to 25 kN. Magnitudes exceeding 30 kN were limited to 27 cycles distributed in five cable lines, two in single span configuration (cable line S03 and S06) and three in multi-span (cable line M03, M04, and M06). Also, for comparison, it was calculated the MCLA during outhaul, similarly to what was done in (Spinelli et al. 2017). The outhaul MCLA ranged from 0.5 to 17 kN and its difference with inhaul

MCLA resulted statistically significant, with inhaul recording values between 2.6 to 7.1 times outhaul (Table 3.4), suggesting a relevant effect of the transported loads.

The oscillation frequency of the cable tensile forces was similar, at line level, between outhaul and inhaul, even if three-quarter of the cable lines showed statistical differences. Average cyclic frequency during outhaul resulted generally briefly higher than inhaul, excluding two cable lines (cable line S05 and M04). The differences, however, were limited to cents of hertz. At general level, the cyclic frequency resulted 0.34 Hz during outhaul and 0.33 Hz during inhaul.

Inhaul MCLA was calculated also as ratio with other variables. The inhaul *MCLA factor*, expressed as ratio between inhaul MCLA and pretension, assumed values ranging from 0.05 up to 0.95 (Figure 3.19), with nearly 75% of the cycles recording values comprised between 0.10 and 0.30. The inhaul *MCLA index*, calculated as ratio between inhaul MCLA and the estimated total load, reported average values per line comprised between 0.55 up to 1.42 (Figure 3.20). The extreme values ranged from 0.21 to an extreme value of 3.82, recorded in a short single span cable line (cable line S02).

Also, it was calculated the ratio between inhaul MCLA and inhaul peak tensile force. This parameter resulted almost constant between the different cable lines, with average values ranging between 0.10 and 0.15 in ten cable lines out of twelve. Values larger than 0.20 were limited to 7.2% of the work cycles, most of them (4.0%) related to cable line S01.

Table 3.4: Maximum cyclic load amplitude and frequency in outhaul and inhaul

Cable	Mean - max MCLA [kN]		p-value		Mean frequency [Hz]		p-value	
line	Outhaul	Inhaul	t-test	MW	Outhaul	Inhaul	t-test	MW
S01	2.0 (0.7) - 3.6	12.4 (3.8) - 19.8	<0.001	-	0.36 (0.08)	0.36 (0.04)	0.780	-
S02	2.5 (1.1) - 7.1	9.7 (4.2) - 20.7	<0.001	-	0.47 (0.06)	0.43 (0.03)	-	<0.001
S03	5.4 (1.8) - 9.9	18.5 (6.8) - 30.0	<0.001	-	0.27 (0.01)	0.25 (0.01)	-	<0.001
S04	7.8 (2.4) - 13.9	19.0 (4.5) - 28.4	<0.001	-	0.35 (0.03)	0.35 (0.03)	-	0.969
S05	5.5 (1.7) - 11.1	14.1 (4.4) - 23.3	<0.001	-	0.34 (0.03)	0.36 (0.03)	0.025	-
S06	7.0 (2.8) - 17.0	26.3 (6.4) - 37.7	-	<0.001	0.39 (0.07)	0.36 (0.02)	-	<0.001
M01	1.6 (0.3) - 2.5	8.8 (2.7) - 15.8	-	<0.001	0.36 (0.02)	0.29 (0.01)	-	<0.001
M02	3.8 (1.9) - 10.8	8.3 (4.5) - 21.4	-	<0.001	0.36 (0.08)	0.34 (0.02)	0.513	-
M03	3.7 (0.6) - 5.7	19.6 (5.7) - 36.8	-	<0.001	0.30 (0.02)	0.29 (0.01)	0.012	-
M04	4.8 (1.9) - 11.0	18.1 (9.2) - 47.3	-	<0.001	0.29 (0.04)	0.32 (0.05)	-	<0.001
M05	3.7 (1.0) - 5.8	13.8 (4.1) - 26.7	<0.001	-	0.39 (0.04)	0.37 (0.03)	0.009	-
M06	7.2 (1.9) - 14.0	18.7 (6.4) - 33.1	-	<0.001	0.27 (0.01)	0.26 (0.01)	-	<0.001

Notes: The brackets report the standard deviations. The significance of the differences between the elements at line level were tested with paired t-test or, in case of assumptions violations, with the Mann-Whitney-Wilcoxon non-parametric test (MW).

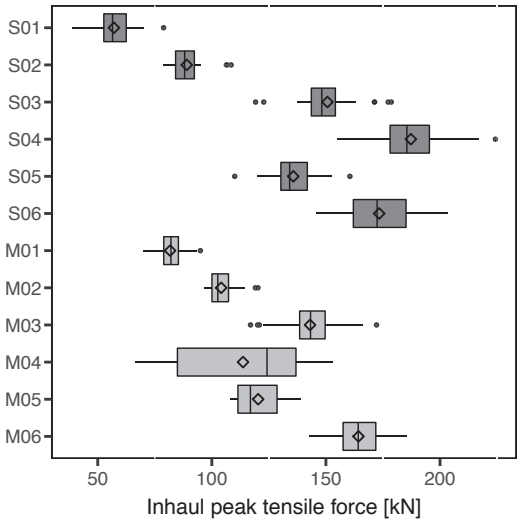

Figure 3.17: Inhaul tensile force per cable line

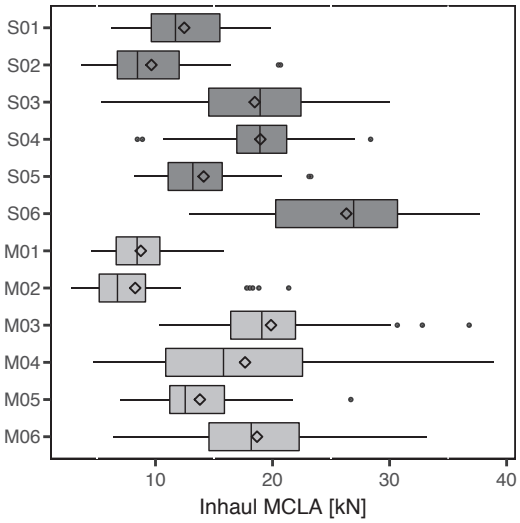

Figure 3.18: Inhaul MCLA per cable line

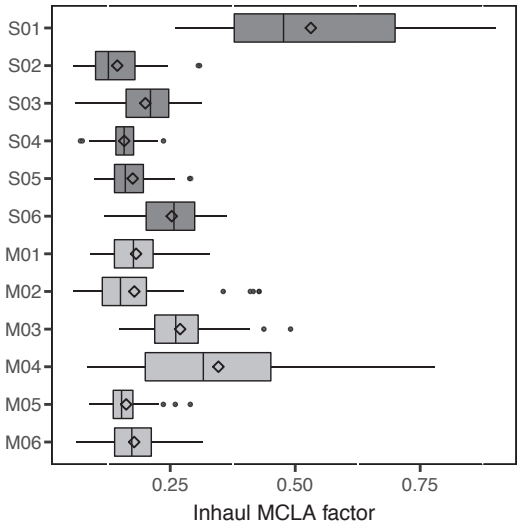

Figure 3.19: Inhaul MCLA factor per cable line

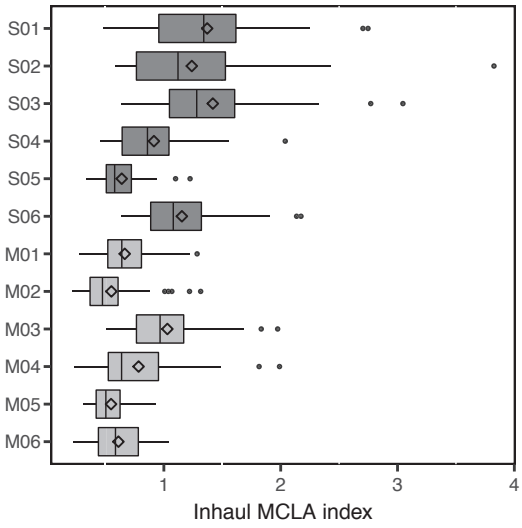

Figure 3.20: Inhaul MCLA index per cable line

3.1.6. REGRESSION ANALYSIS RESULTS

Random intercept linear mixed-effect models were applied on BOTF and inhaul peaks, as well as on dynamic amplifications factors and indexes, to identify the significant variables. This statistical tool allowed to analyze the dataset without averaging per cable line. Estimators, standard errors and significance of the explanatory variables are reported in Table 3.5. Table 3.6 shows the goodness-of-fit and the results related to the random effects.

The analysis of the BOTF recorded in the different work cycles (model A) was limited to the 443 cycles were the logs pulled during the lateral skid are the same size as the logs measured at the landing. The pretension, the estimated total load, the horizontal length of the span in which the lateral skid occurred and its slope, and the carriage position during lateral skid, expressed as percentage distance from the mid-span (0=at the supports, 100=at the mid-span), resulted significant variables able to explain, all together, more than 57% of the BOTF data variability. The estimators resulted positive for all of the variables, with exception of the span slope.

Both the BOTF increase and its log-transformed ratio with the pretension (*BOTF increase factor*) resulted affected by the same variables influencing the absolute value of BOTF (model B and model C, respectively) with the exception of the pretension which was not significant for the tensile force increase, and the span slope which was not significant for the log-transformed BOTF increase factor. The coefficient of determinations resulted very similar to model A.

The regression analysis of the log-transformed BOTF increase index (model D) showed as significant variables the pretension, the estimated total load, the horizontal span length, and the carriage position during lateral skid (expressed in terms of percentage distance from the mid-span). Also, statistical differences were recorded between single and multi-span configurations, where the load had a larger effect on the tensile force increase in single span cable lines. The pretension and the estimated total load reported negative estimators leading to a decrement of the BOTF increase index at higher values. This model explained nearly 60% of the data variability. Residuals plots of models A, B, C, and D are reported in Figure 3.21, Figure 3.22, Figure 3.23, Figure 3.24, respectively.

Similarly to the break-out analysis, random intercept linear mixed models were applied for identifying the main variables influencing inhaul peaks and MCLA, setting the cable lines as random factor. The log-transformed pretension, the log-transformed estimated total load, and the horizontal length of the main span crossed during the cycle resulted as significant variables in the regression analysis of the log-transformed inhaul peak tensile forces (model E), able to explain more than 72% of the variability.

Table 3.5: Explanatory variables of the random intercept linear mixed models

Model	Response variable	Explanatory variables						
		Coefficient	Unit	Estim.	SE	t-value	χ^2	p-value
model A	break out tensile force [kN]	pretension	kN	0.8612	0.1042	8.267	46.70	<0.001
		total load	kN	0.7538	0.0742	10.158	92.66	<0.001
		span length	m	0.2482	0.0166	14.959	179.59	<0.001
		span slope	%	-0.4366	0.1389	-3.143	9.74	0.002
		mid-span distance	%	0.2307	0.0221	10.430	97.17	<0.001
model B	break out tensile force increase [kN]	total load	kN	0.7481	0.0741	10.099	91.38	<0.001
		span length	m	0.2473	0.0167	14.847	178.04	<0.001
		span slope	%	-0.4812	0.1403	-3.431	11.59	0.001
		mid-span distance	%	0.2321	0.0221	10.499	98.26	<0.001
model C	LOG break out tensile force increase factor	pretension	kN	-0.0200	0.0026	-7.729	43.08	<0.001
		total load	kN	0.0149	0.0017	8.610	68.53	<0.001
		span length	m	0.0053	0.0004	13.635	154.83	<0.001
		mid-span distance	%	0.0055	0.0005	11.119	109.04	<0.001
model D	LOG break out tensile force increase index	pretension	kN	-0.0057	0.0019	-2.999	7.75	0.005
		total load	kN	-0.0302	0.0018	-16.737	215.30	<0.001
		span length	m	0.0048	0.0004	12.791	138.63	<0.001
		mid-span distance	%	0.0057	0.0005	11.084	108.23	<0.001
		span conf. (single)	-	0.2951	0.1120	2.635	5.00	0.025
model E	LOG Inhaul peak tensile force [kN]	LOG pretension	kN	0.4136	0.0431	9.587	82.57	<0.001
		LOG total load	kN	0.1571	0.0080	19.757	287.28	<0.001
		main span length	m	0.0026	0.0010	28.853	487.07	<0.001
model F	LOG Inhaul MCLA [kN]	total load	kN	0.0189	0.0022	8.624	68.07	<0.001
		main span length	m	0.0031	0.0004	7.306	50.70	<0.001
		span conf. (single)	-	0.3692	0.1463	2.524	5.11	0.024
model G	LOG Inhaul MCLA factor	pretension	kN	-0.0154	0.0028	-5.582	21.82	<0.001
		total load	kN	0.0186	0.0022	8.318	64.42	<0.001
		main span length	m	0.0033	0.0005	7.265	49.91	<0.001
		span conf. (single)	-	0.4619	0.1820	2.538	5.20	0.023
model H	LOG Inhaul MCLA index	total load	kN	-0.0274	0.0022	-12.647	138.45	<0.001
		main span length	m	0.0031	0.0004	7.401	51.91	<0.001
		span conf. (single)	-	0.4613	0.1385	3.331	7.82	0.005

Notes: LOG: log-transformation of the variable; Total load: estimated total load including logs load and carriage load; Span length: horizontal length of the span in which occurred the lateral skid of the logs; Span slope: slope of the span in which occurred the lateral skid of the logs; Mid-span distance: carriage position during lateral skidding, expressed as percentage distance from the mid-span (0=at the supports, 100=at the mid-span); Main span length: horizontal length of the main span crossed during the cycle.

Table 3.6: Random intercepts information and goodness-of-fit of linear mixed models

Model	N	Random intercept		AIC	BIC	L_M	L_0	R^2_{LM}
		variance	st.dev.					
model A	443	139.37	11.81	3395.8	3428.6	-1689.9	-1879.3	0.575
model B	443	168.13	12.97	3395.4	3424.1	-1690.7	-1874.6	0.564
model C	443	0.1019	0.3191	64.6	93.3	-25.3	-196.7	0.539
model D	443	0.0335	0.1831	95.4	128.2	-39.7	-242.1	0.599
model E	502	0.0336	0.1832	-1318.0	-1292.8	665.0	343.7	0.722
model F	502	0.0604	0.2458	341.4	366.7	-164.7	-224.4	0.212
model G	502	0.0912	0.3020	357.7	387.2	-171.8	-237.4	0.230
model H	502	0.0539	0.2321	330.1	355.3	-159.0	-248.2	0.299

Notes: N = number of observations; AIC = Akaike Information Criterion; BIC = Bayesian Information Criterion; L_M = log likelihoods of the model; L_0 = log likelihoods of the intercept only model; R^2_{LM} = coefficient of determination proposed by Magee (1990).

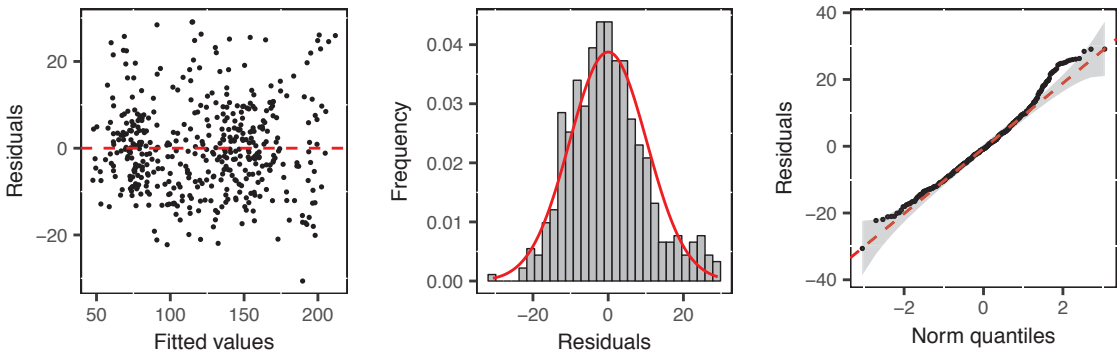

Figure 3.21: Residuals distribution plots related to Model A

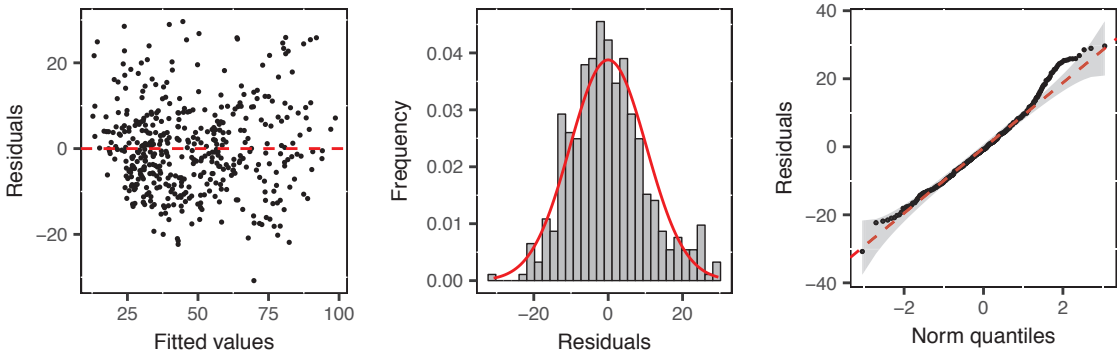

Figure 3.22: Residuals distribution plots related to Model B

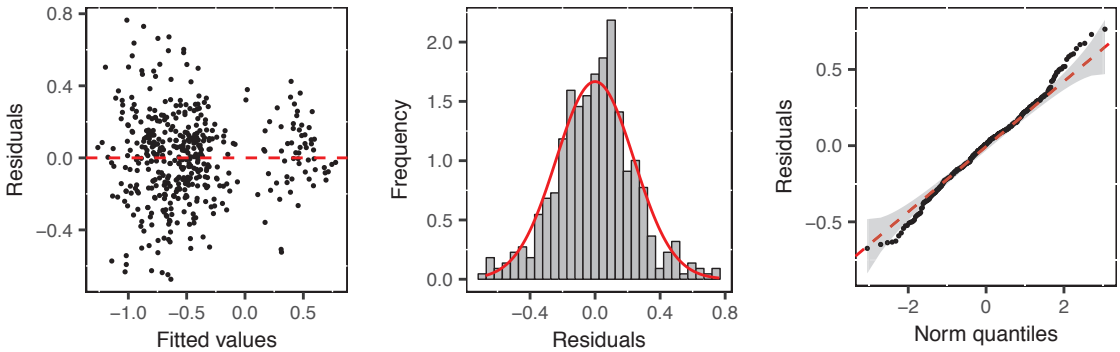

Figure 3.23: Residuals distribution plots related to Model C

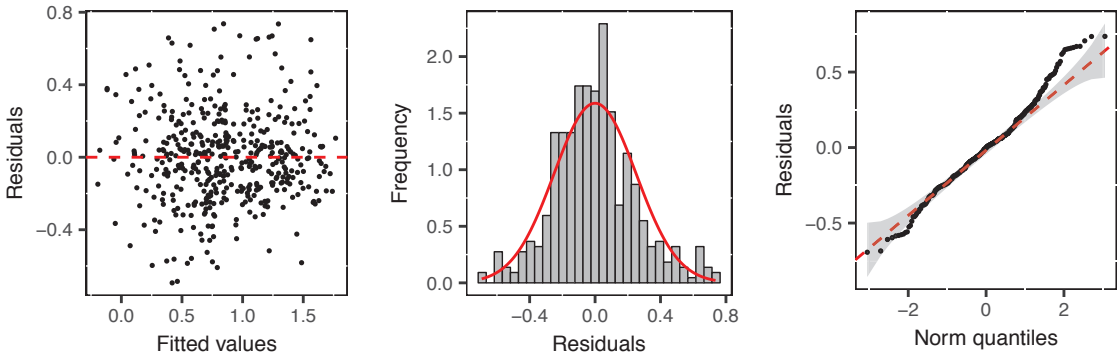

Figure 3.24: Residuals distribution plots related to Model D

A deeper analysis focused on the cyclic load behavior of cable tensile forces during inhaul. The estimated total load and the horizontal length of the main span crossed during the cycle, both reporting a positive estimator, were two significant variables in the regression analysis of the log-transformed inhaul MCLA (model F). Also, the cable line configuration was another significant variable, showing a broader effect on the cyclic load amplitude for the single span cable lines. These variables, all together, were able to explain only 21% of the observed variation.

Main variables influencing the log-transformed MCLA factor and the log-transformed MCLA index (model G and model H, respectively) resulted similar to the variable identified for absolute values of MCLA, with exception of the pretension which was significant for the MCLA factor. Also, the pretension for the MCLA factor and the estimated total load for the MCLA index assumed negative estimators. The coefficient of determinations, again, resulted grossly low for both the parameters. The MCLA index model showed the best goodness-of-fit in the MCLA analysis, being able to explain almost 30% of the observed variability. Residuals plots for model E, F, G, and H are reported in Figure 3.25, Figure 3.26, Figure 3.27, Figure 3.28, respectively.

3.2. RESULTS RELATED TO THE WINCH-ASSIST HARVESTING SYSTEMS CASE STUDIES

A total of 14.7 PMH_{15} of winch-assist forwarding operations were monitored, recording more than 5.3 million rows of tensile force data. The study included 28 forwarder loads drove by four different operators on eight different trails. All operators were less than 40 years of age and had at least two years' experience in winch-assist operations.

The number of cycles per site change considering the forwarder availability in the harvesting site in the monitored weeks. In the first two study sites (Site N and Site O) the forwarders actively operated for only one day, and the cycles were collected on one trail per site. In Site P, where the forwarder operated for the whole week, 19 loads on six different trails were monitored. The number of cycles per trail ranged from two to six.

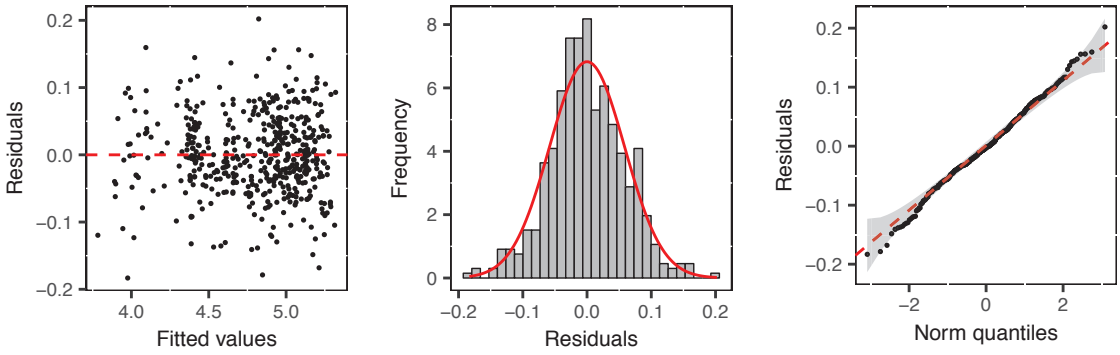

Figure 3.25: Residuals distribution plots related to Model E

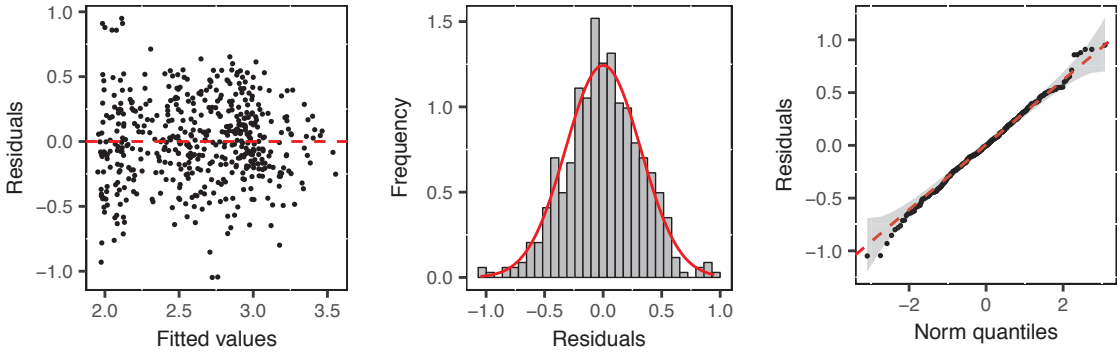

Figure 3.26: Residuals distribution plots related to Model F

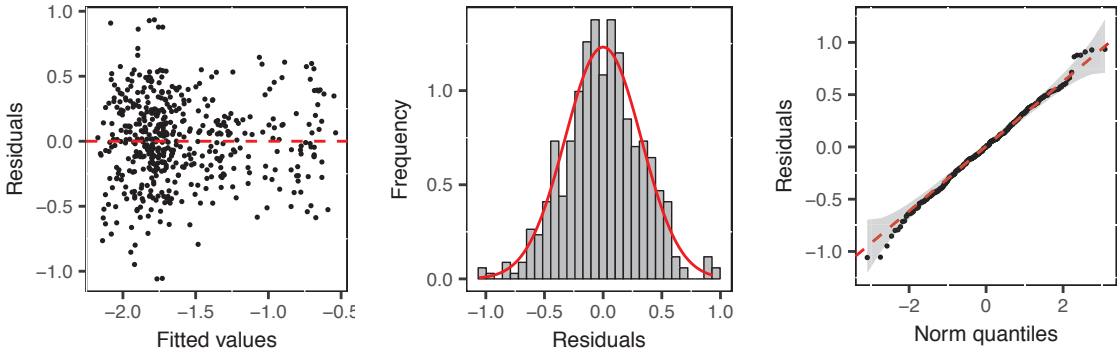

Figure 3.27: Residuals distribution plots related to Model G

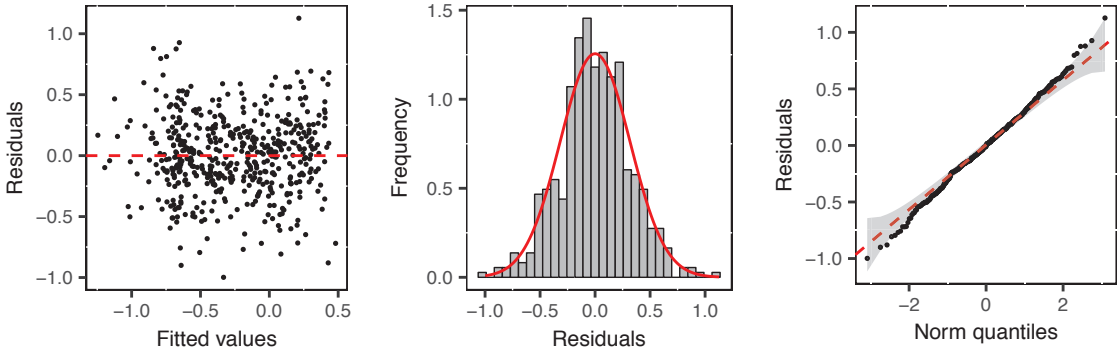

Figure 3.28: Residuals distribution plots related to Model H

The trails (Table 3.7) measured average slopes ranging from 25 to 45%, but in six of them the maximum slope exceeded 55%, with a peak of almost 76% in trail CR02. The horizontal length was longer than 200 m in seven trails, with a maximum of 260 m. Only trail CR05 recorded a shorter length (90 m). Downhill forwarding direction was the most commonly observed method (21 on 28 cycles).

3.2.1. TIME STUDY AND PRODUCTIVITY

The average delay-free work cycle was 30.8 $PMmin_0$ long, with loading accounting for more than one-third of the total time (Figure 3.29). Loading and unloading accounted for 52.2% of the total recorded time, while travelling was 44.8%. Delays shorter than 15 minutes were recorded in 57% of the work cycles, with an average duration of 1.53 minutes. Forwarders operated for 72.0% of the time on trails and 28.0% of the time on forest roads.

The total wood volume forwarded during the study was 523 m^3. Volume forwarded by trail showed a wide range, from 28 to 110 m^3, mainly because of the different number of cycles monitored per trail. The average wood volume extracted for each cycle was 18.7 m^3, ranging between a minimum of 10.9 to a maximum of 24.1 m^3 per cycle . A total of 1054 logs were counted and measured by photo analysis. The general average log size was 0.50 m^3, while a consistent difference was recorded between the trails.

The forwarder travel distances were measured as the horizontal distances from the forest road center line in proximity of the trail, assumed as the reference starting point. The

Table 3.7: Trails configuration and geometries

Trail	Operator	Forwarding direction	Ground slope			Horizontal length	Inclined length
			Mean	st.dev.	Max		
-	-	-	%	%	%	m	m
CR01	A–B	down	25.4	8.1	39.1	210.4	218.6
CR02	C	up	36.6	19.0	75.8	238.6	261.3
CR03	D	down	44.2	12.3	68.2	201.4	224.9
CR04	D	down	40.6	12.2	58.0	208.7	232.3
CR05	D	up	32.6	8.8	42.3	89.4	95.8
CR06	D	down	36.1	19.6	55.0	204.4	225.7
CR07	D	down	45.3	10.9	58.3	203.4	226.6
CR08	D	down	37.1	19.7	66.4	200.0	220.5

distance travelled on the trails, measured as the farthest loading point of the cycle, ranged from 43 to 203 m, with an average of 149 m. Forwarder distances travelled on the roads, measured as the farthest unloading point of the cycle, ranged from 14 to 204 m, with an average of 68 m. Details on the time study, load information and travel distances per trails are reported in Table 3.8.

Integrating the load information with the time study, the productivity recorded in the forwarding cycles ranged, on average, from 28 up to 46 m^3 PMH_{15}^{-1} (Figure 3.30), with a general mean value between the work cycles of 36 $m^3PMH_{15}^{-1}$.

Table 3.8: Average forwarding distance and load per trail

Trail	Total time	Work cycles	Work cycle duration	Trail distance	Road distance	Total wood volume	Load volume	Log size
-	PMH_{15}	no.	$PMmin_{15}$	m	m	m^3	m^3	m^3
CR01	3.5	6	34.7	142 (53)	61 (27)	95.9	16.0	0.34
CR02	1.6	3	32.5	137 (49)	75 (22)	50.6	16.9	0.22
CR03	1.1	2	31.8	159 (37)	24 (4)	32.7	16.4	0.55
CR04	0.9	2	26.6	149 (37)	37 (9)	28.7	14.4	0.50
CR05	1.8	4	27.4	80 (10)	47 (11)	84.4	21.1	0.74
CR06	2.1	4	31.6	169 (35)	139 (81)	75.9	19.0	0.66
CR07	2.8	5	33.8	195 (3)	64 (75)	109.8	22.0	1.02
CR08	1.0	2	30.6	165 (19)	61 (13)	45.0	22.5	0.95

Notes: The values between the brackets report the standard deviations

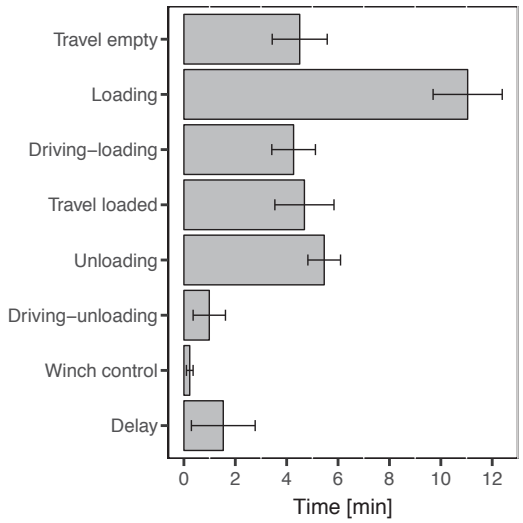

Figure 3.29: Work element time distribution in winch-assist forwarding

Notes: The error bars report the 95% confidence interval

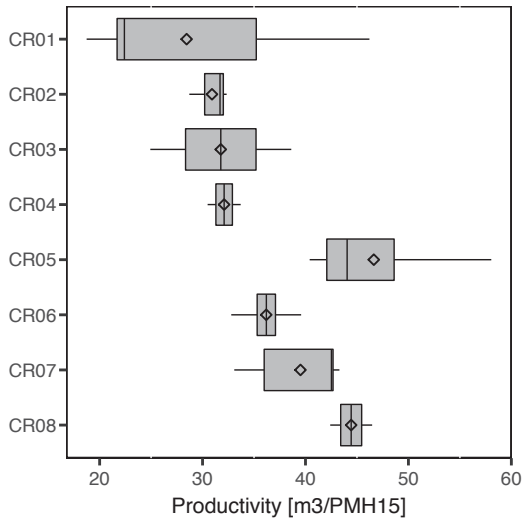

Figure 3.30: Winch-assist forwarding cycle productivity recorded per trail

3.2.2. CABLE WORKING LOAD AND TENSILE FORCE VARIABILITY

The cable working load distribution (Figure 3.31) showed a sort of bimodal shape, similar to the working load distribution presented by Holzleitner et al. (2018). A first peak at the lower working loads, ranging from two to five percent, and a second peak at a working load close to 25%. The maximum working load recorded in the study was 40.1%. Considering the cycle as the observational unit, however, the cable tensile force was lower than the SWL of the cable in almost all the cycles (Figure 3.32). Only four peak cycles, recorded in three different trails of Site P (trails CR03, CR05, CR07), reached and exceeded the SWL for a total of just 7.3 seconds.

The cable working load distributions by the trails (Figure 3.33) and their further decomposition in the different work elements (Figure 3.34) provided more information on the general cable tensile force distributions. The highest frequency, related to the lower working loads, resulted mainly due to the contribution of trail CR01 (Site N) - where the cable tensile forces were generally low - and to the contribution of unloading and driving-unloading occurred at the road side - where the tensile force generally ranged from 8 to 15 kN. The second frequency peak in the general cable working load distribution, related to working loads of approximately 25%, was mainly related to the cable tensile forces recorded during the work elements occurred on the steep trails, in particular in five trails of Site P (CR03,

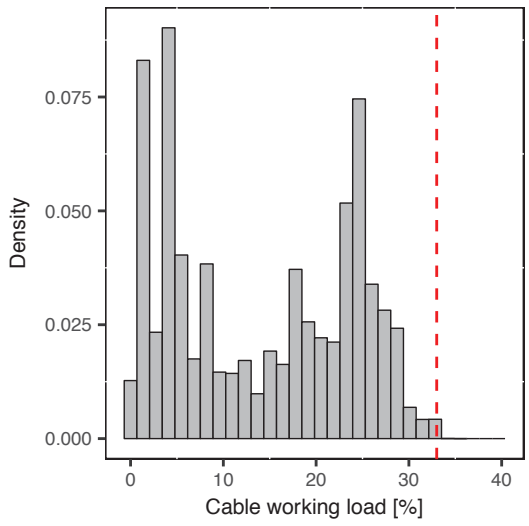

Figure 3.31: Cable working load distribution recorded in the whole dataset

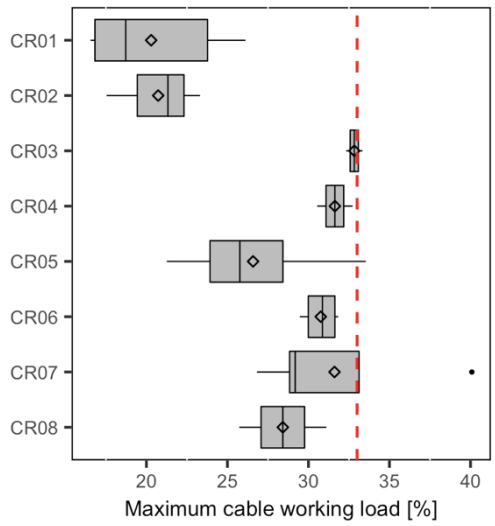

Figure 3.32: Maximum cycle cable working load distribution per trail

Notes: The dashed red lines indicate the cable Safe Working Load (one-third of the Minimum Breaking Load)

CR04, CR06, CR08). A more limited intermediate spike in the frequency of the cable working load, nearly to 18%, resulted mainly as a contribution from active work elements occurred on trail CR02, CR05, and CR07. The winch control element occurred most frequently while the forwarders were operating in the loading area, setting the winch considering the trail conditions. Thus, the cable working loads recorded during this element assumed values similar to loading and driving on the trails.

The cable tensile force behavior of a forwarder completing one cycle is shown in Figure 3.35. This example shows a forwarder starting from the forest road located at the bottom part of the block, moving empty uphill and forwarding logs downhill. The first five minutes of data show tensile force peaking and then receding to about 5 kN. This was because the forwarder had to return to the road and lower the tensile force because of the cable was wedged in a stump. When the cable was released, the tensile force was increased again for climbing the hill, moving the forwarders on its back side. The highest cable tensile forces were recorded while traveling empty uphill and driving between the first two load spots. Following, the forwarder started to move downhill, partially loaded, decreasing the cable tensile force. A sequence of several spikes between the loading and driving on the trail resulted as non-perfect synchronization between the machine movements and the winch. The cable tensile force decreased by approximately 10 kN when the forwarder began moving uphill after being stationary. Again, when the machine started moving downhill after a stationary element, there were positive spikes due to the machine moving in the opposite direction of the winch force. The cable tensile force fell to the lowest values when the forwarder reached the forest road for unloading the logs.

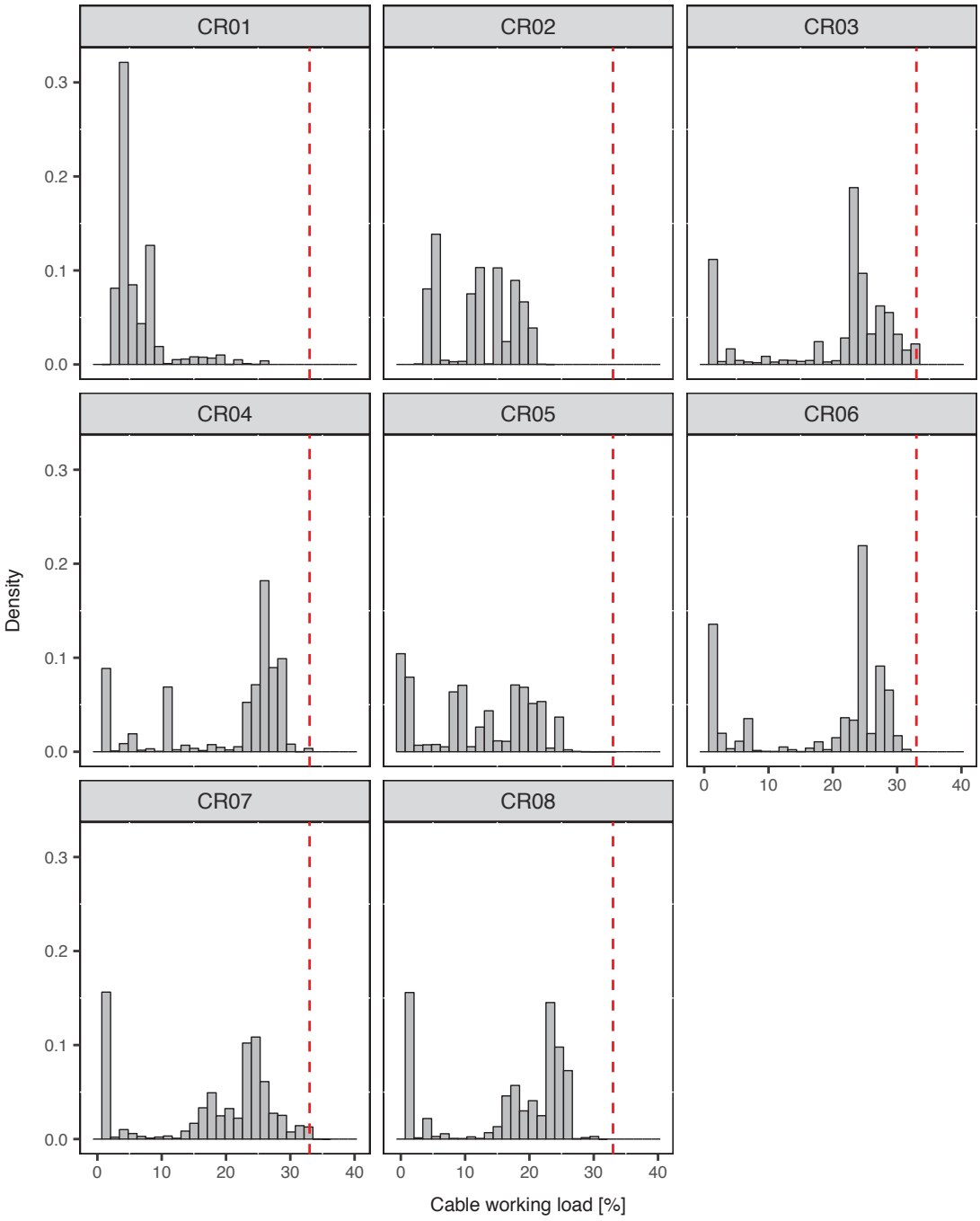

Figure 3.33: Cable working load distribution per trail

Notes: The dashed red lines indicate the cable Safe Working Load (one-third of the Minimum Breaking Load)

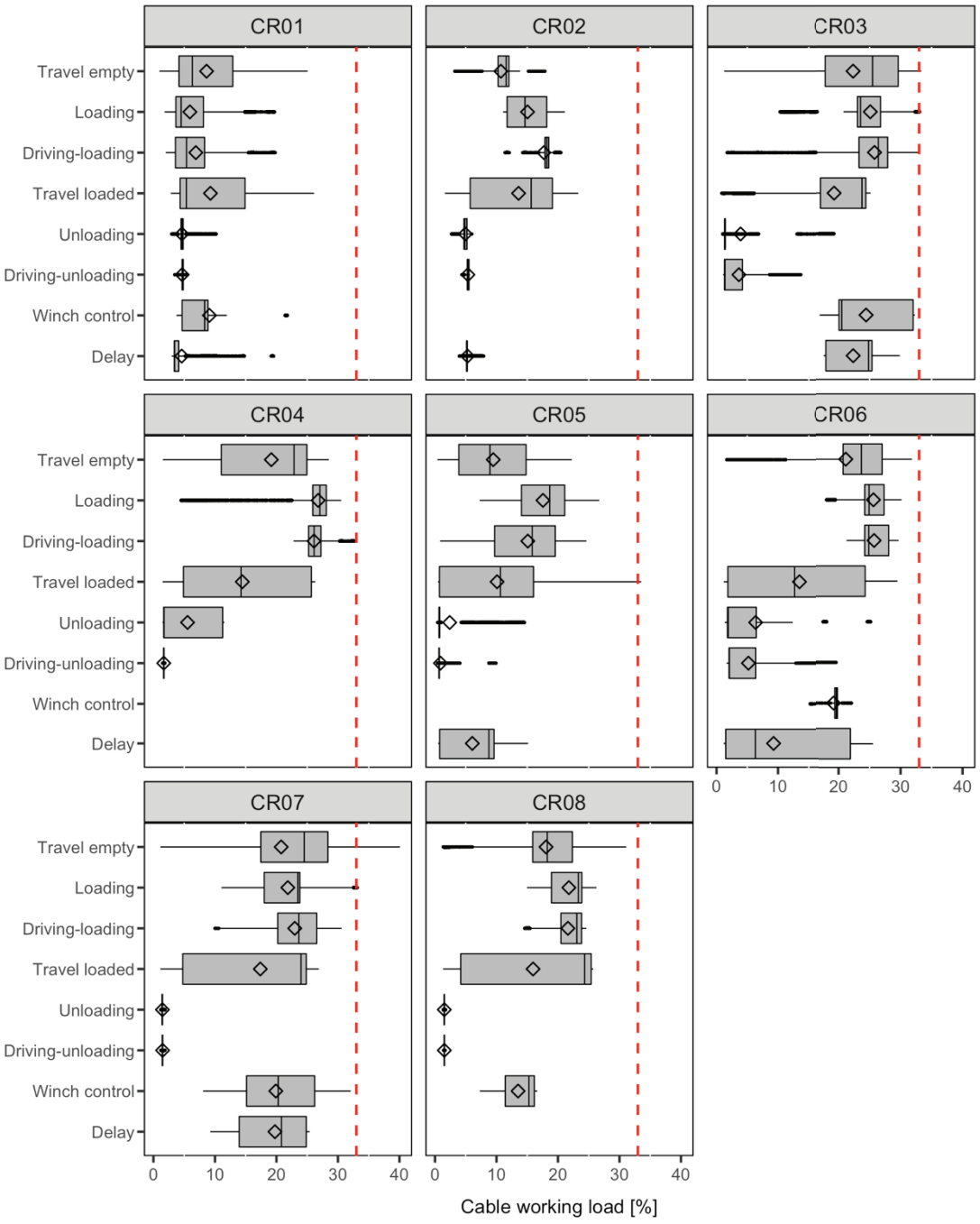

Figure 3.34: Cable working load distribution per trail and work element

Notes: The dashed red lines indicate the cable Safe Working Load (one-third of the Minimum Breaking Load)

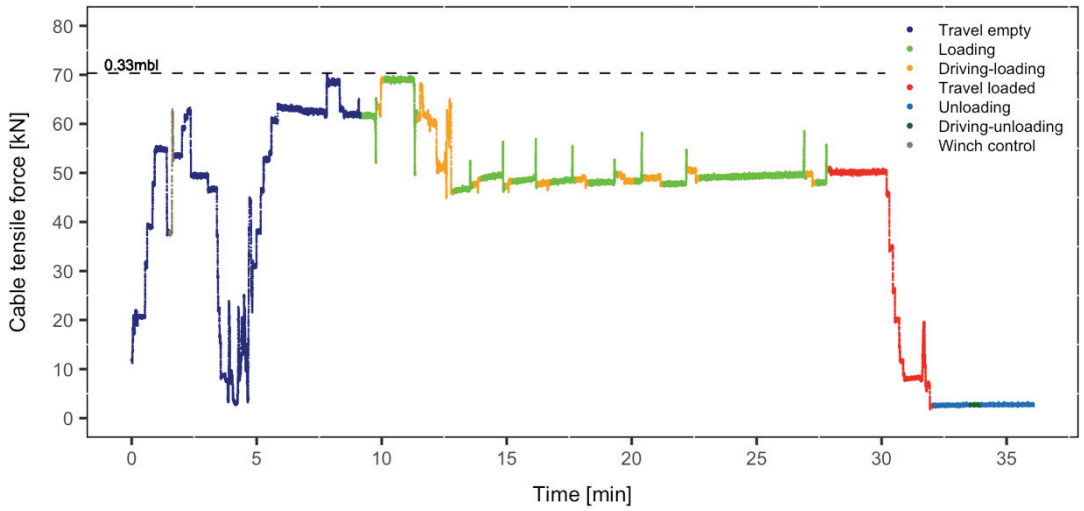

Figure 3.35: Cable tensile force plotted over the time for a whole forwarding cycle

3.2.3. MEAN AND PEAK CABLE TENSILE FORCES

The highest mean cable tensile forces were recorded for loading and driving between the different loading spots (driving-loading), considering both the whole set of data and the subsamples of downhill oriented cycles (logs forwarded downhill to the landing) and uphill oriented cycles (logs forwarded uphill to the landing). Lower and similar tensile forces were recorded for travel empty, travel loaded, winch control and delay. The minimum values were recorded for the unloading elements (unloading and driving-unloading) at the landing.

Regarding peak tensile forces, which represent one of the main concerns in tensile force analysis, on average, the highest and similar values were recorded again during the work elements operating on the steep trail and in particular during loading and travel empty. Travel empty was also the element during which recorded the highest peak tensile force of the whole dataset (84.6 kN). However, analyzing separately the subsample of uphill oriented cycles, the highest average peak tensile forces were recorded during travel loaded. These considerations suggested the absence of correlation between the total machine weight and the cable tensile force while prevailing the travel direction. Table 3.9 shows the results of the *Mann-Whitney-Wilcoxon* non-parametric tests which was applied instead of the ANOVA because of the violation of the normality of the data distribution and/or the homogeneity of the variance.

Table 3.9: Cable tensile force data aggregated per work element

Work element	Mean tensile force	Average peak tensile force	Max peak tensile force
-	kN	kN	kN
Travel empty	31.6 (14.85) [ab]	48.0 (17.4) [a]	84.6
Loading	38.5 (16.6) [b]	50.6 (14.6) [a]	69.9
Driving – loading	37.9 (16.4) [b]	46.7 (17.1) [ab]	69.6
Travel loaded	27.3 (10.9) [a]	46.2 (15.7) [a]	70.8
Unloading	8.1 (7.0) [c]	12.6 (13.4) [c]	53.1
Driving – unloading	6.8 (4.8) [c]	10.2 (10.2) [c]	41.4
Winch control	27.6 (14.4) [ab]	37.5 (21.2) [b]	68.2
Delay	25.0 (15.6) [a]	35.8 (16.3) [b]	63.0

Notes: Mean tensile force and Average peak tensile force represent the data aggregate per work element calculated as the mean of the different cycles. The Max peak tensile force represents the maximum tensile force recorded in the whole dataset for any work element (just one value for any work element). Between the brackets, it is reported the standard deviation. The letters close to the brackets represent the statistical differences between the work elements tested through the Kruskal- Wallis and Mann-Whitney-Wilcoxon non-parametric tests because of ANOVA assumptions violations

The frequency with which a work element recorded the highest cycle tensile force value in the cycle changed considering the forwarding direction. For uphill oriented forwarding operations, the maximum tensile force was mainly recorded during travel loaded (71.4%). Instead, for the downhill oriented operations, which represent the majority of the analyzed cycles, the highest cycle peak tensile forces were recorded during travel empty (47.6% of the cycles) and loading (28.6%).

3.2.4. WINCH SETTINGS SELECTED BY THE OPERATOR

Cable tensile forces in winch-assist harvesting systems were continuously selected by the operator who was driving the machine, considering the ground conditions. The settings choose by the operator, thus, had a direct effect on the cable working load. The analysis of the winch setting was based on the video analysis of the second camera installed in the forwarder cabs, linked to the time study of the forwarding operations. The data processing is very time-consuming, and the analysis was limited to one working day, recording 4.5 PMH_{15} of active logging operations. A total of eight cycles on two different trails were monitored: three cycles on trail CR06, five cycles on trail CR07.

The plot distribution of the winch settings (Figure 3.36) and the decomposition between the different work elements (Figure 3.37) highlighted the dominance of values ranging from 40 to 60 kN, related to the loaded phase on the steep trail, and a peak at 0 kN, related

to the operations at the forest road (unloading and driving-unloading). Winch-setting during travel empty and travel loaded recorded a more limited mean value because parts of these work elements were carried out at the forest road, where the cable was lowered to the ground. The differences between the cable tensile forces and the winch settings normally ranged between plus or minus 15 kN (Figure 3.38). An extra tensile force, ranging from 2 kN to 6 kN, resulted when the forwarders were operating at the forest road (Figure 3.39).

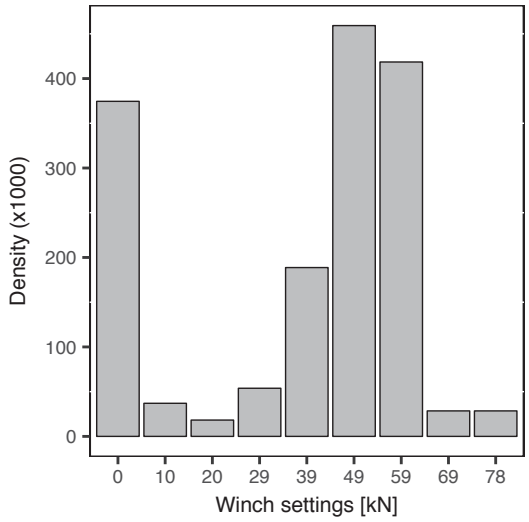

Figure 3.36: Density plot of the winch settings

Figure 3.37: Winch settings distribution per work element

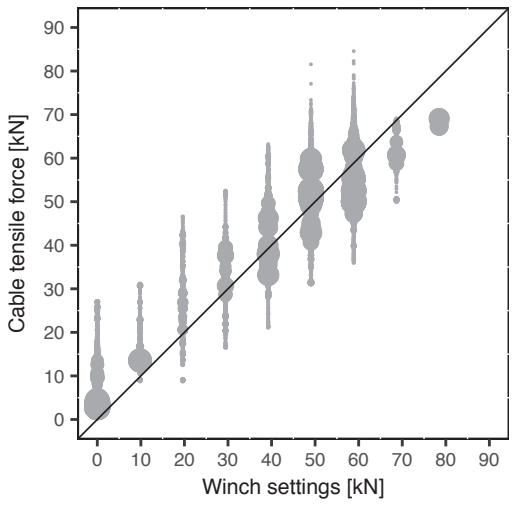

Figure 3.38: Relationship between cable tensile force and winch settings

Notes: The point size represents the point density

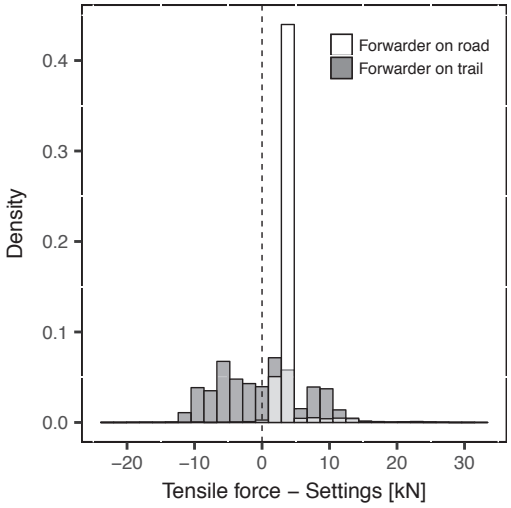

Figure 3.39: Differences between cable tensile force and winch settings

3.2.5. REGRESSION ANALYSIS RESULTS

Regression analysis was first applied on the highest cycle peak tensile force. Subsequently, considering the manageable dimension of data (less than six million row data), multiple regression analyses were applied at the whole dataset recorded with a frequency of 100 Hz in order to identify the actual cable tensile force values. Also, a separate analysis was dedicated to the winch settings and its relationship with the actual tensile forces. Estimates, coefficients, standard errors and significance of the explanatory variables are reported in Table 3.10. The coefficient of determination, the statistic parameters related to the different models, and the reference datasets are reported in Table 3.11.

At cycle level, no statistically significant relationships were found between the highest cycle peak tensile force and the load volume, as well as for the forwarding direction (uphill or downhill orientation) or the maximum trail slope. Only the average trail slope was significant (Model I), and able to explain 46% of the variability.

Table 3.10: Explanatory variables of the simple and multiple linear regressions

Model	Response variable	Explanatory variables					
		Coefficient	Unit	Estimat.	SE	t-value	p-value
model I	Max cycle cable tensile force [kN]	intercept		12.7523	9.5857	1.330	0.1950
		mean profile slope	%	1.2314	0.2617	4.706	<0.001
model L	Cable tensile force [kN]	intercept		6.1720	0.0270	228.906	<0.001
		ground slope	%	0.9355	0.0005	1864.653	<0.001
		travel direction (stationary)	-	-1.1999	0.0147	-81.805	<0.001
		travel direction (uphill)	-	3.6435	0.0181	201.255	<0.001
		anchor distance	m	-0.0505	0.0001	-411.133	<0.001
model M	Cable tensile force [kN]	intercept		5.4580	0.0075	727.120	<0.001
		settings	kN	0.8773	0.0002	5225.429	<0.001
model N	Cable tensile force [kN]	intercept		12.7150	0.0185	686.108	<0.001
		settings	kN	0.7390	0.0004	2042.367	<0.001
model O	Cable tensile force [kN]	intercept		12.2073	0.0200	613.451	<0.001
		settings	kN	0.7496	0.0004	1947.304	<0.001
model P	Residuals model M [kN]	intercept		-5.3312	0.0242	-219.943	<0.001
		slope	%	0.0974	0.0005	186.408	<0.001
		travel direction (stationary)	-	0.1478	0.0110	13.439	<0.001
		travel direction (uphill)	-	-0.5004	0.0125	-39.975	<0.001
		anchor distance	m	0.0087	0.0001	79.142	<0.001

Table 3.11: Goodness-of-fit and statistical parameters of the linear regressions

Model	Dataset	N	degree of freedom	F-statistic	p-value	R^2
model I	cycle aggregated data	28	1/26	22.14	<0.001	0.460
model L	limited to steep trail	3822.39 e^{+03}	4/3822.38 e^{+03}	929.37 e^{+03}	<0.001	0.493
model M	settings	1607.00 e^{+03}	1/1607.00 e^{+03}	27305.11 e^{+03}	<0.001	0.944
model N	settings, trails	1205.20 e^{+03}	1/1205.19 e^{+03}	4171.26 e^{+03}	<0.001	0.776
model O	settings, trails, active mov.	706.30 e^{+03}	1/706.29 e^{+03}	3791.99 e^{+03}	<0.001	0.843
model P	settings, trails	1205.20 e^{+03}	4/1205.19 e^{+03}	15668.37	<0.001	0.049

A similar coefficient of determination was recorded in the multiple regression analysis applied to the actual cable tensile forces. When the forwarders were operating on the trails, the slope, the travel direction, and the distance from the anchors (derived by the distance from the mid-road) resulted as the main significant variables influencing the cable tensile force and able to explain 49% of the data variability (model L).

In the subsample of data where setting information was analyzed, settings the operator choose were able to explain alone the 94% of the tensile force variability measured at the anchor (model M), representing the main variable in the cable tensile forces. The analysis of the elements influencing the residuals of the tensile force-setting regression did not show a satisfying result because of the limited data available (one-day recording on two trails). Slope, travel direction, and distance from the anchor were able to explain just 5% of the residual's variability. However, the same limited dataset explained only 15% of the cable tensile force variability - compared to the 49% of the whole dataset on the trail - and did not show a normal residuals distribution even if transformed.

Limiting the analysis to the subsample of data related on forwarding operations on the steep trails (thus excluding operations occurred when the machines were located on the forest roads), the relationship between the cable tensile force and the operator settings decreases in strength but still maintain high determination (model N). The relationship increased by considering just the data related to active machine movements uphill or downhill (model O). Residual plots of the models I, L, M, N, O, and P are reported in Figure 3.40, Figure 3.41, Figure 3.42, Figure 3.43, Figure 3.44, Figure 3.45, respectively.

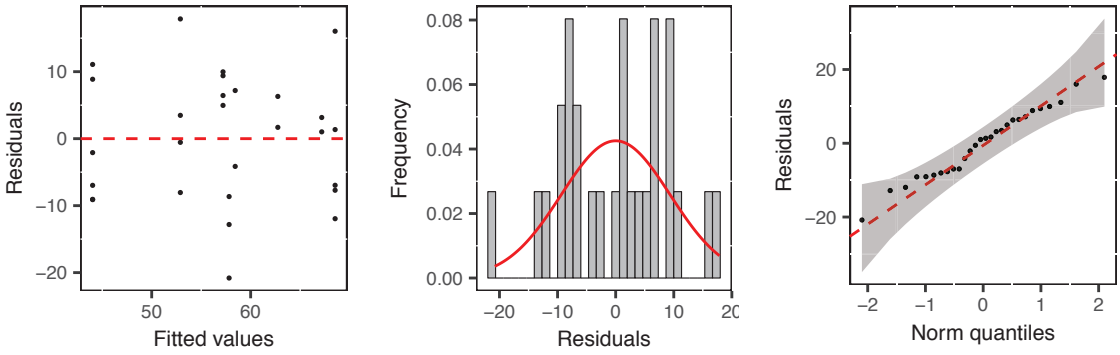

Figure 3.40: Residuals distribution plots related to model I

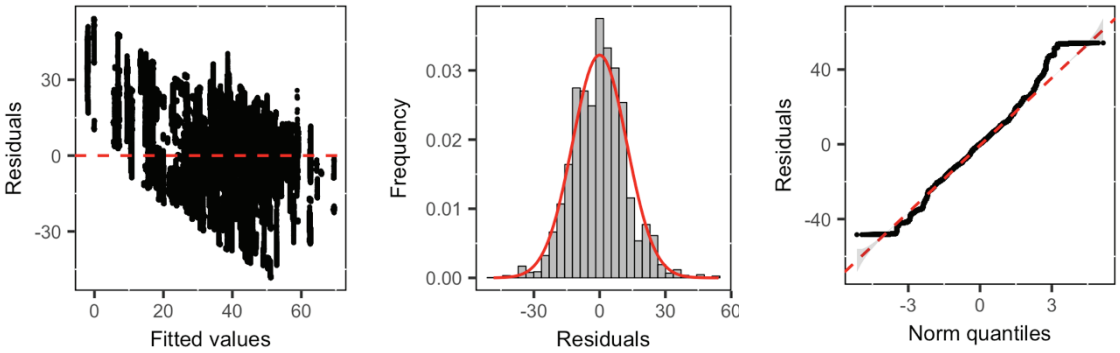

Figure 3.41: Residuals distribution plots related to model L

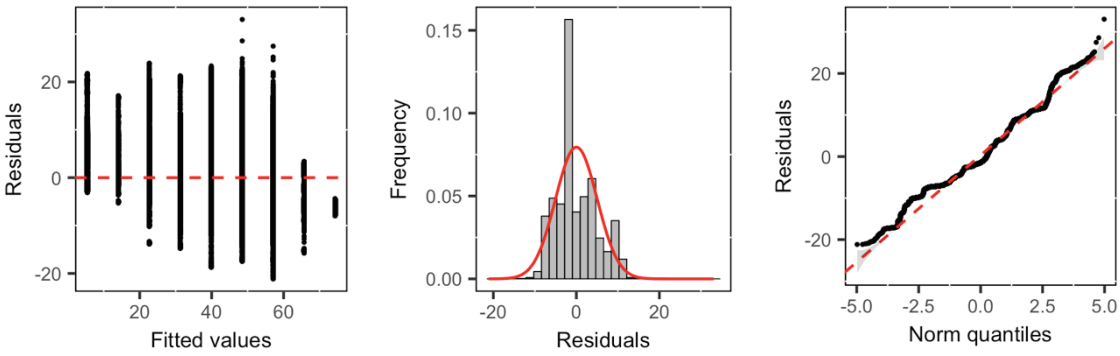

Figure 3.42: Residuals distribution plots related to model M

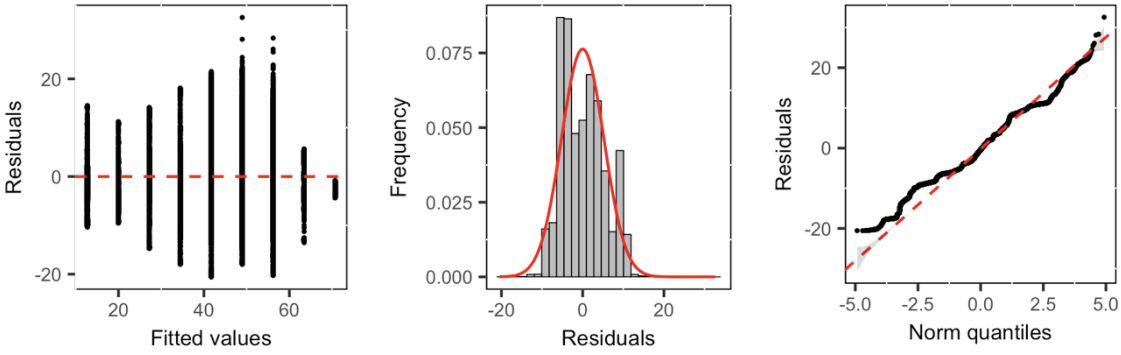

Figure 3.43: Residuals distribution plots related to model N

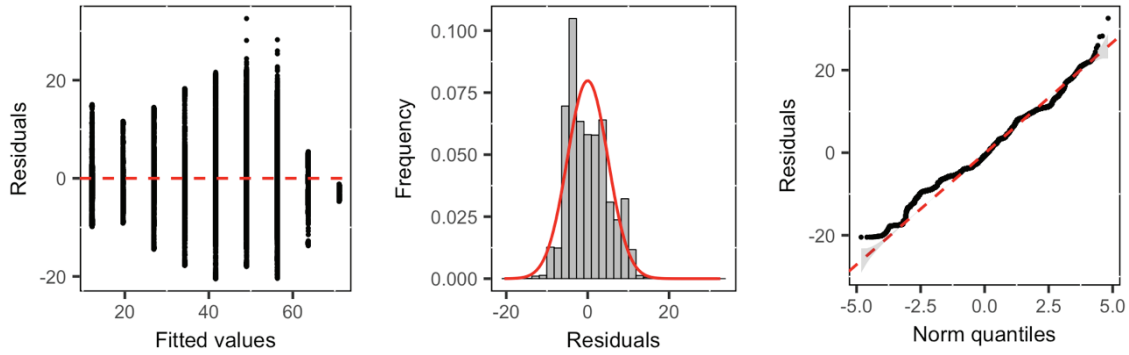

Figure 3.44: Residuals distribution plots related to model O

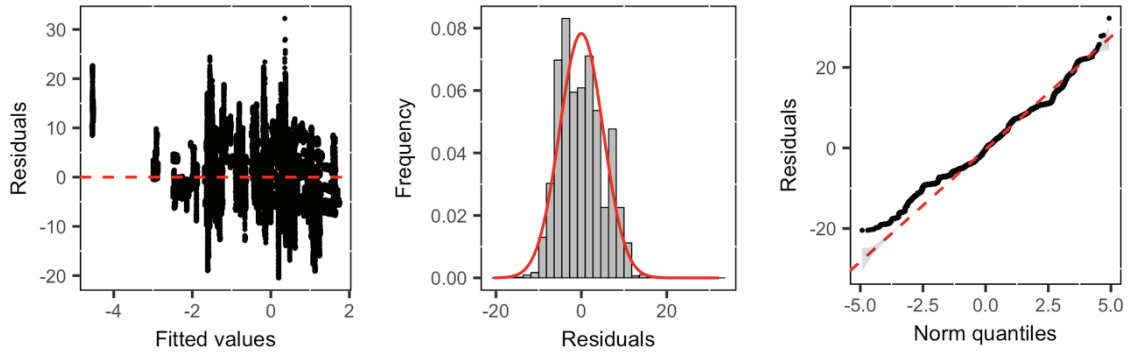

Figure 3.45: Residuals distribution plots related to model P

4. DISCUSSIONS

Cable tensile force monitoring on ordinary harvesting sites are limited due to the high costs and the specific equipment required for the analysis, as already mentioned by Dupire et al. (2015). Also, logging contract's collaboration and specific safety procedures and organization are required for effectively and safely collect the data. Thus, the main merit of this work was the extended and detailed analysis of cable tensile force behavior in steep slope forest operations, strongly enriching the available information related to the operational conditions in ordinary harvesting sites.

The analysis of two different steep slope harvesting solution was carried on different forestry conditions, in terms of both management systems and average block sizes. Significant differences were also related to the organization of the logging operations. These differences, however, did not exchange the cable tensile force behaviors, the issues on operating in steep grounds and the related safety considerations.

The observation of ordinary harvesting sites instead of a controlled environment did not allow to control or standardize the variables but had the merit to record actual operational conditions and analyze real behaviors. The high recording frequency (100 Hz) of cable tensile forces guaranteed the detection of the peak tensile forces, dynamic amplifications and shock events. The main weakness of the study, instead, was the payload estimation in cable logging operations and the volume estimation in winch-assist operations, based on unavoidable approximations. For the finality of the present study, however, the accuracy of these estimations was considered more than sufficient.

The clamped-on tensiometer resulted particularly suitable and efficient for the cable tensile force monitoring, with the possibility to monitor the logging operations without any interruption in the work cycles. The tensiometer, however, showed more troubles in

monitoring the support cable of winch-assist harvesting systems because of the particularly high risk of damaging the sensor. This is mainly because the cable is not stable in a fixed position, but it moves laterally following the machine movements, often directly in contact the ground. The cable movements, which are normally limited to few meters, largely increase when the machines move from the trail to the forest road and vice versa. A further element of potential risk of damage, mainly on the connections of the sensor, is represented by the abrupt released of the cable when stacked in a stump. The clamped-on tensiometer required particular attention to avoid damages in winch-assist monitoring but resulted particularly precise in recording the cable tensile forces. As reported also by Holzleitner et al. (2018), however, it is only usable on integrated-winch machines, where the cable is anchored to a tree or a stump and is not moving longitudinally on the ground. It is not usable for monitoring winch-assist solutions based on anchor machines.

While the general approach resulted efficient in the data collection, the main procedural limit in the analysis was the time-consuming of the video analysis to assess the time and motion studies of the logging operations and to identify particular events during the operations. The GNSS-IMU sensor was developed to facilitate this process. It allows the identification of about 90% of the different work elements (Lezier 2016), similarly to other prototype monitoring systems recently developed (Pierzchała et al. 2017). The automatic detection of the work element through the GNSS-IMU sensor, however, was considered not sufficiently accurate for the detailed skyline tensile force analysis. Moreover, due to the frozen conditions, this sensor was not suitable for the secure external installation on the forwarders, and it was set in the self-levelling and rotating cabs. Thus, pitch and roll information were not usable to measure the machine inclinations. The GNSS-IMU sensor, however, resulted particularly efficient in the medium-term machine monitoring, allowing continuous recording of carriage/machine position and inclination for several days without downloading any data or recharge the battery.

The number of observations was largely different between the two analyzed harvesting systems. The primary reason was the different accessibility to logging companies equipped with the two technological solutions. The standing skyline cable yarders are widely spread in the European Alps, in particular in Italy where there are more than 300 contractors operating with different cable systems (Spinelli et al. 2013). The winch-assist systems, as oppose, are still limited in Italy and the organization of the field studies required the

collaboration of foreign research institutions. Moreover, even if the number of days spent in the field was even larger for the winch-assist systems compared to the cable-based systems (15 and 14 days, respectively), the possibility to monitor effectively the integrated-winch forwarders was limited to seven days because of change in the logistics of the operations. Finally, a third reason of different amount of monitored work cycles between cable-based and winch-assist systems is the different average cycle time duration. Almost seven cycles per hour were recorded monitoring cable-based harvesting systems, while only less than two cycles per hour were recorded during winch-assist forwarding operations.

4.1. Discussions related to the cable-based harvesting systems case studies

The mobile tower yarders analyzed in this research include some of the most representative cable yarders used in the Alps and, in particular, in the Italian mountain regions (Mologni and Cavalli 2015; Mologni et al. 2017). The analysis of cable logging operations highlighted the large versatility of this harvesting solution, with applications from short distance wood extraction on trafficable terrain, up to long distances cable yarding in extremely steep and rocky grounds. Light, mean, and heavy machines were monitored exploiting from small broadleaves for woodfuel production up to large conifer whole trees for roundwood production.

The monitoring of ordinary harvesting sites allowed to record the actual operational conditions of different contractors in several applications and rigging configurations. The possible combinations of rigging configurations, machine size, and operational conditions in standing skyline mobile tower yarders, however, are wider than the analyzed case studies. Thus, this study is not representative of the whole possible applications of standing skyline logging, even if it provided a large improvement on the data available at international level. The large variability of case studies and cable lines did not allow to standardize any variable in the analysis, leading to a more complex analysis. This limit was addressed through the application of random intercept linear mixed-effect models, assuming the single cable lines as random factor.

At general level, the cable tensile force monitoring showed a large frequency in exceeding the recommended requirements during cable yarding operations. The SWL was exceeded in eleven of the twelve cable lines, during 55% of the 502 work cycles. This result is similar to previously published results. For example, Hartsough (1993) reported that up to 50% of the cycles recorded in twelve of 14 cable yarders exceeded the SWL. Harrill and Visser (2016) showed that 53% of 259 work cycles, across 14 of the 16 analysed cable lines, exceeded the SWL. Spinelli et al. (2017) reported a larger frequency of exceeding the SWL, ranging from 60 to 80% of the cycles, in the two tested applications. Exceeding of the recommended SWL is partially justified by the fact that adopting static empirical procedures for cable layout design, at operational level, the unavoidable dynamic forces may lead the peak tensile forces to exceed the statically calculated SWL. The current results, however, show peak tensile forces even exceeding the endurance limit (50% of MBL) during the break-out of the loads, mainly because of the improper selection of pretension and/or payload. The endurance limit is considered the working load which should never be exceeded because of the linked reduction of the economic rope lifespan and the increasing of the related potential safety risks (Wenger 1984).

The peak tensile forces shown in the present work are comparable with previous studies, functionally to the machine size considered by the different authors. Most of the work cycles monitored in the current study interested cable yarders equipped with 22mm-diameter skylines. Peak tensile forces operating with these machines exceeded 180 kN in five cable lines, with a maximum close to 240 kN. Smaller machines recorded lower peak tensile forces. For example, cable line S01, operating with a 16mm-diameter skyline, reached a maximum peak tensile force of 94.6 kN, not so different from the 80 kN reported by Pyles et al. (1994) monitoring a similar small-size machine. Spinelli et al. (2017), monitoring a 24mm-diameter skyline, recorded a maximum peak tensile force of 269 kN. Harrill and Visser (2016) reported even larger peak tensile forces related to the heavy New Zealand cable yarders.

As supposed, the highest peak tensile forces were recorded during lateral skid and inhaul. Lateral skid peaks were particularly relevant in single span cable lines, where the break-out of the loads caused the highest tensile forces recorded in the whole dataset and the most critical skyline working loads. Peak tensile forces at the break-out point resulted relevant also in multi-span cable lines, mainly in those cycles where the carriage was stopped close

to the mid-length of long spans. Inhaul peak tensile forces, as oppose, exceeded the lateral skid peaks when the hooking point was close to an intermediate support or, in case of multi-span configurations, when the hooking point was located in a minor short span. The absolute maximum peak tensile force recorded per cable line, however, was mainly recorded at the break-out point during lateral skid. This consideration is particularly relevant considering that the actual procedures for the skyline layout calculations do not consider the break-out tensile forces.

The BOTF and the MCLA recorded in the current work resulted in the same order of the values reported in previous publications (Table 4.1), functionally to the machine size analysed by the different authors. Only Harrill and Visser (2016) highlighted large differences in the maximum values reported in their paper. However, these largest dynamic amplifications were recorded monitoring a Falcon slackline rigging configuration, with a totally different functionality compared to a standing skyline system.

The BOTF did not differ significantly between single and multi-span configurations and resulted proportional to the machine size and power, directly correlated with the skyline capacity and maximum payload. Large differences, however, resulted from the set-up of the system and the operational conditions.

The pretension, the estimated total load, the span length and slope, and the carriage distance from mid-span were the significant variables in the BOTF analysis, able to explain more than 56% of the data variability. As a comparison, Spinelli et al. (2017) showed only the estimated total load as significant variables for the BOTF, able to explain 35% of the dataset. Harrill and Visser (2017) suggested the difficulty in lateral skid as a primary variable in the dynamic amplification during the break-out of the load. The difficulty of break-out

Table 4.1: Dynamic amplification results comparison with previous publications

Reference	BOTF increase		BOTF factor		Inhaul MCLA		In. MCLA factor	
	Mean	CV	Mean	CV	Mean	CV	Mean	CV
	kN	%	-	%	kN	%	-	%
Present work	27-77	18-49	0.4-1.5	19-52	8.3-26.3	24-54	0.2-0.5	24-56
Spinelli et al. 2017	60-71	-	1.0-1.1	-	25.6-30.4	37-46	0.3[1]	-
Harrill & Visser 2016	37-166	23-107	0.4-2.4	31-166	26.5-74.4	37-89	0.2-4.6	51-106
Pyles et al. 1994	13-14	56-66	0.5	76-79	13.6	40	0.4	36

Notes: [1] Calculated from the mean values reported in the paper; CV= coefficient of variation. The Table reports the minimum and maximum mean values reported in the papers for the different application/configuration considered in the research works. The present work results report the minimum and the maximum mean values recorded in the different cable lines.

was not considered in the present research because of its subjective nature and uncertainty in the estimation. However, it probably represents one of the main parameters in explaining the residuals of the identified model.

The large range of the BOTF between the different cable lines was strongly reduced considering the tensile force increase, for which the pretension did not result statistically significant. Pretension, thus, represented the baseline from which the estimated total load and the cable line geometry influenced the peak tensile forces. As a consequence, obviously, pretension was a significant variable for the BOTF increase factor, reporting a negative estimator.

The calculation of the ratio between BOTF increase and pretension (BOTF increase factor) showed only two cable lines (cable line S01 and M04) frequently recording values larger than one. Both of them were characterized by a ratio between the estimated total load and the pretension larger than 0.40, while this value in other ten cable lines ranged between 0.14 and a maximum of 0.32. The wide range in terms of BOTF increase and BOTF increase factor recorded in the cable line M04 was due to the different conditions in which were monitored the work cycles during two working days, as shown by the large standard deviation of the yarding distance (Table 3.2). The first monitoring session, related to the lower BOTF increase values, was localized in proximity of an intermediate support, between the first and the second span. In a second monitoring session, related to the higher BOTF increase values, the cycles were localized in proximity to the mid-length of the primary span of the cable structure.

Another relevant result of the break-out analysis is related to the ratio between tensile force increase and estimated total load (BOTF increase index). This parameter was also a function of the cable line configuration, with significantly larger values recorded for single span cable lines, where the peaks frequently exceeded a value of five. This is probably because in multi-span cable lines the intermediate supports absorb part of the static and dynamic forces occurring during the work cycles (Spinelli et al. 2017), and the tensile force increases are smoothed through the rope feeding from the conterminous spans, due to the skyline movement on the jack supports (Lysons and Mann 1967). Other works reporting a similar index are those related to the mainline and choker analysis (Henshaw 1977; Falk 1980; Peters and Biller 1984; Harrill and Visser 2017) showing amplification factors, calculated as ratio between mainline/choker tensile force and payload, ranging from 0.8 to four.

The analysis of the inhaul tensile forces showed a large effect of the interaction between the loads and the ground profiles. Inhomogeneities on the ground profiles, in particular, lead to the variation of the skyline catenary clearances and, sometimes, changes in the transportation system, from semi-suspended to fully-suspended and vice versa. This was the case, for example, of several cycles recorded in cable line S01, S06, and M03. The variations of the transportation system from semi-suspended to fully-suspended, in particular, caused the largest dynamic amplifications of the skyline tensile force during inhaul. This is shown in Figure 3.7, where the load, crossing a valley (shown in Annex 5), was abruptly enterally suspended to the skyline. At that point, the dynamic release of the logs to fully suspension led to a large increase in the magnitude of the tensile force and of the cyclic oscillations of the cable structure (MCLA). Several variables were calculated and considered in the regression analysis to take into account the interactions between the load and the ground profile, as for example the log length, the variation of the chord clearance, and the interaction between the two variables. However, none of them resulted statistically significant.

Inhaul peaks tensile forces reached absolute magnitudes comparable to the BOTF. Similarly to the results found by Spinelli et al. (2017), the log-transformed inhaul peak tensile forces were a function of the log-transformed estimated total load and the log-transformed pretension. Also, according to Fabiano et al. (2002, 2011), the length of the main span crossed during the cycle was another significant variable. The model was able to explain more than 72% of the observed variation. This is in line with the goodness-of-fit of the model identified by Spinelli et al. (2017), reporting a coefficient of determination equal to 0.689. The better prediction of the inhaul peak tensile force models compared to the BOTF ones could be related to the generally limited ratio between MCLA and peak tensile forces. The MCLA showed values mostly lower than 25 kN, similarly to the values reported by the other studies on standing skyline configuration, functionally to the machine size. These values resulted generally limited to 10-15% of the inhaul peak tensile forces. Thus, the parameters normally used in the static tensile force calculations were able to explain most of the observed variability. Limited peaks exceeding 30 kN were recorded in the single span cable line S06 and in the multi-span M03, M04, and M06.

The MCLA is a combination of the static engineering behaviour of the cable structure (mainly due to the skyline weight and the line geometry) and the effect of a concentrate

and moving load which interacts with the ground profile (Pyles et al. 1994). The complexity of this phenomena is witnessed by the very low coefficient of determination of the regression found in this research and in previously published papers. The significance of the cable line configuration variable, which highlighted for the same load and span length a more limited dynamic amplification (in terms of absolute and relative values) for multi-span cable lines, was particularly interesting. This effect, again, could probably be due to the damping capacity of the intermediate supports (Pyles et al. 1994). As a comparison, Spinelli et al. (2017), analysing a single span cable line, detected as significant variable for inhaul MCLA only the estimated total load, with a very limited goodness-of-fit (R^2 lower than 0.10). Harrill and Visser (2016) affirmed a larger inhaul MCLA for semi-suspended loads. The transportation system, however, did not result significant in the current dataset, probably because of the limited number of fully-suspended loads. Moreover, contrary to what was supposed by Pyles et al. (1994), the pretension did not result as a statistically significant variable for MCLA, even if it apparently showed a brief positive trend. It was significant in the MCLA factor analysis.

MCLA was mainly recorded at the mid-length of the main span crossed during the work cycle, in the proximity of the largest peak tensile forces. The inhaul peak tensile force variable, however, was excluded from the analysis because directly correlated with the estimated total load. Largest values of MCLA seemed mainly related to the dynamic load movements caused by the interaction with the ground.

The MCLA factor resulted almost constant between the different cable lines, excluding values recorded in the cable lines S01 and in M04. Cable line S01, in particular, reported an average value more than double compared to the general average. As described in the discussion of the BOTF increase factor results, these two cable lines showed the highest ratio between estimated total load and pretension. No publications reporting a comparable MCLA index were found in the literature.

The oscillation frequency of the cyclic load during inhaul was, on average, 0.33 Hz, ranging between 0.25 and 0.43 Hz, on average, between the different cable lines. These data derived from the average cyclic period, identified in the inhaul peak and valleys detection during the MCLA analysis, and not from a spectral analysis of the dataset. The results are comparable with the 0.40 Hz discussed in the oscillation analysis by Visser (1998), while quite a bit lower than a frequency of 0.55 Hz reported by Pyles et al. (1994). These latter

authors, however, referred to a single span line configuration shorter than 100 m, which tent to oscillate at higher frequency.

Both single and multi-span were considered in the present work, while most of the previous studies on tensile force monitoring focused on single span configurations. Results confirmed the single span configuration as the most critical condition regarding the skyline tensile forces, even if not in terms of absolute peak. Main differences resulted in the BOTF increase index and in the MCLA. In multi-span cable lines, the damping effect of the intermediate supports as well as the rope feeding of the conterminous spans significantly reduced the tensile force increase and the magnitude of the oscillations of the cable structure.

4.2. Discussions related to the winch-assist harvesting systems case studies

The cable tensile force analysis of winch-assist harvesting systems focused on large integrated-winch forwarders operating in extended Canadian clear cuts. The standardization of the machine type allowed to simplify the data elaboration processes, applying simple and multiple linear regressions without consideration of any random factors. As oppose, however, this work investigated the cable tensile force only on a very specific option between the multiple possibilities available in the market, in term of machine size and winch-assist systems.

The discussion of the cable tensile force monitoring results for winch-assist logging operations cannot be referred to research works carried out during the last 25 years, as done for the cable-based harvesting systems. Only one recent scientific publication reports tensile force monitoring of integrated-winch forwarders (Holzleitner et al. 2018), focusing on the methodological approach. Also, brief data related to integrated-winch machines are reported in some technical reports elaborated by the *KWF* (Weise and Burk 2011, 2016; Debnar 2014).

The integrated-winch forwarders were observed operating on trails in which the maximum slope was at least almost 40%. No winch-assist operations were observed at lower slopes because in these conditions cheaper conventional systems easily operated.

Most of the cycles were downhill-oriented. The operators noted this is because of lower fuel consumption, better traction, and overall improved efficiency compared to uphill forwarding. Even if downhill oriented, however, the contractors always provided an access road or a back trail to quickly access the anchor at the top of the block. In Central European application (Holzfeind et al. 2018; Holzleitner et al. 2018) reported a frequent use of a strawline for set-up the system, starting from the road located at the bottom of the block up to the anchor. This was not recorded in the present study.

The analysis of the cable tensile forces and time duration per work element was function of the priority assigned. Loading resulted the longest element in the average work cycle and the work element in which were recorded several tensile force spikes. The spikes, however, included tensile forces of forwarders which were moving along the trail but still were completing the loading of the logs. A different definition of the priority between the different work elements, thus, could differently distribute the tensile force and the duration between the loading and the driving-loading elements.

The maximum recorded cable tensile force was 84.6 kN, corresponding to a cable working load of 40.1%, which is larger than the maximum working load recorded by Holzleitner et al. (2018) in Central European winch-assist forwarding. However, exceeding of the SWL was limited to less than 15% of the work cycles and for an extremely limited time.

Considering the cycle as the observational unit, the highest cycle cable tensile force did not resulted function of the maximum slope of the trail, as it was initially supposed. The only significant variable was the average ground slope. While the slope was measured at any significant slope change in the ground profile, micro variations related to the presence of obstacles (e.g., stumps) could generate limited extreme climbing conditions, leading to an increase of tensile force even on the trail sections with a general more limited slope. Average trail slope resulted a better indicator of the potential presence of critical spots in the trail.

The cable tensile force distribution per work element, resulted generally in line with the paper published by Holzleitner et al. (2018). Largest tensile forces were recorded while the forwarders were moving uphill, during travel empty for downhill oriented operations, and during travel loaded for the uphill oriented ones.

The regression analysis applied to the whole dataset showed the actual cable tensile force as a function of local trail slope, travel direction, and anchor distance. While increasing

slope is easily connected to the cable tensile force increase, the reduction in the cable tensile force at an increased distance from the anchor could be mainly connected to losses due to the friction of the cable on the ground, which exceed the effect of tensile force increasing due to an increased difference in altitude (rope weight effect). The increase in the cable tensile force moving the forwarders uphill could be associated with the necessity to contrast the slipping of the wheels. Moreover, there is also a technical reason why maximum tensile force moving uphill and downhill were different. The Haas winch has a maximum pulling force of 90 kN moving uphill (wrapping up the cable) but a pulling force of just 60 kN while moving downhill (unwinding the cable).

A more detailed analysis showed the winch settings the operators choose as the main variable in the determining the cable tensile forces. The difference between the actual tensile forces and the winch settings were mostly lower than 10 kN. A negative difference was mainly recorded while the forwarders were operating on the steep trails, where the rope was strongly pressed to the ground and the friction reduced the tensile force measured ad the anchor. While the forwarders were unloading at the forest roads, considering most of the cycles where downhill-oriented, they were located at about 50 m less in altitude and 200 m far from the anchor and the tensile force measuring system. The weight per unit of length of the cable, multiplied for the difference in altitude and reduced by the partial force losses due to the friction on the ground (limited in case of very low tensile forces), caused this almost constant extra tensile force during unloading at the forest road. Residuals larger than 25 kN were recorded only in 5.53 seconds, corresponding to 0.03% of the total recorded time in which the settings information are available. These limited differences, distributed in three different cycles, could also be related to a non-perfect synchronization at cents per second of the winch control systems and the analysis procedures.

Regarding the analysis of the winch settings the operator chose, the limited availability of data usable for the analysis, reduced to one working day on two different trails, was not sufficient for identify any significant variable.

5. CONCLUSIONS

Cable tensile force monitoring has an important role in assessing long-term cable performance and developing safety guidelines for cable-supported steep slope forest operations. This research allowed to collect relevant and primary data on cable tensile force behavior, focusing on standing skyline mobile tower yarders and integrated-winch forwarders. The results largely extended the limited information available for ordinary logging operations in real harvesting sites.

Regarding the cable-based harvesting system case studies, twelve different cable lines, for a total of 502 work cycles, were analysed. Results showed a broader effect of dynamic amplifications connected with a frequent exceeding of the safety limit, partially reaching critical values. The study, in particular, highlighted the difficulties of experienced logging contractors to keep the skyline tensile forces lower than the recommended safety limits. Working loads exceeding 40% and 50% (endurance limit) of the skyline MBL, seems mainly due to the low perception of the operators regarding: i) the effects of payload, pretension, line geometry and configuration to the actual skyline tensile forces; and ii) the magnitude of dynamic amplifications, mainly during the break-out of the loads. This consideration suggests, at a general level, the need for a larger effort to promote best practices in cable yarding.

Also, the results showed that the use of slip brake to the skyline drum was mostly ineffective to prevent the largest peak tensile forces, probably because of the use of clamped carriages. This common type of carriage leads to different tensile forces during lateral skid (and thus during the break-out of the loads) in the two sections of skyline separated by the clamps of the carriage, as shown by Miles et al. (1993) and Tuor et al. (1998). This aspect should be considered in the discussion about the update of the European Union legislation

currently oriented on changing the safety factor from three to 2.5 for the cable yarders equipped with a calibrated slip break on the skyline drum (CEN 2017).

The complexity in identifying reliable theoretical models including the dynamic amplifications, the inefficacy of the current load limiters, and the low perception of several operators regarding the magnitude of skyline peak tensile forces and dynamic amplifications also suggest the necessity to adopt solutions for the continuous tensile force monitoring through systems mounted at the tail anchor and able to record the peak tensile force even while working with automatic clamped carriages. The continuous tensile force monitoring, proposed since at least 25 years, could help the cable logging system to maintain its social and economic acceptability, improving the safety of the operations and, at the same time, improving their efficiency.

Cable tensile force monitoring of integrated-winch forwarding operations analyzed 28 work cycles on eight different trails. The study showed cable tensile forces never reaching extreme peak values or critical conditions. Most of the work cycles recorded tensile forces lower than one-third of the MBL of the cable, which is for example the legal requirement in New Zealand (MBIE 2012). The discussion of the safety requirements for traction aid winches at international level, however, is considering a safety factor of two, assuming the cable only as a support to the traction (ISO 2018). Thus, the tensile force recorded in the monitored case studies largely satisfied these potential legal requirements.

A primary result of this study was that the winch settings chosen by the forwarder operators account for most of the tensile force variability, suggesting the need for a primary consideration of the human factor in the safety procedures. A deeper investigation should also focus on the analysis of the relevance of the operator experiences in winch-assist operations and its relationship with the settings chosen. The present study involved four different operators. However, all of them had a similar age and experience, and most of the cycles were drove by the same operator. The analysis of the winch settings the operator choose should be properly expanded, identifying an alternative more efficient and less time-consuming procedure able to automatically record the data.

No clear dynamic amplifications resulted from the cable tensile force analysis of winch-assist forwarder, were the cable should only provide an assistance to the vehicle traction. Only a series of short duration spikes in the cable tensile force was observed when the

forwarder started moving between the loading spots. This was attributed to a time lag between when the wheels started moving and the response of the winch, indicating synchronization between the winch and the wheel movement was not perfectly matched.
The cable tensile force monitoring on integrated winch-forwarders carried out in this research referred to a limited number of work cycles and operational conditions and cannot be considered representative at general level. Operators indications highlighted potential critical conditions in case of operator errors or winch malfunctions or failures. Thus, further analyses should deeper investigate the cable tensile force related to the use of winch-assist systems in steep slope forest operations.
A larger effort, in particular, should focus on extending the cable tensile force monitoring to the anchor machine based winch-assist option, single and double cable solutions, and to the analysis of integrated-winch harvesting machine for which there is still an extremely limited information available. Research should also consider the development of protocols to analyze localized cable damages which could represent the worst safety limits in winch-assist operation based on integrated-winch machines.

Finally, the analysis of steep slope harvesting operations based on the use of both cable-based and winch-assist harvesting solutions showed the needed of improving the analysis and knowledge of the anchoring capacity of trees and stumps in forest operations, for which there is an extremely large gap of knowledge in the literature, and for which there is large uncertainty throughout the operators.

6. REFERENCES

Ackerman S., Immelman A., McEwan A., Naidoo S., Upfold S. (Eds.). (2017). ***South African cable yarding safety and operating handbook***. Forest Engineering Southern Africa and Institute for Commercial Forestry Research.

Acuna M., Bigot M., Guerra S., Hartsough B.R., Kanzian C., Kärhä K., Lindroos O., Magagnotti N., Roux S., Spinelli R., Talbot B., Tolosana E., Zormaier F. (2012). ***Good practice guidelines for biomass production studies***. (Magagnotti N. and Spinelli R., Eds.). Sesto Fiorentino (FI) Italy: CNR IVALSA.

Alam M., Acuna M., Brown M. (2013). ***Self-levelling feller-buncher productivity based on LiDAR-derived slope***. *Croatian Journal of Forest Engineering 34(2*), 273–281.

Alexandru V., Ticu S. (2012). ***Road transportation of timber and forest zones pollution***. *Bulletin of the Transilvania University of Brasov, Series II: Forestry, Wood Industry, Agricultural Food Engineering*, *5(1),* 1-6.

Amishev D. (2016). ***Winch-assist technologies available to Western Canada***. Technical report No. 37, FPInnovations. Vancouver, BC (Canada).

Amishev D., Evanson T. (2010). ***Innovative methods for steep terrain harvesting***. In *Proceedings of the 43th International Symposium on forestry mechanization - FORMEC 2010. 11-14 July* (p. 9). Padua, Italy.

B.C. Reg. 296/97. ***Workers compensation act. Occupational health and safety regulation***. Part 26 - Forestry operations and similar activities. Equipment operations - 26.16 Slope limitations.

Baral A., Malins C. (2014). ***Assessing the climate mitigation potential of biofuels derived from residues and wastes in the European context***. International Council on Clean Transportation. Washington, DC (US).

Bayne K.M., Parker R.J. (2012). ***The introduction of robotics for New Zealand forestry operations: Forest sector employee perceptions and implications***. *Technology in Society*, *34(2)*, 138–148. doi.org/10.1016/j.techsoc.2012.02.004

BC Forest Safety Council (2017). ***Update on steep slope developments at TLA convention***. *Forest Safety News 4*(1), 1–2.

Bell J.L. (2002). ***Changes in logging injury rates associated with use of feller-bunchers in West Virginia***. *Journal of Safety Research*, *33*(4), 463–471. doi.org/10.1016/S0022-4375(02)00048-8

Bennett N. (2016). ***Timber supply crunch drives loggers to more dangerous terrain***. *Business in Vancouver*. Vancouver, BC (Canada).

Biller C.J., Baumgras J.E. (1987). ***Failure loads of small-diameter hardwood stumps***. *Transactions of the American Society of Agricultural Engineers*, *30*(6), 1587–1590.

Binkley V.W., Gosh J., Studier D.D., Warner J. (1978). ***Skyline anchor dynamic test***. Project

Record San Dimas Equipment Develoment Center. USDA Forest Service.
Björheden R. (1991). ***Basic time concepts for international comparisons of time study reports***. *Journal of Forest Engineering*, *2*(2), 33–39. doi.org/10.1080/08435243.1991.10702626
Blyth S., Groombridge B., Lysenko I., Miles L., Newton A. (2002). ***Mountain watch: environmental change and sustainable development in mountains***. UNEP-WCMC.
Bont L.G. (2012). ***Spatially explicit optimization of forest harvest and transportation system layout under steep slope conditions***. PhD dissertation. ETH. Zürich, Switzerland.
Bont L.G., Heinimann H.R. (2012a). ***Optimum geometric layout of a single cable road***. *European Journal of Forest Research*, *131*(5), 1439–1448. doi.org/10.1007/s10342-012-0612-y
Bruinsma J. (2009). ***The resource outlook to 2050: by how much do land, water and crop yields need to increase by 2050?*** In *Expert Meeting on How to Feed the World in 2050. 24-26 June* (p. 33). FAO Economic and Social Development Department.
Buttoud G. (2000). ***Approaches to multifunctionality in mountain forests***. In *Forests in sustainable mountain development: a state of knowledge report for 2000*, 187-194.
Byrne K.E., Mitchell S.J. (2007). ***Overturning resistance of western redcedar and western hemlock in mixed-species stands in coastal British Columbia***. *Canadian Journal of Forest Research*, *37*(5), 931–939. doi.org/10.1139/X06-291
Carson W.W. (1983). ***Is New Zealand ready for steep country logging?*** *New Zealand Journal of Forestry*, *28*(1), 24–34.
Cavalli R. (2012). ***Prospects of research on cable logging in forest engineering community***. *Croatian Journal of Forest Engineering*, *33*(2), 339–356.
Cavalli R. (2015). ***Forest operation in steep terrain***. In *Proceedings of the Conference CROJE 2015. Forest Engineering - Current situation and future challenges. March 18-20*. (p. 3). Zagreb, Croatia.
Cavalli R., Amishev D. (2017). ***A case study: ground yarding operations in mountainous terrain***. In *Proceedings of the 27th Club of Bologna Members' Meeting - Session 3 - KNR 3.2. November 12-13* (p. 7). Hanover, Germany.
Cavalli R., Grigolato S., Bergomi L.Z. (2009). ***Esbosco in ambiente montano con cable-forwarder***. In *Atti del Terzo Congresso Nazionale di Selvicoltura per il miglioramento e la conservazione dei boschi italiani* (Vol. pp. 3:1476-1481). Taormina, Italy. Accademia Italiana di Scienze Forestali. doi.org/10.4129/CNS2008.212
CEN (2017). prEN 16517:2017 (E). ***Agricultural and forestry machinery. Mobile yarders for timber logging. Safety***. European Committee for Standardization. Technical Committee CEN/TC 144. Working Group 8.
Charland J.W., Hernried A.G., Pyles M.R. (1994). ***Cable systems with elastic supporting elements***. *Journal of Structural Engineering*, *120*(12), 3649–3665.
Chung W., Sessions J. (2003). ***A computerized method for determining cable logging feasibility using a dem***. In *Council on Forest Engineering (COFE) conference proceedings: Forest operations among competing forest uses. September 7-10. Bar Harbor, Maine (US)*.
Davis C.J., Reisinger T.W. (1990). ***Evaluating terrain for harvesting equipment selection***. *Journal of Forest Engineering*, *2*(1), 9-16. doi.org/10.1080/08435243.1990.10702618
Debnar E. (2014). ***Traktionshilfswinden HAAS typen THSW 07 und THSW 09 für harvester und rückezug***. Kuratorium für Waldarbeit und Forsttechnik e.V. (KWF).
Dupire S., Bourrier F., Berger F. (2015). ***Predicting load path and tensile forces during cable***

yarding operations on steep terrain. *Journal of Forest Research*, *21*(1), 1–14. doi.org/10.1007/s10310-015-0503-4

Dykstra D.P., Heinrich R. (1992). ***Sustaining tropical forests through environmentally sound harvesting practices***. *Unasylva*, *43*(169), 9–15.

Dyson P., Boswell B. (2016). ***Winch-assisted feller-buncher equipped with a continuous-rotation disc saw: short-term productivity assessment***. Technical report No. 46, FPInnovations. Vancouver, BC (Canada).

Enache A., Kühmaier M., Visser R., Stampfer K. (2016). ***Forestry operations in the European mountains: a study of current practices and efficiency gaps***. *Scandinavian Journal of Forest Research*, *31*(4), 412–427. doi.org/10.1080/02827581.2015.1130849

Erber G., Holzleitner F., Kastner M., Stampfer K. (2016). ***Effect of multi-tree handling and tree-size on harvester performance in small-diameter hardwood thinnings***. *Silva Fennica*, *50*(1), 17. doi.org/10.14214/sf.1428

Erickson M.D., Virginia W. (1991). ***Productivity and cost estimator for conventional ground-based skidding on steep terrain using preplanned skid roads***. In *McNeel, JF; Andersson, Bjorn, eds. Forestry operations in the 1990's; challenges and solutions, Proceedings of the 14th annual meeting of the Council of Forest Engineers, July 22-25* (pp. 92–96). Nanaimo, BC (Canada).

Evanson T., Amishev D. (2010). ***Productivity impacts of bunching for yarder extraction***. In *Proceedings of the 43th International Symposium on forestry mechanization - FORMEC 2010. 11-14 July*. Padua, Italy.

Fabiano F., Hippoliti G., Marchi E., Piegai F. (2002). ***Analisi delle sollecitazioni in funi portanti di gru a cavo forestali***. *Annali*, 121–158.

Fabiano F., Marchi E., Neri F., Piegai F. (2011). ***Skyline tension analysis in yarding operation: case studies in Italy***. In *Proceedings of the 44th International Symposium on Forestry Mechanisation - FORMEC 2011. October 9 -13.* (p. 12). Graz, Austria.

Falk G.D. (1980). ***A study of lateral yarding forces in cable thinning***. Master thesis. Oregon State University, Corvalliss, OR (US).

Falk G.D. (1981). ***Predicting the payload capability of cable logging systems including the effect of partial suspension***. Broomall, PA (US): US Department of Agriculture, Forest Service, Northeastern Forest Experiment Station.

FAO (1985). ***Logging and transport in steep terrain***. *FAO Forestry Paper 14 Rev.1*. Rome, Italy.

FAO (2004). ***Reduced Impact Logging***. *Forest Harvesting and Engineering Working Paper No.1*. Rome, Italy.

FAO (2015a). ***Global Forest Resources Assessment 2015. Desk reference***. Rome, Italy.

FAO (2015b). ***Global Forest Resources Assessment 2015. How are the world's forests changing?*** Rome, Italy.

FAO (2016). ***Forestry for a low-carbon future: Integrating forests and wood products in climate change strategies***. *FAO Forestry Paper 177*, 151. Rome, Italy.

FAO (2017). ***Forests and Energy***. Rome, Italy.

FAO (2018a). ***State of the world's forests 2018 - Forest pathways to suistanble development***. Rome, Italy.

FAO (2018b). ***FAOSTAT***. Rome, Italy.

FAO (2018c). ***Mountain forests***. *Mountain Forests Module*. Rome, Italy

Fernandez-Lacruz R., Di Fulvio F., Bergström D. (2013). ***Productivity and profitability of harvesting power line corridors for bioenergy***. *Silva Fennica*, *47*(1), 23. doi.org/10.

14214/sf.904
Feyrer K. (2015). ***Wire ropes: Tension, endurance, reliability*** (Second Edi). Springer Berlin Heidelberg. doi.org/10.1007/978-3-642-54996-0
FITEC (2005). ***Best practice guidlines for Cable Logging***.
Forest Europe. (2011). ***State of Europe's Forests 2011. Status and trends in Sustainable Forest Management in Europe***. In *Ministerial Conference on the Protection of Forests in Europe, Forest Europe, Liaison Unit Oslo* (p. 344).
Gerasimov Y., Sokolov A. (2014). ***Ergonomic evaluation and comparison of wood harvesting systems in Northwest Russia***. *Applied Ergonomics*, *45*(2), 318–38. doi.org/10.1016/j.apergo.2013.04.018
Ghaffarian M.R., Stampfer K., Sessions J. (2009). ***Comparison of three methods to determine optimal road spacing for forwarder-type logging operations***. *Journal of Forest Science*, *55*(9), 423–431.
Ghaffariyan M.R., Stampfer K., Sessions J. (2010). ***Optimal road spacing of cable yarding using a tower yarder in Southern Austria***. *European Journal of Forest Research*, *129*(3), 409–416.
Ghaffariyan M.R., Stampfer K., Sessions J. (2013). ***Production equations for tower yarders in Austria***. *International Journal of Forest Engineering*, *20*(1), 17–21.
Glück P. (2002). ***Property rights and multipurpose mountain forest management***. *Forest Policy and Economics*, *4*(2), 125–134. doi.org/10.1016/S1389-9341(02)00012-6
González-García S., Gasol C.M., Lozano R.G., Moreira M.T., Gabarrell X., i Pons, J.R., Feijoo G. (2011). ***Assessing the global warming potential of wooden products from the furniture sector to improve their ecodesign***. *Science of the Total Environment*, *410–411*, 16–25. doi.org/10.1016/j.scitotenv.2011.09.059
Grabherr G. (2000). ***Biodiversity of mountain forests. In Forests in sustainable mountain development: a state of knowledge report for 2000***. *Task Force on Forests in Sustainable Mountain Development.* (pp. 28–38). doi.org/10.1079/9780851994468.0028
Grigolato S., Panizza S., Pellegrini M., Ackerman P., Cavalli R. (2016). ***Light-lift helicopter logging operations in the Italian Alps: a preliminary study based on GNSS and a video camera system***. *Forest Science and Technology*, *12*(2), 88–97. doi.org/10.1080/21580103.2015.1075436
Grigolato S., Pellegrini M., Cavalli R. (2013). ***Temporal analysis of the traffic loads on forest road networks***. *IForest*, *6*(5), 255–261. doi.org/10.3832/ifor0773-006
Gumus S., Acar H.H. (2010). ***Evaluation of consecutive skylines yarding and gravity skidding systems in primary forest transportation on steep terrain***. *Journal of Environmental Biology*, *31*(1–2), 213-218.
Harrill H. (2014). ***Improving cable logging operations for New Zealand ' s steep terrain forest plantations***. PhD dissertation. University of Canterbury. Christchurch, New Zealand
Harrill H., Visser R. (2013). ***Simulating skyline tensions of rigging configurations***. *Harvesting Technical Note HTN05-12*. Future Forest Research Limited. Rotorua, New Zealand.
Harrill H., Visser R. (2016). ***Skyline tension behavior of rigging configurations used in New Zealand cable logging***. In *Proceedings of the Demo International Conference. September 19-21.* (p. 11). Vancouver, BC (Canada).
Harrill H., Visser R. (2017). ***A study of breakout forces in cable logging***. *Harvesting Technical Note HTN09-06*. Forest Growers Research Ltd. Rotorua, New Zealand.
Hartsough B.R. (1993). ***Benefits of remote tension monitoring***. *Report 18-23*. Logging

Industry Research Organisation. Rotorua, New Zealand.
Heinimann H.R. (2004). ***HARVESTING | Forest Operations under mountainous conditions***. In Burley J., Evans J., Youngquist J.A. (Eds.), *Encyclopedia of Forest Sciences* (pp. 279-285). Oxford: Elsevier. doi.org/10.1016/B0-12-145160-7/00011-9
Heinimann H.R. (2007). ***Forest operations engineering and management - The ways behind and ahead of a scientific discipline***. *Croatian Journal of Forest Engineering*, *28*(1), 107–121.
Heinimann H.R., Stampfer K., Loschek J., Caminada L. (2001). ***Perspectives on Central European cable yarding systems***. In *The International Mountain Logging and 11th Pacific Northwest Skyline Symposium 2001* (pp. 268–279). Seattle, WA (USA).
Henshaw J.R. (1977). ***A study of the coefficient of drag resistance in yarding logs***. Master thesis. Oregon State University. Corvallis, OR (USA).
Hittenbeck J. (2007). ***Limits of wheel based timber harvesting in inclined areas***. In *Proceedings of the 40th International Symposium on Forestry Mechanisation: Meeting the Needs of Tomorrows´ Forests – New Developments in Forest Engineering - FORMEC 2007, October 7–11* (p. 10). Vienna and Heiligenkreuz, Austria.
Holzfeind T., Stampfer K., Holzleitner F. (2018). ***Productivity, setup time and costs of a winch-assisted forwarder***. *Journal of Forest Research*, *23*(4), 1–8. doi.org/10.1080/13416979.2018.1483131
Holzleitner F., Kastner M., Stampfer K., Höller N., Kanzian C. (2018). ***Monitoring tensile forces at cables of winch-assisted harvesters and forwarders in steep terrain cut-to-length harvesting operations***. *Forests*, *9*(2), 13. doi.org/10.3390/f9010000
Horodnic S.A. (2015). ***A risk index for multicriterial selection of a logging system with low environmental impact***. *Environmental Impact Assessment Review*, *51*, 32–37. doi.org/10.1016/j.eiar.2015.02.002
Huber C, Stampfer K (2015). ***Efficiency of topping trees in cable yarding operations***. Croatian Journal of Forest Engineering 36:185–194.
ILO (1998). ***Safety and health in forestry work***. *The Annals of the American Academy of Political and Social Science* (Vol. 108). doi.org/10.1177/000271622310800139
Inoue K., Kobayashi H. (1996). ***Operators' Physical Strain in Operating the High Proficient Forestry Machines***. *Journal of Forest Research*, *1*(3), 111–115.
IPCC (2014). ***Climate Change 2014: Mitigation of Climate Change***. *Working Group III Contribution to the Fifth Assessment Report of the Intergovernmental Panel on Climate Change*. doi.org/10.1017/CBO9781107415416
ISO (2018) 19472-2 ***Machinery for Forestry. Winches - Dimensions, performance and safety - Part 2: Tethering and Tractions Assistance Winches***. International Organisation for Standardization.
Jarmer C., Sessions J. (1992). ***Logger-PC for improved logging planning***. In *Proceedings of Planning and Implementing Future Forest Operations, International Mountain Logging and 8th Pacific Northwest Skyline Symposium, Schiess, P. and J. Sessions [Eds.]*.
Kapos V., Rhind J., Edwards M., Price M.F., Ravilious C. (2000). ***Developing a map of the world ' s mountain forests***. In *Forests in sustainable mountain development: a state of knowledge report for 2000* (pp. 4–9).
Klun J., Medved M. (2007). ***Fatal accidents in forestry in some European countries***. *Croatian Journal of Forest Engineering*, *28*(1), 55–62.
Knobloch C, Bont L (2018) ***A new method to compute mechanical properties of a cable road skyline***. In: FORMEC 2018. Proceedings of the 51st International Symposium on forest

mechanization. 24-28 September. Madrid, Spain.
Kühmaier M., Stampfer K. (2010). ***Development of a multi-attribute spatial decision support system in selecting timber harvesting systems***. *Croatian Journal of Forest Engineering*, *31*(2), 75–88.
Leshchinsky B., Sessions J., Wimer J., Clauson M. (2016). ***Designing mobile anchors to yield : A tension relief system for tail anchoring***. *Croatian Journal of Forest Engineering*, *37*(2), 269–278.
Lezier A. (2016). ***Sviluppo e applicazione di uno strumento per il rilievo automatico dei tempi di lavoro nelle operazioni di esbosco con gru a cavo***. Master thesis. University of Padova. Padua, Italy
Liniger H., Weingartner R. (2000). ***Mountain forests and their role in providing freshwater resources***, In *Forests in sustainable mountain development: a state of knowledge report for 2000* (pp. 370–380).
Lundström T., Jonas T., Stöckli V., Ammann W. (2007). ***Anchorage of mature conifers: resistive turning moment, root-soil plate geometry and root growth orientation***. *Tree Physiology*, *27*(9), 1217–1227. doi.org/10.1093/treephys/27.9.1217
Lundström T., Jonsson M.J., Kalberer M. (2007). ***The root–soil system of Norway spruce subjected to turning moment: resistance as a function of rotation***. *Plant and Soil*, *300*(1–2), 35–49. doi.org/10.1007/s11104-007-9386-2
Lyons K.C., McNeel J. (2004). ***Partial retention and helicopter turn volume***. *Forest Products Journal*, *54*(1), 58–61.
Magaud P., Grulois S., Boggio B., Sandmeier F. (2018). ***Cable yarding in france and in swiss romandie: status quo and adapted measures within the two different organisations***. In *6th International Forest Engineering Conference "Quenching our thirst for new Knowledge" April 16th - 19th* (p. 6). Rotorua, New Zealand,.
Magee L. (1990). ***R2 measures based on Wald and liklihood ratio joint significance tests***. *The American Statistician*, *44*(3), 250–253.
Manzone M., Balsari P. (2011). ***Forestry use of the helicopter***. In *Proceedings of the 44th International Symposium on Forestry Mechanisation - FORMEC 2011. October 9 -13.* Graz, Austria.
Marchi E., Chung W., Visser R., Abbas D., Nordfjell T., Mederski P.S., McEwan A., Brink M., Laschi, A. (2018a). ***Sustainable Forest Operations (SFO): a new paradigm in a changing world and climate***. *Science of the Total Environment*, *634*, 1385–1397. doi.org/10.1016/j.scitotenv.2018.04.084
Marchi L., Grigolato S., Mologni O., Scotta R., Cavalli R., Montecchio L. (2018b). ***State of the art on the use of trees as supports and anchors in forest operations***. *Forests*, *9*(467), 17. doi.org/10.3390/f9080467
MBIE. (2012). ***Approved Code of Practice for Safety and Health in Forest Operations***. Wellington, New Zealand: Ministry of Business, Innovation and Employment.
Mccool S.F., Lachapelle P.R. (2000). ***Recreational uses of mountain forests***. In *Forests in sustainable mountain development: a state of knowledge report for 2000. Task Force on Forests in Sustainable Mountain Development.* (pp. 330–337).
Millennium Ecosystem Assessment (2005). ***Ecosystems and human well-being: synthesis***. Washington, DC (USA): Island Press.
Miles J.A., Zeni S.T., Hartsough B.R. (1993). ***Comparison of clamped and unclamped carriages for downhill yarding in partial cut situations***. *Transactions of the ASAE*, *36*(6), 1929–1933.

Mologni O, Antonioli S, Grigolato S, Cavalli R (2017) ***Gru a cavo nelle Alpi Centrali. Caratteristiche delle linee e osservazioni sui tempi di montaggio e smontaggio***. Sherwood - Foreste ed Alberi Oggi 23:7–11.

Mologni O, Cavalli R (2015) ***Gru a cavo nelle imprese forestali lombarde***. Sherwood - Foreste ed Alberi Oggi 21:11–15.

Moore J.R. (2000). ***Differences in maximum resistive bending moments of Pinus radiata trees grown on a range of soil types***. *Forest Ecology and Management*, *135*(1–3), 63–71. doi.org/10.1016/S0378-1127(00)00298-X

Moore J.R., Gardiner B.A. (2001). ***Relative windfirmness of New Zealand-grown Pinus radiata and Douglas-fir: a preliminary investigation***. *New Zealand Journal of Forestry Science*, *31*(2), 208–223.

Nagelkerke N.J.D. (1992). ***Maximum Likelihood Estimation of Functional Relationships***. (J. Berger, S. Fienberg, J. Gani, K. Krickeberg, I. Olkin, & B. Singer, Eds.) (Vol. 69). New York, NY: Springer New York. doi.org/10.1007/978-1-4612-2858-5

OECD (2016). ***Policy Guidance on Resource Efficiency***. Paris, France: OECD Publishing. http://doi.org/10.1787/9789264257344-en

OR-OSHA (2010). **Yarding and loading handbook**, (pp. 164). Salem, OR (USA): Oregon Occupational Safety and Health Division.

OR-OSHA (2016). ***Oregon OSHA's revised guidelines for using tethered logging systems*** 6/2016. Salem, OR (USA): Oregon Occupational Safety and Health Division.

Orazio C., Kies U., Edwards D. (2017). ***Handbook for wood mobilisation in Europe. Measures for increasing wood supply from sustainably managed forests***. (pp 116). doi.org/10.13140/RG.2.2.30261.78568

Owende P.M., Lyons J., Haarlaa R., Peltola A., Spinelli R., Molano J., Ward S.M. (2002). ***Operations protocol for eco-efficient wood harvesting on sensitive sites***. *The Ecowood Partnership*.

Owende P.M., Tiernan D., Ward S.M., Lyons J. (2001). ***Is there a role for cable extraction on low gradient sensitive sites?*** In *Workshop on New trends in wood harvesting with cable systems for sustainable forest management in the mountains. 18-24 June*. Ossiach, Austria.

Papesch A.J.G., Moore J.R., Hawke A.E. (1997). ***Mechanical stability of pinus radiata trees at Eyrewell Forest investigated using static tests***. *New Zealand Journal of Forestry Science*, *27*(2), 188–204.

Pellegrini M., Grigolato S., Cavalli R. (2013). ***Spatial multi-criteria decision process to define maintenance priorities of forest road network : an application in the Italian Alpine region***. *Croatian Journal of Forest Engineering*, *34*(1), 31–42.

Pentek T., Poršinsky T., Sušnjar M., Stankić I., Nevećerel H., Sporcić M. (2008). ***Environmentally sound harvesting technologies in commercial forests in the area of Northern Velebit. Functional terrain classification***. *Periodicum Biologorum*, *110*(2), 8.

Pertlik E. (1992). ***Spannungsermittlung an forstlichen seilgeraeten*** *[Tensile force detection on forestry ropes]*.

Pestal E. (1961). ***Seilbahnen und seilkrane für holz un materialtransport***. Horn, Austria: Verlag Georg Fromme & Co.

Peters P.A., Biller C.J. (1984). ***Evaluation of log attachment methods by a latin square design***. *Transactions of the ASAE*, *27*(2), 382–384.

Pierzchała M., Kvaal K., Stampfer K., Talbot B. (2017). ***Automatic recognition of work phases in cable yarding supported by sensor fusion***. *International Journal of Forest*

Engineering, *29*(1), 1–9. doi.org/10.1080/14942119.2017.1373502

Price M.F., Butt N. (Eds.). (2000). ***Forests in sustainable mountain development: a state of knowledge report for 2000***. *IUFRO Research Series 5*. CABI Publishing. doi.org/10.1079/9780851994468.0004

Price M.F., Georg G., Duguma L.A., Kohler T., Maselli D., Romeo R. (Eds.) (2011). ***Mountain Forests in a Changing World: Realizing values, addressing challenges***. FAO/MPS and SDC, Rome.

PWC (2016). ***British Columbia ' s Forest industry and the BC economy in 2016***.

Pyles M.R., Anderson J.W., Stafford S.G. (1991). ***Capacity of second-growth Douglas-fir and western hemlock stump anchors for cable logging***. *Journal of Forest Engineering*, *3*(1), 29–37.

Pyles M.R., Stoupa J. (1987). ***Load-carrying capacity of second-growth Douglas-Fir stump anchors***. *Western Journal of Applied Forestry*, *2*(3), 77–80. doi.org/10.1093/wjaf/2.3.77

Pyles M.R., Womack K.C., Laursen H.I. (1994). ***Dynamic characteristics of a small skyline logging system with a guyed tailspar***. *International Journal of Forest Engineering*, *6*(1), 35–49.

Raymond K. (2012). ***Innovation to increase profitability of steep terrain harvesting in New Zealand***. *New Zealand Journal of Forestry*, *57*(2), 19–23.

Safe Work Australia (2013). ***Guide to managing risks in cable logging***.

Samset I. (1985). ***Winch and Cable System*** (1st ed., Vol. 1). Dordrecht (NL): Springer. doi.org/10.1017/CBO9781107415324.004

Schönenberger W. (2000). ***Silvicultural problems in subalpine forests in the Alps***. In *Forests in sustainable mountain development: a state of knowledge report for 2000* (pp. 197–203).

Scion T.E. (2009). ***Use of tension monitors to estimate payload***. *Harvesting Technical Note, 1*(8). Future Forest Research Limited. Rotorua, New Zealand.

Sessions J., Garland J.J. (1999). ***Logging - McGraw-Hill Encyclopedia of Science and Technology***. McGraw-Hill Professional Publishing.

Sessions J., Leshchinsky B., Chung W., Boston K., Wimer J. (2017). ***Theoretical stability and traction of steep slope tethered feller-bunchers***. *Forest Science*, *63*(2), 192–200. doi.org/10.5849/forsci.16-069

SFC (2010). ***Climate Change and Forestry***. Standing Forestry Committeed Ad Hoc Working Group III on Climate Change and Forestry.

Smith J., McMahon S. (1995). ***Stump anchorage capacity on two contrasting soil types***. *LIRO Report 20(22)*. Logging Industry Research Organization. Rotorua, New Zealand.

Spinelli R., Magagnotti, N. (2011). ***The effects of introducing modern technology on the financial, labour and energy performance of forest operations in the Italian Alps***. *Forest Policy and Economics*, *13*(7), 520–524. doi.org/10.1016/j.forpol.2011.06.009

Spinelli R., Magagnotti N., Aminti G., De Francesco F., Lombardini C. (2016). ***The effect of harvesting method on biomass retention and operational efficiency in low-value mountain forests***. *European Journal of Forest Research*. doi.org/10.1007/s10342-016-0970-y

Spinelli R., Magagnotti N., Facchinetti D. (2013). ***Logging companies in the European mountains: an example from the Italian Alps***. *International Journal of Forest Engineering*, *24*(2), 109–120. doi.org/10.1080/14942119.2013.838376

Spinelli R., Marchi E., Visser R., Harrill H., Gallo R., Cambi, M., Neri F., Lombardini C.,

Magagnotti, N. (2017). ***Skyline tension, shock loading, payload and performance for a European cable yarder using two different carriage types***. *European Journal of Forest Research*, *136*(1), 161–170. doi.org/10.1007/s10342-016-1016-1

Spinelli R., Nati C., Magagnotti N. (2006). ***Recupero di biomassa, alcune utilizzazioni in boschi alpini***. *Sherwood - Foreste Ed Alberi Oggi*, *119*, 1–7.

Spinelli R., Visser R., Thees O., Sauter U.H., Krajnc N., Riond C., Magagnotti N. (2015). ***Cable logging contract rates in the Alps: the effect of regional variability and technical constraints***. *Croatian Journal of Forest Engineering*, *36*(2), 195–203.

Stampfer K. (1999). ***Influence of terrain conditions and thinning regimes on productivity of a track-based steep slope harvester***. In *Proceedings of the International Mountain Logging and 10th Pacific Northwest Skyline Symposium* (Vol. 20, pp. 78–87).

Stampfer K., Gridling H., Visser R. (2002). ***Analyses of parameters affecting helicopter timber extraction***. *International Journal of Forest Engineering*, *13*(2), 61–68.

Stampfer K., Leitner T., Visser R. (2010). ***Efficiency and ergonomic benefits of using radio controlled chokers in cable yarding***. *Croatian Journal of Forest Engineering*, *31*(1), 1–9.

Stampfer K., Steinmüller T. (2001). ***A new approach to derive a productivity model for the harvester "Valmet 911 Snake"*** In *The International Mountain Logging and 11th Pacific Northwest Skyline Symposium 2001* (pp. 254–262).

Stampfer K., Visser R., Kanzian C. (2006). ***Cable corridor installation times for European yarders***. *International Journal of Forest Engineering*, *17*(2), 71–77.

Strandgard M., Alam M., Mitchell R. (2014). ***Impact of slope on productivity of a self-levelling processor***. *Croatian Journal of Forest Engineering*, *35*(2), 193–200.

Studier D.D., Binkley V.W. (1974). ***Cable logging systems***. USDA Forest Service. Pacific Northwest Region. Portland, Oregon (USA).

Talbot B., Stampfer K., Visser R. (2015). ***Machine function integration and its effect on the performance of a timber yarding and processing operation***. *Biosystems Engineering*, *135*, 10–20. doi.org/10.1016/j.biosystemseng.2015.03.013

Toupin R., Pyles M.R., Tuor B. (1985). ***Modelling and testing two-stump anchors***. *LIRA Technical release* 7(4). Logging Industry Research Association. Rotorua, New Zealand

Tsioras P.A., Rottensteiner C., Stampfer K. (2011). ***Analysis of accidents during cable yarding operations in Austria 1998-2008***. *Croatian Journal of Forest Engineering*, *32*(2), 549–560.

Tsioras P.A., Rottensteiner C., Stampfer K. (2014). ***Wood harvesting accidents in the Austrian State Forest Enterprise 2000–2009***. *Safety Science*, *62*, 400–408. doi.org/10.1016/j.ssci.2013.09.016

Tuor B., Palmer D., McMahon S. (1998). ***Clamping carriages and skyline tensions***. *LIRO Report* 23(9). Logging Industry Research Organization. Rotorua, New Zealand.

Twining-Ward L. (2010). ***Global Report on Women in Tourism 2010***.

UNCED (1992). ***Agenda 21***. *United Nations Conference on Environment and Development Rio de Janerio, Brazil, 3-14 June.*

UNFCCC (2015). ***Paris Agreement***. *Conference of the Parties on Its Twenty-First Session*.

United Nations (2015). ***Transforming our world: the 2030 Agenda for Sustainable Development***. *General Assembley 70 Session*, *16301*(October), 1–35. doi.org/10.1007/s13398-014-0173-7.2

United Nations (2017a). ***United Nations strategic plan for forests 2017–2030 and quadrennial programme of work of the United Nations Forum on Forests for the period***

2017–2020.
United Nations. (2017b). ***World Population Prospects. The 2017 Revision Key Findings and Advance Tables***. Department of Economic and Social Affairs Population Division.
Valente C., Spinelli R., Hillring B.G. (2011). ***LCA of environmental and socio-economic impacts related to wood energy production in alpine conditions: Valle di Fiemme (Italy)***. *Journal of Cleaner Production*, *19*(17–18), 1931–1938. doi.org/10.1016/j.jclepro.2011.06.026
Valente C., Spinelli R., Hillring B.G., Solberg B. (2014). ***Mountain forest wood fuel supply chains: comparative studies between Norway and Italy***. *Biomass and Bioenergy*, *71*, 370–380. doi.org/10.1016/j.biombioe.2014.09.018
Vinet L., Zhedanov A. (2011). ***A 'missing' family of classical orthogonal polynomials***. *Journal of Physics A: Mathematical and Theoretical*, *44*(8), 085201.
Visser R. (1998). ***Tensions monitoring of forestry cable systems***. PhD dissertations. Bodenkultur University, Wien, Austria.
Visser R. (2013). ***Tension monitoring of a cable assisted machine***. *Harvesting Technical Note* HTN05-11. Future Forest Research Limited. Rotorua, New Zealand.
Visser R. (2014). ***New harvesting innovations to improve heath and safety***. In *Second International Congress of Silvicolture - November 26-29* (pp. 813–817). Florence, Italy.
Visser R. (2016). ***Cable-Assist in forest harvesting: developments and operating limits***. At *Demo International and COFE Meeting*. Vancouver, BC (Canada).
Visser R., Berkett H. (2015). ***Effect of terrain steepness on machine slope when harvesting***. *International Journal of Forest Engineering*, *26*(1), 9.
Visser R., Harrill H. (2017). ***Cable yarding in North America and New Zealand: a review of developments and practices***. *Croatian Journal of Forest Engineering*, *38*(2), 209–217.
Visser R., Raymond K., Harrill H. (2014). ***Developing fully mechanised steep terrain harvesting operations***. In *Proceedings of the 47th International Symposium on Forestry Mechanisation - FORMEC 2014. September 23 - 26.* (p. 8). Gerardmer, France: Forest Research Institute.
Visser R., Stampfer K. (2015). ***Expanding ground-based harvesting onto steep terrain: a review***. *Croatian Journal of Forest Engineering*, *36*(2), 321–331.
WCED (1987). ***General assembly***, *05445*, 1–13.
Weise G., Burk, J. (2011). ***Traktionshilfswinde Komatsu SPW***. Kuratorium für Waldarbeit und Forsttechnik e.V. (KWF).
Weise G., Burk, J. (2016). ***Traktionshilfswinde HSM HSW 15***. Kuratorium für Waldarbeit und Forsttechnik e.V. (KWF).
Wenger K.F. (1984). ***Forestry handbook*** (Vol. 84). John Wiley & Sons.
West P.W. (2014) ***Tree and Forest Measurement***. *Third edition*. Springer
Wihersaari M. (2005). ***Greenhouse gas emissions from final harvest fuel chip production in Finland***. *Biomass and Bioenergy*, *28*(5), 435–443. doi.org/10.1016/j.biombioe.2004.11.007
Womack K.C. (1989). ***The dynamic behavior of a cable logging skyline and its effect on the tailspar***. PhD dissertation. Oregon State University. Corvallis, OR (USA).
Womack K.C., Pyles M.R., Laursen H.I. (1994). ***Computer model for dynamic skyline behaviour***. *International Journal of Forest Engineering*, *5*(2), 55–62.
Work Safe BC. (2006). ***Cable yarding systems handbook***. *Second edition*.
Zanzi Sulli, A. (2000). ***The cultural value of forests***. In *Forests in sustainable mountain development: a state of knowledge report for 2000. Task Force on Forests in*

Sustainable Mountain Development. (pp. 170–176).

Zhang Y., Mckechnie J., Cormier D., Lyng R., Mabee W., Ogino A., Maclean H.L. (2010). ***Life cycle emissions and cost of producing electricity from coal, natural gas, and wood pellets in Ontario, Canada***. *Environmental Science and Technology*, *44*(1), 538–544. doi.org/10.1021/es902555a

Zingari P.C. (2000). ***Sustainably balancing downstream and upstream benefits in European mountain forest communities***. In *Forests in sustainable mountain development: a state of knowledge report for 2000* (pp. 155–165).

Annex 1: List of tables and figures

LIST OF TABLES

LIST OF FIGURES

Annex 2: Wire ropes technical description

This section reports some general information about the wire ropes used in forestry operations. This information refers to the contents reported in the standards UNI EN 12385-4:2008 (*Steel wire ropes - Safety- Part 4: Stranded ropes for general lifting applications*) and in (Feyrer 2015).

The wire ropes consist of three main elements: i) the wires, representing the basic building units of a wire rope; ii) the strands, consisting of several individual wires laid about a central wire (the strand must be pre-formed to give them the permanent helical twist mechanically imparted); iii) the core representing the central element on which the strands are stranded to make a wire rope. The greatest differences in wire ropes are found in terms of number of strands, constructions of strands, the type of the core and the lay of directions of the strands versus the core.

Grade

The wires of the wire rope are made of high-carbon steel. The grade is the expression of the material tensile strength used to make the wire rope and it is indicated in N mm^{-2}. There are many different strength grades of rope made. Some are listed below:

- 1370 N mm^{-2} - mild plow steel (MPS);
- 1570 N mm^{-2} - plow steel (PS);
- 1770 N mm^{-2} - improved plow steel (IPS);
- 1960 N mm^{-2} - extra improved plow steel (EIPS);
- 2160 N mm^{-2} - enhanced o extra-extra improved plow steel (EEIPS).

Core

The core acts supporting the strands in their relative positions and cushions the wires to prevent their nicking each other. There are many different types of cores, including:

- IWRC (independent wire rope core): the core is a wire rope itself;
- WSC (wire strand core): core is a wire strand structure;
- FC (fiber core): the core is made of synthetic or natural fiber.

Strand wire construction

Most of the different wire construction used in the strands of the wire rope can be classified into 3 general types: Seale, Warrington and Filler. Wire inner and outer layer positioning and diameter are the basis to assign the right strand wire construction.

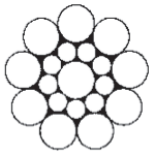

S: Seale

They have the same number of wires on both layers. The wires of the outer layer are thicker than those of the inner layer and each layer wires have the same diameter.

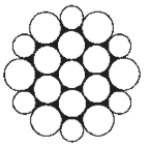

W: Warrington

type differs from the others in that: the outside layer is composed of twice numbers of wires alternately large and small and the inner layer consist of wires of the same diameter.

F: Filler

The outside layer's wires are uniform in size. The outer layer has twice number of wires compared to the inner layers. The wires of the inside layers are made up of a combination of main wires each of the same size, and smaller filler wires each of the same size, nested between the main wires.

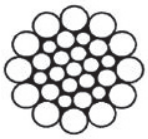

WS: Warrington-Seale

Combinations of the Filler, Seale and Warrington types are commonly used. The most popular combination is given the best features of each strand wire arrangement more flexibility and more resistant to abrasion and pressure.

Wire rope lays

Lays denotes the direction in which the strands are laid, as well as the relationship between the direction of the wires in the strand and the direction of the strands in the wire rope. Right or left are used to refer to the lay of the strands. Ordinary lay, as opposed to lang lay, denotes the direction of wire twist in the strands. In ordinary lay-rope, the wires in each

strand lie in the opposite direction from the strands. “sZ” or “zS”. In Lang lay rope the wires in each strand lie in the “same” direction as the strands. “zZ or “sS”. The wire ropes used in forestry operations, as the ropes used in the analyzed harvesting sites, are right-hand ordinary lay (RHOL).

Rope compaction

Rope compaction can occur through two different processes, one at the strand level (compacted ropes) and one at the rope level (swaged ropes). Both the compaction processes allow to get ropes with higher minimum breaking load at same diameters compared to ordinary ropes or ropes with the same minimum breaking loads but thinner diameters. These manufacturing process causes higher rope performances and manufacturing costs.

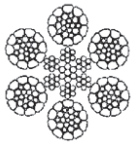

C: compacted ropes

these ropes consist of strands reduced on size in diameter by drawing them one by one through a flattener die that works on outside wires. The strands are then laid up to manufacture the wire rope;

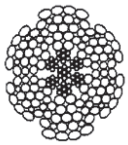

S: swaged ropes

these ropes are obtained from ordinary or compacted ropes reducing the diameter by a pounding action.

The skyline monitored in the cable-based harvesting system case studies are identified using the standard nomenclature. The ropes were named considering the number of strands, the number of wires per strand, the construction, the core, and the compaction. As example, 6x26WS IWRC (C+S) indicates a rope with six strands, each one composed by 26 wires (6x26), in Warrington-Seale construction (WS), with an independent wire rope core (IWRC). The strands were compacted (C) and the rope swaged (S)

No detailed descriptions have been provided for the cable used in winch-assist forwarding.

Annex 3: Study site details: Cable-based harvesting systems

Site A

Site A was located in a mixed spruce-silver fir public forest own by the municipality of Cinte Tesino (Trento - Italy). The administration prescribed a five hectares patch-cut. The logging operations were managed by a contractor, here named "T1", employing three long-experienced operators. Two cable lines were initially planned, but only one cable line was installed by the contractor. The skyline tensile force monitoring interested two consecutive working days on a single cable line (cable line M06).

The cable line was in double-span downhill-oriented configuration, with the tower yarder located on a forest road at the bottom of a valley. The observed work cycles were located in the second half of the first span, up to the intermediate supports. No cycles were monitored on the second span. A large track-based cable yarder (Valentini V600/M/3/1000/B10/R) and an automatic clamped carriage (Hochleitner BW4000) were used for yarding the logs (cable system 4B in Table 2.3). The cable system included a 22 mm-skyline, a 12 mm-mainline, and a 11 mm-haul-back line. Four 18 mm-guylines anchored the tower yarder on its back side. A fifth guyline was installed in the front size as safety protection against tower overturning in case of skyline or anchor failure. Whole trees were used as anchors, tail spar and intermediate support.

Whole trees or partially sorted stems (when the load was too heavy) were yarded to the landing. Both the cable yarder and the carriage were operated through the use of two remote radio controls, one located at the choker-man and a second one at the pole-man. The hauling phases were automatized through the use of the programmable software installed on the machine. Electronic chockers were used for improving the efficiency of the operations. The yarding operations involved two operators at the loading area and one operator at the landing. The operator at the landing drove a Konrad Highlander with a Woody 60 processor head for the mechanical processing of the logs. In case of too large log size, a chainsaw operator completed the processing of the logs. A self-loading log-truck continuously removed the logs processed because of the limited available space at the landing. Residues were chipped for wood energy production. Photos of the block, machines, and anchor are reported in Figure 6.1.

Figure 6.1: Photos of Site A. From the top left: Loading area; landing, Log processing; Log truck; Carriage; Anchor

Site B

This site was located in a spruce-dominated private forest stand in Bieno (Trento - Italy). A 1.5 hectares patch-cut was managed by a contractor, here named "T2", employing three long-experienced operators and two young operators. The skyline tensile force monitoring interested one cable line (cable line S06) monitored for one working day.

The cable line was a single span uphill-oriented line, with the tower yarder located on a narrow forest road. The work cycles were located in the second half of the span. A two-axes truck-based cable yarder (Valentini V600/M/3/1000/LKW) and an automatic clamped carriage (Hochleitner BW4000) were used for yarding the logs (cable system 5B in Table

2.3). The cable system included a 22 mm-skyline and 12 mm-mainline. Four 18 mm-guylines anchored the tower yarder on its back side. A fifth guyline was installed in the front size as safety protection. Two trees were used as multiple tail anchor. A tree without the top section was used as tail spar.

Whole trees and semi-processed stems were yarded to the landing. The operations involved two operators hooking the logs and three operators at the landing. One of the operators at the landing unhooked the loads and remotely controlled the cable yarder and the carriage. A second operator processed the logs using a chainsaw. A third operator moved and piled the logs using a CAT 314E track excavator-base grapple loader. Logs were piled on one side of the road and a self-loading log-truck continuously removed the logs because of the limited available space. Residues were chipped for wood energy production. Photos of the block, machines, and anchor are reported in Figure 6.2.

Site C

Site C was located in a young private spruce plantation in Castello Tesino, in the Autonomous Province of Trento (Italy). Two hectares of this stand were clear-cut for land use conversion to grass. The logging operations were managed by the contractor "T2", employing six operators. Four of them had long-experience in cable yarding. Two operators were younger and with a more limited experience. The skyline tensile force monitoring interested two working day on two different cable lines (cable line S04 and S05).

Both the cable lines were in single span downhill-oriented configuration, with the tower yarders located at the landing at the bottom of the stand. The work cycles were located at the mid-span for the cable line S04 and in the second half of the span for the cable line S05. In cable line S04, a trailer-based cable yarder (Valentini V600/M/3/1000) and an automatic clamped carriage (Hochleitner BW4000) were used for yarding the logs (cable system 3B in Table 2.3). The cable system used a 22mm-skyline, a 12mm-mainline and a 11mm-haul-back line. Four 18mm-guylines anchored the tower yarder on its back side, while a fifth guyline was installed in the front size for safety reasons. Cable line S05 used the same cable system monitored in Site B. In Site C, however, this cable system also involved a 11mm-haul-back line. Braced whole trees were used as anchors. No intermediate supports or tail

Figure 6.2: Photos of Site B. From the top left: Loading area; Cable yarder; Unloading; Landing; Carriage; Multiple anchor

spar were set-up. The two cable lines were almost parallel, and the trees used for setting-up the haul-back line pulleys were partially shared. Only whole trees were yarded to the landing. In cable lines S05 the cable system was managed through a radio remote control by the pole-man, who also unhooked the chains at the landing. A choker-man hooked the logs. The same working system was applied in cable line S04, in which were involved a choker-man and a pole-man. In this case, both of them had the radio remote controls.

The yarder also had the possibility to automatize the hauling phases, but this function was not used during the cable tensile force monitoring. Chains were used to hook the logs. Other two employers operated at the landing, one driving a CTA 314E track excavator-base

grapple loader, a the other one driving an excavator-based processor, based on a New Holland E245 track excavator with a Konrad Woody 60 processor head. These two machines periodically exchange their position from one line to the other. A truck chipper, self-loading log-trucks and chip-tucks continuously operate to clean the landing. Photos of the block, machines, and anchor are reported in Figure 6.3.

Site D

This site was located on a spruce and silver fir-dominated public forest own by the municipality of Zuglio (Udine -Italy). The logging plan prescribed a 22 hectares of shelter wood

Figure 6.3: Photos of Site C. From the top left: Loading area; Landing; Machine operating at the landing; Haul-back line shared supports; Carriage; Anchor

cut, partially integrated with clearance cut in proximity of the natural regeneration. The harvesting operations were managed by a contractor, here named “F1”, employing two experienced and a young operator. Eleven cable lines were planned to exploit the wood. The skyline tensile force monitoring interested one of these cable lines (cable line M05), for one working day.

The observed cable line was an uphill-oriented four-span line, with the tower yarder located in proximity of a hairpin bend of the forest road. The observed work cycles were mainly located between the second and the third span. A trailer-based cable yarder (Valentini V600/M/3/850/spec.) and an automatic clamped carriage (Hochleitner BW4000) were used for yarding the logs (cable system 1B in Table 2.3). The cable system used a 22 mm-skyline and a 12 mm-mainline. Also, because of the limited chord slope of the first two spans, an 11 mm-haul-back line was used. Five 18 mm-guylines anchored the tower yarder, four on its back side and one in the front size as security against tower overturning. Whole trees were used as anchors and intermediate supports.

Stems, whole trees and sorted logs were yarded to the landing. Both the cable yarder and the carriage were operated by two remote radio controls, one at the loading area and one at the landing. The hauling phases were automatized through the use of the programmable software installed on the machine. The yarding operations involved two operators hooking the loads and two operators at the landing site. The pole-man controlled the unloading phase, unhooked the loads and processed the logs. A second operator drove a Hitachi Zaxis 110 track excavator-based grapple loader, moving the logs and assisting the processing. A two-staging log transport was required because of the limited width of the forest road. Thus, logs were initially removed using a tractor and trailer with a loading hydraulic arm. Photos of the block, machines, and anchor are reported in Figure 6.4.

Site E

Site E was located in beech-dominated public stand with inclusions of spruce, in the municipality of Verzegnis (Udine - Italy). The harvesting plan prescribed 17.6 hectares of shelter wood cut, mainly focused on small trees (diameter less than 17.5 cm). The logging operations were managed by a contractor, here named “F2”, employing three long-

Figure 6.4: Photos of Site D. From the top left: Lateral skid; Landing; Unloading; Cable yarder; Carriage; Anchor

experienced and a young operator. Eight different cable lines were planned for logging the stand. The skyline tensile force monitoring interested one working day on a single cable line (cable line S03). Because of a mechanical problem to the carriage, the monitoring was stopped in the early afternoon.

The observed cable line was a downhill-oriented single span line with the tower yarder located on the forest road at the bottom of the stand. The observed work cycles were mainly located in the upper part of the line. A trailer-based cable yarder (Greifenberg TG T3) and an automatic time-triggered clamped carriage (Koller HUSK2002) were used for yarding the logs (cable system 2B in Table 2.3). The cable system used a 22 mm-skyline, a

11 mm-mainline and a 11mm-haulback line. Four 18 mm-guylines anchored the tower yarder on its back side. One front guyline secured the tower against overturning. Whole trees were used as anchors.

The work flow was based on the whole tree harvesting method, extracting whole trees and processing them at the landing. Two operators hooked the logs using chains. Two other operators were employed at the landing, one operating the cable yarder through the use of an electro-hydraulic control panel and unhooking the logs (pole-man), a second one processing the logs operating a track excavator-based processor, based on a JCB JS220 equipped with a Konrad Woody 60 processor head. A self-loading log-truck removed the logs from the landing once per day. Residues were chipped for wood energy production. Photos of the block, machines, and anchor are reported in Figure 6.5.

Site F

This study site was located on a private spruce-dominated forest stand in Raveo (Udine – Italy). A 0.6 hectares patch-cut was yarded by a contractor, here named "F3", employing two experienced and a young operator. The monitoring interested one working day on a single cable line (cable line S01).

The observed cable road was a short uphill-oriented single span cable line, with the tower yarder located on the upper side of a forest road. An intermediate artificial support on the other side of the forest road, just before a rock jump, was used to guarantee enough clearance for the processing operations. This 7m-span was not considered as significant in the cable structure behavior, and the cable line was considered as a single span configuration. A whole tree tail spar was located at the bottom part of the block. The tail anchor was located 40 m far from the spar tree because of a better line geometry configuration. The observed work cycles were concentrated in the second half of the primary span. A tractor-based cable yarder (Valentini V400/2T), pulled and powered by a Same Antares 110 wheeled tractor, and an automatic clamped carriage (Hochleitner BW3000) were used for yarding the logs (cable system 2A in Table 2.2). The cable system used a 16 mm-skyline and a 10 mm-mainline. Four 14 mm-guylines anchored the tower yarder on the back side. A safety guyline was frontally mounted as security against tower overturning.

Figure 6.5: Photos of Site E. From the top left: Upper section of the Loading area; Landing; Unloading; Cable yarder; Carriage; Anchor

Logs where mostly debranched and partially sorted in the forest, except the top sections of the trees. A mix of long stems, top tree sections, and sorted logs were yarded to the landing. The yarding operations involved one operator hooking the logs (choker-man) and two operators at the landing site. A pole-man controlled the cable yarder and carriage movements trough a radio remote control and unhook the loads. A second operator completed the processing phase and piled the logs driving the grapple hydraulic loading arm of a Galvagni trailer, pulled and powered by a Same Silver 100.4 wheeled tractor. The tractor and trailer were also used to transport the logs. Photos of the block, machines, work elements, and structural elements are reported in Figure 6.6.

Figure 6.6: Photos of Site F. From the top left: Inhaul; Landing; Unloading; Artificial support; Carriage; Anchor

Site G

Site G was located in a private mixed stand of beech and spruce in Lauco (Udine - Italy). The stand was partially harvested using a selective approach for fire wood production. The logging operations were managed by a contractor, here named “F4”, employing two experienced and a young operator. The monitoring interested one working day on a single cable line (cable line S02).

The observed cable road was a short slightly inclined uphill-oriented single span cable line with the tower yarder located on a trail. The observed work cycles were distributed on the whole operative cable line length. A single-axe trailer-based cable yarder (Greifenberg

TG700) and an automatic time-triggered clamped carriage (Greifenberg CRG15) were used for yarding the logs (cable system 3A in Table 2.2). The cable system used a 20 mm-skyline and a 10 mm-mainline. Four 16 mm-guylines anchored the tower yarder on its back side. A spruce was used as tail spar, while the tail anchor was a beech stump.

No partial processing was carried out in the forest and only whole trees were yarded to the landing. The yarding operations involved one operator hooking the loads and two operators at the landing site. A pole-man controlled the yarding movements through an electro-hydraulic control panel. A second operator unhooked the load and move the trees out from unloading area using a Deutz-Farh Agroton K430 tractor equipped with a forest winch. The trees were motor-manually processed by two operators in the late afternoon using chain-saws, when the yarding phase was stopped. A self-loading log-truck was used to move and pile the logs. Residues were chipped for energy production. Photos of the block, machines, work elements, and anchor are reported in Figure 6.7.

Site H

This study site was located on a larch-spruce mixed public forest in the municipality of Spriana (Sondrio -Italy). More than 20 hectares of this forest were logged through patch-cuts by a contractor, here named “L1”, employing two experienced and a young operator. The harvesting plan initially accounted five different cable lines. Later, the contractor changed the landing position and the line distribution. The skyline tensile force monitoring interested two working days in two different weeks on a single cable line (cable line M04).

The observed cable road was an uphill-oriented multi-span cable line with three spans and the tower yarder located in proximity of a hairpin bend of the forest road. The observed work cycles were mainly located between the first and the second spans during the first day, and in the middle of the third span during the second day. A trailer-based cable yarder (Konrad KMS12U) and a motorized carriage with independent drop line (Konrad Liftliner 4000) were used for yarding the logs (cable system 6A in Table 2.2). The cable system used a 22 mm-skyline and a 12 mm-mainline. The carriage used a 12 mm-drop line with total length of 85 m. Four 20 mm-guylines anchored the tower yarder on its back side. Two

Figure 6.7: Photos of Site G. From the top left: Inhaul; Unloading; Tractor and winch used for cleaning the landing; Cable yarder; Carriage; Anchor

larches were used as in-line double tail anchor. Whole trees and topped trees were used as intermediate supports.

Heavy trees were partially processed in the forest. Logs, whole trees, and topped trees were yarded to the landing. The cable yarder and the carriage were operated through two remote radio controls. The hauling phases were automatized through the use of the programmable software installed on the machine. Chockers were used for hooking the load. The yarding operations involved one choker-man hooking the logs and two operators at the landing site. The pole-man controlled the unloading phase and unhook the loads, a second operator processed the logs driving an excavator-based processor, based on a CASE

1188 wheeled excavator equipped with a Konrad Woody 60 processor head. Because of the steep and the limited width of the access road, a two-staging log transportation was required. Thus, logs were initially transported using a tractor and trailer with a loading hydraulic arm. Frequent chipping of the residues, using a trailer chipper, was required by the limited dimension of the landing. Photos of the block, machines, and structural supports are reported in Figure 6.8.

Site I

Site I was located on a mixed spruce-silver fir public forest in the municipality of Bema (Sondrio - Italy). Ten hectares of this stand were patch-cut by a contractor, here named "L2", employing five experienced operators. The administration planned three cable lines, but the contractor yarded the whole area with a single cable line. The skyline tensile force monitoring interested two consecutive working day on a single cable line (cable line M03). The observed cable road was an uphill-oriented multi-span line with three spans and the tower yarder located at a landing on one side of the forest road. The observed work cycles were distributed in the third span. A trailer-based cable yarder (Greifenberg TG860) and an automatic active slack-pulling clamped carriage (Greifenberg HT30) were used for yarding the logs (cable system 5A in Table 2.2). The cable system used a 22 mm-skyline and a 12 mm-mainline. Also, because of the limited slope of the first two spans, a 11 mm-haul-back line was used. Five 16 mm-guylines anchored the tower yarder, four on its back side and one in the front size as security against tower overturning. Whole trees were used as anchors and intermediate supports.

Large trees, mainly silver firs, were partially sorted in the forest. The rest of the material was yarded as whole trees. The cable yarder was operated through an electro-hydraulic control panel. It also had the possibility to automatize the hauling phases, but it was programmed just for reducing the speed in proximity of the intermediate supports. The clamping system of the carriage and the active slack pulling of the mainline were controlled through two radio controls. Chockers were used for hooking the load. The yarding operations involved one choker-man who also controlled of the carriage moving during the loading steps. Four operators were employed at the landing site. A pole-man operated the cable

Figure 6.8: Photos of Site H. From the top left: Loading area; Landing; Excavator-based processor; Intermediate support; Motorized carriage; In-line double anchor

yarder and the carriage. Two operators unhook the chockers and motor-manually processed the logs using chainsaws. The last operator moved and piled the logs and the residues driving a Volvo 400L track excavator-based grapple loader. Self-loading log-trucks periodically cleaned the landing. Residues were chipped for wood energy production. Photos of the block, machines, work elements, and structural supports are reported in Figure 6.9.

Figure 6.9: Photos of Site I. From the top left: Loading area; Landing; Lateral skid; Inhaul; Carriage; Anchor

Site L

This site was located in a private larch-spruce mixed stand in the municipality of Villa di Tirano (Sondrio - Italy). A 3.3 hectares patch-cut was managed by a contractor, here named "L3", employing three experienced and a young operator. The skyline tensile force monitoring interested one working day on a single cable line (cable line M01).

The observed cable road was a four-spans uphill-oriented cable line with the tower yarder located at a landing close to an ordinary road. The observed work cycles were concentrated in the last span. A tractor-based cable yarder (Valentini V400/2T), pulled and powered by a FiatAgri F110 wheel tractor, and an automatic time-triggered clamped carriage (Koller

HSK2002) were used for yarding the logs (cable system 1A in Table 2.2). This cable yarder was manufactured to work with a 16 mm-skyline with a maximum length of 400 m. However, in this site, the contractor used a 20 mm-skyline with a total length of 600 m. This cable cannot be wrapped on the skyline drum of the cable yarded and was wrapped on a dedicated coil once the yarding operation was completed. A 10 mm-mainline and five 14 mm-guylines complete the cable system. Whole and topped trees were used as anchors, tail spars and intermediate supports.

Most of the trees were halved in the forest to allow an easier yarding operation. The yarding operations involved a choker-man hooking the loads and two operators at the landing site. Chockers were used for hooking the load. At the landing, a pole-man controlled the yarding movements through an electro-hydraulic control panel. An operator unhooked the load and processed the logs. A third operator assisted the processing phase and piled the logs driving a Neuson 8002 tracked excavator-based grapple loader. A self-loading truck and trailer transported the logs. Residues were chipped for wood energy production. Photos of the block, machines, work elements, and anchor are reported in Figure 6.10.

Site M

Site M was located in a mixed spruce-larch-Scotch pine public forest in the Chiesa di Valmalenco (SO), in Lombardy Region. The harvesting plan focused on a path-cuts and cleanup in proximity of the sky facilities. The logging operations were managed by a contractor, here named “F4”, employing three experienced operators. The skyline tensile force monitoring interested one working day on a single cable line (cable line M02).

The observed cable road was a downhill-oriented double-span cable line with the tower yarder located at the forest road at bottom of the stand. Almost one-third of the second span, starting from the tail anchor, was in contact with the ground. The observed work cycles were located in the upper part of the first span and in the first half of the second one. A trailer-based cable yarder (Valentini V600/M/2/1000) was used in compliance with a self-propelled carriage (Konrad Woodliner3000) for yarding the logs (cable system 4A in Table 2.2). The cable system used a 22 mm-skyline. No mainline or haul-back line were required because of the use of a self-propelled carriage. Four 18 mm-guylines anchored

Figure 6.10: Photos of Site L. From the top left: Loading area; Landing; Inhaul; Excavator-based grapple loader; Carriage; Anchor

the tower yarder. Two spruces were used as double in-line tail anchor. A larch was used as intermediate support.

Mostly whole trees were yarded to the landing. Once the skyline was pretensioned, the cable system was managed directly operating the self-propelled carriage through two radio controls with the possibility to automatize the hauling phases. Chains were used for hooking the load. The yarding operations involved two operators at the loading hooking the loads and one operator at the landing site. The operator at the landing controlled the unloading phase, unhook the load and process the logs. During the monitoring, most of the material was not usable for industrial purposed and it was directly piled without any

processing step for the further chipping. The loads were moved directly by the operator at the landing driving a New Holland E145 track excavator-based grapple loader. Photos of the block, machines, anchors, and monitoring are reported in Figure 6.11.

Figure 6.11: Photos of Site M. From the top left: Harvested area; Landing; Unloading; Cable yarder; Carriage; First of the in-line double anchor

Annex 4: Study site details: Winch-assist harvesting systems

Site N

Site N was located in Clearwater, in the North Thompson River valley (British Columbia - Canada). The forest was managed by Canfor, a North American forest company accounting more than 4000 employers in British Columbia (PWC 2016). A 50 hectares block was clear-cut by a contractor, here named "BC1", original from Switzerland and specialized in steep slope harvesting. The block, initially partially planned for cable logging, was exploited combining conventional and winch-assist ground machines.

The logging operations were monitored for a whole week. Differently from what was initially planned, during the first days any forwarder was operating in the area and the measurements were limited to the harvesting machines (not reported in this work). The forwarding operations were monitored during the last day of the week, observing a John Deere 1910E integrated-winch forwarder working on a single trail (CR01), driven by two different operators. The portion of the block where the forwarder was monitored is highlighted in Figure 6.12. The forwarding direction was downhill-oriented. The stump anchor was reached through a lateral access trail. The steepest slope of the trail was limited to a short section in proximity of the forest road.

The harvesting machine used to cut the steepest section of the block, including the observed area, was a John Deere 1470G harvester equipped with semi-tracks and integrated HAAS synchro-winch GEN2, with a 90 kN maximum pulling force. The original hydraulic crane of the harvester was substituted with a more powerful Mesera 285H 97. The harvesting head was a Waratah H290. Photos describing the block, the machines, and the monitoring are reported in Figure 6.13.

Site O

Site O was located in Kamloops (British Columbia - Canada), 180 km far from Site N, where the North and South Thompson rivers meet. The forest was managed by Interfor, a North American forest company accounting 1160 employers in British Columbia (PWC 2016). A

17 hectares clear-cut was carried out by a contractor, here named “BC2”, historically operating in the Thompson River valley.

The logging operations were monitored for a whole week. Again, similarly to Site O, any forwarder operated in the area during the first days, differently from what was initially planned. Thus, the tensile force monitoring initially focused on the harvesting machines (not reported in the present work). Two John Deere 1910E integrated-winch cable-forwarders started to operate during the last monitored day. The cable tensile force interested one of these forwarders, operating in the block section highlighted in Figure 6.14. The analysis interested one trail (CR02) and one operator.

The forwarding operations were uphill-oriented. The anchor was a large Douglas fir. The cable was deviated on a medium-size stump to center the line along the trail. Similarly to the Site N, the harvesting machine was a John Deere 1470G equipped with chains and semi-tracks and integrated with a Haas Highgrade synchro-winch GEN2, with a maximum pulling force of 90 kN. The harvesting head was a Waratah H290. Photos of the block, machine and monitoring are reported in Figure 6.15.

Site P

This site was located 100 km east from Prince George (British Columbia - Canada). The forest was managed by Canfor. A large block (116 ha) was clear-cut by one of the largest contractors in the world, here named “BC3”. A logging camp was available for the loggers and the researchers because the first town was two-hours far from the block.

The John Deere 1910E forwarder operated for the whole observed week. Six trails were monitored (CR03-CR08) in the block section reported in Figure 6.16. Forwarding operations were downhill-oriented in most of the trails. Only one short trail was uphill-oriented. Two forest roads were available at the top and the bottom of the block. Both large trees and stumps were used as anchors. The harvesting machine which felled the block was a 34-tons Tigercat 1185 harvester (the largest harvester available in the market), equipped with a Tigercat 570 harvester head. The harvester was tethered by an Austrian made anchor winch machine Ecoforst T-winch, with a maximum pulling force of 80 kN. Photos of the block, machine and monitoring are reported in Figure 6.17.

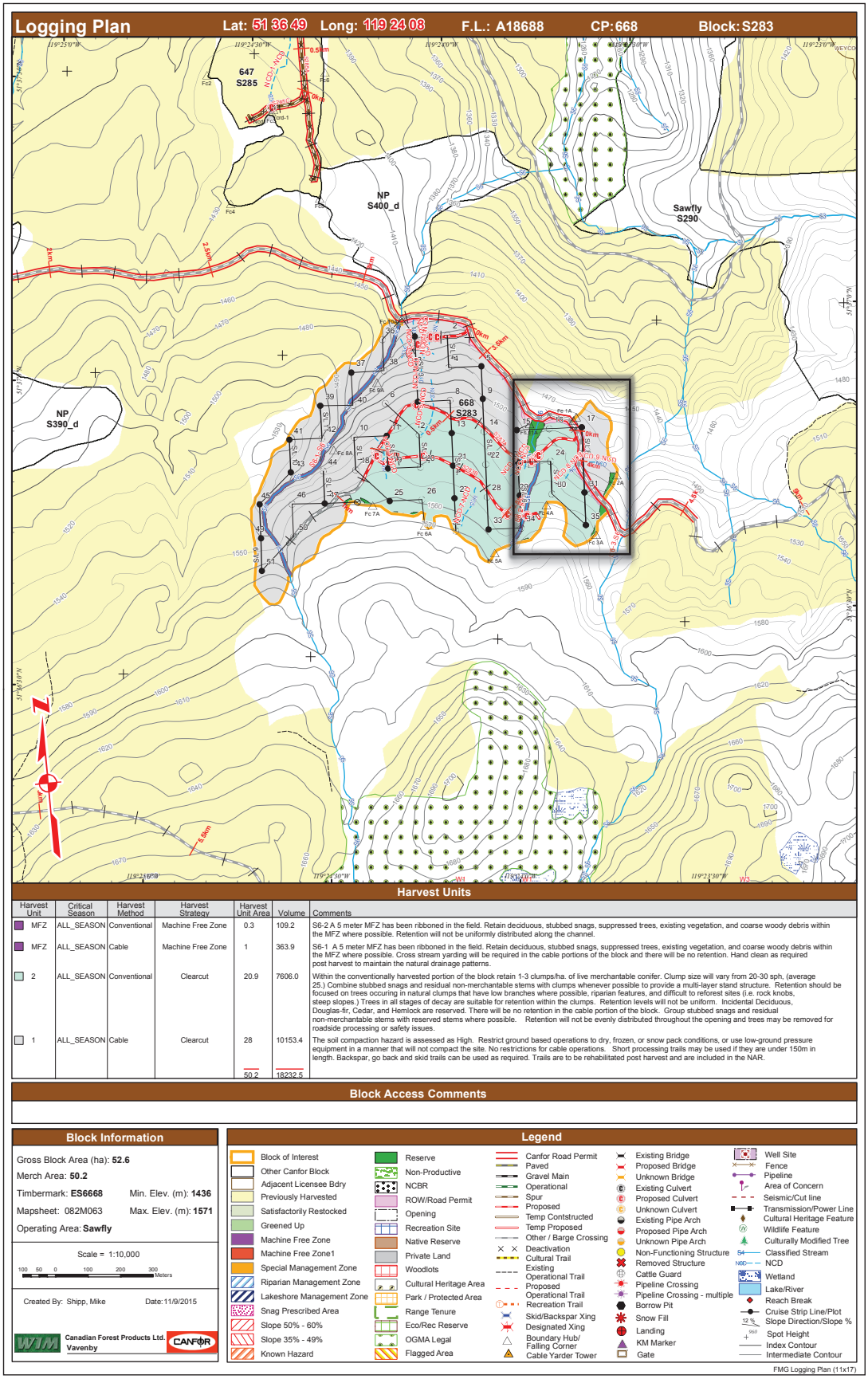

Figure 6.12: Logging plan of Site N with evidence of the area interested by the monitoring

Figure 6.13: Photos of Site N. From the top left: Winch-assist harvesting operations; Harvester; Landing; Log-Truck; Winch-assist forwarding; Forwarder; Cable tensile force monitoring system; Anchor

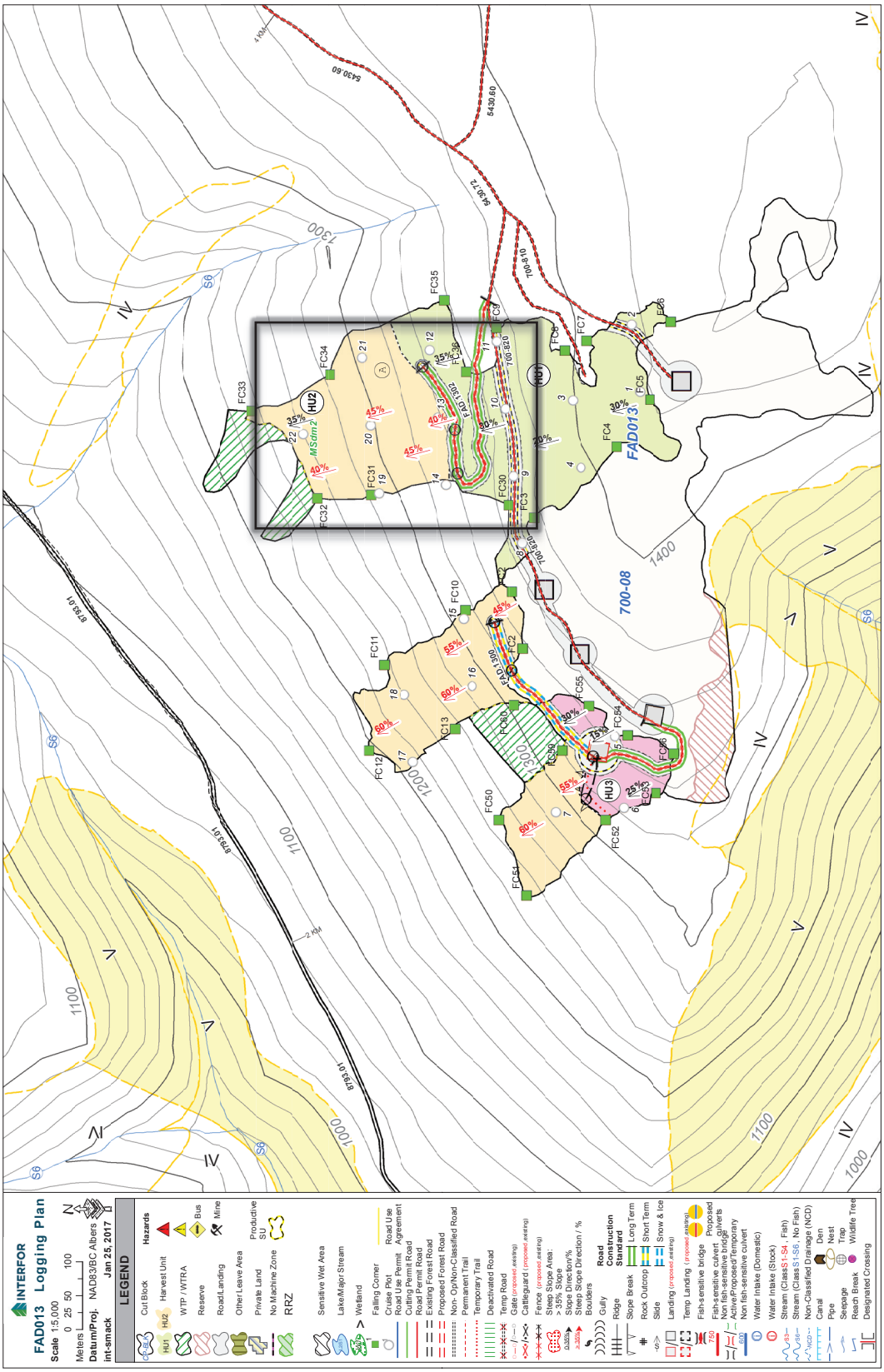

Figure 6.14: Logging plan of Site O with evidence of the area interested by the monitoring

Figure 6.15: Photos of Site O. From the top left: Winch-assist harvesting operations; Harvester; Harvested area; Unloading at the Landing; Winch-assisted forwarder close to the landing; Deviating system used to center the cable on the trail; Cable tensile force monitoring system; Anchor

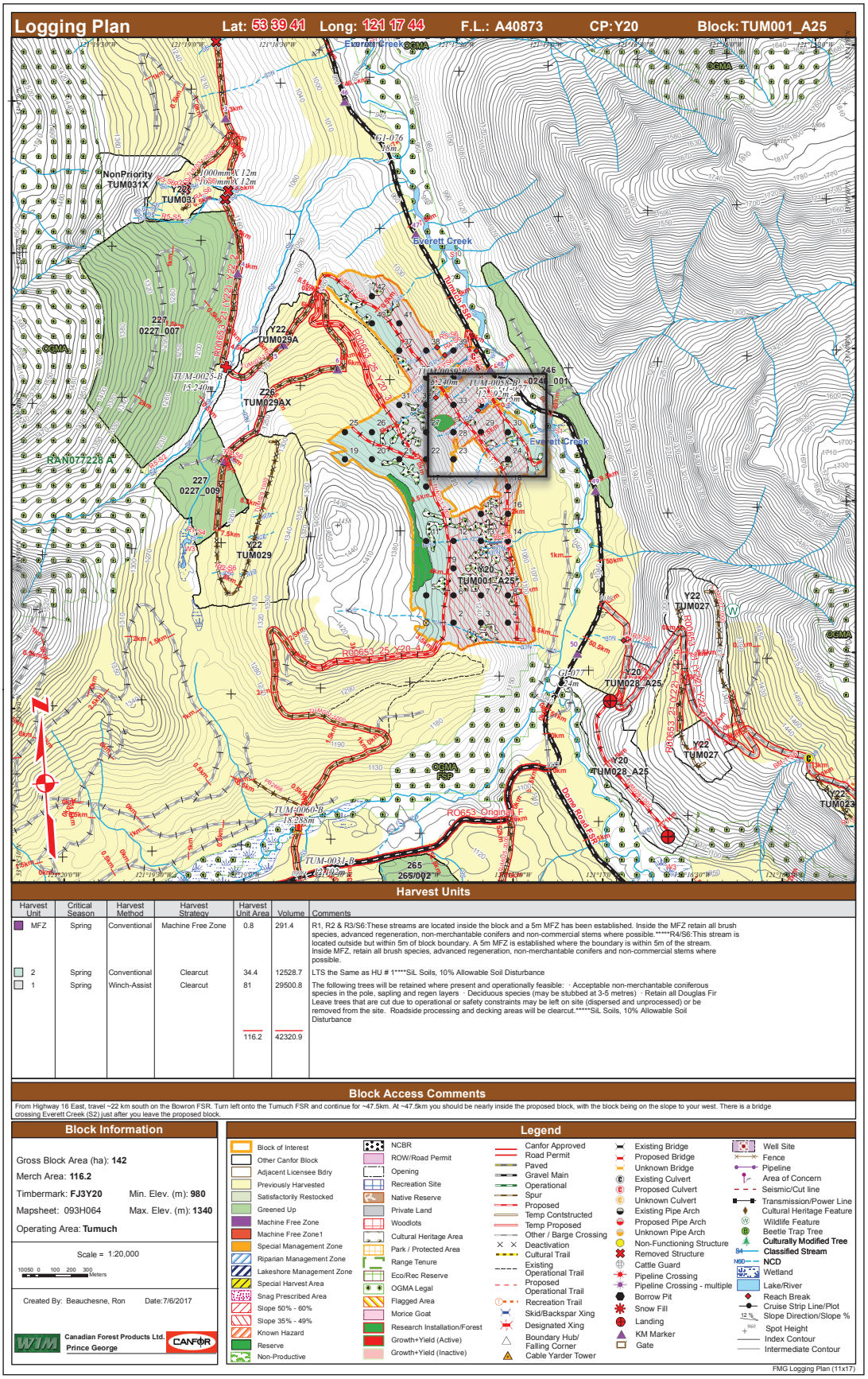

Figure 6.16: Logging plan of Site P with evidence of the area interested by the monitoring

Figure 6.17: Photos of Site P. From the top left: Winch-assist harvesting operations; Harvester; Anchor based machine; Harvested area; Winch-assist forwarding; Forwarder; Cable tensile force monitoring system; One of the anchors

Annex 5: Profiles and maps of the monitored cable lines

This section reports for each monitored cable line: the graphical representation of the longitudinal profile, a summary table with the main features of the skyline structural element supports, and a map showing the skyline and its structural element position. When appropriate, also the haul-back lines and their supports are reported in the map. In case of multiple anchor, only the first one is reported in the longitudinal profile and in the map.

The longitudinal profiles show the different type of anchors (whole trees or stumps) and intermediate supports (whole trees or topped trees). Also, the different spans described in Table 3.1 are highlighted. The ground profile; the supports heights, and the skyline position at the supports is in scale. The representation of anchors and support is not representing the real tree species or type. It is only used to identify the type of support.

The tables report the details of each element reported in the profile representations and in the maps. In the specie column it is also indicated when the support is artificial. The "DBH" column reports the diameter at breast height (nearly 1.30 m). In case of stumps, this column reports the diameter measured at the highest point. The columns "H tot", "H rope", and "H force" report, respectively: the total height of the support; the clearance of the skyline at that point; the height of the application of the force at the support. In case of anchors, "H rope" and "H force" are approximated to zero. The "Distance" column indicates the horizontal distance from the tower yarder. Also, the tables report the ground profile slope.

The maps show the skylines and the haul-back lines, when appropriate, with their relative structural element positions on the hillshade. Also, the maps report the evidence of the ground slope (with 40% transparency) and the contour lines (reported every 5 m) derived by the high-quality Digital Elevation Models.

Cable line S01 (Site F)

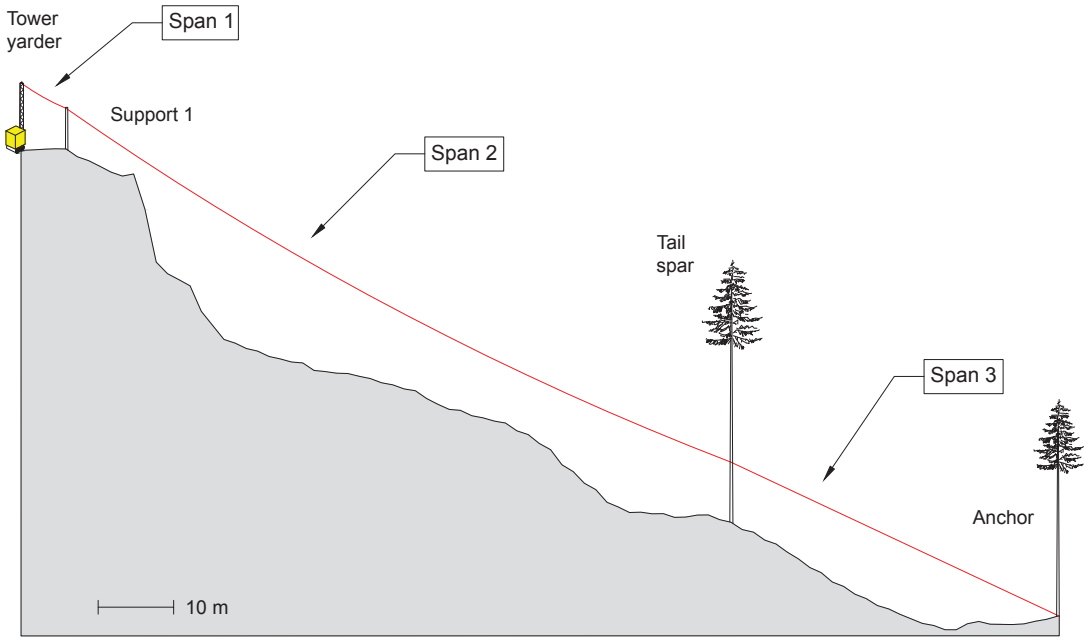

Element -	X coord. m	Y coord. m	Altitude m a.s.l.	Specie -	DBH cm	H tot m	H rope m	H force m	Distance m
Tower yarder	796603.12	5149985.79	793	-	-	9	9	9	0
Support 1	796603.99	5149979.52	793	artificial	-	6	5.4	6	6
Tail spar	796616.15	5149892.63	744	spruce	55	30	8	11	94
Anchor	796622.26	5149848.93	731	beech	70	20	0	0	138

Profile slope [%]: mean 67.6; st.dev. 46.3; max 534.4

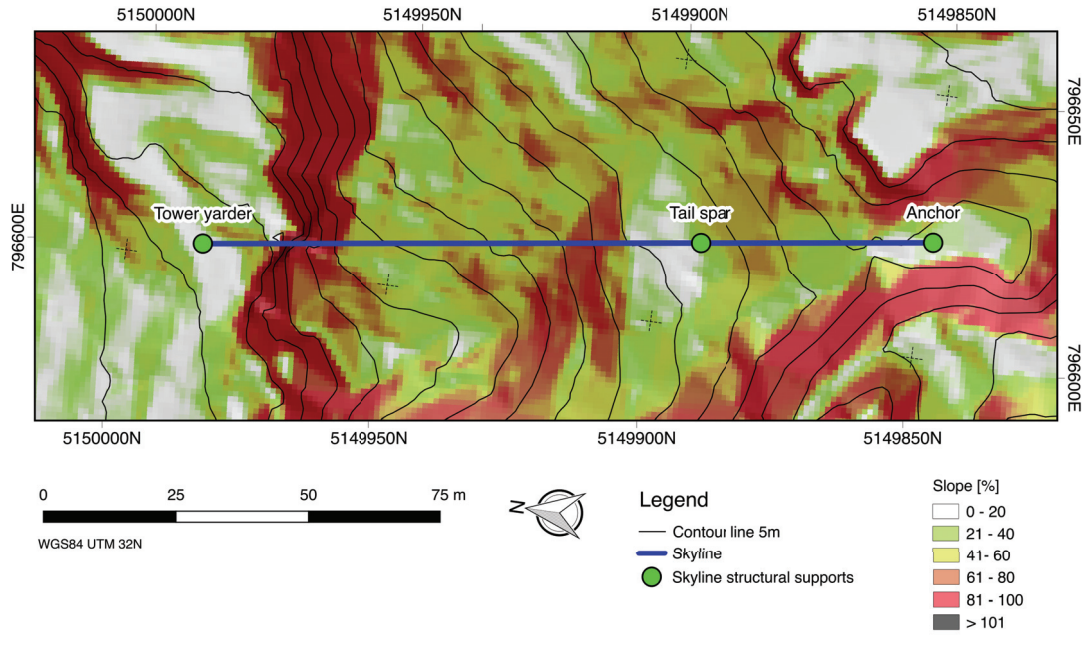

Cable line S02 (Site G)

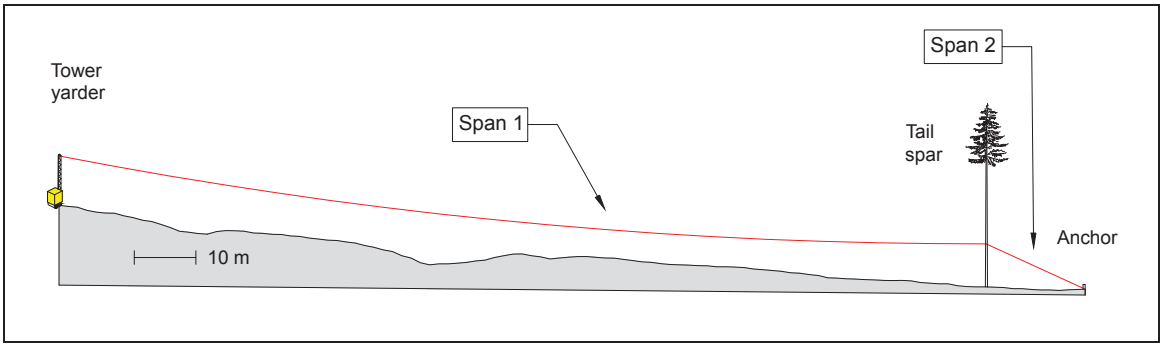

Element -	X coord. m	Y coord. m	Altitude m a.s.l.	Specie -	DBH cm	H tot m	H rope m	H force m	Distance m
Tower yarder	802454.97	5150039.07	965	-	-	8	8	8	0
Tail spar	802446.97	5150189.12	951	spruce	59	30	7	8.8	150
Anchor	802446.12	5150204.99	951	beech	55	0	0	0	166

Profile slope [%]: mean 26.5; st.dev. 18.3; max 126.0

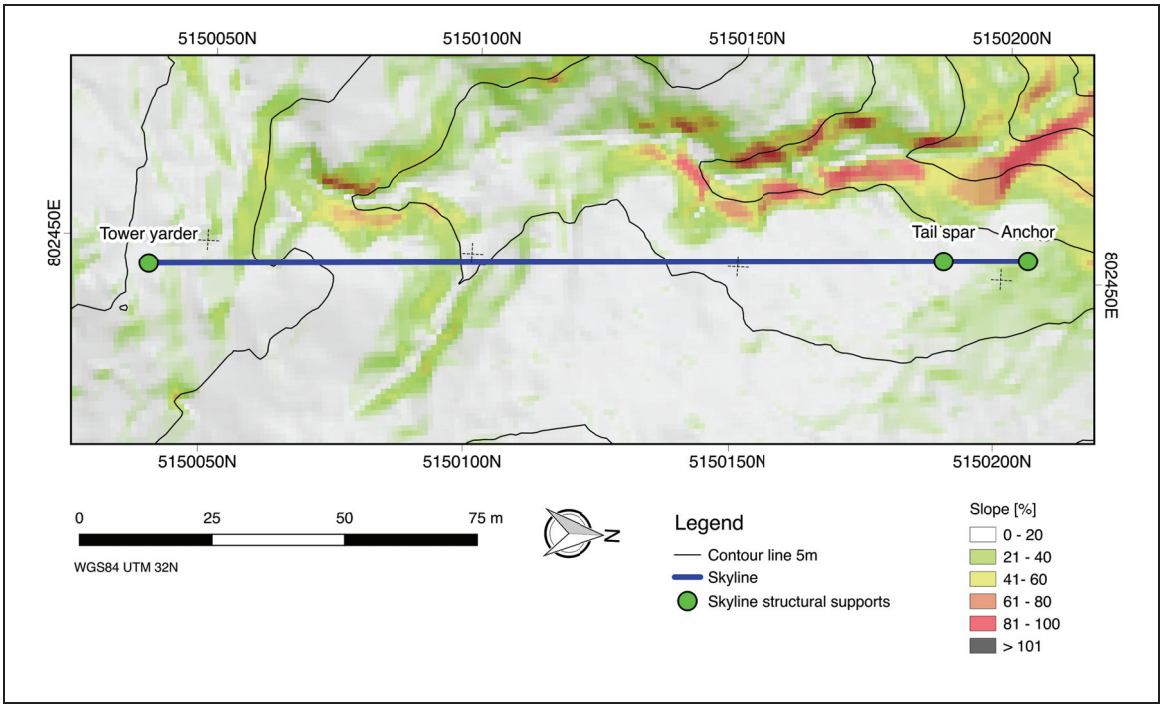

Cable line S03 (Site E)

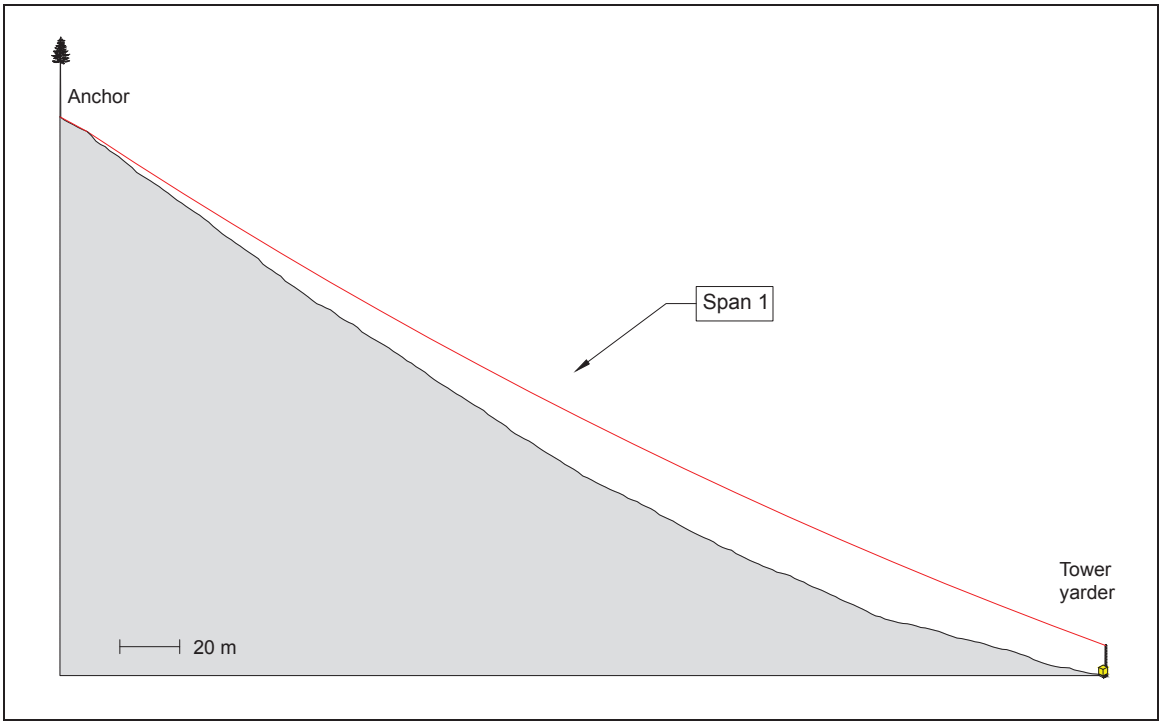

Element -	X coord. m	Y coord. m	Altitude m a.s.l.	Specie -	DBH cm	H tot m	H rope m	H force m	Distance m
Tower yarder	802939.13	5141039.70	950	-	-	10	10	10	0
Anchor	803203.59	5140812.36	1137	beech	48	24	0	0	349

Profile slope [%]: mean 54.7; st.dev. 19.4; max 148.2

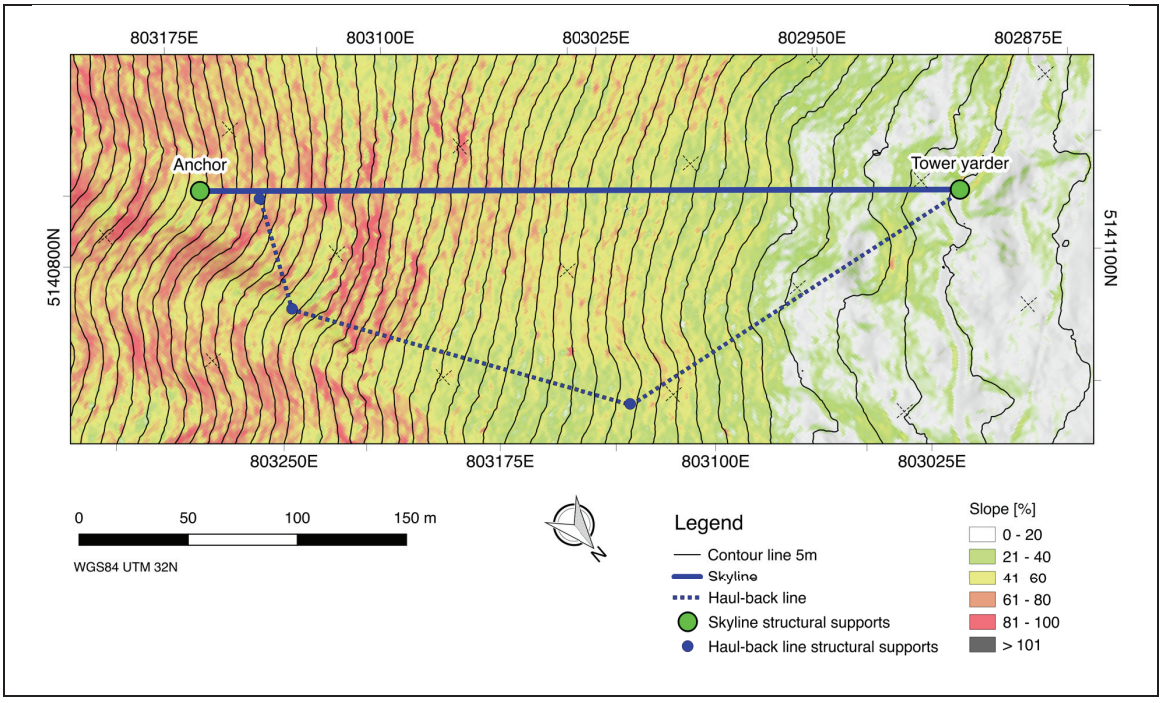

Cable line S04 (Site C)

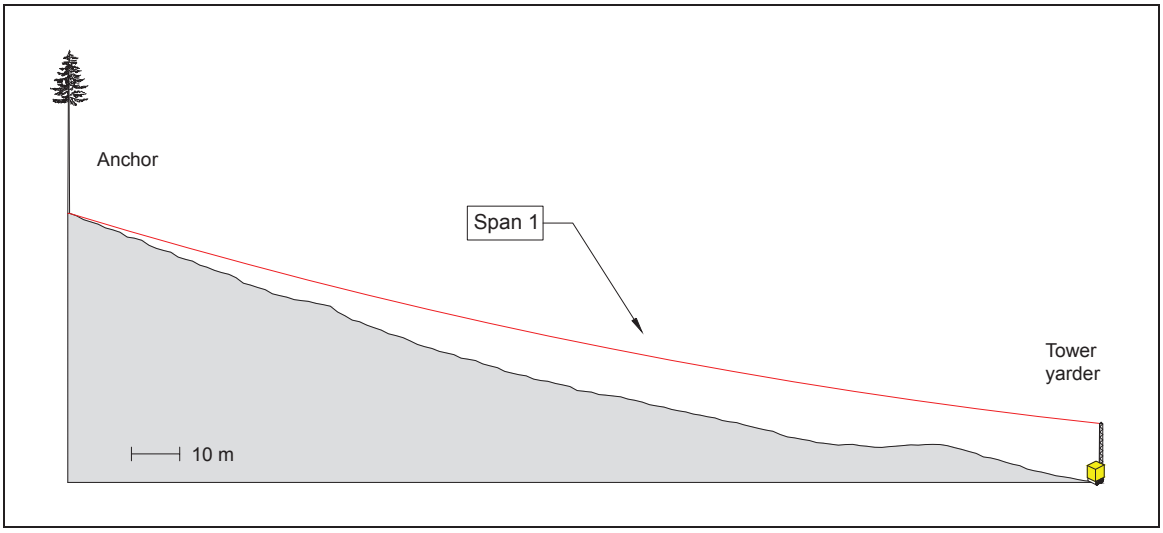

Element -	X coord. m	Y coord. m	Altitude m a.s.l.	Specie -	DBH cm	H tot m	H rope m	H force m	Distance m
Tower yarder	704594.82	5106199.00	1142	-	-	12.2	12.2	12.2	0
Anchor	704780.61	5106303.83	1197	spruce	52	25.2	0	0	213

Profile slope [%]: mean 28.5; st.dev. 10.2; max 47.9

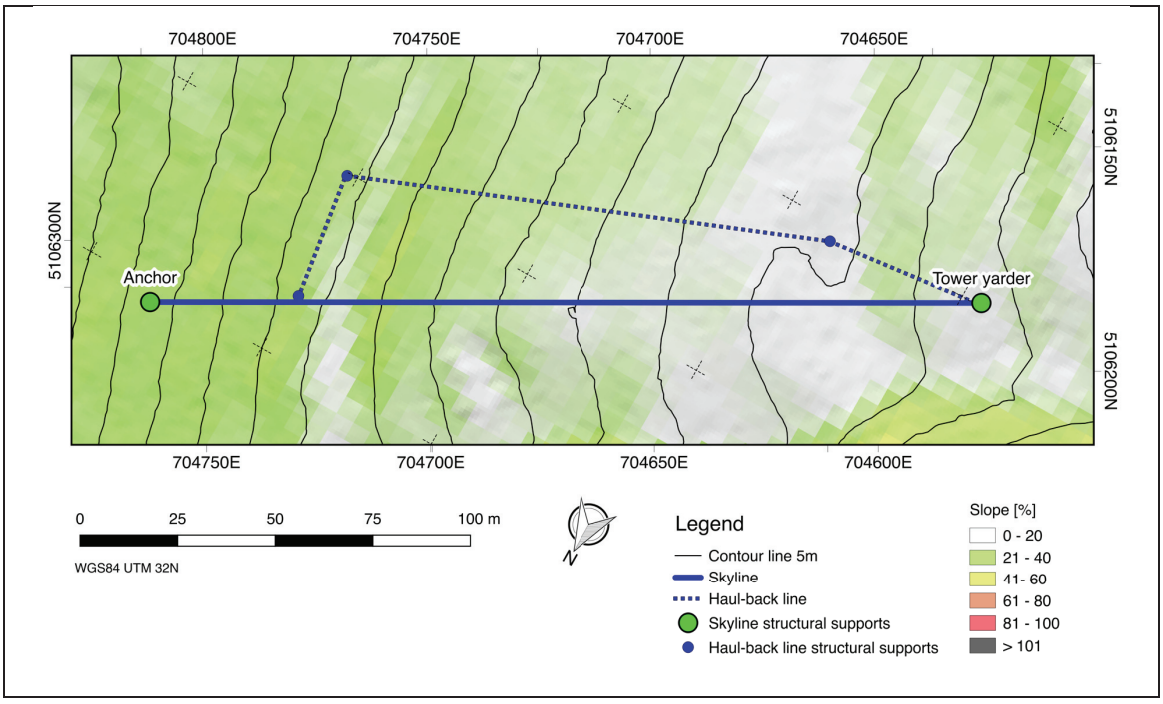

Cable line S05 (Site C)

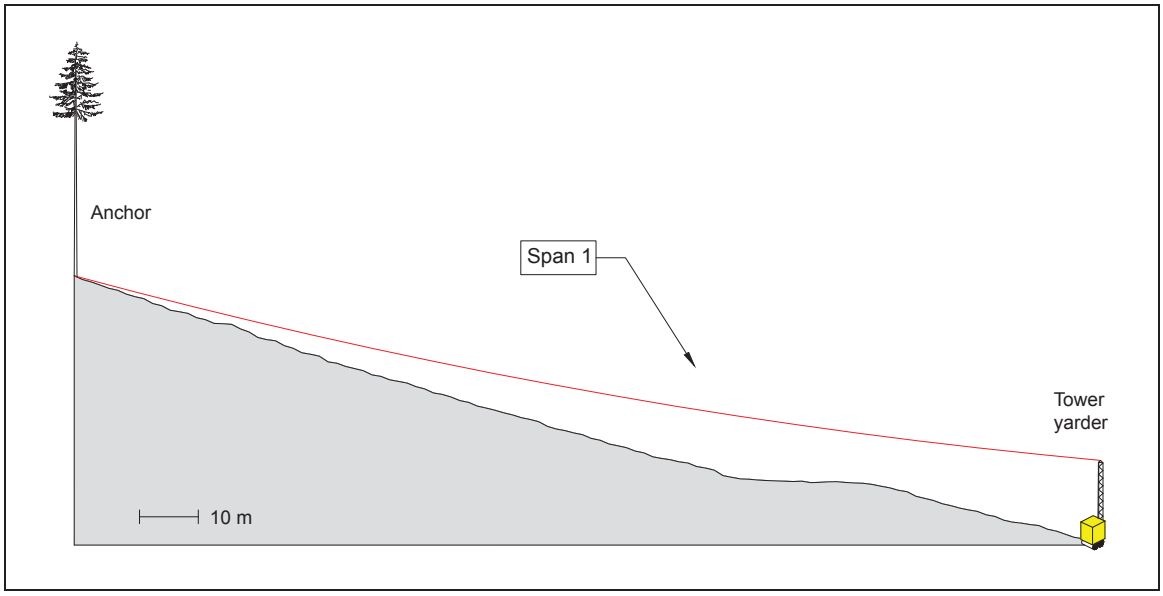

Element -	X coord. m	Y coord. m	Altitude m a.s.l.	Specie -	DBH cm	H tot m	H rope m	H force m	Distance m
Tower yarder	704605.50	5106170.48	1141	-	-	14.5	14.5	14.5	0
Anchor	704769.22	5106233.48	1187	spruce	57	26	0	0	175

Profile slope [%]: mean 28.2; st.dev. 7.6; max 42.3

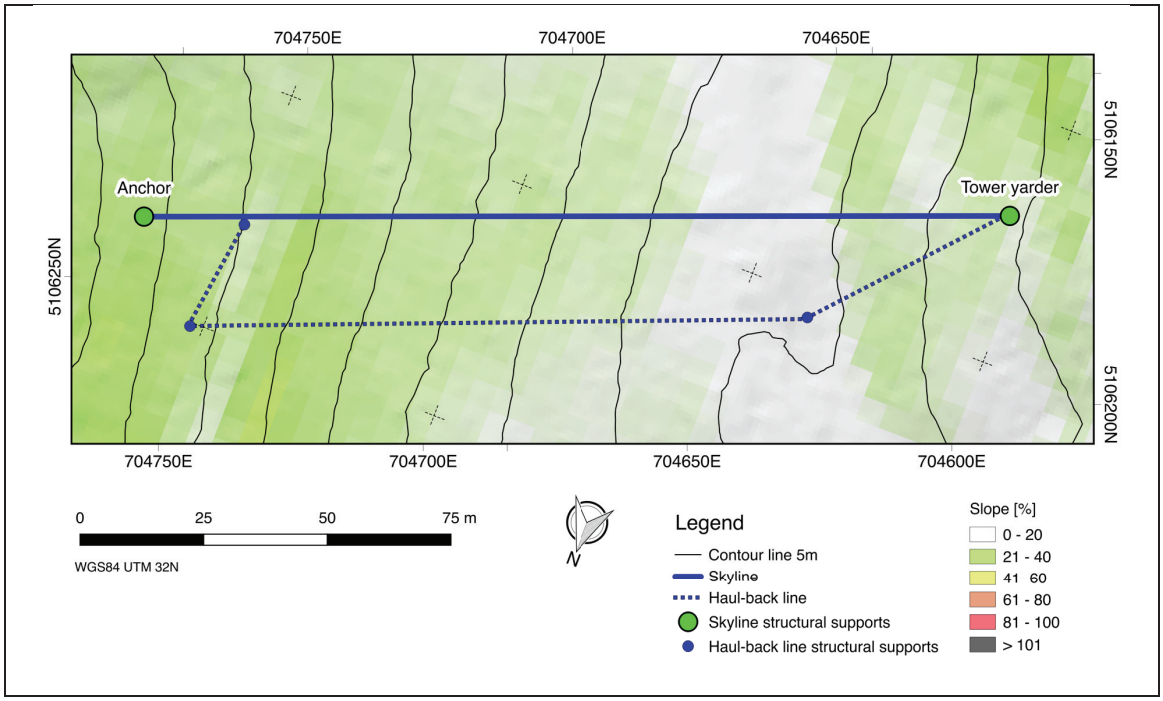

Cable line S06 (Site B)

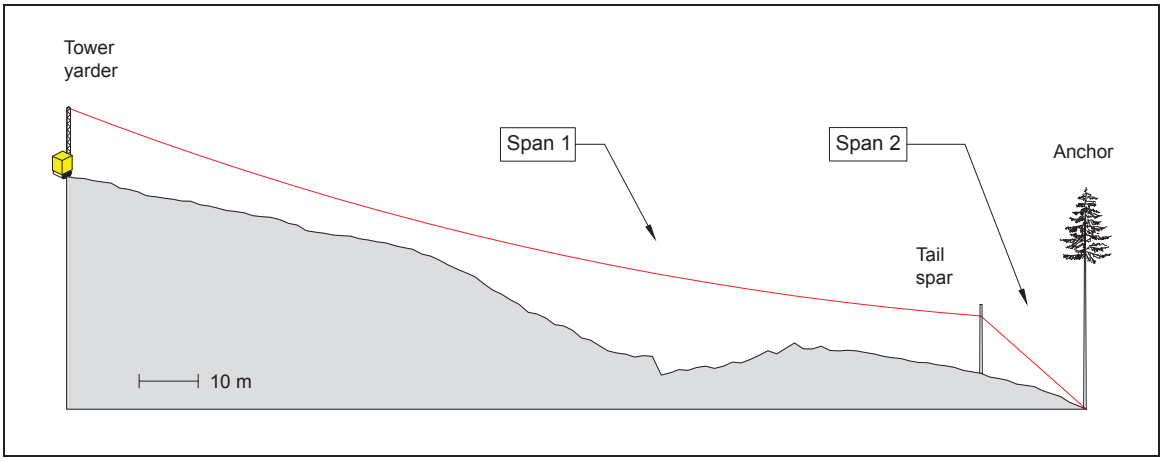

Element -	X coord. m	Y coord. m	Altitude m a.s.l.	Specie -	DBH cm	H tot m	H rope m	H force m	Distance m
Tower yarder	698154.52	5106802.72	975	-	0	11.7	11.7	11.7	0
Tail spar	698226.93	5106666.19	941	spruce	51	10.2	7.3	9.7	155
Anchor	698235.27	5106650.48	935	spruce	51	26.1	0	0	172
Anchor 2	698238.19	5106645.96	933	larix	76	27.3	0	0	178

Profile slope [%]: mean 39.9; st.dev. 15.0; max 100.1

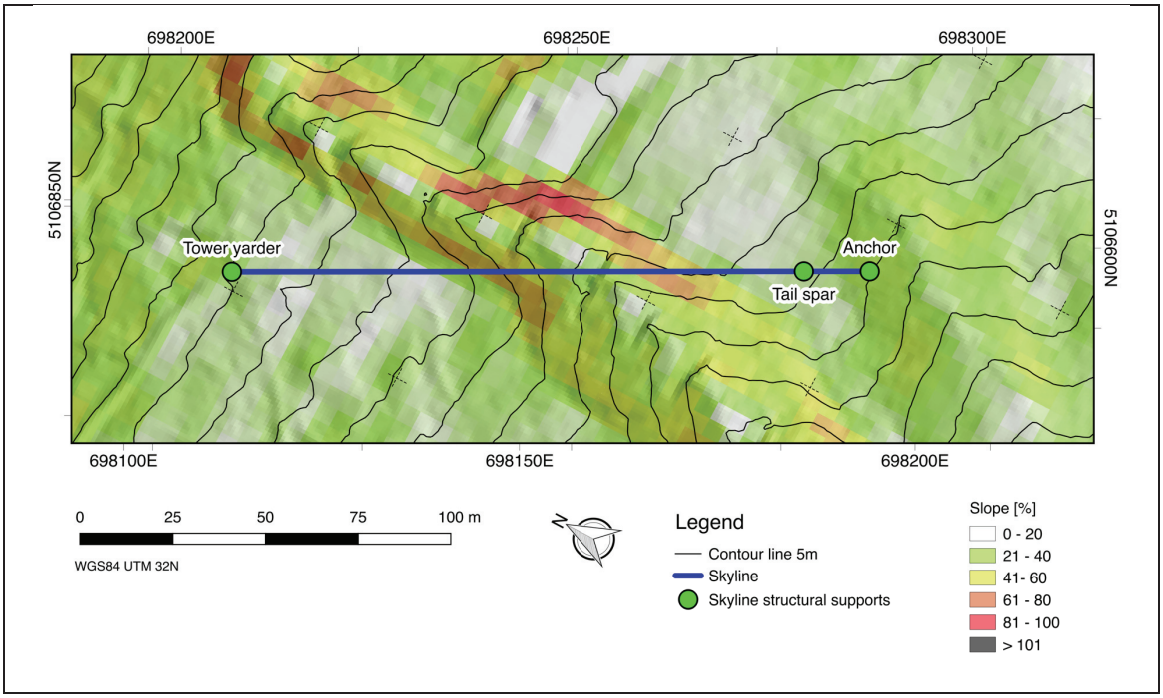

Cable line M01 (Site L)

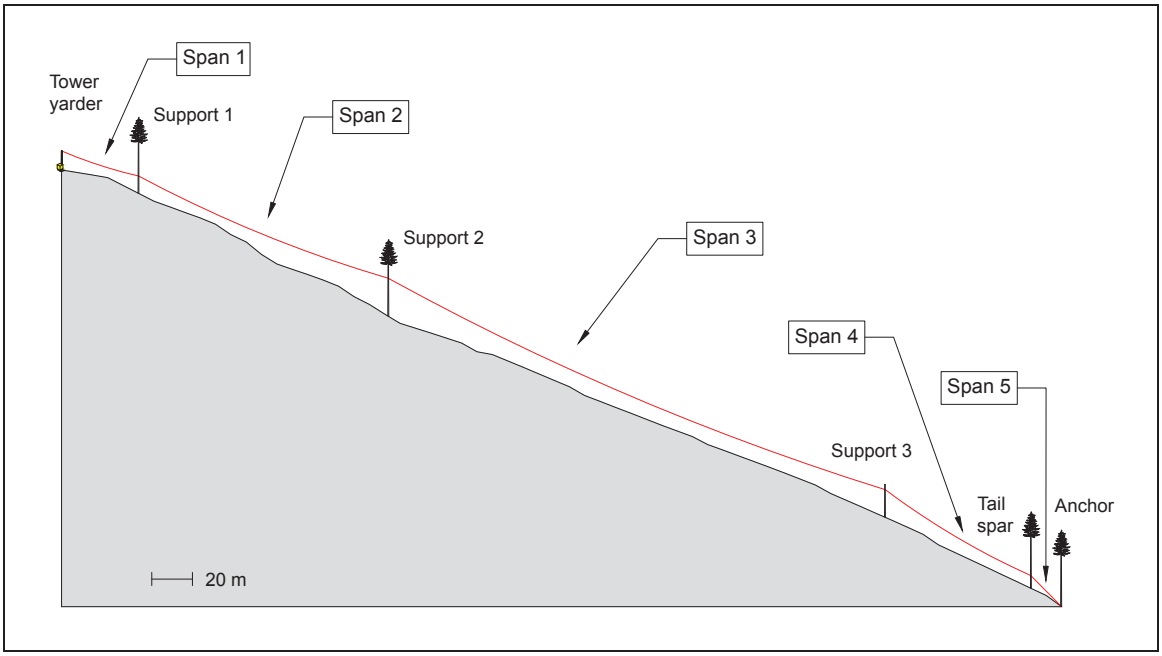

Element -	X coord. m	Y coord. m	Altitude m a.s.l.	Specie -	DBH cm	H tot m	H rope m	H force m	Distance m
Tower yarder	590394.06	5114528.29	1575	-	-	9.3	9.3	9.3	0
Support 1	590365.51	5114553.57	1564	spruce	45	16	8.5	13	38
Support 2	590274.09	5114633.05	1505	spruce	76	30.5	18.5	20	159
Support 3	590091.19	5114792.10	1404	spruce	59	16.5	13.5	15.5	402
Tail spar	590038.14	5114838.24	1371	larix	64	25.7	6.2	8	472
Anchor	590024.80	5114849.84	1362	spruce	45	30	0	0	490

Profile slope [%]: mean 44.1; st.dev. 10.6; max 90.1

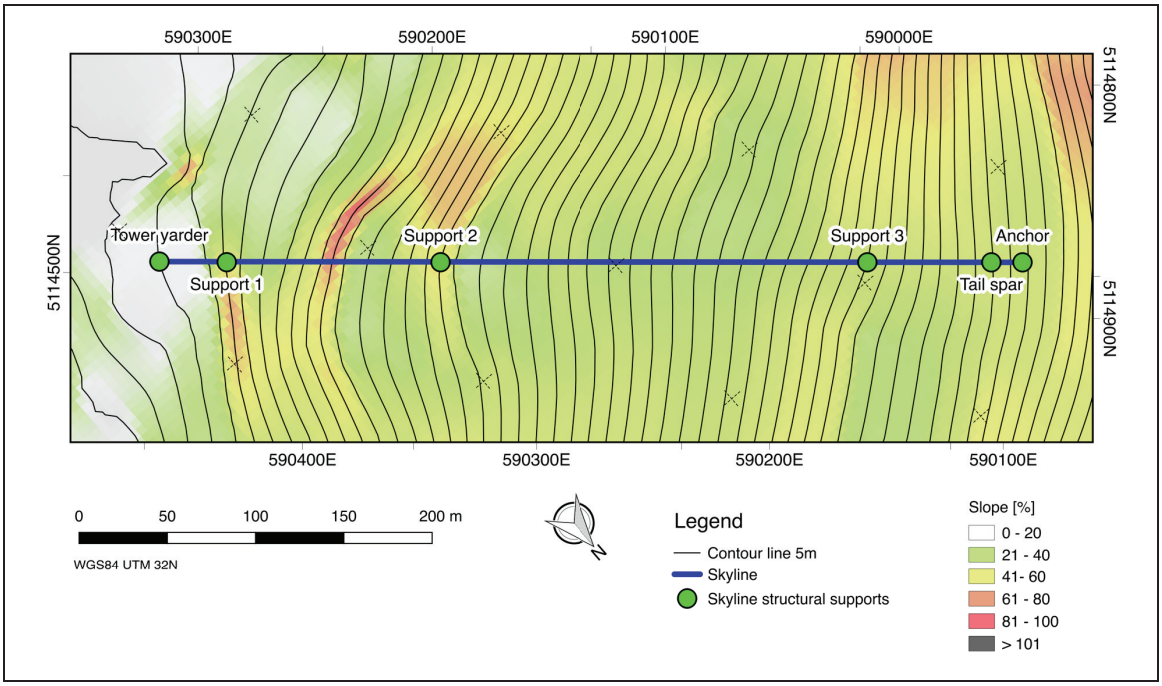

Cable line M02 (Site M)

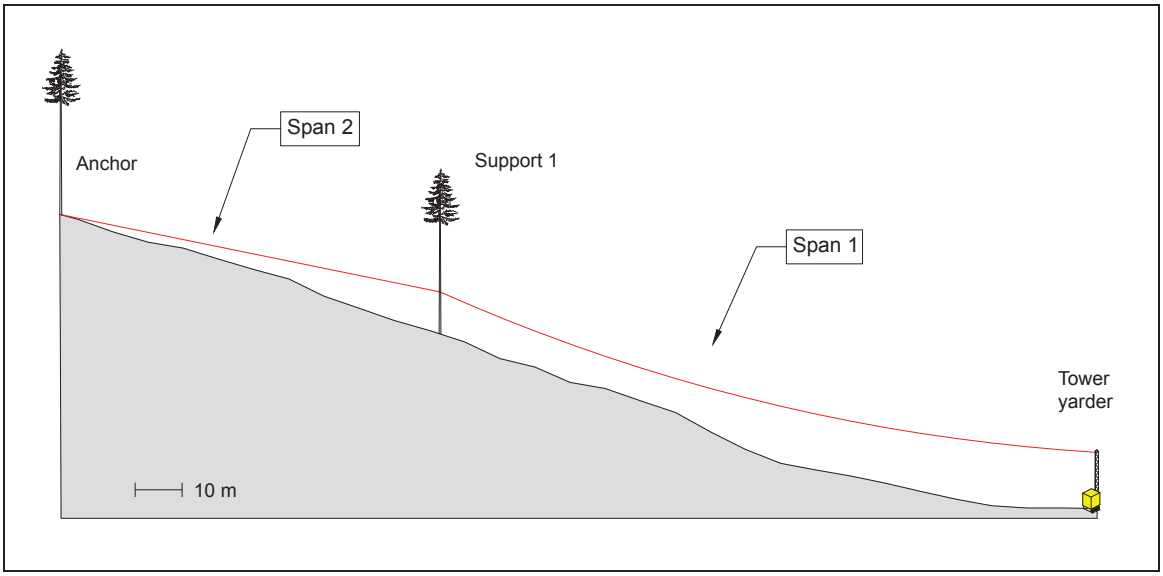

Element -	X coord. m	Y coord. m	Altitude m a.s.l.	Specie -	DBH cm	H tot m	H rope m	H force m	Distance m
Tower yarder	565992.82	5127567.43	1820	-	-	12	12	12	0
Support 1	566078.71	5127456.56	1857	larix	65	25	9	12	140
Anchor	566128.31	5127392.31	1883	spruce	43	19	0	0	222
Anchor 2	566135.78	5127389.06	1884	spruce	43	19.5	0	0	229

Profile slope [%]: mean 30.6; st.dev. 14.7; max 82.1

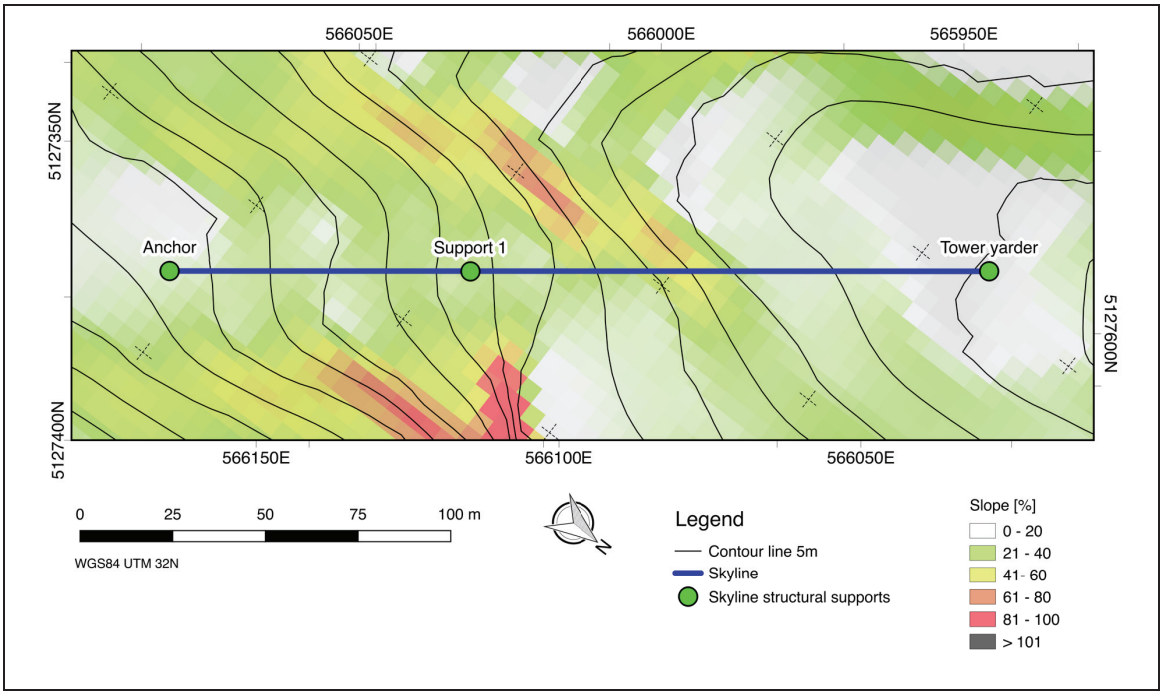

Cable line M03 (Site I)

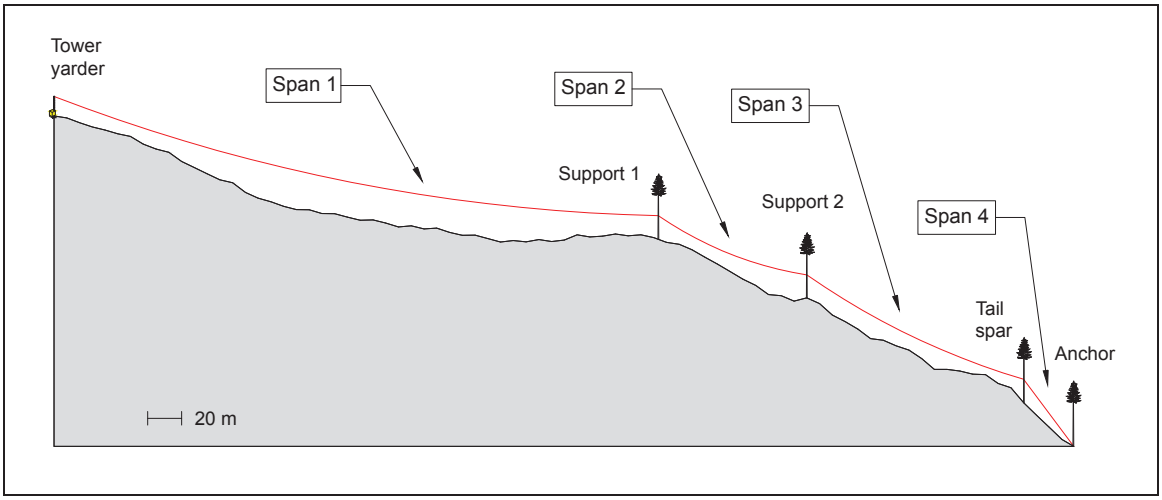

Element -	X coord. m	Y coord. m	Altitude m a.s.l.	Specie -	DBH cm	H tot m	H rope m	H force m	Distance m
Tower yarder	544680.22	5104547.36	1290	-	-	11.5	11.5	11.5	0
Support 1	545003.23	5104694.78	1218	silver fir	65	33.8	13.5	25.5	355
Support 2	545083.80	5104731.55	1180	spruce	51	26	13.5	18	444
Tail spar	545197.78	5104783.59	1121	spruce	65	38	13.8	15	569
Anchor	545225.50	5104796.21	1095	spruce	62	35	0	0	600

Profile slope [%]: mean 59.6; st.dev. 24.1.; max 188.8

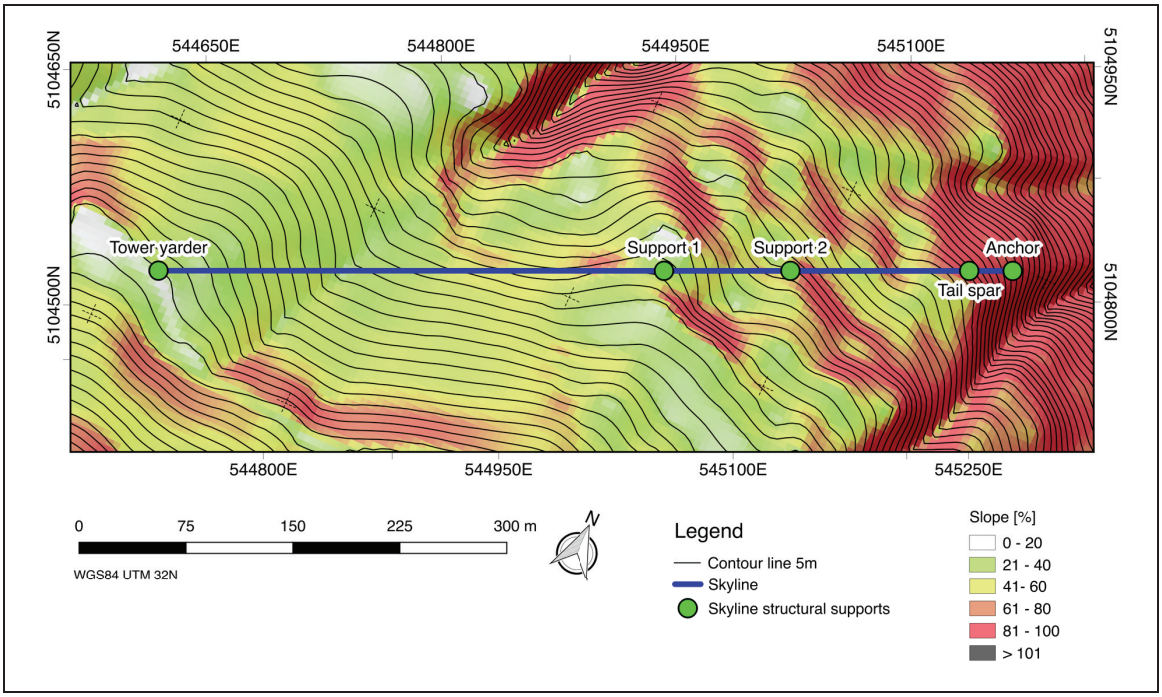

Cable line M04 (Site H)

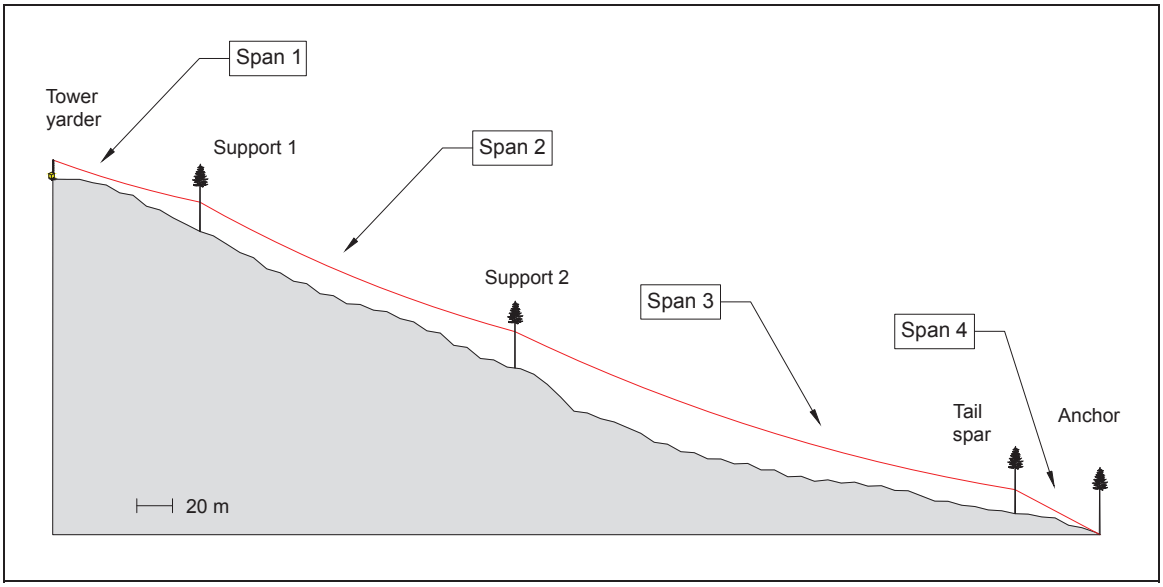

Element -	X coord. m	Y coord. m	Altitude m a.s.l.	Specie -	DBH cm	H tot m	H rope m	H force m	Distance m
Tower yarder	562902.71	5121257.52	1810	-	-	10.8	10.8	10.8	0
Support 1	562979.63	5121229.13	1781	spruce	58	28.5	16.5	19.5	82
Support 2	563146.05	5121167.71	1704	larix	62	25	20.5	22.5	260
Support 3	563407.80	5121071.10	1622	larix	60	34.5	13.5	16	539
Anchor	563454.01	5121054.05	1610	larix	45	12.5	0	0	588
Anchor 2	563458.48	5121050.03	1605	larix	60	27	0	0	595

Profile slope [%]: mean 59.8; st.dev. 21.5; max 126.0

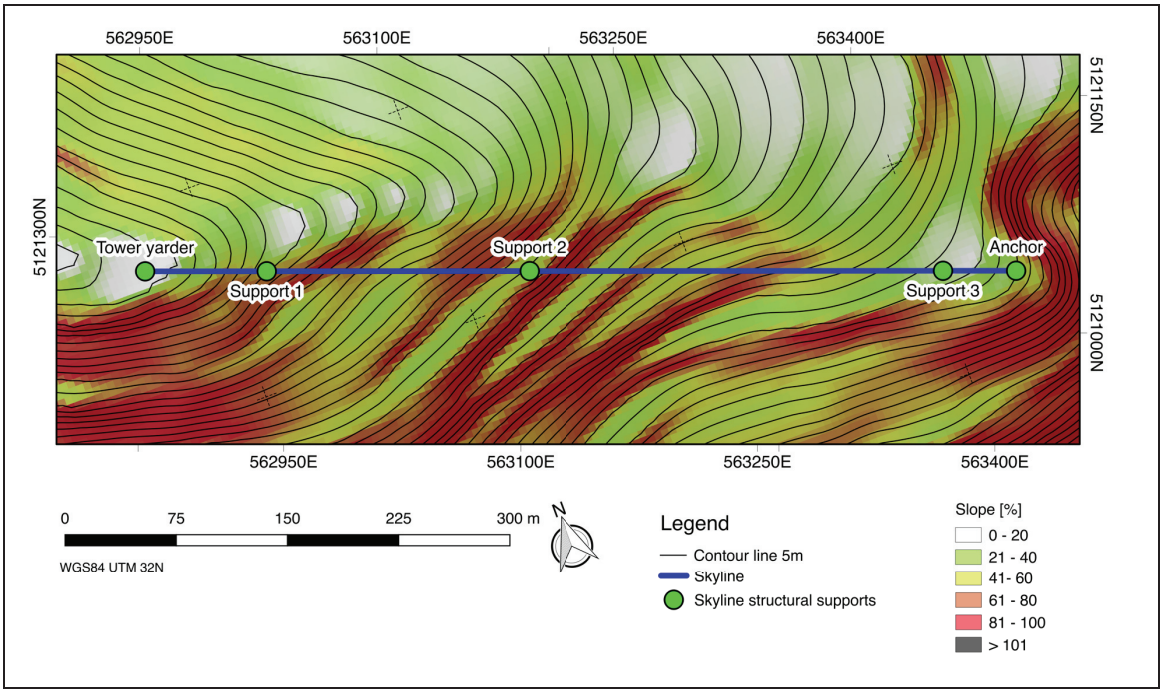

Cable line M05 (Site D)

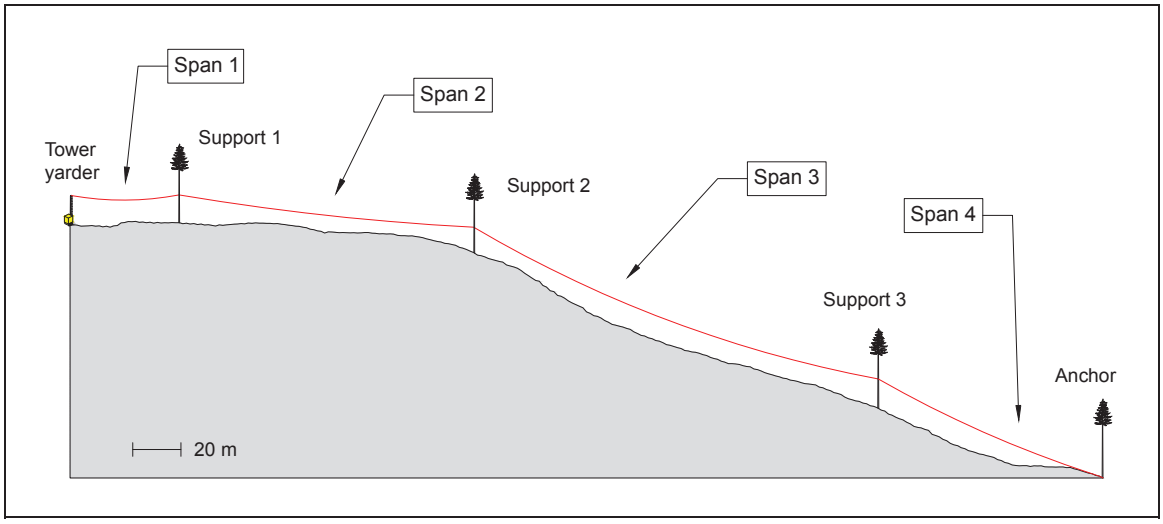

Element -	X coord. m	Y coord. m	Altitude m a.s.l.	Specie -	DBH cm	H tot m	H rope m	H force m	Distance m
Tower yarder	806680.05	5154599.81	1095	-	-	12	12	12	0
Support 1	806723.07	5154587.73	1096	spruce	75	36.5	11.5	13.5	45
Support 2	806840.22	5154554.83	1084	silver fir	51	31	10.5	13	166
Support 3	807002.03	5154509.40	1019	silver fir	50	35	12	13.5	334
Anchor	807090.89	5154484.44	991	spruce	56	30	0	0	426

Profile slope [%]: mean 38.0; st.dev. 15.6; max 120.5

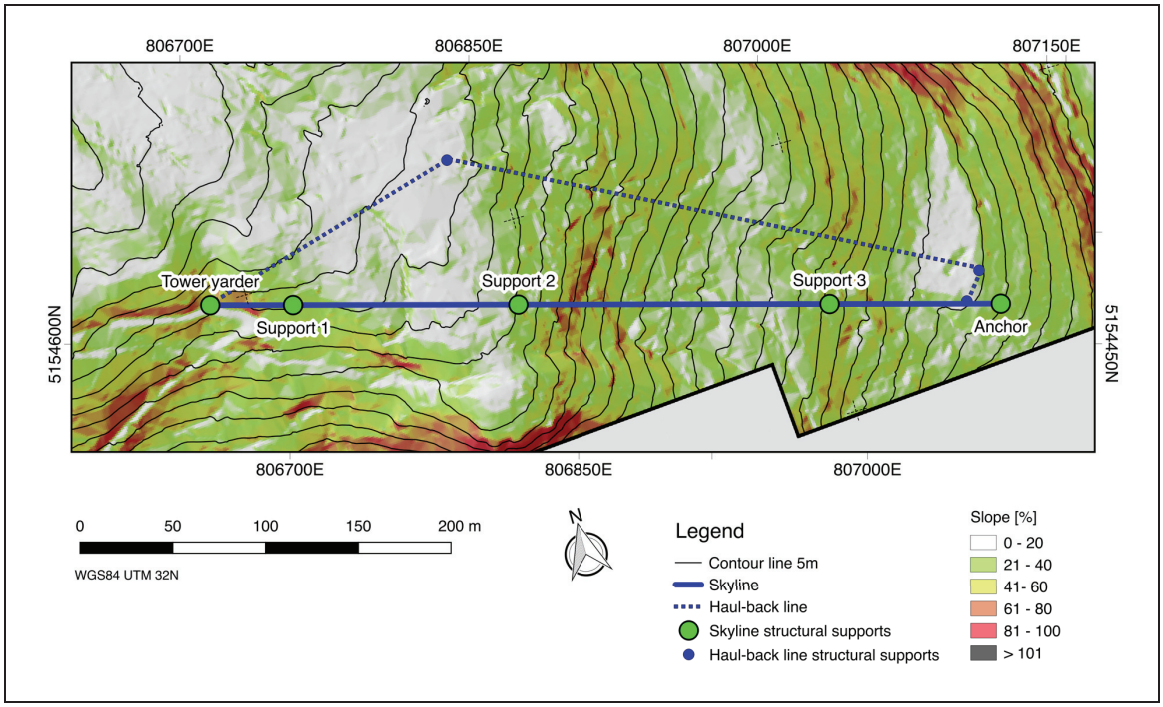

Cable line M06 (Site A)

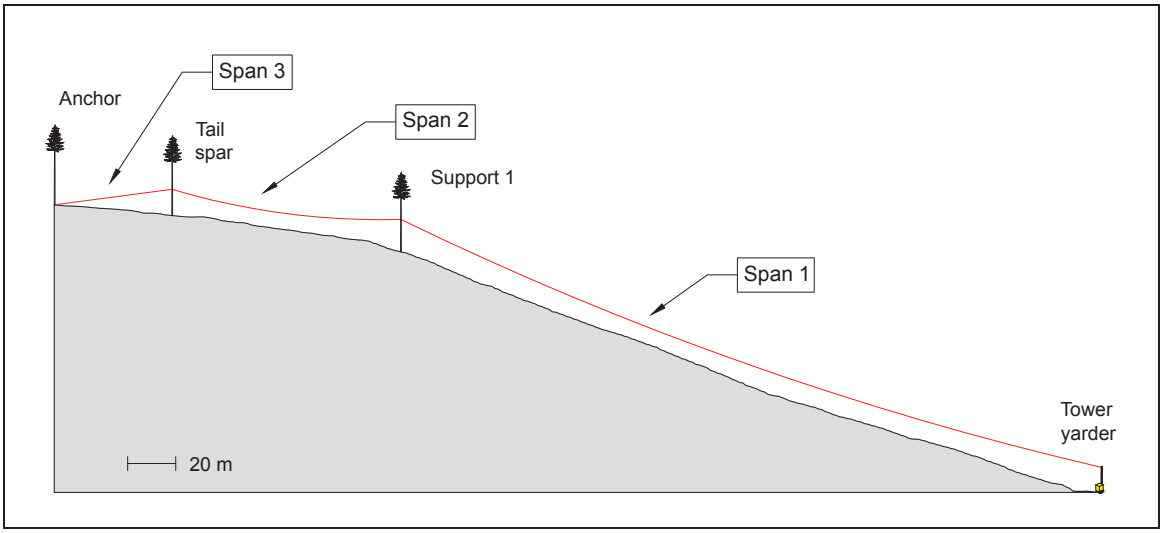

Element -	X coord. m	Y coord. m	Altitude m a.s.l.	Specie -	DBH cm	H tot m	H rope m	H force m	Distance m
Tower yarder	711094.12	5109970.39	1218	-	-	10.5	10.5	10.5	0
Support 1	711107.99	5109677.62	1318	silver fir	62	32	13.6	15.8	293
Tail spar	711112.52	5109582.05	1333	spruce	63	30	11	12	389
Anchor	711114.84	5109533.16	1338	spruce	76	32	0	0	438

Profile slope [%]: mean 30.7; st.dev. 10.4; max 46.9

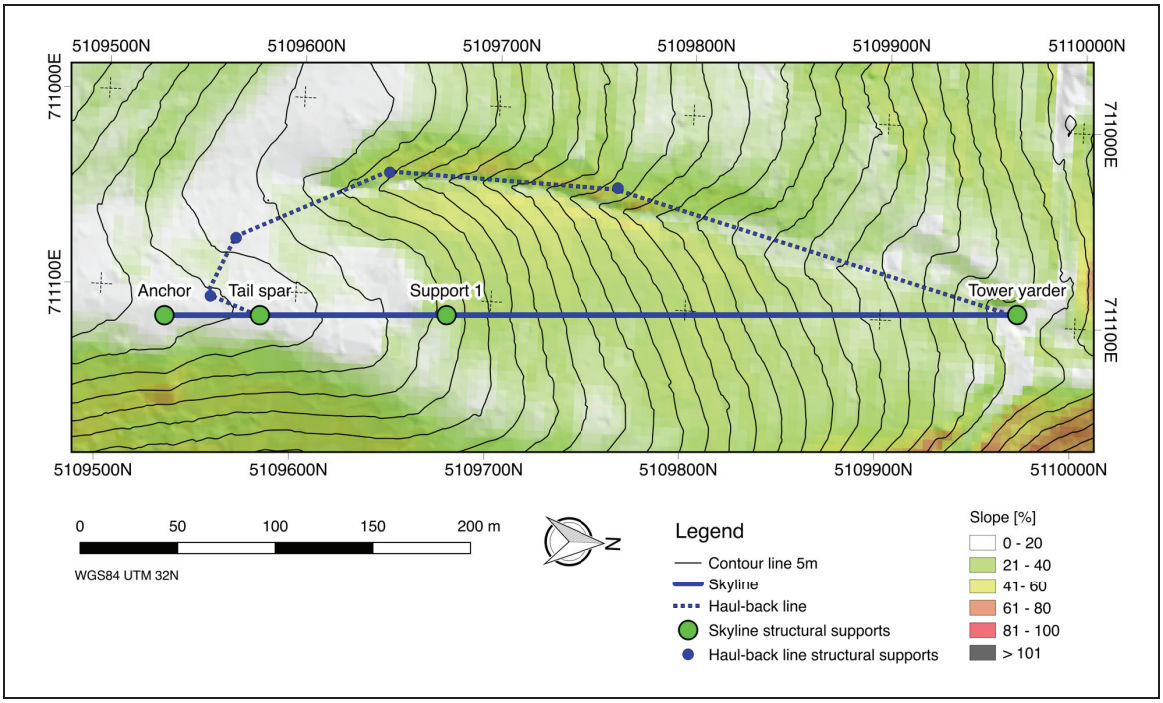

Annex 6: Profiles and maps of the monitored trails

This section, similarly to Annex 4 for cable lines, reports the graphical representation of the longitudinal profile and the map of each observed trail where the winch-assist forwarder operated.

The longitudinal profiles show the different type of anchors (whole trees or stumps), described in Table 6.1. Also, the picture indicates the position of the forest roads. The ground profile and the anchor heights are in scale.

The maps show the position of anchor, monitored trail, forest road, and access trails, if appropriate. Also, the maps report the evidence of the ground slope (as discrete values with 20% transparency) and the contour lines (reported every 10 m), derived by 30m-grid Digital Elevation Models. The black narrows show the forwarding direction.

The tables report the details of each element reported in the profile representations and in the maps. The "DBH" column reports the diameter at breast height (nearly 1.30 m). In case of stumps, this column reports the diameter measured at the highest point. The columns "H tot" shows the total height of the anchors.

Table 6.1: Anchors used in the winch-assist study sites

Trail -	Site -	Specie -	Element -	Type	DBH cm	H tot m
CR01	A	hybrid spruce	anchor	stump	55	0
CR02	B	Douglas fir	anchor	tree	76	41.2
	B	Douglas fir	deviator	stump	32	0
CR03	C	hybrid spruce	anchor	tree	52	36
CR04	C	hybrid spruce	anchor	tree	67	38.5
CR05	C	hybrid spruce	anchor	tree	67	38.5
CR06	C	hybrid spruce	anchor	tree	58	37
CR07	C	hybrid spruce	anchor	tree	54	36
CR08	C	hybrid spruce	anchor	tree	64	38

Trail CR01 (Site N)

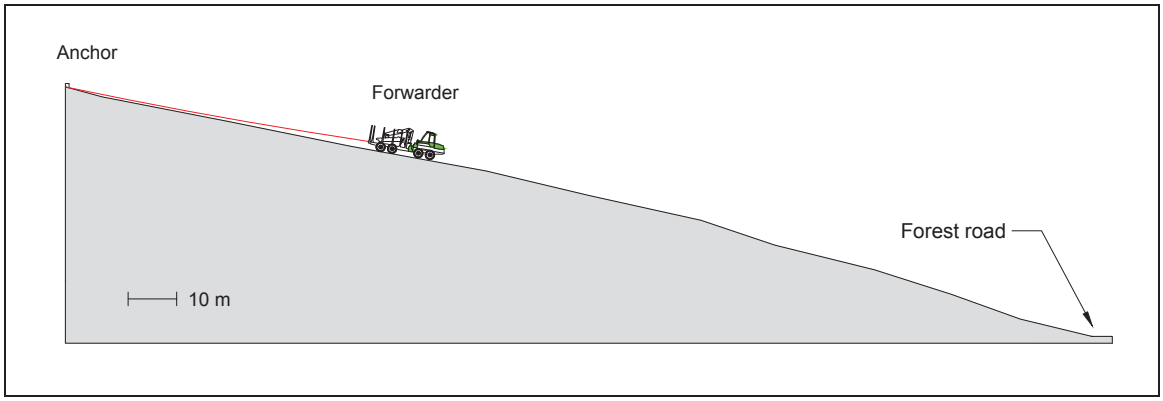

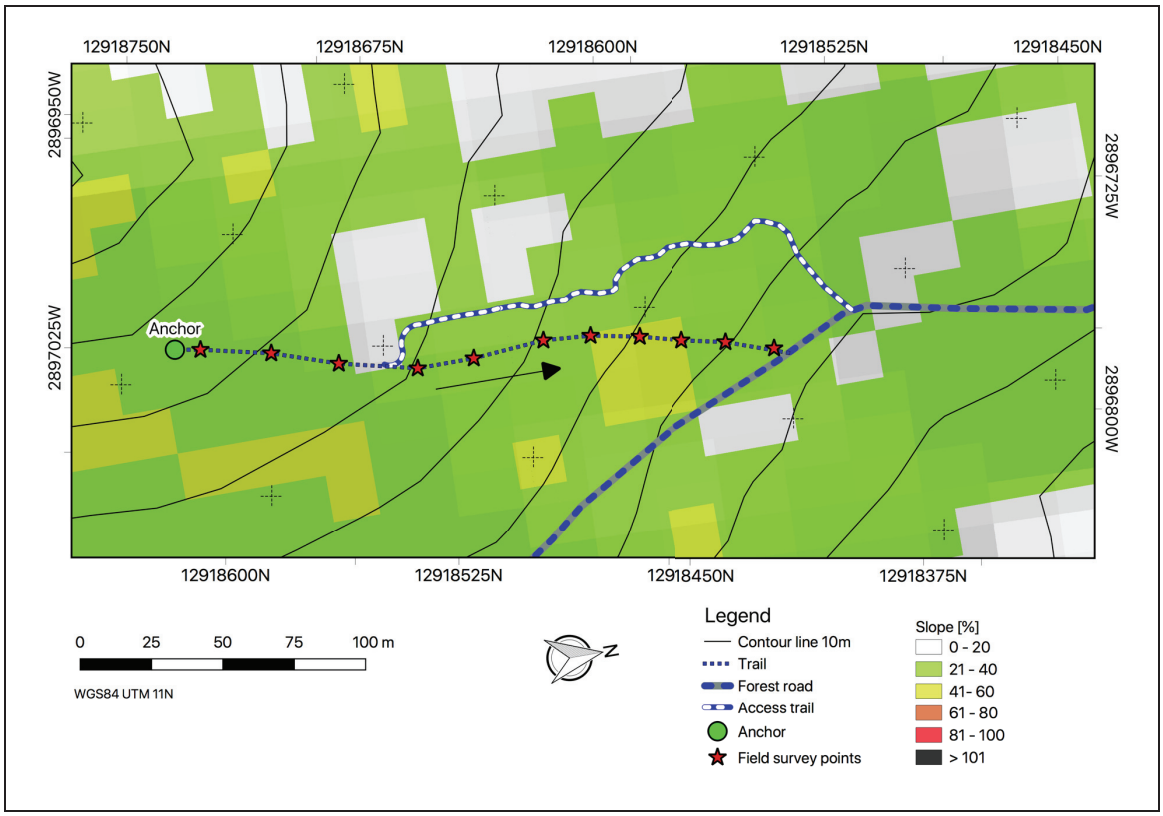

Trail CR02 (Site O)

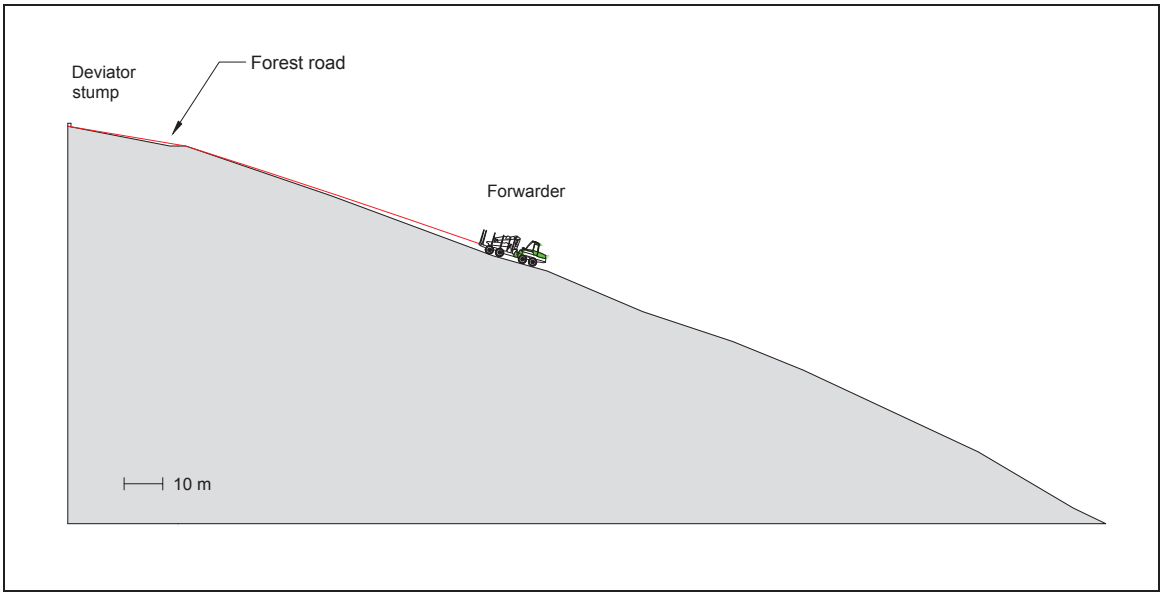

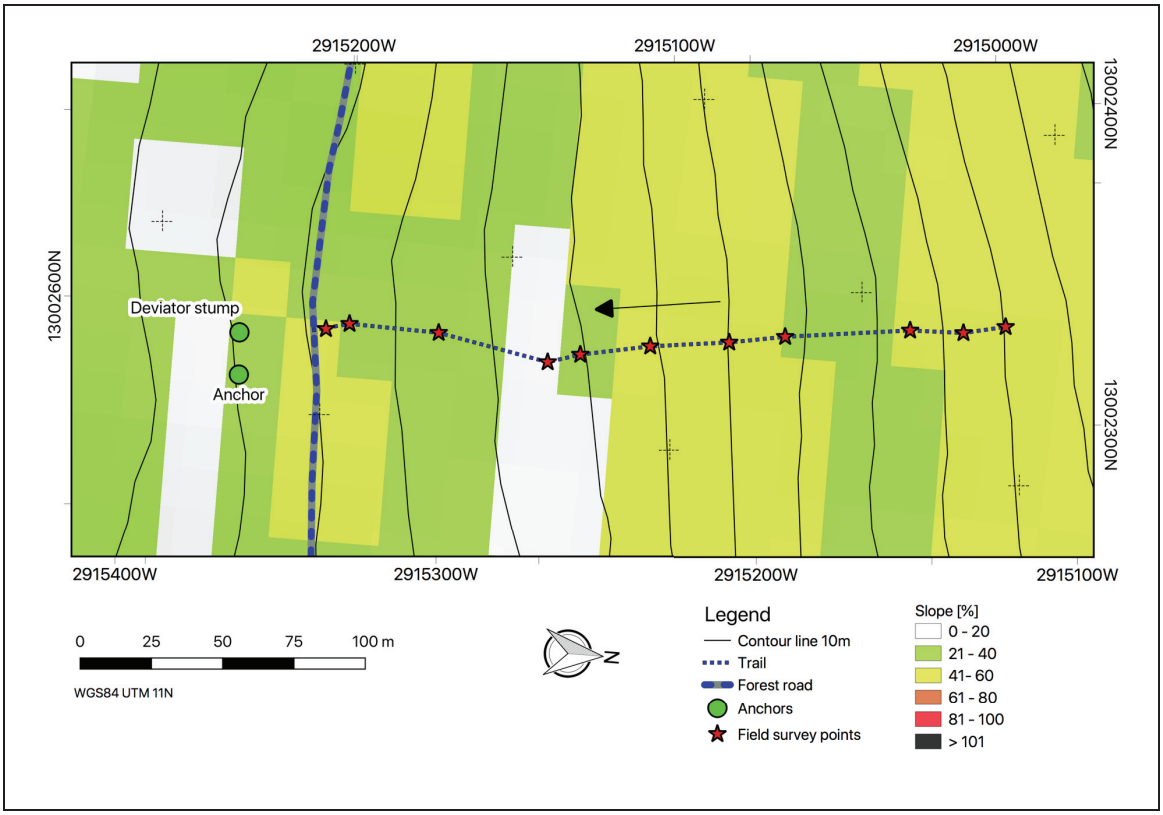

Trail CR03 (Site P)

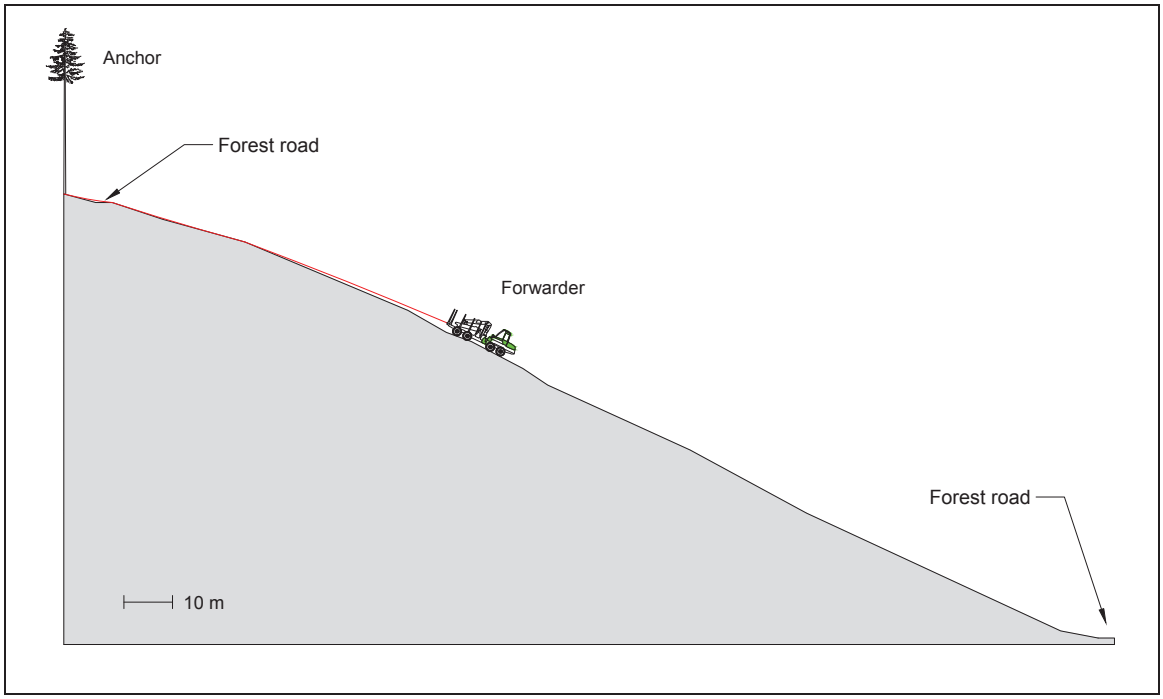

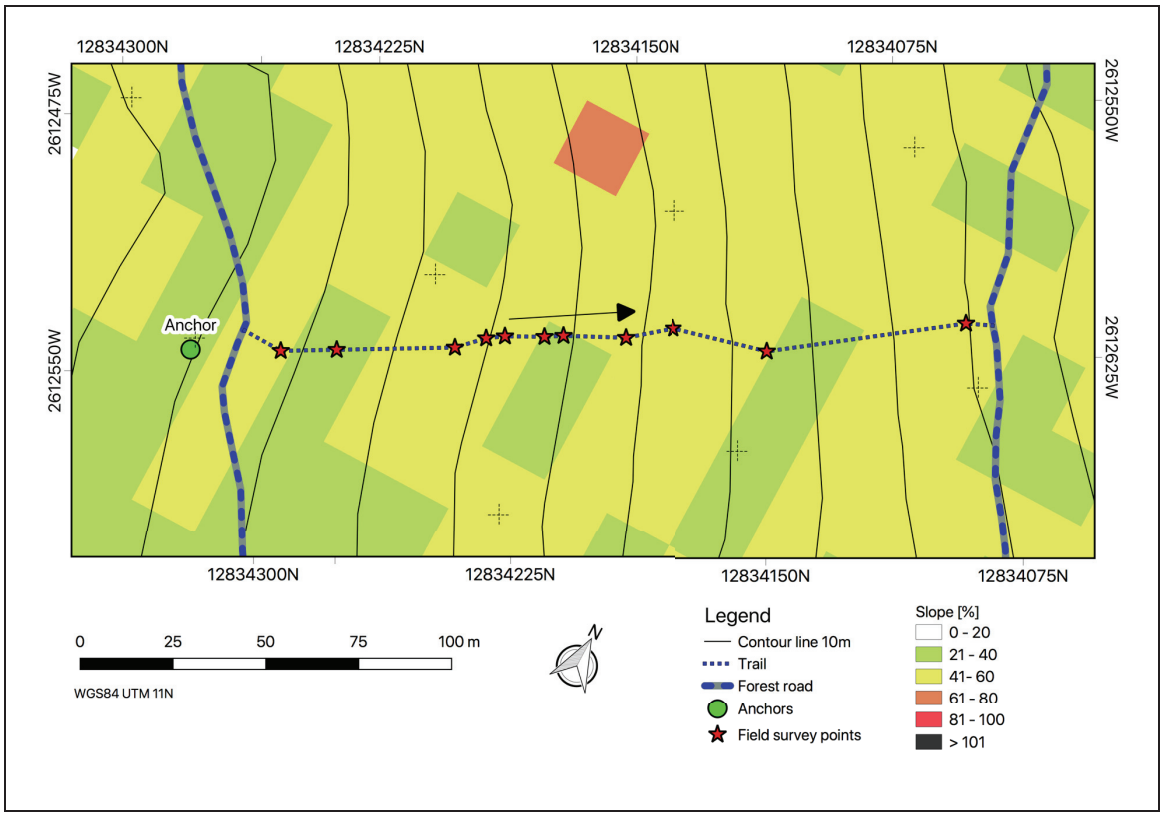

Trail CR04 (Site P)

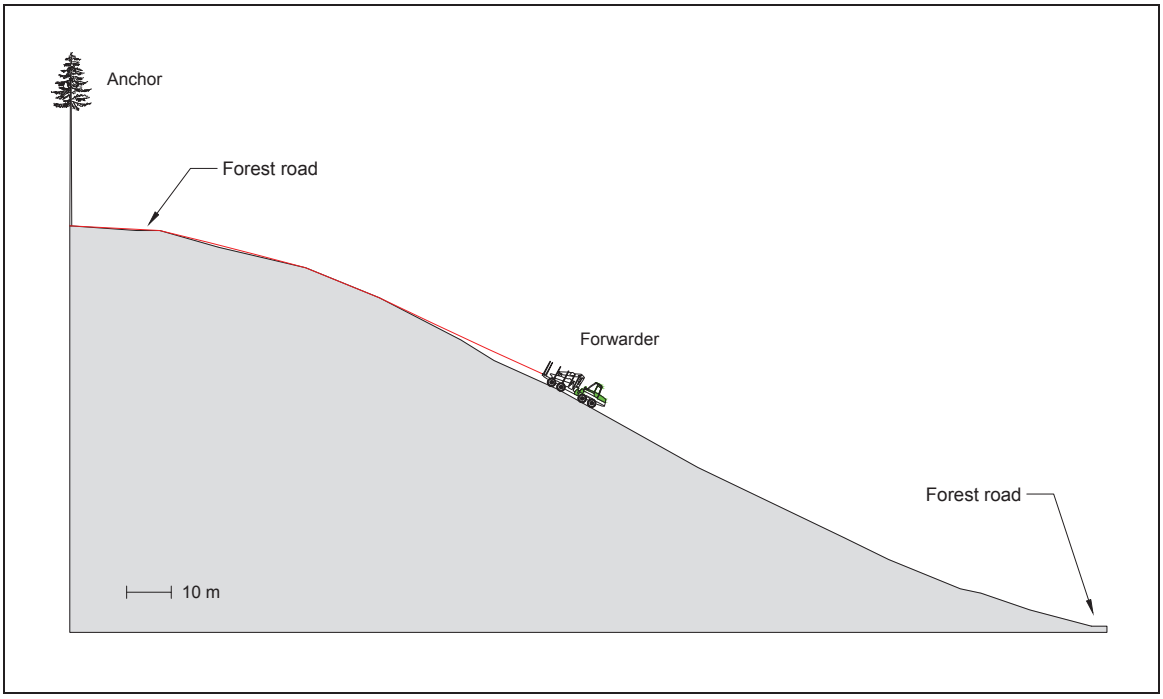

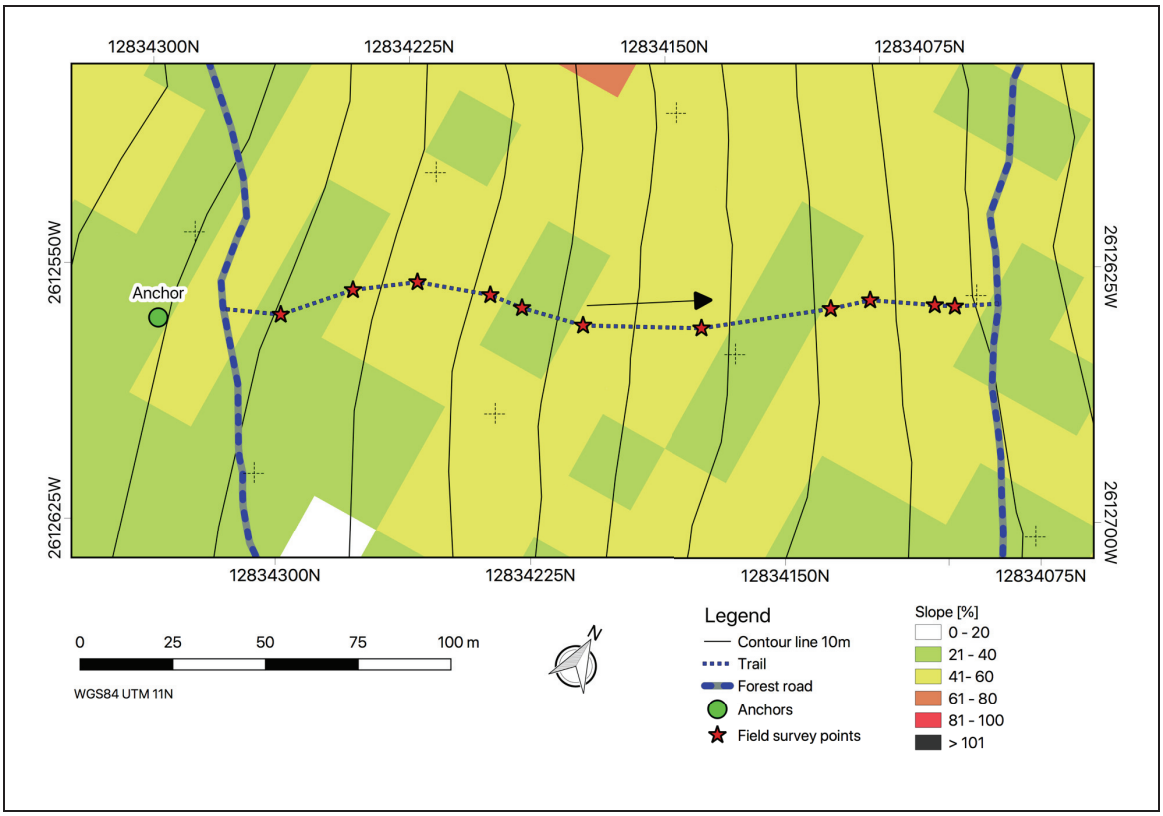

Trail CR05 (Site P)

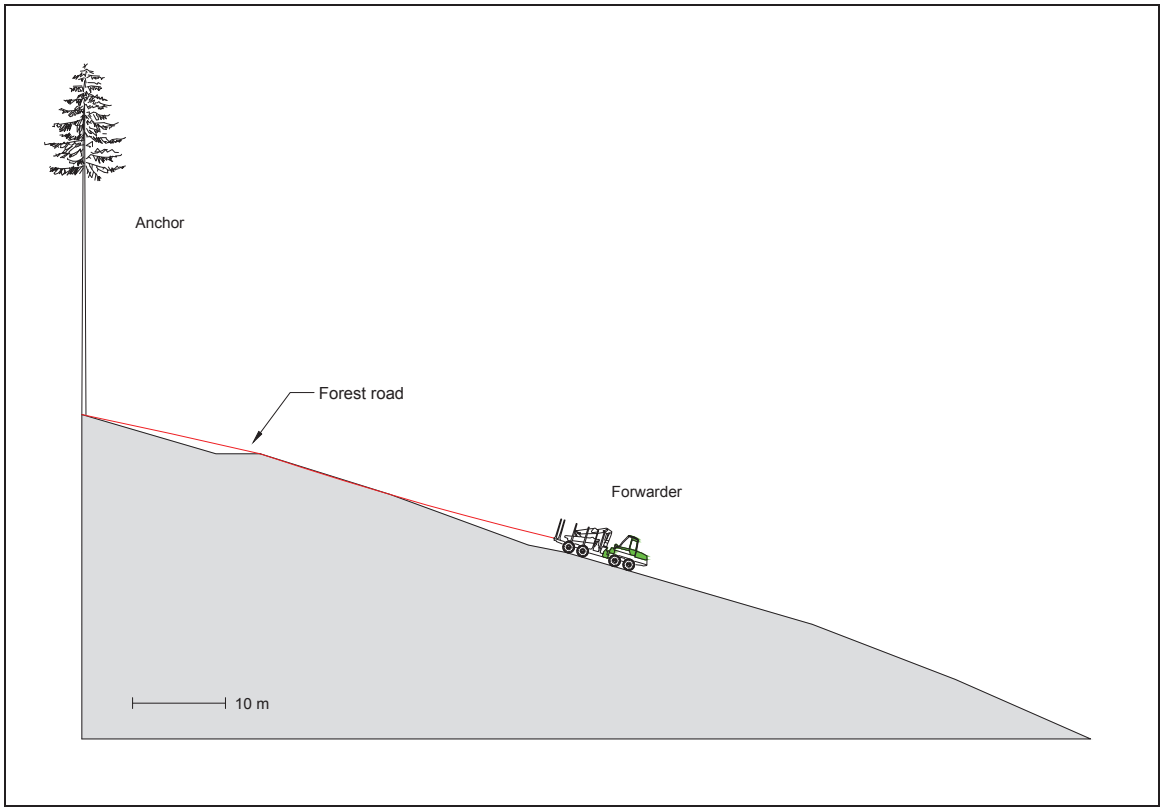

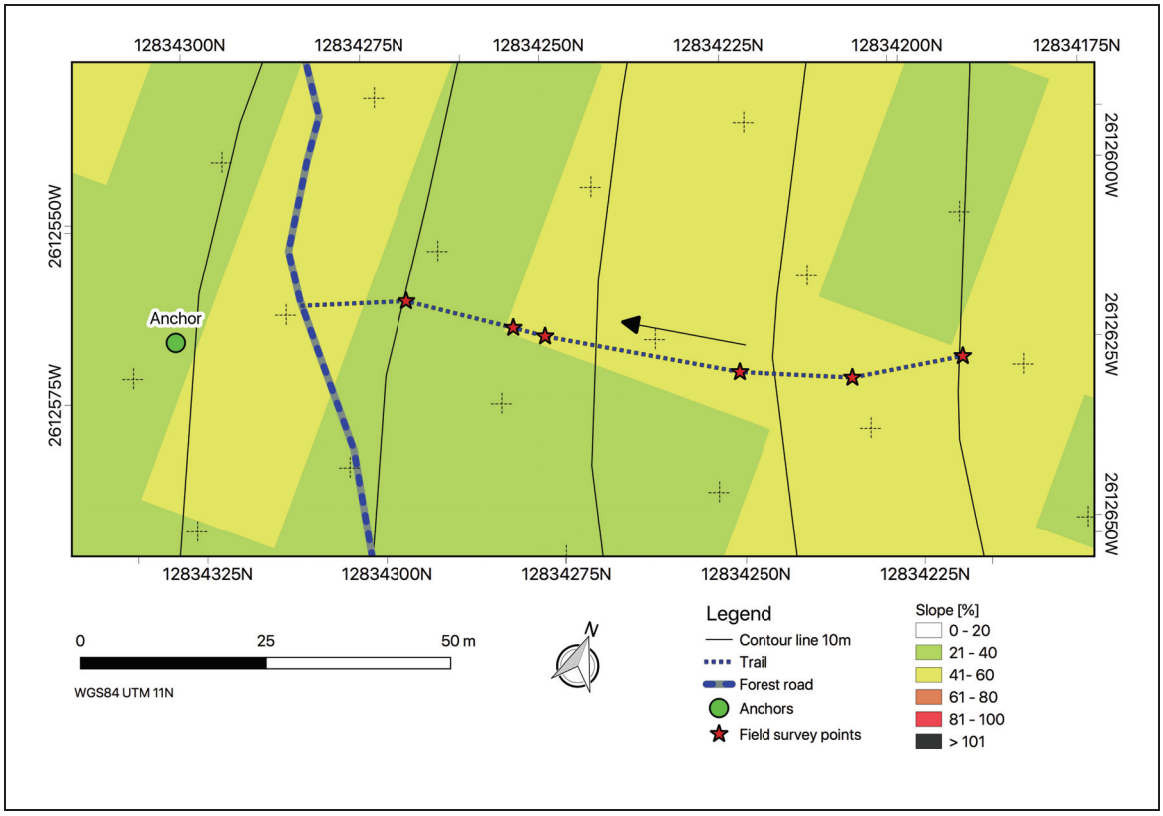

Trail CR06 (Site P)

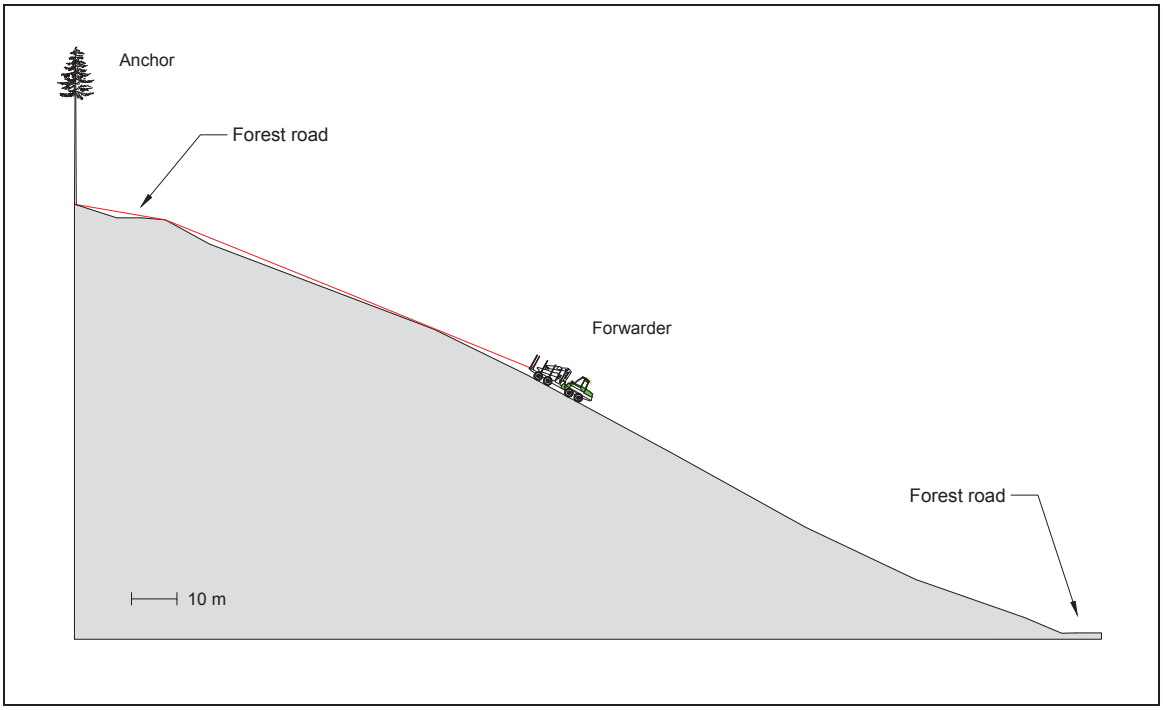

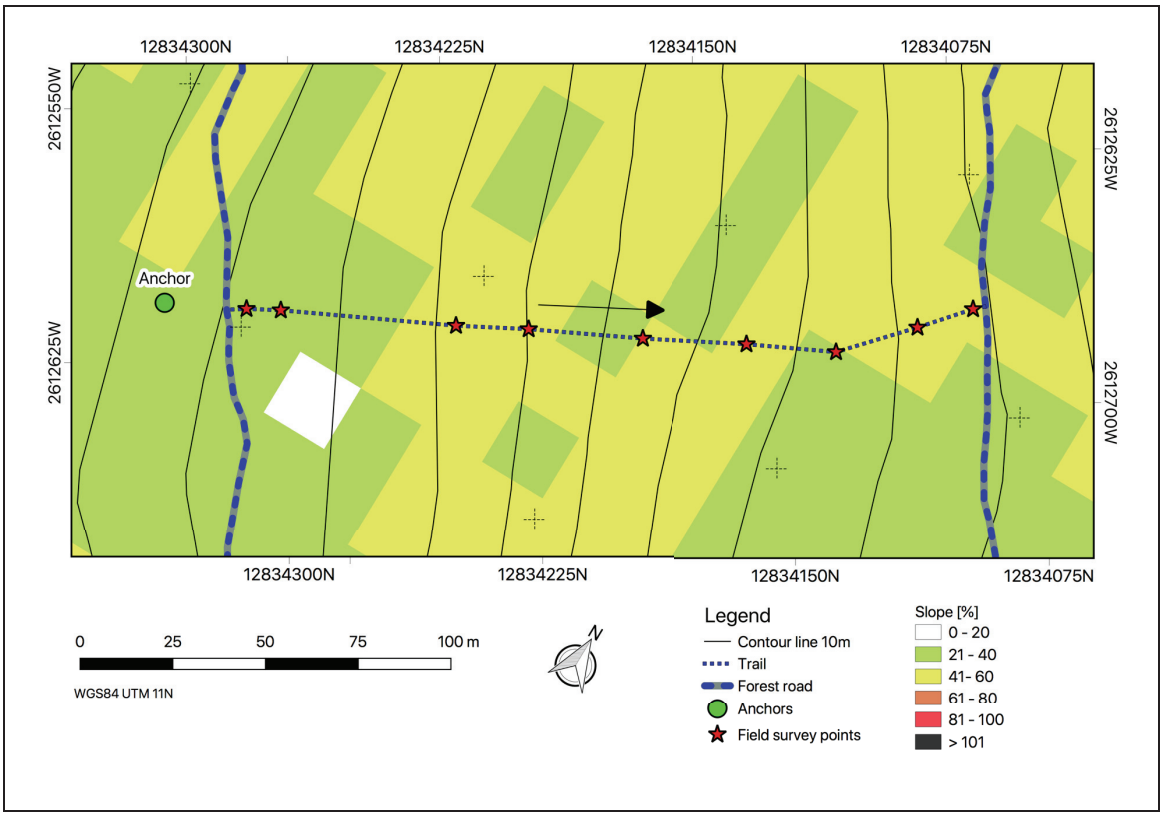

Trail CR07 (Site P)

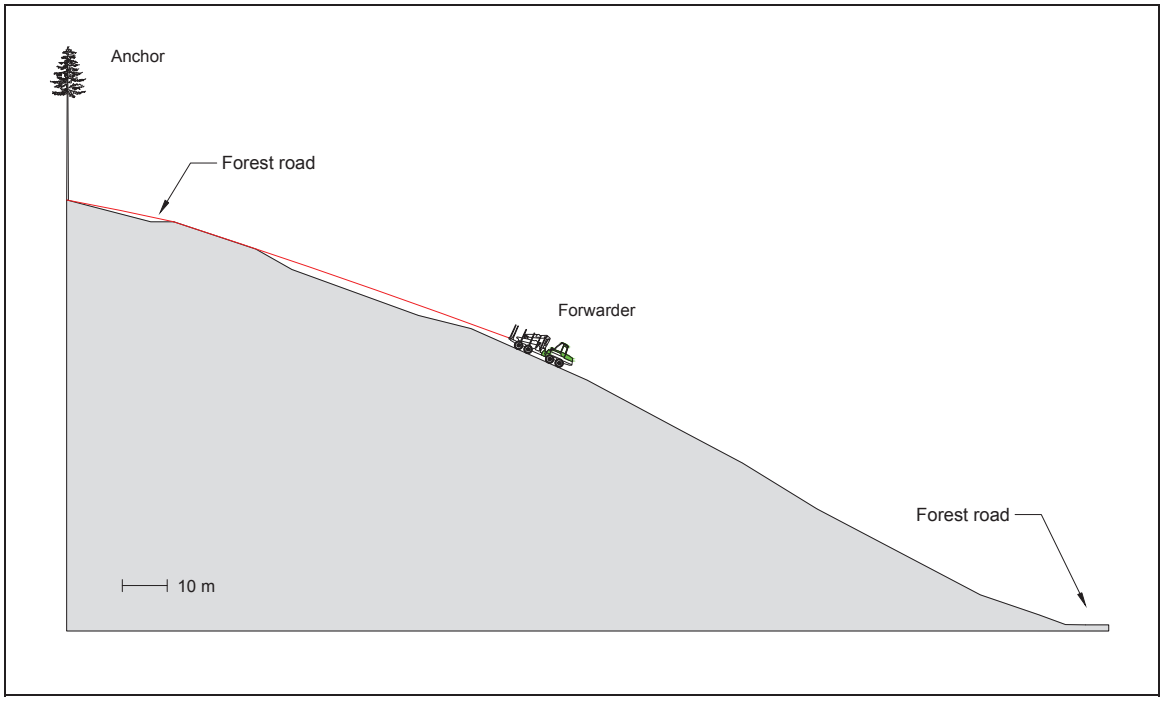

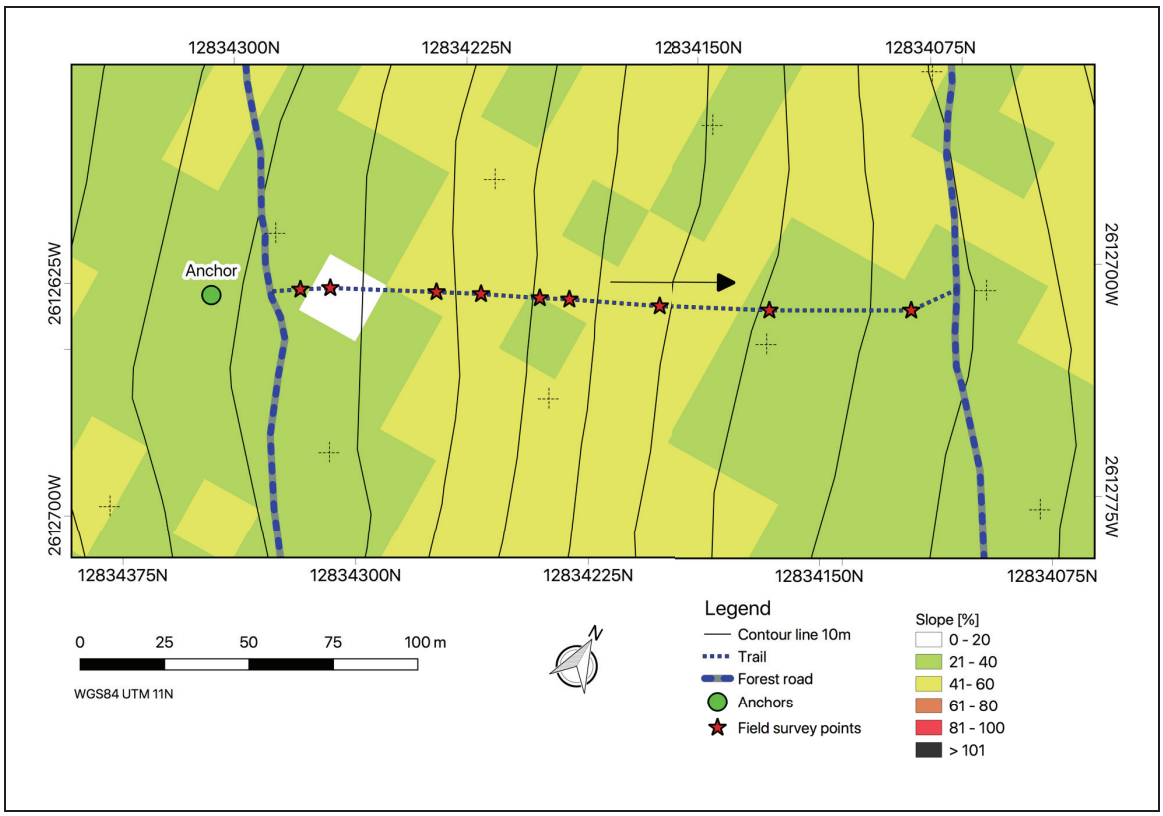

Trail CR08 (Site P)

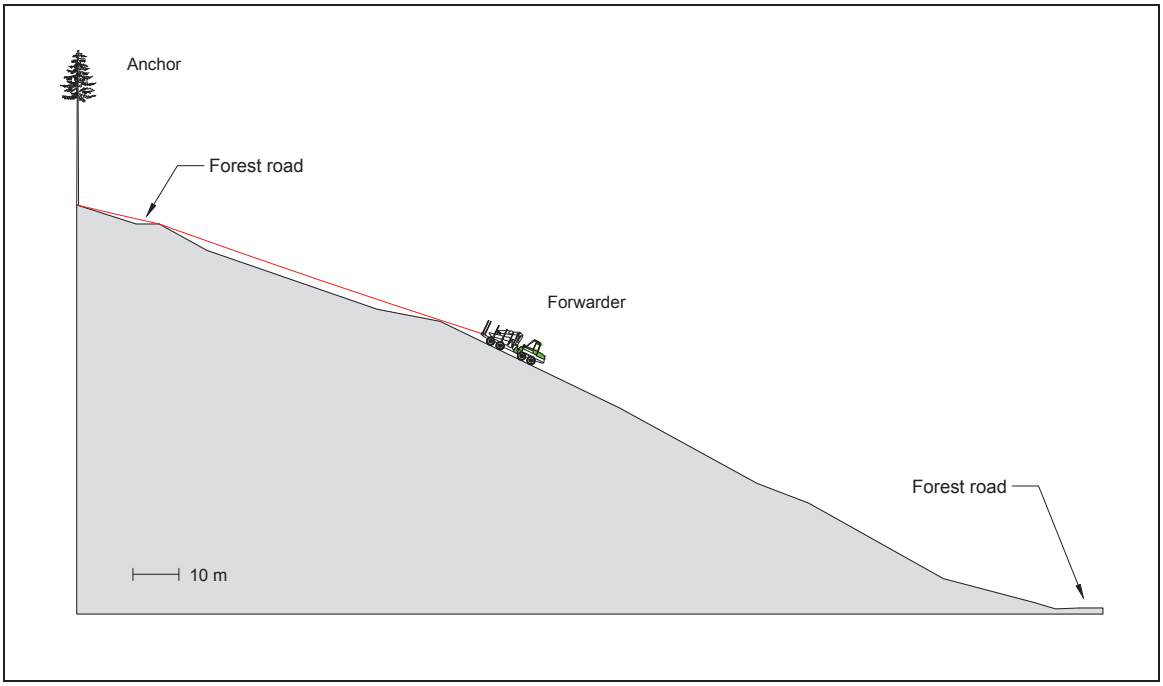

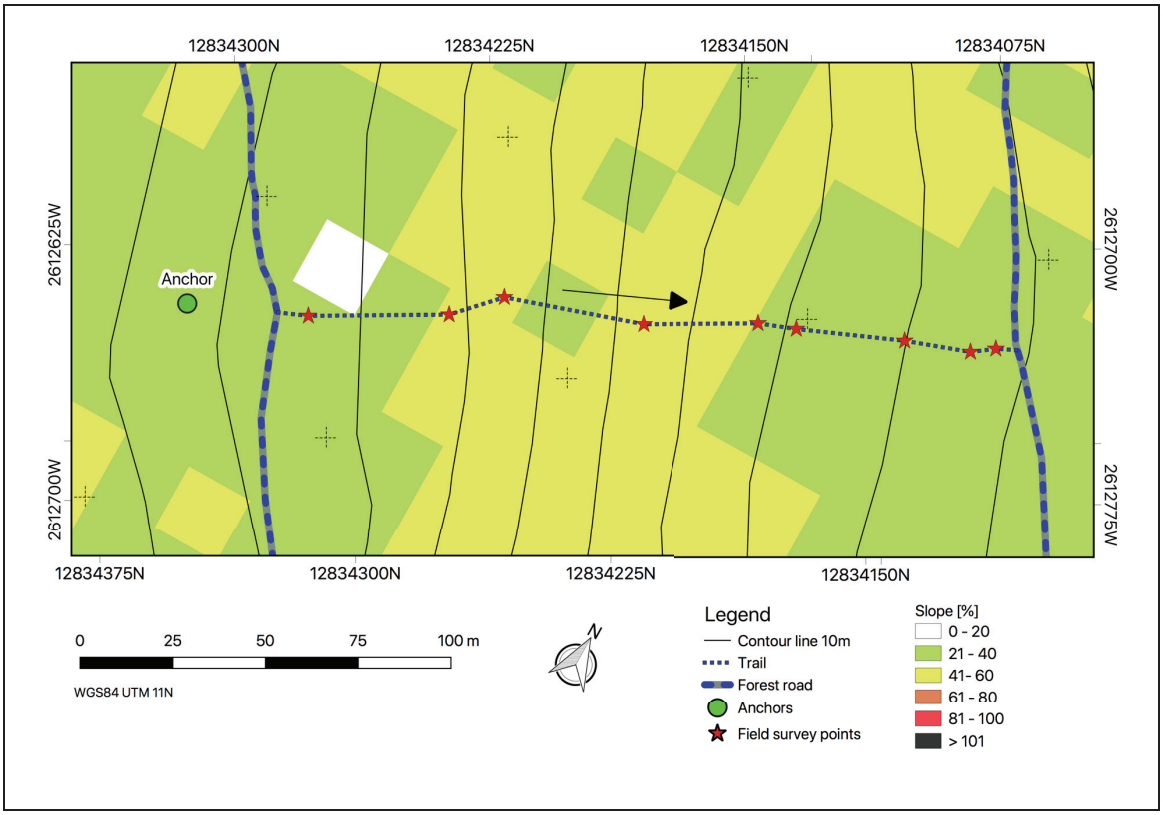

Overview trails CR03-CR08 (Site P)